

CM<P 2021 | Kharkiv, Ukraine



B. Verkin Institute for Low Temperature
Physics and Engineering of NAS of Ukraine



Abstracts book

II International Advanced Study Conference

**CONDENSED MATTER &
LOW TEMPERATURE PHYSICS**

6 – 12 June 2021
Kharkiv, Ukraine



II International Advanced Study Conference Condensed Matter and Low Temperature Physics

CM<P 2021

6 - 12 June 2021 | Kharkiv, Ukraine

Conference Program

Book of Abstracts

Kharkiv 2021

UDK 536.48

**I-69
BBK 22.36**

Scientific Edition

Scientific International Conference – Conference Program and Book of Abstracts

**II International Advanced Study Conference
Condensed Matter and Low Temperature Physics 2021
CM<P 2021**

Organised by B. Verkin Institute for Low Temperature Physics and Engineering (ILTPE) of NAS of Ukraine
Council of Young Scientists of B.Verkin ILTPE of NAS of Ukraine

6-12 June 2021 | Kharkiv, Ukraine

Editorial board: Yurii Naidyuk
Aleksandr Dolbin

Layout Editor: Nina Gamayunova
Valentin Koverya

Design: Razet Basnukaeva

I-69 II International Advanced Study Conference Condensed Matter and Low Temperature Physics 2021 (6-12 June 2021, Kharkiv): Conference Program and Book of Abstracts / Editor: Nataliia Mysko-Krutik. – Kharkiv: FOP Brovin O.V., 2021. – 240 p.

ISBN 978-617-8009-12-0

This book is the proceedings of the II International Advanced Study Conference Condensed Matter and Low Temperature Physics 2021. The proceedings contain 196 peer-reviewed abstracts. These materials present the studies of modern aspects of condensed matter and low temperature physics including electronic properties of conducting and superconducting systems, magnetism and magnetic materials, optics, photonics and optical spectroscopy, quantum liquids and quantum crystals, cryocrystals, nanophysics and nanotechnologies, biophysics and physics of macromolecules, materials science, theory of solid state physics, technological peculiarities of the instrumentation for physical experiments, and related fields.

The conference proceeding is published as a printed edition.
All rights reserved.

**UDK 536.48
BBK 22.36**

ISBN 978-617-8009-12-0

© B. Verkin Institute for Low Temperature Physics and Engineering NAS of Ukraine, 2021

FOREWORD

Dear Participants of the Conference,

On behalf of the Organizing Committee I am glad to welcome you to the II International Advanced Study Conference “Condensed Matter and Low Temperature Physics 2021” (CM<P - 2021) organized at the B.Verkin Institute for Low temperature Physics and Engineering (ILTPE) of the National Academy of Sciences of Ukraine (NASU), Kharkiv, Ukraine.

The CM<P – 2021 has evolved from the previous International Conference for Professionals and Young Scientists “Low Temperature Physics” (ICPYS LTP). Now, for recent 11 years, we have been enjoying the tradition of fruitful contacts among professional experts in the field of condensed matter and low temperature physics and young researchers – all this owing to the international conferences organized by the ILTPE.

The program of CM<P 2021 covers all presently important experimental and theoretical aspects of condensed matter physics, including low temperature physics, superconductivity, magnetism, optics, nanophysics, biophysics, materials science and related areas. CM<P 2021 is intended to be a platform for scientists to share their knowledge, to exchange new information and ideas, and to find collaborators and co-partners.

This scientific event offers broad opportunities for researchers engaged in academic and research institutions, as well as in industrial companies for exchanging information and launching cooperation. This will attract the attention of the young scientists of the region to multifaceted present-day solid state physics and its applications – this will encourage them to start a career as a researcher. A special lecture will be delivered concerning the problems of career promotion.

The Conference will host over 200 scientists from 25 countries, in particular from Austria, Algeria, China, Finland, France, Georgia, Germany, Israel, India, Japan, Kazakhstan, Latvia, Poland, Republic of Belarus, Romania, Russian Federation, South Africa, South Korea, Slovak Republic, Spain, Turkey, Ukraine, United Kingdom, United Arab Emirates and USA.

I hope you will gain unforgettable impression of our conference – its interesting high-quality scientific program, offered opportunities of meetings and discussions. And may the meetings be fruitful. Get the most of them!

Prof. Yurii Naidyuk
Director of B.Verkin Institute for Low Temperature
Physics and Engineering of the National
Academy of Sciences of Ukraine

PROGRAM COMMITTEE

Chair: Prof. Yurii Naidyuk, ILTPE NASU (Kharkiv, Ukraine)
Vice-chair: Prof. Aleksandr Dolbin, ILTPE NASU (Kharkiv, Ukraine)
Dr. Mykola Glushchuk, ILTPE NASU (Kharkiv, Ukraine)
Dr. Viktor Chabanenko, DonFTI NASU (Kyiv, Ukraine)
Prof. Gennadiy Grechnev, ILTPE NASU (Kharkiv, Ukraine)
Prof. Andrzej Jezowski, INTiBS PAN (Wroclaw, Poland)
Dr. Oleksandr Kalinenko, ILTPE NASU (Kharkiv, Ukraine)
Dr. Gennadii Kamarchuk, ILTPE NASU (Kharkiv, Ukraine)
Prof. Viktor Karachevtsev, Corr. Member of NASU, ILTPE NASU (Kharkiv, Ukraine)
Prof. Mykola Kharchenko, Full Member of NASU, ILTPE NASU (Kharkiv, Ukraine)
Prof. Yuriy Kolesnichenko, ILTPE NASU (Kharkiv, Ukraine)
Dr. Oleksandr Kordyuk, Corr. member of NASU, IMP NASU (Kyiv, Ukraine)
Dr. Volodymyr Kurnosov, ILTPE NASU (Kharkiv, Ukraine)
Dr. Volodymyr Maidanov, ILTPE NASU (Kharkiv, Ukraine)
Prof. Vasyliy Natsik, ILTPE NASU (Kharkiv, Ukraine)
Dr. Anatoliy Negriyko, Corr. Member of NASU, IOP NASU (Kyiv, Ukraine)
Prof. Oleksandr Omelyanchouk, Corr. Member of NASU, ILTPE NASU (Kharkiv, Ukraine)
Dr. Pavlo Pal-Val, ILTPE NASU (Kharkiv, Ukraine)
Prof. Leonid Pastur, Full Member of NASU, ILTPE NASU (Kharkiv, Ukraine)
Prof. Elena Savchenko, ILTPE NASU (Kharkiv, Ukraine)
Dr. Sergiy Shevchenko, ILTPE NASU (Kharkiv, Ukraine)
Dr. Svyatoslav Sokolov, ILTPE NASU (Kharkiv, Ukraine)
Prof. Victor Slavin, ILTPE NASU (Kharkiv, Ukraine)
Prof. Andrzej Szewczyk, IF PAN (Warsaw, Poland)
Prof. Yevgen Syrkin, ILTPE NASU (Kharkiv, Ukraine)
Prof. Alexander Vasiliev, MSU (Moscow, Russia)

ORGANIZING COMMITTEE

Chair: Dr. Nataliia Mysko-Krutik
Vice-chair: Dr. Maryna Kolodiazhnna
Secretary: Dr. Anastasiya Lyogenkaya

Dr. Maksym Barabashko	Diana Hurova
Dr. Razet Basnukaeva	Dr. Olga Ilinskaya
Dr. Nina Gamayunova	Dr. Valentin Koverya
Ann Boychenko	Volodymyr Meleshko
Vusal Geidarov	Dr. Yevhen Petrenko
Anna Herus	Dr. Sergii Poperezhai

SECTION 1. ELECTRONIC PROPERTIES OF CONDUCTING AND SUPERCONDUCTING SYSTEMS

Chair: Dr. Valentin Koverya

PLENARY LECTURES

The strain impact on ferromagnetic/graphene/ferroelectric nanostructures ..44

M.V. Strikha^{1,2}, E.A. Eliseev³, A.N. Morozovska⁴

¹Taras Shevchenko National University of Kyiv, Faculty of Radiophysics, Electronics and Computer Systems, Kyiv, Ukraine,

²V.Lashkariov Institute of Semiconductor Physics NASU, Kyiv, Ukraine

³Institute for Problems of Materials Science NASU, Kyiv, Ukraine

⁴Institute of Physics NASU, Kyiv, Ukraine

Ultra-fast vortex dynamics in nanoengineered superconductors ..32

O.V. Dobrovolskiy

Faculty of Physics, University of Vienna, Vienna, Austria

Influence of pressure and stoichiometry on the Ginzburg-Landau parameter in superconducting YB₆ ..34

S. Gabáni¹, K. Flachbart¹, E. Gažo¹, J. Kačmarčík¹, M. Marcin¹, T. Mori², M. Orendáč¹, Z. Pribulová¹, G. Pristáš¹, P. Samuely¹, N. Shitsevalova³, N. Sluchanko⁴

¹Institute of Experimental Physics, SAS, Košice, Slovakia

²National Institute for Materials Science, ICMN & CFSN, Tsukuba, Japan

³Frantsevich Institute for Problems of Materials Science, NASU, Kyiv, Ukraine

⁴Prokhorov General Physics Institute, RAS, Moscow, Russia

ORAL PRESENTATIONS

Fractal analysis of the critical state of the NbTi superconductor ..52

O.M. Chumak^{1,2}, V.V. Chabanenko¹, V.F. Rusakov³, O.I. Kuchuk¹, I. Abaloszewska², O. Abaloszewska², A. Nabiałek², R. Puźniak²

¹O.Galkin Donetsk Institute for Physics and Engineering NASU, Kyiv, Ukraine

²Institute of Physics, Polish Academy of Sciences, Warsaw, Poland

³Vasyl' Stus Donetsk National University, Vinnytsia, Ukraine

Shift of the electronic bands in Fe(Se,Te) in the vicinity of the superconducting transition ..53

Yu.V. Pustovit^{1,2}, D.P. Menesenko¹, A.A. Kordyuk²

¹T.Shevchenko National University of Kyiv, Kyiv, Ukraine

²Kyiv Academic University, Kyiv, Ukraine

Possibility for the anisotropic acoustic plasmons in LaH₁₀ and their role in enhancement of the critical temperature of superconducting transition ..54

E.A. Pashitskii, V.I. Pentegov, A.V. Semenov

Institute of Physics NASU, Kyiv, Ukraine

The unusual microwave response of chalcogenide FeSe_{1-x}Te_x film compared to other superconductors ..55

Y. Wu¹, A.A. Barannik², L. Sun¹, Y-S. He¹, N.T. Cherpak²

¹Institute of Physics of Chinese Academy of Sciences, National Laboratory for Superconductivity, Beijing, China

²O. Usikov Institute for Radiophysics and Electronics NASU, Kharkiv, Ukraine

POSTERS

Low field high-harmonic generation in Mo₆S₆I₂ Chevrel-phase superconductor	..56
I.R. Metskhvarishvili ^{1,2} , <u>B.G. Bendeliani</u> ¹ , G.N. Dgebuadze ¹ , G.R. Giorganashvili, M.R. Metskhvarishvili ² , T.E. Lobzhanidze ³	
¹ Ilia Vekua Sukhumi Institute of Physics and Technology, Laboratory of Cryogenic Technique and Technologies, Tbilisi, Georgia	
² Georgian Technical University, Faculty of Informatics and Control Systems, Department of Microprocessor and Measurement Systems, Tbilisi, Georgia	
³ Ivane Javakhishvili Tbilisi State University, Faculty of Exact and Natural Sciences, Department of Chemistry, Tbilisi, Georgia	
 Spin Nernst effect in the platinum and tungsten samples	..57
Yu.N. Chiang, <u>M.O. Dzyuba</u>	
B. Verkin Institute for Low Temperature Physics and Engineering NASU, Kharkiv, Ukraine	
 Superconductivity in hole-doped Ge detected by Point-Contact Spectroscopy	..58
N.V. Gamayunova ¹ , P. Szabó ² , J. Kačmarčík ² , P. Samuely ² , O.E. Kvintitskaya ¹ , L.V. Tyutrina ¹ , Yu.G. Naidyuk ¹	
¹ B.Verkin Institute for Low Temperature Physics and Engineering NASU, Kharkiv, Ukraine	
² Centre of Low Temperature Physics, Institute of Experimental Physics SAS, Košice, Slovakia	
 The influence of magnetic field on phase dynamics of stacks of long Josephson junctions	..59
A. Grib	
V. N. Karazin National University, Kharkiv, Ukraine	
 Magnetic transition in RuSr₂(Eu_{1.5}Ce_{0.5})Cu₂O_{10-δ} ceramic samples and VRH law	..60
E.Yu. Beliayev, I.G. Mirzoev, <u>V.A. Horielyi</u>	
B. Verkin Institute for Low Temperature Physics and Engineering NASU, Kharkiv, Ukraine	
 The effect of hydrogen thermo diffusion on the superconducting properties of FeTe_{0.65}Se_{0.35} single crystals	..61
S.I. Bondarenko ¹ , <u>A.I. Prokhvatilov</u> ¹ , R. Pužniak ² , J.Piętosa ² , A.A. Prokhorov ³ , V.V. Meleshko ¹ , V.P. Timofeev ¹ , <u>V.P. Koverya</u> ¹ , D.J. Gawryluk ^{2,4} , A. Wiśniewski ²	
¹ B. Verkin Institute for Low Temperature Physics and Engineering NASU, Kharkiv, Ukraine	
² Institute of Physics of the Polish Academy of Sciences, Warsaw, Poland	
³ Institute of Physics of the Czech Academy of Sciences, Praha, Czech Republic	
⁴ Laboratory for Scientific Developments and Novel Materials, Paul Scherrer Institute, Villigen, Switzerland	
 Josephson properties of phase-slip centers in narrow channels made of a bimetallic superconducting-normal film	..62
A.G. Sivakov, <u>S.O. Kruhlav</u> , A.S. Pokhila	
B. Verkin Institute for Low Temperature Physics and Engineering NASU, Kharkiv, Ukraine	
 Magnetic and structural properties of La_{1-x}Gd_xCoO₃ compounds	..63
A.S. Panfilov ¹ , <u>A.A. Lyogenkaya</u> ¹ , G.E. Grechnev ¹ , V.A. Pashchenko ¹ , L.O. Vasylechko ² , V.M. Hreb ² , A.V. Kovalevsky ³	
¹ B. Verkin Institute for Low Temperature Physics and Engineering NASU, Kharkiv, Ukraine	
² Lviv Polytechnic National University, Lviv, Ukraine	
³ Department of Materials and Ceramic Engineering, CICECO - Aveiro Institute of Materials, University of Aveiro, Aveiro, Portugal	

Magnetoresistive study of the excess conductivity in YBCO monolayers	..64
E.V. Petrenko ¹ , L.V. Omelchenko ¹ , A.L. Solovjov ¹ , N.V. Shitov ¹ , K. Rogacki ²	
¹ B. Verkin Institute for Low Temperature Physics and Engineering NASU, Kharkiv, Ukraine	
² Institute for Low Temperatures and Structure Research, Polish Academy of Sciences, Wroclaw, Poland	
Effect of MWCNT content on electrical properties of ternary PVDF/PANI/MWCNT nanocomposite at low temperature	..65
R.M. Rudenko ¹ , O.O. Voitsihovska ¹ , V.M. Poroshin ¹ , M.V. Petrychuk ² , A.S. Nikolenko ¹ , N.A. Ogurtsov ³ , Yu.V. Noskov ³ , D.O. Sydorov ³ , A.A. Pud ³	
¹ Institute of Physics NASU, Kyiv, Ukraine	
² Taras Shevchenko National University of Kyiv, Kyiv, Ukraine	
³ V.P. Kokhar Institute of Bioorganic Chemistry and Petrochemistry NASU, Kyiv, Ukraine	
Electrical properties of molybdenum disulfide MoS₂ nanopowder	..66
R.M. Rudenko, O.O. Voitsihovska, G.I. Dovbeshko, V.M. Poroshin	
Institute of Physics, NASU, Kyiv, Ukraine	

Generalized nonlinear magnetic susceptibility of superconductive disk in transverse AC field and its dependence on the pick-up coil size	..67
A.V. Semenov	
Institute of Physics NASU, Kyiv, Ukraine	

Challenge in microwave study of unconventional superconductors in normal state and near the critical temperature	..68
A.A. Barannik ¹ , S.A. Vitusevich ² , M.V. Vovnyuk ¹ , A.I. Shubnyi ¹ , S.K. Dukhnovskiy ^{1,3}	
¹ O. Usikov Institute for Radiophysics and Electronics NASU, Kharkiv, Ukraine	
² Institute of Biological Information Processing (IBI-3): Bioelectronics, Forschungszentrum Juelich, Juelich, Germany	
³ National University of Radioelectronics, Kharkiv Ukraine	

SECTION 2. MAGNETISM AND MAGNETIC MATERIALS

Chair: Dr. Maryna Kolodiazhna

PLENARY LECTURES

Nonlinear and chiral response of topological semimetals and other chiral media	..36
F. Büscher ¹ , V. Gnezdilov ^{1,2} , D. Wulferding ^{1,3} , S. Müllner ¹ , Yu. G. Pashkevich ⁴ , C. Felser ⁵ , Ch. Shekhar ⁵ , K. Manna ⁶ , P. Lemmens ¹	
¹ IPKM and LENA, TU-Braunschweig, Germany	
² B.Verkin Institute for Low Temperature Physics and Engineering of NASU, Kharkiv, Ukraine	
³ IBS, Center for Correlated Electron Systems, Seoul Nat. Univ, Seoul, Korea	
⁴ Donetsk IPE O.O. Galkin NAS, Kyiv, Ukraine	
⁵ MPI Dresden, Germany	
⁶ Quantum Materials Magneto-Transport Laboratory, IIT, New Delhi, India	

Magnetochiral effect of phonons	..47
S. Zherlitsyn	
Hochfeld-Magnetlabor Dresden, Helmholtz-Zentrum Dresden-Rossendorf, Dresden, Germany	

Pressure-tuned magnetic interactions in a triangular-lattice quantum antiferromagnet	..49
S. Zvyagin	
Dresden High Magnetic Field Laboratory, Helmholtz-Zentrum Dresden Rossendorf, Dresden, Germany	

Massive magnetostriction of the KEr(MoO₄)₂	..35
D. Kamenskyi ^{1,2} , B. Bernath ³ , S. Khmelevskyi ⁴ , L.V. Pourovskii ⁵ , S. Poperezhai ⁶ , K. Kutko ⁶	
¹ Experimental Physics V, Institute of Physics, University of Augsburg, Augsburg, Germany	
² Molecular Photoscience Research Center, Kobe University, Kobe, Japan	
³ High Field Magnet Laboratory (HFML-EMFL), Radboud~University, Nijmegen, Netherlands	
⁴ Research Center for Materials Science and Engineering, Vienna University of Technology, Vienna, Austria	
⁵ CPHT, CNRS, Ecole Polytechnique, Institut Polytechnique de Paris, Palaiseau, France	
⁶ B.Verkin Institute for Low Temperature Physics and Engineering of NASU, Kharkiv, Ukraine	

ORAL PRESENTATIONS

Magnetic frustration in insulating Jahn-Teller manganite crystals	..70
L. Gonchar ^{1,2}	
¹ Ural State University of Railway Transport, Yekaterinburg, Russia	
² Ural Federal University named after First President of Russia B.N.Yeltsin, Yekaterinburg, Russia	
Effect of Kink Scattering on their Confinement in Quasi One-Dimensional Magnetically ordered quantum spin systems	..71
S.B. Rutkevich	
Bergische Universität Wuppertal, Wuppertal, Germany	

POSTERS

Magnetocaloric effect in [Ni(fum)(phen)] – the ferromagnetic Dimer with Spin 1	..72
P. Danylchenko ¹ , V. Tkáč ¹ , A. Orendáčová ¹ , E. Čižmár ¹ , A. Uhrinová ^{2,3} , M. Orendáč ¹ , R. Tarasenko ¹	
¹ Institute of Physics, Faculty of Science, P.J. Šafárik University, Košice, Slovak Republic	
² Institute of Chemistry, Faculty of Science, P.J. Šafárik University, Košice, Slovak Republic	
³ Department of Chemistry, Biochemistry, and Biophysics, Institute of Pharmaceutical Chemistry, University of Veterinary Medicine and Pharmacy, Košice, Slovakia	

Low Temperature Thermodynamics of the Finite Spin-1/2 XX Chain Decorated by Some Ising Impurities	..73
O. Dzhenzherov ¹ , E. Ezerskaya ¹	
¹ V.N. Karazin Kharkiv National University, Kharkiv, Ukraine	

The Antiferromagnetic Phase Transition in the Lamellar Cu_{0.15}Fe_{0.85}PS₃ Semiconductor: Experiment and DFT Modeling	..74
V. Pashchenko ¹ , O. Bludov ¹ , D. Baltrunas ² , K. Glukhov ³ , Yu. Vysochanskii ³	
¹ B.Verkin Institute for Low Temperature Physics and Engineering, Kharkiv, Ukraine	
² Department of Nuclear Research Center for Physical Sciences and Technology Savanoriu, Vilnius, Lithuania	
³ Institute for Solid State Physics and Chemistry, Uzhhorod University, Uzhhorod, Ukraine	

Antiferromagnetic spin chains formed in novel TCNQ-based organic magnets	..75
M. Holub ¹ , E. Čižmár ¹ , T.N. Starodub ² , A. Feher ¹ , V.A. Starodub ²	
¹ Institute of Physics, Faculty of Science, P. J. Šafárik University, Košice, Slovakia	
² Institute of Chemistry, Jan Kochanowski University, Kielce, Poland	

On the Spin-Wave Analysis of Narrow Graphene Nanoribbons with Periodically Embedded Impurities	..76
E. Ezerskaya, A. Kabatova, V. Zaytseva	
V.N.Karazin Kharkiv national University, Kharkiv, Ukraine	

Giant fourfold magnetic anisotropy in nanotwinned NiMnGa epitaxial film	..77
J. Kharlan ¹ , P. Bondarenko ¹ , A. Marinchenko ² , V. Golub ¹	
¹ Institute of Magnetism NAS of Ukraine and MES of Ukraine, Kyiv, Ukraine	
² National Aviation University, Aerospace faculty, Kyiv, Ukraine	
Hidden magnetism of superconducting iron chalcogenides	..78
V.D. Fil ¹ , D.V. Fil ^{2,3} , G.A. Zvyagina ¹ , K.R. Zhekova ¹ , I.V. Bilych ¹ , D.A. Chareev ^{4,5,6} , M.P. Kolodiazhnaya ¹ , A.N. Bludov ¹ .	
¹ B.Verkin Institute for Low Temperature Physics and Engineering, Kharkiv, Ukraine	
² Institute for Single Crystals, NAS of Ukraine, 60 Nauky Avenue, Kharkiv, 61072, Ukraine	
³ V.N. Karazin Kharkiv National University, 4 Svobody Square, Kharkiv, 61022, Ukraine	
⁴ Institute of Experimental Mineralogy, RAS, Chernogolovka, 142432, Russia	
⁵ National University of Science and Technology "MISiS", Moscow, 119049, Russia	
⁶ Ural Federal University, Ekaterinburg, 620002, Russia	
Electric and Magnetic Properties of Fe_{7-x}A_xSe₈ Single Crystals	..79
Y.T. Konopelnyk ¹ , M. Pękała ² , I. Radelytskyi ¹ , P. Iwanowski ¹	
¹ Institute of Physics, Polish Academy of Sciences, Warsaw, Poland	
² Chemistry Department, Warsaw University, Warsaw, Poland	
Pressure induced modification of the magnetic properties of triangular antiferromagnet KFe(MoO₄)₂	..80
D. Kamenskii ^{1,2} , K. Kutko ³ , L. Prodan ¹ , T. Sakurai ² , H. Ohta ²	
¹ Experimental Physics V; Center for Electronic Correlations and Magnetism; Institute of Physics; University of Augsburg, Augsburg; Germany	
² Molecular Photoscience Research Center; Kobe University; Kobe; Japan	
³ B.Verkin Institute for Low Temperature Physics and Engineering, Kharkiv, Ukraine	
Temperature Evolution of Magnetooptic Spectra of YIG:Co as a Marker of Changes of Magnetic Anisotropy	..81
E. Kychka ² , O.V. Miloslavskaya ¹ , Yu.M. Kharchenko ¹ , M.F. Kharchenko ¹	
¹ B.Verkin Institute for Low Temperature Physics and Engineering, Kharkiv, Ukraine	
² V.N.Karazin Kharkiv National University, Kharkiv, Ukraine	
The study of lattice dynamics in Cu(en)₂SO₄ - the low-dimensional Heisenberg quantum antiferromagnet with spin ½	..82
O. Vinnik ¹ , L. Lederová ¹ , R. Tarasenko ¹ , L. Kotvyska ¹ , K. Zakut'anská ² , N. Tomašovičová ² , A. Orendáčová ¹	
¹ Institute of Physics, P. J. Šafárik University, Košice, Slovakia	
² Institute of Experimental Physics of SAS, Košice, Slovakia	
SECTION 3. OPTICS, PHOTONICS AND OPTICAL SPECTROSCOPY	
<i>Chair: Dr. Sergii Poperezhai</i>	
PLENARY LECTURES	
GHz-THz Nonlinearities in Semiconductor Superlattices	..38
M.F. Pereira	
Department of Physics, Khalifa University of Science and Technology, Abu Dhabi, UAE	
Goos-Haenchen Effect and Brillouin Light Scattering	..50
I. Lyubchanskii	
O. Galkin Donetsk Institute for Physics and Engineering of NASU, Kyiv, Ukraine	

Features of the exciton self-trapping in molecular aggregates	..43
<u>A.V. Sorokin</u> , I.I. Grankina, I.Yu. Ropakova, S.L. Yefimova	
Institute for Scintillation Materials of NAS of Ukraine, Kharkiv, Ukraine	

Implementation of a simultaneous message-passing protocol using optical vortices	..45
<u>M. Szatkowski</u> ¹ , J. Koechlin ² , J. Masajada ¹ , D. Lopez-Mago ³	
¹ Wrocław University of Science and Technology, Dept. of Optics and Photonics, Wrocław, Poland	
² University of Basel, Department of Physics, Basel, Switzerland	
³ Tecnológico de Monterrey, Escuela de Ingeniería y Ciencias, Monterrey, Mexico	

ORAL PRESENTATIONS

Optical Response of Airplanes with Novel Coatings	..84
<u>L. Illyashenko</u>	
Kharkiv National University of Radio Electronics, Kharkiv, Ukraine	

Simulation of elliptically polarized light propagation in turbid tissue-like scattering media with Monte Carlo method	..85
<u>I.V. Lopushenko</u> ¹ , M. Borovkova ¹ , A. Bykov ¹ , I. Meglinski ^{1,2}	
¹ OPEM, ITEE, University of Oulu, Oulu, Finland	
² College of Engineering and Physical Sciences, Aston University, Birmingham, UK	

Correlation Picture in Dicke Superradiance	..86
<u>S. Lyagushyn</u>	
O. Honchar Dnipro National University, Dnipro, Ukraine	

Transverse Anderson Localization Versus Evanescent Waves Confinement	..87
<u>S.S. Melnyk</u> ¹ , O.V. Usatenko ¹ , V.A. Yampol'skii ^{1,2}	
¹ A.Ya. Usikov Institute for Radiophysics and Electronics of NAS of Ukraine, Kharkiv, Ukraine	
² V.N. Karazin Kharkov National University, Kharkiv, Ukraine	

Spectral properties of thiacarbocyanine J-aggregates depending on formation conditions	..88
<u>P. Pisklova</u> , I. Ropakova, A. Sorokin, S. Yefimova	
Institute for Scintillation Materials of NAS of Ukraine, Kharkiv, Ukraine	

Scattering of Surface Plasmon-Polaritons by a Segment of Metal-Dielectric Boundary with Randomly Fluctuating Impedance	..89
<u>Yu. Tarasov</u> ¹ , O. Stadnyk ^{1,2}	
¹ O. Ya. Usikov Institute for Radiophysics and Electronics of NAS of Ukraine, Kharkiv, Ukraine	
² Kharkiv National University of Radio Electronics, Kharkiv, Ukraine	

Surface Plasmon-Polaritons at Two-Dimensional Resonant Anisotropic Systems	..90
<u>O. Yermakov</u> ^{1,2}	
¹ Department of Computer Physics, V. N. Karazin Kharkiv National University, Kharkiv, Ukraine	
² Department of Physics and Engineering, ITMO University, St. Petersburg, Russia	

Photoelectric properties of heterostructures with GeSn thin films	..91
<u>S. Derenko</u> , S. Kondratenko	
Taras Shevchenko National University of Kyiv, 64 Volodymyrs'ka St. 01601, Kyiv, Ukraine	

POSTERS

Impurity-based emitting centers of different types in doped molecular crystals: formation and spectral multiplicity	..92
<u>M.D. Curmei</u> , V.I. Melnyk, G.V. Klishevich, T.V. Bezrodna, V.V. Nesprava, O.M. Roshchin	
Institute of Physics, NAS of Ukraine, Kyiv, Ukraine	

Absolute cross sections of bremsstrahlung induced by 0.3–1 keV electron scattering by free xenon clusters.	..93
Yu.S. Doronin, A.A. Tkachenko, V.L. Vakula, G.V. Kamarchuk	
B.Verkin Institute for Low Temperature Physics and Engineering of NASU, Kharkiv, Ukraine	
Effect of annealing on optical properties of cadmium sulfide thin films	..94
A. Kashuba ¹ , R. Guminilovych ¹ , H. Ilchuk ¹ , B. Andriyevsky ² , V. Kordan ³ , I. Semkiv ¹ , R. Petrus ¹ , T. Malyi ³	
¹ Lviv Polytechnic National University, Lviv, Ukraine	
² Koszalin University of Technology, Koszalin, Poland	
³ Ivan Franko National University of Lviv, Lviv, Ukraine	
Effect of titanium doping on the structural and optical properties of spinel crystals	..95
V. Gritsyna ¹ , V. Kobyakov ¹ , V. Hryshko ¹ , Yu. Kazarinov ^{1,2}	
¹ V.N. Karazin Kharkiv National University, Kharkiv, Ukraine	
² NSC “Kharkov Institute of Physics and Technology”, Kharkiv, Ukraine	
IR spectrometric studies of recondensates CCL₄ obtained by the method of cryomatrics isolation.	..96
E. Korshikov, D. Sokolov, A. Nurmukan, D. Zhaxybekov	
Al-Farabi Kazakh National University, Institute of Experimental and Theoretical Physics, Almaty, Kazakhstan	
Features of light absorption by a model molecular aggregate	..97
I.Yu. Ropakova ¹ , A.A. Zvyagin ^{2,3}	
¹ Institute for Scintillation Materials of NAS of Ukraine, Kharkiv, Ukraine	
² B.Verkin Institute for Low Temperature Physics and Engineering of NASU, Kharkiv, Ukraine	
³ Max-Planck für Physik komplexer Systeme, Dresden, Germany	
X-ray luminescence spectra of the undoped ZnTe crystal	..98
M. Rudko ¹ , V. Kapustianyk ¹ , V. Mykhailyk ²	
¹ Ivan Franko Lviv National University, Lviv, Ukraine	
² Diamond Light Source, Harwell Campus, Didcot, UK	
Photoluminescence of Ag₈SnSe₆ argyrodite	..99
I. Semkiv ¹ , H. Ilchuk ¹ , M. Pawłowski ² , N. Kashuba ¹	
¹ Lviv Polytechnic National University, Lviv, Ukraine	
² Warsaw University of Technology, Warszawa, Poland	
Single-photon switch controlled by an artificial atom in an engineered electromagnetic environment	..100
E.V. Stolyarov	
Institute of Physics of the National Academy of Sciences of Ukraine, Kyiv, Ukraine	
New opportunities of the optical investigation of distant scattering objects	..101
V.M. Tkachuk	
Yuriy Fedkovych Chernivtsi National University, Chernivtsi, Ukraine	

SECTION 4. QUANTUM LIQUIDS AND QUANTUM CRYSTALS, CRYOCRYSTALS

Chair: Dr. Nataliia Mysko-Krutik

PLENARY LECTURES

Latest Advances in Theory of Logarithmic Fluids: Polycrystalline Metals and Superfluid Stars	..48
K.G. Zloshchastiev	
Institute of Systems Science, Durban University of Technology, Durban, South Africa	

ORAL PRESENTATIONS

Second sound resonances in superfluid ^3He - ^4He mixtures	..103
T.G. Vikhtinskaya, <u>N.O. Herashchenko</u> , K.E. Nemchenko	
V. N. Karazin Kharkiv National University, Kharkiv, Ukraine	
Magnetoelectric Properties of Quantized Vortices and Vortex Rings	..104
<u>A.M. Konstantinov</u> , S.I. Shevchenko	
B. Verkin Institute for Low Temperature Physics and Engineering NASU, Kharkiv, Ukraine	
NMR investigation phases of ^3He adsorbed on MCM-41 one-dimensional nanotubes	..105
<u>N.P. Mikhin</u> , S.S. Sokolov	
B. Verkin Institute for Low Temperature Physics and Engineering NASU, Kharkiv, Ukraine	
Desorption of excited H^* atoms from free clusters Ar/CH_4 and solid Ar doped with CH_4	..106
Yu.S. Doronin, V.L. Vakula, G.V. Kamarchuk, A.A. Tkachenko, I.V. Khyzhniy, S.A. Uyutnov,	
M.A. Bludov, <u>E.V. Savchenko</u>	
B. Verkin Institute for Low Temperature Physics and Engineering NASU, Kharkiv, Ukraine	
Radiolysis of Pyridine-Water-Ices by swift Ions	..107
P. Ada Bibang ¹ , A.N. Agnihotri ^{1,2} , P. Boduch ¹ , A. Domaracka ¹ , Z. Kanuchova ³ , <u>H. Rothard</u> ¹	
¹ Centre de Recherche sur les Ions, les Matériaux et la Photonique, Normandie Univ, Caen, France	
² Indian Institute of Technology Delhi, India	
³ Astronomical Institute of the Slovak Academy of Science, Tatranska Lomnica, Slovak Republic	

POSTERS

Low-temperature features in heat capacity of complex molecular crystals	..108
<u>Yu.V. Horbatenko</u> , O.A. Korolyuk, A.I. Krivchikov, O.O. Romantsova	
B. Verkin Institute for Low Temperature Physics and Engineering NASU, Kharkiv, Ukraine	
Mean squared displacement of molecules in the low-temperature phase of solid Nitrogen	..109
L.A. Alekseeva ¹ , E.S. Syrkin ¹ , <u>D.E. Hurova</u> ¹ , N.A. Aksanova ^{1,2} , N.N. Galtsov ¹	
¹ B. Verkin Institute for Low Temperature Physics and Engineering NASU, Kharkiv, Ukraine	
² Ukrainian State University of Railway Transport, Kharkiv, Ukraine	
Thermal activation heat transfer in dynamically disordered phases of molecular crystals	..110
<u>A.V. Karachevtseva</u> , V.A. Konstantinov, A.I. Krivchikov, V.V. Sagan	
B. Verkin Institute for Low Temperature Physics and Engineering NASU, Kharkiv, Ukraine	
V(T) Phase diagrams of the Fluoroethanes	..111
V.V. Sagan, V.A. Konstantinov, <u>A.V. Karachevtseva</u>	
B. Verkin Institute for Low Temperature Physics and Engineering NASU, Kharkiv, Ukraine	

Radiation-induced non-stationary processes in solid Ar doped with CH₄	..112
I.V. Khyzhniy, E.V. Savchenko, S.A. Uyutnov, M.A. Bludov	
B. Verkin Institute for Low Temperature Physics and Engineering NASU, Kharkiv, Ukraine	
Vibrations Localized on Defects in One-Dimensional Atomic Structures Adsorbed on Bundles of Carbon Nanotubes	..113
E.V. Manzhelii, S.B. Feodosyev	
B. Verkin Institute for Low Temperature Physics and Engineering NASU, Kharkiv, Ukraine	
Based on cluster model analysis of the oreintational order in CO-Ar alloys	..114
N.S. Mysko-Krutik, A.O. Solodovnik	
B. Verkin Institute for Low Temperature Physics and Engineering NASU, Kharkiv, Ukraine	
Nanostructured phases in Ar-Kr condensed mixtures	..115
A.O. Solodovnik, N.S. Mysko-Krutik	
B. Verkin Institute for Low Temperature Physics and Engineering NASU, Kharkiv, Ukraine	
The Structure and Collective Mibrations of Electronic Systems Consisting of Several Chains	..116
V. Syvokon, E. Sokolova, S. Sokolov	
B. Verkin Institute for Low Temperature Physics and Engineering NASU, Kharkiv, Ukraine	
Viscosity measurement of superfluid solutions ³He - ⁴He using a quartz tuning fork	..117
V.A. Vrakina ¹ , S.S. Kapuza ¹ , V.K. Chagovets ^{1,2}	
¹ B. Verkin Institute for Low Temperature Physics and Engineering NASU, Kharkiv, Ukraine	
² V. N. Karazin Kharkiv National University, Kharkiv, Ukraine	

SECTION 5. NANOPHYSICS AND NANOTECHNOLOGIES

Chair: Dr. Maksym Barabashko

PLENARY LECTURES

Optical Horn Effect via Plasmonic Hour-Glass Nano-Aperture	..30
S.S. Choi	
Research Center for Nano-Bio Science, SunMoon University, Ahsan, South Korea	

ORAL PRESENTATIONS

Structural Models for the Diffraction Analysis of Various Carbon Honeycombs	..119
D.G. Diachenko, N.V. Krainyukova	
B.Verkin Institute for Low Temperature Physics and Engineering NASU, Kharkiv, Ukraine	

Research of impact of presence of vitamins B2, B3, and C on calcium oxalate monohydrate crystallization processes in simulated body fluid	..120
M. Dryhailo ¹ , Yu. Taranets ²	
¹ V.N. Karazin Kharkiv National University, Kharkiv, Ukraine	
² Institute for Single Crystals of the National Academy of Sciences of Ukraine, Kharkiv, Ukraine	

Phonon models of thermal conductivity of nanosized structures	..121
T.V. Medintseva, K.E. Nemchenko T.G. Vikhtinskaya	
V.N. Karazin Kharkiv National University, Kharkiv, Ukraine	

Fundamental description of Wannier qubits in semiconductor	..122
K. Pomorski ^{1,2}	
¹ Cracow University of Technology, Faculty of Computer Science and Telecommunications, Krakow, Poland	
² Quantum Hardware Systems, Lodz, Poland	

On the problem of charge transfer and phototransfer in nonregular condensed media	..123
<u>G.D. Tatischvili</u> , T.A. Marsagishvili, M.N. Matchavariani	
Iv. Javakhishvili Tbilisi State University, R. Agladze Institute of Inorganic Chemistry and Electrochemistry, Tbilisi, Georgia	
 A New Method for Real-Time Selective Detection in Complex Gas Mixtures	..124
Using Yanson Point Contacts	
<u>V. Vakula</u> ¹ , A. Pospelov ² , V. Belan ¹ , D. Harbuz ^{1,2} , L. Kamarchuk ³ , Yu. Volkova ³ , G. Kamarchuk ¹	
¹ B.Verkin Institute for Low Temperature Physics and Engineering of NASU, Kharkiv, Ukraine	
² National Technical University “Kharkiv Polytechnic Institute”, Kharkiv, Ukraine	
³ SI “Institute for Children and Adolescents Health Care” of NAMS of Ukraine, Kharkiv, Ukraine	
 Base Pressure Effect on Electrical Properties of Chromium Nanofilms	..125
<u>S.L. Udachan</u> ¹ , N.H. Ayachit ¹ , L.A Udachan ² , S. Siddanna ³ , S.S. Kolkundi ⁴ , S. Ramya ⁵	
¹ Dept of Physics, Rani Channamma University, Belagavi, Karnataka, India	
² S.S. Tegnoor Degree College, Kalaburagi, Karnataka, India	
³ Dept of PG Studies & Research in Physics, Kuvempu University Jnanasahyadri, Shankaraghata, Shimoga, Karnataka, India	
⁴ Government First Grade College, Shahapur, Yadgir, Karnataka, India	
⁵ Shree Sangam Vidya Mandir, Kalaburagi, Karnataka, India	
 POSTERS	
 Influence of the Aharonov-Bohm Effect on the Eigenmodes Spectra of a Semiconductor Nanotube With a Dielectric Filling	..126
<u>Yu. Averkov</u> ^{1,2} , Yu. Prokopenko ^{1,3} , V. Yakovenko ¹	
¹ O.Usikov Institute for Radiophysics and Electronics of NAS of Ukraine, Kharkiv, Ukraine	
² V.Karazin Kharkiv National University, Kharkiv, Ukraine	
³ Kharkiv National University of Radio Electronics, Kharkiv, Ukraine	
 Influence of grinding and oxidation of carbon nanotubes on their heat capacity	..127
<u>M.S. Barabashko</u> ¹ , D. Szewczyk ² , M.I. Bagatskii ¹ , V.V. Sumarokov ¹ , A. Jejowski ² , V.L. Kuznetsov ^{3,4} , S.I. Moseenkov ³ , A.N. Ponomarev ⁶	
¹ B. Verkin Institute for Low Temperature Physics and Engineering, NASU, Kharkiv, Ukraine	
² W. Trzebiatowski Institute of Low Temperature and Structure Research, Wroclaw, Poland	
³ Boreskov Institute of Catalysis, Novosibirsk, Russia	
⁴ National Research Tomsk State University, Tomsk, Russia	
⁵ National Research Tomsk Polytechnic University, Tomsk, Russia	
⁶ Institute of Strength Physics and Materials Science of SB RAS, Tomsk, Russia	
 Preparation of colloidal aqueous solution of C₆₀ fullerene by the sublimation method	..128
<u>R.M. Basnukaeva</u> , A.V. Dolbin, N.A. Vinnikov, A.M. Plohotnichenko, V.B. Esel'son, V.G. Gavrilko, S.V. Cherednychenko	
B.Verkin Institute for Low Temperature Physics and Engineering of NASU, Kharkiv, Ukraine	
 Analysis of energy spectrum of tunable superconducting flux qubit intended for single microwave photon counting	..129
<u>A.P. Boichenko</u> ¹ , O.G. Turutanov ¹ , V.Yu. Lyakhno ¹ , A.A. Soroka ² , V.I. Shnyrkov ³	
¹ B.Verkin Institute for Low Temperature Physics and Engineering of NASU, Kharkiv, Ukraine	
² National Science Center “Kharkiv Institute of Physics and Technology”, Akhiezer Institute for Theoretical Physics, Kharkiv, Ukraine	
³ Kyiv Academic University, Kyiv, Ukraine	
 Graphene-based nanocomposite adhesive compounds	..130
<u>S.V. Cherednychenko</u> , A.V. Dolbin, N.A. Vinnikov, V.B. Esel'son, V.G. Gavrilko, R.M. Basnukaeva, N.V. Isaev, P.A. Zabrodin	
B.Verkin Institute for Low Temperature Physics and Engineering of NASU, Kharkiv, Ukraine	

Study of the mechanism of the cyclic switchover effect for quantum sensing with dendritic Yanson point contacts	..131
<u>A.O. Herus</u> ¹ , A.V. Savytskyi ¹ , A.P. Pospelov ² , Yu.S. Doronin ¹ , V.L. Vakula ¹ , G.V. Kamarchuk ¹	
¹ B. Verkin Institute for Low Temperature Physics & Engineering, Kharkiv, Ukraine	
² National Technical University "Kharkiv Polytechnic Institute", Kharkiv, Ukraine	
Small orthovanadate nanocrystals with controlled redox-activity	..132
<u>K.O. Hubenko</u> , S.L. Yefimova, P.O. Maksimchuk, N.S. Kavok, V.K. Klochkov	
Institute for Scintillation Materials of NAS of Ukraine, Kharkiv, Ukraine	
Electron diffraction diagnostics of N₂-Kr binary cluster beams	..133
<u>O.P. Konotop</u> , O.G. Danylchenko	
B.Verkin Institute for Low Temperature Physics and Engineering of NASU, Kharkiv, Ukraine	
Gold-Fullerene Heterojunctions for Thermoelectricity	..134
V. Kozachenko, V. Shmid, A. Podolian, A. Nadtochiy, <u>O. Korotchenkov</u>	
Taras Shevchenko National University of Kyiv, Kyiv, Ukraine	
Size oscillations of the frequency of surface plasmons in metal nanowires with an elliptical cross section	..135
<u>A. Korotun</u> ¹ , A. Babich ²	
¹ National University "Zaporizhzhia Politechnic", Zaporizhzhya, Ukraine	
² Max Planck Institute for Solid State Research, Stuttgart, Germany	
Softening of the Metastable Bi-43wt.%Sn Eutectic under Repeated Loading in the Region of Microplasticity	..136
V. Korshak	
V. N. Karazin Kharkiv National University, Kharkiv, Ukraine	
Low-temperature magnetoresistance of multiwall carbon nanotubes with perfect structure	..137
<u>T. Len</u> ¹ , I. Ovsienko ¹ , I. Mirzoiev ² , E. Beliayev ² , V. Andrievskii ² , D. Gnida ³ , L. Matzui ¹ , V. Heraskevych ¹	
¹ Taras Shevchenko National University of Kyiv, Department of Physics, Kyiv, Ukraine	
² B.Verkin Institute for Low Temperature Physics and Engineering of NASU, Kharkiv, Ukraine	
³ Institute of Low Temperature and Structure Research, Polish Academy of Sciences, Wroclaw, Poland	
Gate-controlled Electroluminescence in a Molecular Photodiode	..138
<u>V.O. Leonov</u> , E.G. Petrov, Ye.V. Shevchenko	
Bogolyubov Institute for Theoretical Physics of NAS of Ukraine, Kyiv, Ukraine	
High-frequency quantum interferometry for a double-quantum dot	..139
<u>M.P. Liul</u> ¹ , A.I. Ryzhov ¹ , S.N. Shevchenko ^{1,2}	
¹ B.Verkin Institute for Low Temperature Physics and Engineering of NASU, Kharkiv, Ukraine	
² V. N. Karazin Kharkiv National University, Kharkiv, Ukraine	
Effect of defects on polarization switching in CuInP₂S₆ crystals	..140
D. Gal, H. Ban, A. Haysak, <u>A. Molnar</u>	
Department of the Physics of Semiconductors, Uzhhorod National University, Uzhhorod, Ukraine	
Split of surface plasmon resonance in metal nanodisks with a small aspect ratio	..141
<u>N. Pavlishche</u> ¹ , A. Korotun ¹ , V. Kurbatsky ¹ , I. Titov ²	
¹ National University "Zaporizhzhia Politechnic", Zaporizhzhya, Ukraine	
² UAD Systems, Zaporizhzhya, Ukraine	

Electron tunneling through graphene-based double-barrier structure	..142
<u>V. Sakhnyuk</u> , A. Shutovskyi, O. Zamurujeva, S. Fedosov	
Lesya Ukrainka Volyn National University, Lutsk, Ukraine	
New scintillation materials based on perovskite nanocrystals with intensive photoluminescence	..143
<u>T.V. Skrypnyk</u> , I.I. Bespalova, A.V. Sorokin, S.L. Yefimova	
Institute for Scintillation Materials NAS of Ukraine, Kharkiv, Ukraine	

SECTION 6. BIOPHYSICS AND PHYSICS OF MACROMOLECULES

Chair: Dr. Anastasiya Lyogenkaya

PLENARY LECTURES

Optical choppers with disks, with an insight in biomedical applications	..33
V.-F. Duma	
3OM Optomechatronics Group, “Aurel Vlaicu” University of Arad, Arad, Romania	
Doctoral School, Polytechnic University of Timisoara, Timisoara, Romania	

ORAL PRESENTATIONS

Melatonin determination in the human organism by a breath test	..145
<u>D.O. Harbuz</u> ¹ , A.P. Pospelov ² , V.I. Belan ¹ , V.A. Gudimenko ¹ , V.L. Vakula ¹ ,	
L.V. Kamarchuk ³ , Y.V. Volkova ³ , and G.V. Kamarchuk ¹	
¹ B.Verkin Institute for Low Temperature Physics and Engineering of NASU, Kharkiv, Ukraine	
² National Technical University “Kharkiv Polytechnic Institute”, Kharkiv, Ukraine	
³ SI “Institute for Children and Adolescents Health Care” of NAMS of Ukraine, Kharkiv, Ukraine	
The limitations of DFT tight-binding approximation and their role in conformational analysis of DNA constituents	..146
<u>O.S. Husak</u> , T.Yu. Nikolaienko	
Faculty of Physics of Taras Shevchenko National University of Kyiv, Kyiv, Ukraine	

Permittivity characterization of aqueous solutions of biological active substances	..147
<u>K.S. Kuznetsova</u> ¹ , V.A. Pashynska ^{1,2} , Z.E. Eremenko ¹ , O.I. Shubniy ¹ , A.V. Martunov ³	
¹ O. Usikov Institute for Radiophysics and Electronics of NASU, Kharkiv, Ukraine	
² B. Verkin Institute for Low Temperature Physics and Engineering of NASU, Kharkiv, Ukraine	
³ Mechnikov Institute of Microbiology and Immunology National Academy of Medical Sciences of Ukraine, Kharkiv, Ukraine	

Detection of carbon monoxide in exhaled air	..148
<u>D. Velyhotskyi</u> , A. Mysiura	
Institute of Applied Problems of Physics & Biophysics, NAS of Ukraine, Kyiv, Ukraine	

POSTERS

Thermodynamic model to dielectric parameters of erythrocytes: effect of temperature	..149
<u>L.V. Batyuk</u> ¹ , N.N. Kizilova ²	
¹ Kharkiv National Medical University, Kharkiv, Ukraine	
² Warsaw University of Technology, Warsaw, Poland	
Binding of proflavin to poly(ethylene glycol): investigation by spectroscopic methods	..150
<u>Iu. Blyzniuk</u> , E. Dukhopelnykov, E. Bereznyak, N. Gladkovskaya	
O. Ya. Usikov Institute for Radiophysics and Electronics of NASU, Kharkiv, Ukraine	

Assessment of the degree of BSA denaturation in solutions with AlCl₃ and FeCl₃ by the parameters of film textures	..151
D. Glibitskiy¹, O. Gorobchenko², O. Nikolov², T. Cheipesh³, T. Dzhimieva^{3,4}, I. Zaitseva^{5,6}, A. Zibarov⁶, A. Roshal⁶, M. Semenov¹, G. Glibitskiy¹	
¹ Dept. of biological physics, Institute for Radiophysics and Electronics NASU, Kharkiv, Ukraine	
² Dept of molecular and medical biophysics, School of radiophysics, biomedical electronics and computer systems, V.N. Karazin Kharkiv National University, Kharkiv, Ukraine	
³ Chemical faculty, V.N. Karazin Kharkiv National University, Kharkiv, Ukraine	
⁴ V.N. Karazin Kharkiv National University, Kharkiv, Ukraine	
⁵ O.M. Beketov National University of Urban Economy, Kharkiv, Ukraine	
⁶ Institute for Chemistry, V.N. Karazin Kharkiv National University, Kharkiv, Ukraine	
Protein Condensation in Solution in the Presence of Vitamin B₁	..152
T.O. Hushcha, M.S. Mykula, A.I. Vovk, V.P. Kukhar	
V.P.Kukhar Institute of Bioorganic Chemistry and Petrochemistry of NASU, Kyiv, Ukraine	
Protein phase behavior in solutions with sodium chloride	..153
T.O. Hushcha, A.I. Vovk	
V.P.Kukhar Institute of Bioorganic Chemistry and Petrochemistry of NASU, Kyiv, Ukraine	
Peculiarities of interaction of short double-stranded polynucleotide poly(A:U) with graphene: molecular dynamics simulation	..154
M.V. Karachevtsev	
B.Verkin Institute for Low Temperature Physics and Engineering of NASU, Kharkiv, Ukraine	
Interaction of organic cations with graphene oxide	..155
M.V. Kosevich, O.A. Boryak, A.M. Plokhotnichenko, V.S. Shekovsky, V.G. Zobnina, V.V. Orlov, V.A. Karachevtsev	
B.Verkin Institute for Low Temperature Physics and Engineering of NASU, Kharkiv, Ukraine	
Interaction of mixture of amino acids with graphene oxide probed by mass spectrometry	..156
M.V. Kosevich, O.A. Boryak, V.V. Orlov	
B.Verkin Institute for Low Temperature Physics and Engineering of NASU, Kharkiv, Ukraine	
The charge ordering of the heavy doped organic crystals	..157
E.S. Syrkin¹, V.A. Lykah², E.N. Trotskii³	
¹ B.Verkin Institute for Low Temperature Physics and Engineering of NASU, Kharkiv, Ukraine	
² National Technical University 'Kharkiv Polytechnic Institute', Kharkiv, Ukraine	
³ V.N. Karazin Kharkiv National University, Kharkiv, Ukraine	
Molecular dynamics simulation of eosin Y and methylene blue aggregates in a water-ion environment	..158
K.V. Miroshnychenko¹, A.V. Shestopalova^{1,2}	
¹ O.Ya. Usikov Institute for Radiophysics and Electronics of NAS of Ukraine, Kharkiv, Ukraine	
² V.N. Karazin Kharkiv National University, Kharkiv, Ukraine	
PVA nanofibers containing Ag nanoparticles formed by ultrasonication	..159
V.A. Karachevtsev, A.M. Plokhotnichenko	
B.Verkin Institute for Low Temperature Physics and Engineering of NASU, Kharkiv, Ukraine	
Förster resonance energy transfer in insulin amyloid fibrils doped by Thioflavin T and novel cyanine dyes	..160
M. Shchuka¹, O. Zhytniakivska¹, A. Kurutos², U. Tarabara¹, K. Vus¹, V. Trusova¹, G. Gorbenko¹	
¹ V.N. Karazin Kharkiv National University, Kharkiv, Ukraine	
² Institute of Organic Chemistry with Centre of Phytochemistry, Bulgarian Academy of Sciences, Sofia, Bulgaria	

SECTION 7. MATERIALS SCIENCE

Chair: Dr. Yevhen Petrenko

PLENARY LECTURES

Peculiarities of dipolar ordering in mixed cation halide perovskites ..29

J. Banys¹, S. Balciunas¹, M. Simenas¹, S. Svirskas¹, M. Kinka¹, V. Samulionis¹, R. Grigalaitis¹, A. Garbaras², A. Gagor³, M. Maczka³, A. Sieradzki³

¹Faculty of Physics, Vilnius University, Vilnius, Lithuania

²Mass Spectrometry Laboratory, Center for Physical Sciences and Technology, Vilnius, Lithuania.

³Institute of Low Temperature and Structure Research, Polish Academy of Sciences, Wroclaw, Poland

High-pressure stabilized oxide perovskite structures ..39

A.N. Salak¹, D.D. Khalyavin², E.L. Fertman³, D. Delmonte⁴, E. Gilioli⁴

¹Department of Materials and Ceramics Engineering, CICECO – Aveiro Institute of Materials, University of Aveiro, Aveiro, Portugal

²ISIS Facility, Rutherford Appleton Laboratory, Chilton, Didcot, UK

³B.Verkin Institute for Low Temperature Physics and Engineering of NASU, Kharkiv, Ukraine

⁴Institute of Materials for Electronics and Magnetism, Parma, Italy

Study of the magnetoelectric effect in multiferroic ferrite-perovskite composite ceramics ..42

V.V. Shvartsman

Institute for Materials Science, University of Duisburg-Essen, Essen, Germany

ORAL PRESENTATIONS

Hydrogen storage properties, structural analysis, elastic and electronic properties of K_2PdH_4 ..162

S. Al¹, C. Kurkcu²

¹Department of Environmental Protection Technologies, Vocational School, Izmir Democracy University, Izmir, Turkey

²Department of Electronics and Automation, Kirsehir Ahi Evran University, Kırşehir, Turkey

Phase transitions, elastic and electronic properties of hydrogen storage Na_2PdH_4 ..163

S. Al¹, C. Kurkcu²

¹Department of Environmental Protection Technologies, Vocational School, Izmir Democracy University, Izmir, Turkey

²Department of Electronics and Automation, Kirsehir Ahi Evran University, Kırşehir, Turkey

Lattice softening at the electric field and pressure-induced Mott insulator to metal transitions ..164

D. Babich, L. Cario, B. Corraze, C. Adda, J. Tranchant, M.- P. Besland, J.-Y. Mévellec,

P. Bertoncini, B. Humbert, E. Janod

Institut des Matériaux Jean Rouxel, Université de Nantes – CNRS, Nantes, France

Hemispherical microwave X-band Fabry-Perot resonator for determining in wide band of dielectric parameters of solid materials ..165

A. Breslavets¹, Z. Eremenko¹, O. Voitovich¹, G. Rudnev¹, Zhu Gang², Li Rong²

¹O.Ya. Usikov Institute for Radiophysics and Electronics of NAS of Ukraine, Kharkiv, Ukraine

²Anhui Huadong Photoelectric Technology Institute, Ltd Wuhu, China

Synchrotron diffraction study of the high-pressure behaviour of the multiferroic BiFe_{0.5}Sc_{0.5}O₃ perovskite	..166
J.P. Cardoso ¹ , D.D. Khalyavin ² , D. Delmonte ³ , E. Gilioli ³ , A. Barbier ⁴ , M.R. Soares ¹ , J.M. Vieira ¹ , A.N. Salak ¹	
¹ Department of Materials and Ceramics Engineering and CICECO - Aveiro Institute of Materials, Aveiro, Portugal	
² ISIS Facility, Rutherford Appleton Laboratory, Chilton, Didcot, UK	
³ Institute of Materials for Electronics and Magnetism, Parma, Italy	
⁴ SPEC, CEA, CNRS, Université Paris-Saclay, CEA-Saclay, Gif-sur-Yvette Cedex, France	
Nanostructures on the (001) surface of strontium titanate	..167
V.O. Hamalii, N.V. Krainyukova	
B.Verkin Institute for Low Temperature Physics and Engineering of NASU, Kharkiv, Ukraine	
Optical response of novel structures to detect approaching vehicles	..168
L. Illyashenko	
Kharkiv National University of Radio Electronics, 14 Nauky Ave., Kharkiv, Ukraine	
Influence of aluminum ion substitution on EPR spectra of lithium ferrites	..169
L. Kaykan ¹ , J. Mazurenko ² , N.V. Ostapovych ² , I.R. Pavliuk ²	
¹ G.V. Kurdyumov Institute for Metal Physics, NAS. of Ukraine, Kyiv, Ukraine	
² Ivano-Frankivsk National Medical University, Ivano-Frankivsk, Ukraine	
Stability of Y₂Ti₂O₇ in ODS steels under swift heavy ions irradiation	..170
E.A. Korneeva ¹ , A. Ibrayeva ² , J. O'Connell ³ , A.S. Sohatsky ¹ , V.A. Skuratov ¹	
¹ Joint Institute for Nuclear Research, Dubna, Russia	
² Nur-Sultan Branch of Institute of Nuclear Physics, Nur-Sultan, Kazakhstan	
³ Centre for HRTEM, Nelson Mandela University, University Way, Summerstrand, Port Elizabeth, South Africa	
CH₄ trapping ability of double vacancy graphene Cu-embedded surface: A DFT study	..171
H. Küçük	
Gazi University, Department of Physics, Emniyet Mahallesi, Teknikokullar, Ankara, Turkey	
Influence of extreme factors (low temperatures, corpuscular and electromagnetic radiation) on the mechanical properties of polyimide Kapton H films of different thicknesses	..172
V.A. Lototskaya ¹ , L.F. Yakovenko ¹ , E.N. Aleksenko ¹ , N.I. Velichko ¹ , G.I. Saltevskiy ¹ , I.P. Zaritskiy ¹ , Yu.S. Doronin ¹ , A.A. Tkachenko ¹ , V.V. Abraimov ² , W.Z. Shao ²	
¹ B.Verkin Institute for Low Temperature Physics and Engineering of NASU, Kharkiv, Ukraine	
² Harbin Institute of Technology, Harbin, the People's Republic of China	
Comparative study of Tl-1223 superconductors prepared by the sol-gel route and solid-state reaction	..173
I.R. Metskhvarishvili ^{1,2} , T.E. Lobzhanidze ³ , G.N. Dgebuadze ¹ , B.G. Bendelian ¹ , M.R. Metskhvarishvili ² , M.Sh. Rusia ³ , G.R. Giorganashvili ¹ , V.M. Gabunia ^{1,4}	
¹ Ilia Vekua Sukhumi Institute of Physics and Technology, Laboratory of Cryogenic Technique and Technologies, Tbilisi, Georgia	
² Georgian Technical University, Faculty of Informatics and Control Systems, Department of Microprocessor and Measurement Systems, Tbilisi, Georgia	
³ Ivane Javakhishvili Tbilisi State University, Faculty of Exact and Natural Sciences, Department of Chemistry, Tbilisi, Georgia	
⁴ Petre Melikishvili Institute of Physical and Organic Chemistry of the Iv. Javakhishvili Tbilisi State University, Tbilisi, Georgia	

- Use of Cr³⁺ and Mn²⁺ ions in study of the structure and radiation defects in Mg-Al spinel ..174**
N. Mironova-Ulmane¹, M. Brik², A.I. Popov, G. Krieke, A. Antuzevics, V. Skvortsova, E. Elsts,
A. Sarakovskis
¹Institute of Solid State Physics, University of Latvia, Kengaraga Street 8, LV-1063 Riga, Latvia
²Institute of Physics, University of Tartu, Tartu, Estonia

- The obtaining of Zn_xMg_{1-x}WO₄ nanopowders for composite scintillators ..175**
V. Tinkova, I. Tupitsyna, A. Yakubovskaya, P. Maksimchuk
Institute for scintillations materials of NAS of Ukraine, Kharkiv, Ukraine

- 2-D multifunctional nanostructures of layered double hydroxides assembled in magnetic field ..176**
D.E.L. Vieira¹, E.L. Fertman², A.V. Fedorchenko², R.Yu. Babkin³, Y.G. Pashkevich³, C.M.A. Brett⁴,
J.M. Vieira¹, A.N. Salak¹
¹Department of Materials and Ceramic Engineering, CICECO – Aveiro Institute of Materials,
University of Aveiro, Aveiro, Portugal
²B. Verkin Institute for Low Temperature Physics and Engineering of NASU, Kharkiv, Ukraine
³O.Galkin Donetsk Institute for Physics and Engineering, NASU, Kyiv, Ukraine
⁴Department of Chemistry, CEMMPRE, Faculty of Sciences and Technology, University of
Coimbra, Coimbra, Portugal

- Low thermal conductivity and the evidence of the glassy behavior in (Pb_{0.7}Sn_{0.25}Ge_{0.05})₂P₂S₆ ..177**
and (Pb_{0.7}Sn_{0.25}Ge_{0.05})₂P₂Se₆ mixed crystals
I. Zamaraitė¹, V. Liubachko^{2,3}, R. Yevych², A. Oleaga³, A. Salazar³, A. Dziaugys¹, J. Banys¹,
Yu. Vysochanskii²
¹Faculty of Physics, Vilnius University, Vilnius, Lithuania
²Institute for Solid State Physics and Chemistry, Uzhhorod University, Uzhhorod, Ukraine
³Departamento de Fisica Aplicada I, Escuela de Ingenieria de Bilbao, Universidad del Pais Vasco
UPV/EHU, Bilbao, Spain

- Cryogenic scintillator based on Li₂MoO₄ single crystal ..178**
A.G. Yakubovskaya¹, I.A. Tupitsyna¹, A.M. Dubovik¹, Yu.A. Hizhnyi²
¹Institute for Scintillation Materials NAS of Ukraine, Kharkiv, Ukraine
²Taras Shevchenko National University of Kyiv, Kyiv, Ukraine

POSTERS

- Catalytic reductive amination of furfural with morpholine at presence of Cu-containing ..179**
composites
V.M. Asaula
L.V.Pisarzhevskii Institute of Physical Chemistry of NASU, Kyiv, Ukraine

- The first principle study of substitutional impurities effect on elastic properties of TlInS₂ ..180**
layered crystal
T. Babuka¹, O.O. Gomonnai², K.E. Glukhov¹, L.Yu. Kharkhalis¹, A.V. Gomonnai³, M. Makowska-Janusik⁴
¹Institute for Physics and Chemistry of Solid State, Uzhhorod National Univ., Uzhhorod, Ukraine
²Uzhhorod National University, Uzhhorod, Ukraine
³Institute of Electron Physics NASU, Uzhhorod, Ukraine
⁴Institute of Physics, Faculty of Mathematics and Natural Science, Jan Dlugosz University in
Czestochowa, Czestochowa, Poland

- Electron microscope study with in situ video recording of crystal growth in amorphous films ..181**
A.G. Bagmut, I.A. Bagmut
National Technical University “Kharkiv Polytechnic Institute”, Kharkiv, Ukraine

Effect of Yb-doping on structural and optical properties of CdTe thin films, their defect structure and type of conductivity	..182
Yu.P. Gnatenko ¹ , P.M. Bukivskij ¹ , R.V. Gamernyk ² , <u>A.P. Bukivskii</u> ¹ , M.S. Furyer ¹ , .M. Kolesnyk ³ , D.I. Kurbatov ³ , A.S. Opanasyuk ³	
¹ Institute of Physics of NAS of Ukraine, Kyiv, Ukraine	
² Lviv National University, Lviv, Ukraine	
³ Sumy State University, Sumy, Ukraine	
Study of the polymer - carbon composites electronic structure by positron spectroscopy	..183
Ye.A. Tsapko, Ye.G. Len, <u>I.Ye. Galstian</u>	
G. V. Kurdyumov Institute for Metal Physics of NASU, Kyiv, Ukraine	
Scattering by molecules of the Kapton H polymer. Amorphous films	..184
D.E. Hurova ¹ , V.G. Geidarov ¹ , N.A. Aksanova ^{1,2} , N.N. Galtsov ¹	
¹ B.Verkin Institute for Low Temperature Physics and Engineering of NASU, Kharkiv, Ukraine	
² Ukrainian State University of Railway Transport, Kharkiv, Ukraine	
Effect of annealing temperature on the elementary composition of CZTSe thin films obtained by 3D printing	..185
S. Kakherskyi, R. Pshenychnyi, O. Dobrozhany, A. Opanasyuk	
Sumy State University, Sumy, Ukraine	
Magnetic composite materials based on chitosan: low temperature synthesis, characterization and application	..186
O. Kalinkevich ¹ , Y. Zinchenko ¹ , V. Bilyk ¹ , A. Kalinkevich ¹ , A. Sklyar ² , S. Danilchenko ¹	
¹ Institute of applied physics of NAS of Ukraine, Sumy, Ukraine	
² A.S. Makarenko Sumy State Pedagogical University, Sumy, Ukraine	
Topology of chemical bonds and electron band structure of In₆Se₇ monoclinic crystal doped by Sn atoms	..187
<u>L.Yu. Kharkhalis</u> , K.E. Glukhov, T.Ya. Babuka, M.V. Liakh	
Institute for Physics and Chemistry of Solid State, Uzhhorod National Univ., Uzhhorod, Ukraine	
Deviation from the Hall-Petch relationship for Cu-Mo vacuum condensates	..188
E. Lutsenko ¹ , A. Zybkov ² , M. Zhadko ²	
¹ National Science Center “Kharkiv Institute of Physics and Technology”, Kharkiv, Ukraine	
² National Technical University “Kharkiv Polytechnic Institute”, Kharkiv, Ukraine	
The formation of ZrO₂-Y₂O₃-nanoparticles from fluoride solutions	..189
E.S. Gevorkyan ¹ , <u>O.M. Morozova</u> ¹ , D.S. Sofronov ² , V.P. Nerubatskyi ¹ , N.S. Ponomarenko ³	
¹ Ukrainian State University of Railway Transport, Kharkiv, Ukraine	
² SSI “Institute for Single Crystals” NAS of Ukraine, Kharkiv, Ukraine	
³ Kharkiv National Medical University, Kharkiv, Ukraine	
Estimation of iron concentration in silicon solar cell by kinetics of light-induced change in short-circuit current	..190
<u>O. Olikh</u> ¹ , V. Kostylyov ² , V. Vlasiuk ² , R. Korkishko ²	
¹ Taras Shevchenko National University of Kyiv, Kyiv, Ukraine	
² V. Lashkaryov Institute of Semiconductor Physic Institute of NAS of Ukraine, Kyiv, Ukraine	
Influence of the structure formed by condensation on thermal stability of Cu-Mo pseudoalloys	..191
<u>V. Riaboshtan</u> , A. Zubkov, V. Kucherskyi, M. Zhadko	
National Technical University «Kharkiv Polytechnic Institute», Kharkiv, Ukraine	

The effect of carbon on the microhardness of $\text{Co}_{0.25-x}\text{Cr}_{0.25}\text{Fe}_{0.25}\text{Ni}_{0.25}\text{C}_x$ alloy	..192
<u>H.V. Rusakova</u> ¹ , L.S. Fomenko ¹ , Y. Huang ^{2,3} , E.D. Tabachnikova ¹ , I.V. Kolodiy ⁴ , A.V. Levenets ⁴ , M.A. Tikhonovsky ⁴ , T.G. Langdon ³	
¹ B.Verkin Institute for Low Temperature Physics and Engineering of NASU, Kharkiv, Ukraine	
² Department of Design and Engineering, Faculty of Science and Technology, Bournemouth University, Poole, Dorset, UK	
³ Department of Mechanical Engineering, University of Southampton, Southampton, UK	
⁴ NSC "Kharkov Institute of Physics and Technology" of NASU, Kharkiv, Ukraine	
Forced elasticity of amorphous polymers	..193
<u>V.D. Natsik</u> , <u>H.V. Rusakova</u>	
B.Verkin Institute for Low Temperature Physics and Engineering of NASU, Kharkiv, Ukraine	
Microhardness of ultrafine-grained oxygen-free copper produced by hydrostatic extrusion	..194
<u>H.V. Rusakova</u> , S.V. Lubenets, L.S. Fomenko	
B.Verkin Institute for Low Temperature Physics and Engineering of NASU, Kharkiv, Ukraine	
The effect of temperature on micromechanical properties of graphene oxide/polypropylene nanocomposite	..195
<u>H.V. Rusakova</u> ¹ , L.S. Fomenko ¹ , S.V. Lubenets ¹ , A.V. Dolbin ¹ , N.A. Vinnikov ¹ , R.M. Basnukaeva ¹ , M.V. Khlistyuck ¹ , A.V. Blyznyuk ²	
¹ B.Verkin Institute for Low Temperature Physics and Engineering of NASU, Kharkiv, Ukraine	
² National Technical University "Kharkiv Polytechnic Institute", Kharkiv, Ukraine	
The effect of casting conditions on superplastic properties of the eutectic alloy Sn-38wt%Pb	..196
<u>Yu.O. Shapovalov</u> ¹ , V.F. Korshak ²	
¹ B.Verkin Institute for Low Temperature Physics and Engineering of NASU, Kharkiv, Ukraine	
² V. N. Karazin Kharkiv National University, Kharkiv, Ukraine	
Some peculiarities of structural changes of the eutectic alloy Bi-43wt%Sn under conditions of superplasticity	..197
Yu.O. Shapovalov	
B.Verkin Institute for Low Temperature Physics and Engineering of NASU, Kharkiv, Ukraine	
Low-temperature physical and mechanical properties of high-entropy alloy $\text{Fe}_{50}\text{Mn}_{30}\text{Co}_{10}\text{Cr}_{10}$..198
T.V. Hryhorova ¹ , S.E. Shumilin ¹ , Yu.O. Shapovalov ¹ , Yu.O. Semerenko ¹ , S.N. Smirnov ¹ , <u>O.D. Tabachnikova</u> ¹ , M.A. Tikhonovsky ³ , A.V. Levenets ³ , M.I. Zehetbauer ² , E. Schafler ²	
¹ B.Verkin Institute for Low Temperature Physics and Engineering of NASU, Kharkiv, Ukraine	
² University of Vienna, Nanocrystalline Materials Department, Wien, Austria	
³ National Science Center Kharkov Institute of Physics and Technology, Kharkiv, Ukraine	
Thermoactivated amplitude-dependent dislocation internal friction in deformed samples of pure magnesium	..199
P.P. Pal-Val ¹ , <u>O.M. Vatazhuk</u> ¹ , A.A. Ostapovets ² , L. Král ² , J. Pinc ³	
¹ B.Verkin Institute for Low Temperature Physics and Engineering of NASU, Kharkiv, Ukraine	
² Institute of Physics of Materials, Czech Academy of Sciences, Brno, Czech Republic	
³ Institute of Physics, Czech Academy of Sciences, Prague, Czech Republic	

SECTION 8. THEORY OF CONDENSED MATTER PHYSICS

Chair: Dr. Olga Ilinskaya

PLENARY LECTURES

Theoretical prediction and subsequent observation of the dynamical Casimir effect in a superconducting circuit	..37
F. Nori	
RIKEN, Saitama, Japan; and the University of Michigan, Ann Arbor, USA	
Dynamical Casimir Effect in Optomechanical systems: Fully Quantum and Non-Perturbative Description	..40
S. Savasta	
Dipartimento MIFT, Università degli Studi di Messina, Messina, Italy	
Thermodynamic properties of coexisting phases of carbon tetrachloride on sublimation and melting lines	..46
L.N. Yakub, O.S. Bodiuł	
Thermophysics Dept., Odessa National Academy of Food Technologies, Odessa, Ukraine	
Nonlinear exciton drift in piezoelectric two-dimensional materials	..41
V. Shahnazaryan ¹ , H. Rostami ²	
¹ Department of Physics, ITMO University, St. Petersburg, Russia	
² Nordita, KTH Royal Institute of Technology and Stockholm University, Stockholm, Sweden	

ORAL PRESENTATIONS

Schrödinger-cat states generation via mechanical vibrations entangled with a charge qubit	..201
O.M. Bahrova ¹ , L.Y. Gorelik ² , S.I. Kulinich ¹	
¹ B. Verkin Institute for Low Temperature Physics and Engineering NASU, Kharkiv, Ukraine	
² Department of Physics, Chalmers University of Technology, Göteborg, Sweden	
Depending on the angle of the functionalization of twisted graphene	..202
A.A. Belosludtseva, Y.A. Chymakov, N.G. Bobenko	
Institute of Strength Physics and Materials Science of Siberian Branch of Russian Academy of Sciences (ISPMS SB RAS), Tomsk, Russia	
Resonant modes in cavity layered microwave resonator with axial symmetry	..203
Z.E. Eremenko, I.N. Volovichev, A.A. Breslavets	
O.Ya. Usikov Institute for Radiophysics and Electronics NASU, Kharkiv, Ukraine	
Nonlinear thermoelectric properties of a magnetic single-electron shuttle	..204
O.A. Ilinskaya ¹ , I.V. Krive ¹ , R.I. Shekhter ²	
¹ B. Verkin Institute for Low Temperature Physics and Engineering NASU, Kharkiv, Ukraine	
² Department of Physics, University of Gothenburg, Göteborg, Sweden	
Strong drag force fluctuations in disordered ensembles of scatterers and effects of nonlinear dynamical screening	..205
O.V. Kliushnichenko, S.P. Lukyanets	
Institute of Physics NASU, Kyiv, Ukraine	
Studying the magnetic peculiarities of the frustrated spin chain using the effective model without frustration	..206
O.O. Kryvchikov	
B. Verkin Institute for Low Temperature Physics and Engineering NASU, Kharkiv, Ukraine	

Thermal Coulomb drag between quantum wires hosting 1D Wigner crystals	..207
<u>M.V. Mazanov</u> ¹ , S.S. Apostolov ^{1,2}	
¹ V.N. Karazin Kharkov National University, Kharkov, Ukraine	
² A.Ya. Usikov Institute for Radiophysics and Electronics NASU, Kharkov, Ukraine	
Propagation and intensity-dependent focusing of THz laser radiation in layered superconductors	..208
<u>H.V. Ovcharenko</u> ¹ , Z.A. Maizelis ^{1,2} , S.S. Apostolov ^{1,2}	
¹ V.N. Karazin Kharkov National University, Kharkiv, Ukraine	
² O.Ya. Usikov Institute for Radiophysics and Electronics NASU, Kharkiv, Ukraine	
Ideal Bose gas in steep traps	..209
<u>A. Rovenchak</u> , Yu. Krynytskyi	
Department for Theoretical Physics, Ivan Franko National University of Lviv, Lviv, Ukraine	
Landau-Zener-Stückelberg-Majorana quantum logic gates	..210
<u>A. I. Ryzhov</u> ¹ , O. V. Ivakhnenko ¹ , S. N. Shevchenko ^{1,2} , Franco Nori ^{3,4}	
¹ B. Verkin Institute for Low Temperature Physics and Engineering NASU, Kharkiv, Ukraine	
² V.N. Karazin Kharkiv National University, Kharkiv, Ukraine	
³ Theoretical Quantum Physics Laboratory, RIKEN Cluster for Pioneering Research, Wakoshi, Saitama, Japan	
⁴ Physics Department, University of Michigan, USA	
Thermoelectric and vibronic effects in tunneling of spin-polarized electrons in a molecular transistor	..211
A.D. Shkop	
B. Verkin Institute for Low Temperature Physics and Engineering NASU, Kharkiv, Ukraine	
Approximately isospectral isomers for antiferromagnetic Heisenberg model	..212
V.V. Tokarev	
V.N. Karazin Kharkiv National University, School of Chemistry, Kharkiv, Ukraine	
Low-temperature phases of SU(4)-symmetric fermionic mixtures in optical lattices	..213
<u>V.I. Unukovych</u> ¹ , A.G. Sotnikov ^{1,2}	
¹ V.N. Karazin Kharkiv National University, Kharkiv, Ukraine	
² Akhiezer Institute for Theoretical Physics, NSC «Kharkov Institute of Physics and Technology», Kharkiv, Ukraine	
POSTERS	
Bose-Einstein condensation of ideal gas in the external harmonic potential	..214
<u>E.O. Bilokon</u> ¹ , A.S. Peletminskii ^{1,2}	
¹ V.N. Karazin Kharkiv National University, Kharkiv, Ukraine	
² Akhiezer Institute for Theoretical Physics, National Science Center «Kharkov Institute of Physics and Technology», Kharkiv, Ukraine	
Thermodynamics of quantum Fermi gases in magneto-optical traps	..215
<u>V.O. Bilokon</u> ¹ , A.G. Sotnikov ^{1,2}	
¹ V.N. Karazin Kharkiv National University, Kharkiv, Ukraine	
² Akhiezer Institute for Theoretical Physics, National Science Center «Kharkov Institute of Physics and Technology», Kharkiv, Ukraine	
Magnetic phases and phase diagram of spin-1 condensate with quadrupole degrees of freedom	..216
<u>M. Bulakhov</u> ^{1,2} , A.S. Peletminskii ^{1,2} , S.V. Peletminskii ¹ , and Yu.V. Slyusarenko ^{1,2}	
¹ Akhiezer Institute for Theoretical Physics, National Science Center «Kharkov Institute of Physics and Technology», Kharkiv, Ukraine	
² V.N. Karazin Kharkiv National University, Kharkiv, Ukraine	

Breather birth and wave radiation in the sine-Gordon systems with oscillating kinks	..217
<u>O.V. Charkina</u> ¹ , M.M. Bogdan ^{1,2}	
¹ B. Verkin Institute for Low Temperature Physics and Engineering NASU, Kharkiv, Ukraine	
² V.N. Karazin Kharkiv National University, Kharkiv, Ukraine	
Raman scattering and theoretical investigations of CuInP₂S₆ layered ferrielectric crystal	..218
<u>K. Glukhov</u> , R. Yevych, A. Kohutych, K. Medulych, V. Hryts, Yu. Shiposh, M. Kundria, Yu. Vysochanskii	
Institute for Solid State Physics and Chemistry, Uzhhorod University, Uzhhorod, Ukraine	
Driven quantum systems: Majorana's approach	..219
<u>P.O. Kofman</u> ¹ , O.V. Ivakhnenko ² , S.N. Shevchenko ^{1,2}	
¹ V.N. Karazin Kharkiv National University, Kharkov, Ukraine	
² B. Verkin Institute for Low Temperature Physics and Engineering NASU, Kharkov, Ukraine	
Simultaneous effect of short-range atomic and magnetic orderings on magnetic phase diagrams of substitution binary alloys	..220
<u>E.G. Len</u> ^{1,2} , T.D. Shatnii ¹ , V.V. Lizunov ¹ , M.V. Ushakov ¹ , T.S. Len ³	
¹ G.V. Kurdyumov Institute for Metal Physics NASU, Kyiv, Ukraine	
² Kyiv Academic University, NAS and MES of Ukraine, Kyiv, Ukraine	
³ National Aviation University, Kyiv, Ukraine	
Theoretical cross-sections of the ionization of the K atom by electron impact	..221
V. Roman	
Institute of Electron Physics NASU, Uzhhorod, Ukraine	
Exploration of the phase diagram of (Pb_ySn_{1-y})₂P₂(Se_xS_{1-x})₆ ferroelectrics within the framework of a combined BEG – ANNNI model	..222
<u>V. Liubachko</u> ¹ , A. Oleaga ² , A. Salazar ² , R. Yevych ¹ , A. Kohutych ¹ , <u>Yu. Vysochanskii</u> ¹	
¹ Institute for Solid State Physics and Chemistry, Uzhhorod University, Uzhhorod, Ukraine	
² Departamento de Fisica Aplicada I, Escuela de Ingenieria de Bilbao, Universidad del Pais Vasco, Bilbao, Spain	

SECTION 9. TECHNOLOGIES AND INSTRUMENTATION FOR PHYSICAL EXPERIMENTS

Chair: Anna Herus

PLENARY LECTURES

Strain modulated ferromagnetic resonance technique as a powerful tool for investigating of thin films magnetoelastic properties	..31
<u>O.M. Chumak</u> ¹ , A. Nabiałek ¹ , V.V. Chabanenko ² , T. Seki ^{3,4} , K. Takanashi ^{3,4,5} , L.T. Baczebski ¹ , H. Szymczak ¹	
¹ Institute of Physics, Polish Academy of Sciences, Warsaw, Poland	
² O.Galkin Donetsk Institute for Physics and Engineering NASU, Kyiv, Ukraine	
³ Institute for Materials Research, Tohoku University, Sendai, Japan	
⁴ Center for Spintronics Research Network, Tohoku University, Sendai, Japan	
⁵ Center for Science and Innovation in Spintronics, Core Research Cluster, Tohoku University, Sendai, Japan	

ORAL PRESENTATIONS

Development of universal experimental cell for Yanson point-contact spectroscopy and sensor research ..224

P.O. Dmitriyev¹, A.V. Savytskyi¹, A.P. Pospelov², E. Faulques³, G.V. Kamarchuk¹

¹B. Verkin Institute for Low Temperature Physics & Engineering, Kharkiv, Ukraine

²National Technical University “Kharkiv Polytechnic Institute”, Kharkiv, Ukraine

³MIOPS, Jean Rouxel Institute of Materials, Nantes, France

Investigation of the Voltage Sensitivity of Selectively Doped Microwave Diodes on "Hot" Electrons in a Wide Temperature Range ..225

V. Derkach¹, R. Golovashchenko¹, Y. Ostryzhnyi¹, J. Gradauskas^{2,3}, A. Sužiedėlis², M. Anbinderis^{2,3}

¹O. Ya. Usikov Institute for Radiophysics and Electronics of NAS of Ukraine, Kharkiv, Ukraine

²Center for Physical Sciences and Technology, Vilnius, Lithuania

³Vilnius Gediminas Technical University, Vilnius, Lithuania

Phase-Resolved Visualization of Radio Frequency Standing Waves in Superconducting Spiral Resonator for Metamaterial Applications ..226

A.P. Zhuravel¹, A. Karpov², A.V. Lukashenko³, A.A. Leha¹, A.V. Ustinov^{2,3}

¹B. Verkin Institute for Low Temperature Physics and Engineering of NASU, Kharkiv, Ukraine

²National University of Science and Technology(MISiS), Moscow, Russia

³Karlsruhe Institute of Technology (KIT), Karlsruhe, Germany

Spatial Distribution of Resonances in rf-SQUIDs Array ..227

A.P. Zhuravel¹, A.V. Lukashenko², A.V. Ustinov^{2,3}, Y.D. Oboznyi^{1,4}, S.M. Anlage⁵

¹B. Verkin Institute for Low Temperature Physics and Engineering of NASU, Kharkiv, Ukraine

²Karlsruhe Institute of Technology (KIT), 76131 Karlsruhe, Germany

³National University of Science and Technology(MISiS), Moscow, Russia

⁴V.N. Karazin Kharkov National University, Kharkiv, Ukraine

⁵Center for Nanophysics and Advanced Materials, Department of Physics, University of Maryland, Maryland, USA

POSTERS

Application of deep learning for improvement of particle flow algorithm for dijet events ..228

A. Charkin-Gorbulin, E. Gross, S. Ganguly

Weizmann Institute of Science, Rehovot, Israel

Creation of a remote presence robot based on the TI-RLSK development board ..229

V. Chekubasheva, O. Glukhov, O. Kravchuk, V. Rohovets

Kharkiv National University of Radio Electronics, Kharkiv, Ukraine

Optimized Model of Hybrid Solar PV/Thermal Systems ..230

K.O. Minakova, R.V. Zaitsev, M.V. Kirichenko

National Technical University “Kharkiv Polytechnic Institute”, Kharkiv, Ukraine

Medical masks filter resistance change measurement for their humidification monitoring ..231

V. Rohovets, Y. Levchenko, O. Kravchuk, V. Chekubasheva

Kharkiv National University of Radio Electronics, Kharkiv, Ukraine

Energy Storage Development for High Voltage Electromagnetic Pulse Generator ..232

D.S. Shkoda, M.V. Kirichenko, K.O. Minakova

National Technical University “Kharkiv Polytechnic Institute”, Kharkiv, Ukraine

On Determination of Neutral Oxygen Atoms Density During Testing of Spacecraft Polymer Materials in a Rarefied Plasma Flow

..233

V. Shuvalov, Yu. Kuchugurnyi, D. Lazuchenkov, G. Kochubei

Institute of Technical Mechanics of NAS of Ukraine and SSA of Ukraine, Dnipro, Ukraine

LISTENERS

Yuri Bohdanov, National Technical Univ. "KhPI", Kharkiv (Ukraine)

Oleksandr Fomin, Kharkiv National Univ. of Radio Electronics, Kharkiv (Ukraine)

Mykyta Hress, V.N.Karazin Kharkiv National Univ., Kharkiv (Ukraine)

Yuliia Kharchenko, V.N.Karazin Kharkiv National Univ., Kharkiv (Ukraine)

Oleksandr Khromiuk, V.N.Karazin Kharkiv National Univ., Kharkiv (Ukraine)

Anna Korsun, V.N.Karazin Kharkiv National Univ., Kharkiv (Ukraine)

Pavel Kurmaz, National Technical Univ. "KhPI", Kharkiv (Ukraine)

Olha Kravchuk, Kharkiv National Univ. of Radio Electronics, Kharkiv (Ukraine)

Egor Levchenko, Kharkiv College of Architecture and Design, Kharkiv (Ukraine)

Yevhen Levchenko, Kharkiv National Univ. of Radio Electronics, Kharkiv (Ukraine)

Hlib Makhlaiov, V.N.Karazin Kharkiv National Univ., Kharkiv (Ukraine)

Nikita Moskovkin, V.N.Karazin Kharkiv National Univ., Kharkiv (Ukraine)

Fedir Novikov, V.N.Karazin Kharkiv National Univ., Kharkiv (Ukraine)

Kateryna Solovian, V.N.Karazin Kharkiv National Univ., Kharkiv (Ukraine)



PLENARY LECTURES OF INVITED SPEAKERS

Peculiarities of dipolar ordering in mixed cation halide perovskites

J. Banys¹, S. Balciunas¹, M. Simenas¹, S. Svirskas¹, M. Kinka¹, V. Samulionis¹, R. Grigalaitis¹, A. Garbaras², A. Gagor³, M. Maczka³, A. Sieradzki⁴

¹*Faculty of Physics, Vilnius University,
Sauletekio 3, LT-10257 Vilnius, Lithuania*

²*Mass Spectrometry Laboratory, Center for Physical Sciences and Technology,
Sauletekio 3, LT-10257 Vilnius, Lithuania*

³*Institute of Low Temperature and Structure Research, Polish Academy of Sciences
PL-50-950 Wroclaw, Poland*

⁴*Institute of Low Temperature and Structure Research, Polish Academy of Sciences
PL-50-370 Wroclaw, Poland
Juras.Banys@ff.vu.lt*

The methylammonium (MA) lead halides MAPbX_3 (where X = I, Br, Cl) are popular perovskite materials among scientists and industry due to their perspectives in effective and cheap solar cells [1]. During the past decade, the power conversion efficiency of cells based on these hybrid compounds exceeded more than 20%. A high performance of these materials results from several physical properties such as large absorption coefficient, optimal bandgap, long carrier diffusion length, low exciton binding energy, exceptional defect tolerance. However, a successful application of hybrid perovskite solar cells is mainly prevented by their lead toxicity and poor both thermal and water stability.

The most stable and efficient solar cells are obtained by using perovskites with mixed cations at the A-site. The most popular alternatives to MA are formamidinium and Cs^+ ions. A Dimethylammonium (DMA) cation has been introduced recently as an alternative A-site modification for these compounds. Several investigations have shown that during certain synthesis procedures high quantities of DMA may be unintentionally introduced into MAPbI_3 and CsPbI_3 . These modifications stabilize the preferable cubic phase of MAPbI_3 and leads to the enhanced performance at ambient condition.

In the field of classical inorganic perovskites it is well known that mixing may significantly perturb structure of resulting compound. Thus, the long-range order can be suppressed and frustrated phases may appear. The dielectric permittivity behavior of lead halides seem to be especially informative for the performance of the perovskite cells, as their relatively high value of the dielectric permittivity results in a pronounced defect tolerance and low exciton binding energy. However, a complete understanding of mixing effects on the dielectric permittivity dynamics and structural phase behavior is still absent. Here, we present a multitechnique experimental study of the mixed hybrid perovskite $\text{MA}_{1-x}\text{DMA}_x\text{PbBr}_3$. Our results show that structural phase transitions are significantly suppressed even for a low substitution of the DMA cations. For higher DMA levels, the long-range dipolar order disappears and dipolar glass dielectric behavior dominates in the dielectric spectra.

Optical Horn Effect via Plasmonic Hour-Glass Nano-Aperture

S.S. Choi

Research Center for Nano-Bio Science, SunMoon University, Ahsan,

Chungnam 314606 South Korea

sscpphy1982@daum.net

sscpphy2010@gmail.com

The hour-glass type nanostructures are fabricated by using the conventional Si processes. When beaming though these structures, we observed that light is collected by the micro scale pyramidal cavity, funneled through the nano-aperture by plasmonic resonance and collimated with enhanced transmission by the surrounding horn-like mirrors (optical horn-effect). Optical transmissions through pyramidal probes with various nano-aperture diameters were measured to be dependent upon the aperture area. For a diameter less than ~ 50 nm or less than area with $\sim 10,000$ nm^2 , the transmitted optical intensities are increasing due to the spp-mediated intra-band emission [1-5]. For the aperture diameter greater than 100 nm, the strong spp-coupled emission is shown in Figure 1 and 2. Without any sophisticated nanofabrication processes, we designed and tested this nano-aperture device surrounded by wave-guiding mirrors for enhanced optical transmission with a focusing ability. The enhanced optical intensity via nano-cavity resonance was also reported [6]. Moreover, this pyramidal structure surrounded by mirror walls is expected to be similar to an optically converging-diverging channel (CDC) [7].

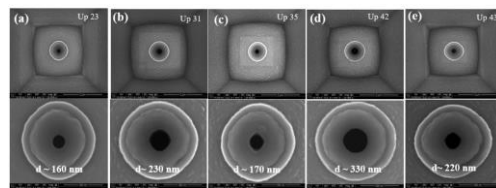


Fig.1. FESEM image of Hourglass Nano-aperture (top view)

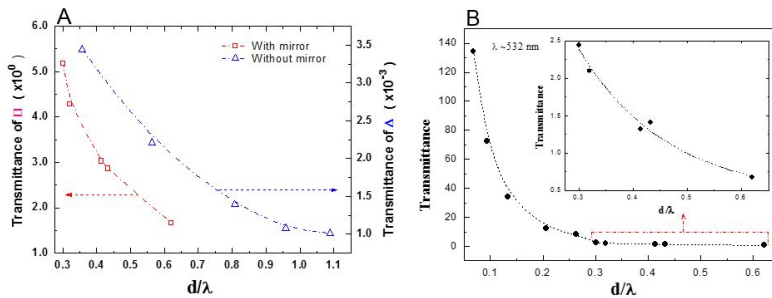


Fig.2. Comparison between transmittances from the hour glass type aperture and pyramidal aperture

- [1] S.S. Choi, S.J. Oh, Y.M. Lee, H.T. Kim, S.B. Choi, B.S. Bae, J. Electrochem. Soc. 167, 027503(2020).
- [2] S.S. Choi, M.J. Park, Y.M. Lee, B.S. Bae, H.T. Kim, S.B. Choi, ECS J. Solid State Sci. Technol. 9, 115015(2020).
- [3] S.S. Choi, S.J. Oh, Y.M. Lee, H.T. Kim, S.B. Choi, B.S. Bae, Mater. Today: Proceedings, <https://doi.org/10.1016/j.matpr.2020.01.359>.
- [4] S.S. Choi, M.J. Park, K.J. Kim, B.S. Bae, Y.M. Lee, H.T. Kim, S.B. Choi, SPIE Proceeding, March, 2021 SPIE Bio, San Francisco, USA.
- [5] M. Consonni, J. Hazart, G. Lerondel, A. Vial, J. Appl. Phys. 105, 084308-6(2009).
- [6] A. Battula, S.C. Chen, Applied Physics Letters 2006, 89, (13), 131113-39(2006), Phys. Rev. B 74, 245407(2006).

Strain modulated ferromagnetic resonance technique as a powerful tool for investigating of thin films magnetoelastic properties

O.M. Chumak¹, **A. Nabialek**¹, **V.V. Chabanenko**², **T. Seki**^{3,4}, **K. Takanashi**^{3,4,5},
L.T. Baczewski¹, **H. Szymczak**¹

¹*Institute of Physics, Polish Academy of Sciences, Al. Lotników 32/46, 02-668 Warsaw, Poland.*

²*O.Galkin Donetsk Institute for Physics and Engineering, NAS of Ukraine,
46 Nauki Ave. 46, 03028, Kyiv, Ukraine.*

³*Institute for Materials Research, Tohoku University, 980-8577 Sendai, Japan*

⁴*Center for Spintronics Research Network, Tohoku University, 980-8577 Sendai, Japan*

⁵*Center for Science and Innovation in Spintronics, Core Research Cluster, Tohoku University,
980-8577 Sendai, Japan
chumak@ifpan.edu.pl*

The presentation is devoted to the Strain Modulated Ferromagnetic Resonance (SMFMR) [1], which is a unique experimental technique enabling determination of the magnetoelastic properties of magnetic thin films or ribbons.

As the illustration of the using of the SMFMR technique, investigation of magnetoelastic properties of Co₂YZ Heusler alloys thin films will be presented [2,3]. Such materials possess a special scientific importance due to their application in spintronic devices as half-metallic electrodes. Study of the magnetoelastic phenomena in spintronic materials have became more and more important in recent years due to possible mechanical control of spin polarization by using magnetoelastic thin films [4].

The investigations by the SMFMR are performed at room temperature in a X-band spectrometer at the frequency of about 9.1 GHz, which is equipped in both magnetic (100 kHz) and strain (48 kHz) modulation systems. The investigated layer is glued to the surface of a polycrystalline quartz rod with a square ($3 \times 3 \text{ mm}^2$) cross-section, which is driven to oscillations by a crystalline quartz generator. The comparison of the amplitudes of the magnetic and strain modulated resonance lines enables to determine the shift of the resonance line caused by the strains, which contains information on the magnetoelastic tensor B_{ijkl} components.

Using of the SMFMR technique to study thin films having different thicknesses of the magnetic layer allows investigation of surface phenomena. In this case the concept of surface magnetoelastic coupling [5] is used to explain the change of the magnetoelastic constants absolute values with changing thickness of the magnetic layers.

Acknowledgements. This work was supported by the grant from Polish National Science Centre – project 2018/31/B/ST7/04006.

- [1] K. Nesteruk, R. Zuberek, S. Piechota, M.W. Gutowski and H. Szymczak, Meas. Sci. Technol. 25, 075502 (2014).
- [2] O.M. Chumak, A. Nabialek, R. Źuberek, I. Radelytskyi, T. Yamamoto, T. Seki, K. Takanashi, L.T. Baczewski, H. Szymczak, IEEE Trans. Magn. 53, 2501906 (2017).
- [3] O.M. Chumak, A. Pacewicz, A. Lynnyk, B. Salski, T. Yamamoto, T. Seki, J.Z. Domagala, H. Głowinski, K. Takanashi, L.T. Baczewski, H. Szymczak and A. Nabialek, *under review*.
- [4] M. Wei, K. Song, Y. Yang, Q. Huang, Y. Tian, X. Hao, W. Qin, Adv. Mater. 32, e2003293 (2020).
- [5] H. Szymczak, R. Źuberek, R. Krishnan, M. Tessier, K.B. Youn and C. Sella, The 12th Int. Colloq. on Mag. Films and Surfaces (Le Creusot), Th3-03 266 (1988).

Ultra-fast vortex dynamics in nanoengineered superconductors

O.V. Dobrovolskiy

*Faculty of Physics, University of Vienna, Boltzmanngasse 5, 1090 Vienna, Austria
oleksandr.dobrovolskiy@univie.ac.at*

The dynamics of vortices at large transport currents is essential for modeling quasiparticle ensembles under far-from-equilibrium conditions and it sets practical limits for the use of superconductors in applications. Recently, two approaches were used to demonstrate ultra-fast vortex motion at velocities $v \gtrsim 5$ km/s: (i) A clean Pb bridge with a short electron-phonon relaxation time was studied [1], with a strongly nonuniform current distribution both across and along the bridge. (ii) An array of ferromagnetic Co nanostripes on top of a superconducting Nb film led to a dynamic ordering of flux quanta guided by the nanostripes and allowed to achieve a narrow distribution of their velocities v [2]. In both of these approaches, specially designed, locally nonuniform structures were used. At the same time, a close-to-ideal uniform system where the fast heat removal from electrons becomes the limiting factor for ultra-fast vortex dynamics was never investigated experimentally. Theoretically, however, it was predicted that dirty superconductors with weak volume pinning and strong edge barrier for vortex entry should also allow for ultra-fast vortex dynamics [3]. The presence of a strong edge barrier in such superconductors leads to a current gradient near the edge where vortices enter the superconductor and where the flux-flow instability (FFI) is actually nucleating.

In my talk, I will present our recent results [4] on the experimental observation of ultra-fast (5-15 km/s) vortex motion in a direct-write Nb-C superconductor (Fig. 1a). The spatial evolution of the FFI implies a chain of nucleation points along the sample edge and their development into self-organized Josephson-like junctions (“vortex rivers”, Fig. 1b). The rarely achieved combination of properties – close-to-depairing critical current, weak volume pinning, and fast heat removal from electrons – make Nb-C a good candidate material for fast single-photon detectors.

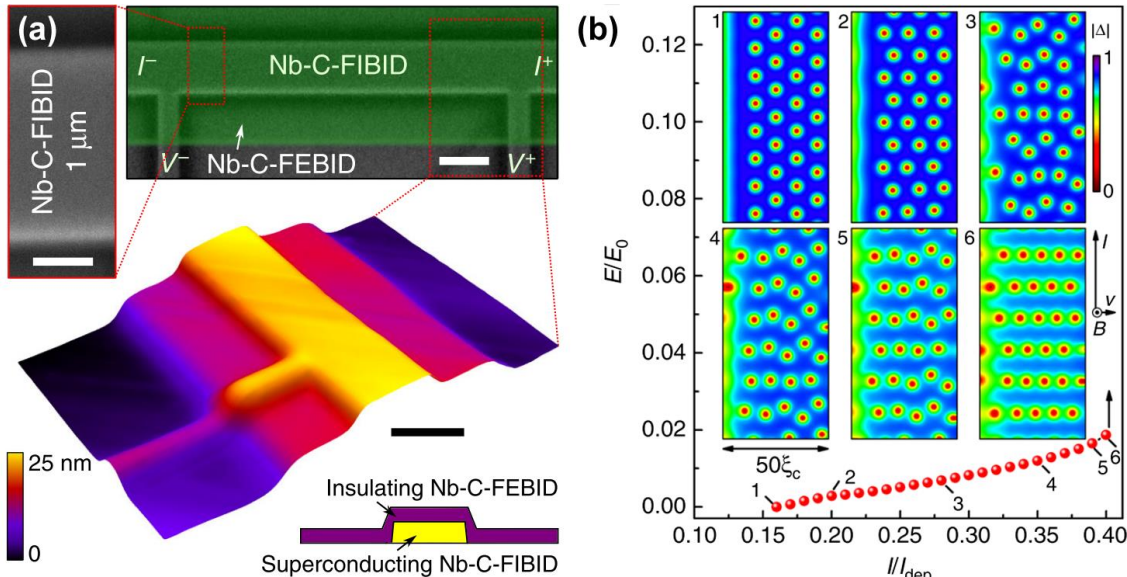


Fig. 1. (a) SEM and AFM images of a 15 nm-thick $1 \times 6.6 \mu\text{m}^2$ superconducting Nb-C-FIBID strip covered with an insulating Nb-C-FEBID layer. (b) I - V curve and the evolution of the superconducting order parameter in the microstrip, calculated relying upon the time-dependent Ginzburg-Landau equation.

- [1] L. Empon, et al. Nat. Commun. 8 (2017) 85.
- [2] O. V. Dobrovolskiy, et al. Phys. Rev. Appl. 11 (2019) 054064.
- [3] D. Y. Vodolazov, Supercond. Sci. Technol. 32 (2019) 115013.
- [4] O. V. Dobrovolskiy, D. Yu. Vodolazov, F. Porriati, R. Sachser, V. M. Bevz, M. Yu. Mikhailov, A. V. Chumak, and M. Huth. Nat. Commun. 11 (2020) 3291.

Optical choppers with disks, with an insight in biomedical applications

V.-F. Duma

*3OM Optomechatronics Group, “Aurel Vlaicu” University of Arad, 77 Revolutiei Ave.,
Arad 310130, Romania*

*Doctoral School, Polytechnic University of Timisoara, 1 Mihai Viteazu Ave.,
Timisoara 300222, Romania
duma.virgil@osamember.org*

We report our one-decade contributions regarding the development of optical choppers. One of the most common devices in optics and photonics (almost as utilized as lenses, mirrors, and prisms), a ‘*classical chopper*’ is essentially a rotational disk with a certain number of windows (and wings) that stops with a corresponding frequency a light (usually, laser) beam. Choppers are employed for the attenuation of light, to eliminate certain wavelengths or spectral intervals, or to produce light (laser) impulses of certain frequencies and profiles [1]. For the latter, laser impulses produced by disk choppers have been usually considered as rectangular, but this is valid only when the beam is perfectly focused in the disk plane. We approached the actual non-linear profiles of laser impulses produced, by performing a multi-parameter theoretical analysis that considered all possible relationships between the dimensions of the disk and of a top-hat transmitted beam (i.e., with a constant intensity on its section) [2]. This theory was confirmed by other groups experimentally [3]. This is the first part of this discussion.

The second part presents the development of novel configurations of disk choppers [4-6]. While classical disks have windows with linear margins, we have introduced [4] and patented [5] chopper disks with windows with non-linear (e.g., semi-circular) margins. We have proposed for them the name of ‘*eclipse choppers*’, because of the way their semi-circular margins obscure the beam section, similarly to a planetary eclipse. The transmission functions of eclipse choppers are the general case of those of classical disk choppers, because the latter can be obtained as a particular case of the former by considering the radius of the window margins going to infinity [6].

While these eclipse choppers can produce other profiles of laser impulses (e.g., approximately triangular) in comparison to classical choppers, their chop frequency (i.e., the frequency of the generated laser impulses) is similar, limited in the literature to 10 kHz [1], although vibrations may already appear around 3 kHz. A research direction to address this issue has been to develop Micro-Electro-Mechanical Systems (MEMS) choppers [7]. However, due to technological and cost limitation of MEMS, we have taken another path, by developing macro-choppers with rotational shafts of different shapes (cylindrical, spherical, or conical)-patent application [8]. This third part of this presentation points out both optical and mechanical aspects of these novel devices [9]. Finally, from the various applications of choppers, we present biomedical imaging ones, using conjugated Optical Coherence Tomography (OCT) and Confocal Microscopy [10].

Acknowledgement: This research was funded by the Romanian National Authority for Scientific Research, CNDI–UEFISCDI grant PN-III-P2-2.1-PED-2020-4423.

- [1] M. Bass, Ed., [Handbook of optics], Mc. Graw-Hill Inc., New York (2010).
- [2] V.-F. Duma, J. of Opt. A: Pure and Appl. Opt. 10(6), 064008 (2008).
- [3] K. Benjamin, A. Armitage, R. South, Measurement 39, 764-770 (2006).
- [4] V.-F. Duma, Comm. in Nonlinear Sc. and Numerical Simulation 16(5), 2218-2224 (2011).
- [5] V.-F. Duma, M. F. Nicolov, C. Mnerie, L. Szanthy, Romanian Patent RO 126505 (2016).
- [6] V.-F. Duma, Latin American J. of Solids and Structures 10(1), 5-18 (2013).
- [7] R. R. A. Syms, H. Zou, J. Stagg, H. Veladi, J. Micromech. Microeng. 14(12), 1700 (2004).
- [8] V.-F. Duma, D. Demian, Romanian Patent RO 129610 (2021).
- [9] E.-S. Csukas, V.-F. Duma, Proc. SPIE 10785, 10785K (2018).
- [10] R. Luca, C. D. Todea, V.-F. Duma, et al., Quant. Im. in Med. and Surgery 9, 782-798 (2019).

Influence of pressure and stoichiometry on the Ginzburg-Landau parameter in superconducting YB₆

S. Gabáni¹, K. Flachbart¹, E. Gažo¹, J. Kačmarčík¹, M. Marcin¹, T. Mori², Mat. Orendáč¹, Z. Pribulová¹, G. Pristáš¹, P. Samuely¹, N. Shitsevalova³, N. Sluchanko⁴

¹*Institute of Experimental Physics, SAS, 04001 Košice, Slovakia*

²*National Institute for Materials Science, ICMN & CFSN, Namiki 1-1, Tsukuba 305-0044, Japan*

³*Frantsevich Institute for Problems of Materials Science, NASU, 03680 Kiev, Ukraine*

⁴*Prokhorov General Physics Institute, RAS, Moscow 119991, Russia*

gabani@saske.sk

After superconducting MgB₂ with a critical temperature of $T_C = 39$ K, yttrium hexaboride YB₆ exhibits the second highest transition temperature $T_C \leq 7.4$ K among borides. From recent studies on the superconducting properties of this compound [1-3] follows that there is still a dispute about, what affects the value of the superconducting transition temperature of various YB₆ samples. To explain such the significant T_C - variation it was suggested in [1] that the transition temperature is controlled by the B/Y ratio (the highest T_C is obtained for a B/Y < 6). Thus, both a growth of the number of boron vacancies, which is associated with the deviation from the stoichiometric composition of the boron sublattice, and a decrease of yttrium vacancies in contrast, which requires an almost stoichiometric metal sublattice composition, result according to [1] in a T_C enhancement in this compound. On the other hand, it is argued in [3] that the T_C enhancement in YB₆ single crystals is determined by the increase of the number of vacancies, both at yttrium and boron sites, leading to a nonstoichiometric composition, which is accompanied by the enhancement of electron-phonon interaction. In mentioned studies [1, 3] also the relevant superconducting state parameters as e.g. the coherence length $\xi(0)$, penetration depth $\lambda(0)$, the Ginzburg-Landau parameters $\kappa(0)$ and the superconducting gap 2Δ were determined. They show that YB₆ compounds exhibit type II superconductivity in “dirty limit” with a medium to strong electron-phonon interaction and *s*-type pairing of charge carriers with $2\Delta(0) / k_B T_C \approx 3 - 4$.

The Ginzburg-Landau parameter $\kappa(0) = \lambda(0) / \xi(0)$ is one of the most important phenomenological parameters of superconductors. As its estimation under the influence of pressure is rather complicated, any new result related with the pressure dependence of this parameter are appreciated. Until now, $\kappa(0)$ was measured under pressure only up to 0.92 GPa [4]. In the present work we estimated the pressure effect on $\kappa(0)$ of YB₆ up to 3 GPa.

Using an array of miniature Hall-probes we have investigated for the first time the penetration of magnetic field and the pinning strength in four YB₆ samples having different stoichiometry and superconducting transition temperatures T_C between 4.2 K and 7.4 K. The obtained results show that except the sample with lowest $T_C = 4.2$ K, which exhibits weak pinning, all others show strong pinning features. On the other hand, the comparison of penetration field H_p temperature dependencies with BCS theory points in all samples to strong *s*-type pairing of charge carriers with $2\Delta / k_B T_C \approx 4$. In addition, based on the temperature and field dependencies of ac-calorimetry, the Ginzburg-Landau as well as another the superconducting state parameters were determined independently and compared with results of previously published works.

- [1] R. Lortz et al., Superconductivity mediated by a soft phonon mode: specific heat, resistivity, thermal expansion, and magnetization of YB₆, Physical Review B 73, 024512 (2006).
- [2] S. Gabani et al., High-pressure effect on the superconductivity of YB₆, Physical Review B 90, 045136 (2014).
- [3] N. Sluchanko et al., Lattice instability and enhancement of superconductivity in YB₆, Physical Review B 96, 144501 (2017).
- [4] R. Khasanov et al., Effect of pressure on the Ginzburg-Landau parameter $\kappa = \lambda / \xi$ in YB₆, Physical Review Letters 97, 157002 (2006).

Massive magnetostriction of the KEr(MoO₄)₂

D. Kamenskyi^{1,2}, B. Bernath³, S. Khmelevskyi⁴, L.V. Pourovskii⁵, S. Poperezhai⁶, K. Kutko⁶

¹*Experimental Physics V, Institute of Physics, University of Augsburg, 86159 Augsburg, Germany*

²*Molecular Photoscience Research Center, Kobe University, 657-8501 Kobe, Japan*

³*High Field Magnet Laboratory (HFML-EMFL), Radboud~University,*

6525 ED Nijmegen, The Netherlands

⁴*Research Center for Materials Science and Engineering, Vienna University of Technology,
A-1040 Vienna, Austria*

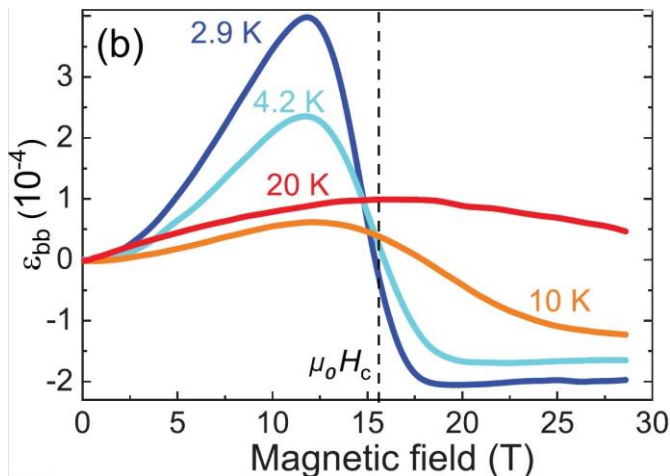
⁵*CPHT, CNRS, Ecole Polytechnique, Institut Polytechnique de Paris, 91128 Palaiseau, France*

⁶*B.Verkin Institute for Low Temperature Physics and Engineering of NAS of Ukraine,*

47 Nauky Ave., Kharkiv, 61103, Ukraine

dmytro.kamenskyi@physik.uni-augsburg.de

The investigation of magnetostrictive properties of ferro- and antiferromagnets helps the fundamental understanding of magnetism and superconductivity and plays an important role in realising technological applications. In paramagnets, however, the magnetostriction is usually significantly smaller, because of the magnetic disorder. Here, we report the observation of a remarkably strong magnetostrictive response ($\varepsilon = \Delta l/l > 10^{-4}$) of the paramagnetic compound KEr(MoO₄)₂ at 15.6 T.



Using low-temperature dilatometry, magnetisation, and THz spectroscopy measurements in magnetic fields up to 30T, in combination with *ab-initio* calculations, we demonstrate that the magnetostriction anomaly is driven by a single-ion effect. Our analysis reveals a strong coupling between the Er³⁺ ions and the crystal lattice, due to the peculiar behaviour of the quadrupolar moments of Er³⁺ ions in the applied field, shedding light on the microscopic mechanism behind the massive lattice response.

Nonlinear and chiral response of topological semimetals and other chiral media

**F. Büscher¹, V. Gnezdilov^{1,2}, D. Wulferding^{1,3}, S. Müllner¹, Yu.G. Pashkevich⁴, C. Felser⁵,
Ch. Shekhar⁵, K. Manna⁶, P. Lemmens¹**

¹*IPKM and LENA, TU-BS, Braunschweig, Germany*

²*ILTPE Kharkiv, Ukraine*

³*IBS, Center for Correlated Electron Systems, Seoul Nat. Univ, Seoul, Korea*

⁴*Donetsk IPE O.O. Galkin NAS, Kyiv, Ukraine*

⁵*MPI Dresden, Germany*

⁶*Quantum Materials Magneto-Transport Laboratory, IIT, New Delhi, India*

p.lemmens@tu-bs.de

Light-matter interaction in chiral media has many important implications from life science to quantum cryptography. Here, we will present a brief overview on chirooptical effects and related light matter interactions. We will discuss the chiral phases of liquid crystals and novel topological semimetals.

One example is the chiral topological semimetal PdGa with a crystal structure that has a well-defined handedness and strong spin orbit interactions. This is the first known compound where electronic bands acquire a maximal Chern number of $C = \pm 4$ [1]. In such a case exotic transport properties are expected, e.g. quantized photocurrents. However, also structural properties are remarkable. Using Raman spectroscopy, we uncover a strong and sharp electronic resonance around $E = 2.35$ eV that allow us to follow changes of electronic Raman scattering occurring in moderate magnetic fields as well as phonon anomalies. Both observations point to a possible modification of the electronic band structure in PdGa in magnetic fields.

Work supported by DFG LE967/16-1, Excellence Cluster QuantumFrontiers, EXC 2123, and Nds. funded QUANOMET NL-4.

[1] Schröter, et al., *Science* **369**, 6500 (2020).

Theoretical prediction and subsequent observation of the dynamical Casimir effect in a superconducting circuit

F. Nori

*RIKEN, Saitama, Japan; and the University of Michigan, Ann Arbor, USA
fnori@riken.jp*

We theoretically investigated [1-5] the dynamical Casimir effect (DCE) in electrical circuits based on superconducting microfabricated waveguides with tunable boundary conditions. We proposed implementing a rapid modulation of the boundary conditions by tuning the applied magnetic flux through superconducting quantum-interference devices that are embedded in the waveguide circuits. We considered two circuits: (i) An open waveguide circuit that corresponds to a single mirror in free space, and (ii) a resonator coupled to a microfabricated waveguide, which corresponds to a single-sided cavity in free space. We analyzed the properties of the DCE in these two setups by calculating the generated photon-flux densities, output-field correlation functions, and the quadrature squeezing spectra. We showed that these properties of the output field exhibit signatures unique to the radiation due to the DCE, and could, therefore, be used for distinguishing the DCE from other types of radiation in these circuits. We also discussed the similarities and differences between the DCE, in the resonator setup, and the down-conversion of pump photons in parametric oscillators.

We observed [2] the dynamical Casimir effect in a superconducting circuit consisting of a coplanar transmission line with a tunable electrical length. The rate of change of the electrical length can be made very fast (a substantial fraction of the speed of light) by modulating the inductance of a superconducting quantum interference device at high frequencies (>10 gigahertz). In addition to observing the creation of real photons, we detected two-mode squeezing in the emitted radiation, which is a signature of the quantum character of the generation process.

- [1] J.R. Johansson, G. Johansson, C.M. Wilson, F. Nori, Phys. Rev. Lett. 103, 147003 (2009). Featured in Physics, Editors' Suggestion
- [2] J.R. Johansson, G. Johansson, C.M. Wilson, F. Nori, Phys. Rev. A 82, 052509 (2010).
- [3] C.M. Wilson, G. Johansson, A. Pourkabirian, J.R. Johansson, T. Duty, F. Nori, P. Delsing, Nature 479, 376-379 (2011).
- [4] P.D. Nation, J. Johansson, M. Blencowe, F. Nori, Rev. Mod. Phys. 84, 1-24 (2012).
- [5] J.R. Johansson, G. Johansson, C.M. Wilson, P. Delsing, F. Nori, Phys. Rev. A 87, 043804 (2013).

GHz-THz Nonlinearities in Semiconductor Superlattices

M.F. Pereira

*Department of Physics, Khalifa University of Science and Technology,
Abu Dhabi 127788, UAE
mauro.pereira@ku.ac.ae*

This talk starts with a short review of the state of the art in nonlinearities in the Gigahertz (GHz) to Terahertz range, followed by an outline of an hybrid approach combining Nonequilibrium Green's Functions and the Boltzmann equation for the nonlinear response of semiconductor superlattices. The nonlinearities are controllable in very good agreement with experiments [1-2].

The Terahertz-Mid Infrared (TERA-MIR) is relatively well understood [3-5] but more work is needed for the next step which is the GIGA-TERA-MIR extended range and a predictive numerical tool is discussed to design materials and devices for a large number of applications for the detection of substances which have strong GHz-THz resonances.

Recent results of control of GHz-THz nonlinearities under will be discussed in detail [6-9].

Possible projects for PhD students with full Fellowship at KU will be discussed. See a video of KU at Ref. [10].

- [1] M.F. Pereira et al, Phys. Rev. B 96, 045306 (2017).
- [2] M.F. Pereira et al, J. Nanophoton 11 (4), 046022 (2017).
- [3] M.F. Pereira, Opt Quant Electron 47, 815 (2015).
- [4] M.F. Pereira, Applied Physics Letters 109, 222102 (2016).
- [5] M.F. Pereira and I.A. Faragai, Optics Express 22 (3), 3439 (2014).
- [6] A. Apostolakis and M.F. Pereira, AIP Advances 9, 015022 (2019).
- [7] A. Apostolakis and M.F. Pereira, J. of Nanophotonics 13, 036017 (2019).
- [8] A. Apostolakis and M.F. Pereira, Nanophotonics (2020)
- [9] M.F. Pereira et al, Sci Rep 10, 15950 (2020).
- [10] <https://www.youtube.com/watch?v=rpGdQapbRd8&t=27s>

High-pressure stabilized oxide perovskite structures

A.N. Salak¹, D.D. Khalyavin², E.L. Fertman³, D. Delmonte⁴, E. Gilioli⁴

¹*Department of Materials and Ceramics Engineering, CICECO – Aveiro Institute of Materials,
University of Aveiro, Aveiro 3810–193, Portugal*

²*ISIS Facility, Rutherford Appleton Laboratory, Chilton, Didcot, Oxon OX11 0QX, UK*

³*B.Verkin Institute for Low Temperature Physics and Engineering of NAS of Ukraine,
Kharkiv 61103, Ukraine*

⁴*Institute of Materials for Electronics and Magnetism, Parma 43124, Italy
salak@ua.pt*

Remarkable properties of the lead zirconate-titanate and other complex oxides with the perovskite-type structure motivated researchers to search for new ABO_3 compounds with the lone electron pair of A-site cation. It turned out that many very promising compositions containing Pb^{2+} or Bi^{3+} do not crystallize in perovskite structure at ambient pressure. Some of those compositions require elevated pressures to transform into the perovskite phase from a single-phase but less compact polymorphs; others form the perovskite compounds under high-pressure & high-temperature conditions only [1]. Beginning with the successful high-pressure synthesis of $BiMnO_3$ and $BiCrO_3$ [2] in the middle of sixties in the last century, a great number of simple and complex perovskite compounds with unique combinations of atomic orderings, oxygen octahedra tilts, atomic displacements and magnetic structures has been produced using the high-pressure & high-temperature technique. High-pressure stabilized Mn_2O_3 perovskite with Mn^{2+}/Mn^{3+} in A-sites and Mn^{3+}/Mn^{4+} in B-sites is one of most prominent recent examples [3]. The unique feature of this binary perovskite that all the A- and B-site cations can be magnetically and electrically active, thus leading to an interplay of multiple structural and electronic instabilities. Another outstanding example is Cu-substituted $BiMn_7O_{12}$ perovskite synthesized under high-pressure [4]. In the case of the particular ($x=0.1$) composition of the $BiCu_xMn_{7-x}O_{12}$ series, the competing interactions arising from the orbital ordering and the stereochemically active lone pair electrons result in the onset of the structural modulation with a complex helical ordering of electric dipoles.

We have recently demonstrated the phenomenon of annealing-stimulated irreversible transformations of the high-pressure stabilized phases (conversion polymorphism) [5] as a new and promising approach to produce novel multiferroic materials. In particular, it has been shown that conversion is the only way to stabilize some of the polymorphs in a bulk form and these polymorphs exhibit unique properties.

Here we report on reversible and irreversible transformations between metastable phases of the Bi-containing perovskite solid solutions $BiFeO_3$ - $BiScO_3$, $BiFeO_3$ - $BiCrO_3$ and $BiMg_{0.5}Ti_{0.5}O_3$ - $BiZn_{0.5}Ti_{0.5}O_3$ below their decomposition temperature. New perovskite polymorphs with interesting combinations of ferroic orders are compared and discussed.

- [1] J. B. Goodenough, J. A. Kafalas and J.M. Longo, High-Pressure Synthesis, in Preparative Methods in Solid State Chemistry, ed. P. Hagenmuller, (Academic Press, New York, 1972).
- [2] F. Sugawara, S. Iida, Y. Syono, and S. Akimoto, J. Phys. Soc. Japan, 20, 1529 (1965).
- [3] J. Cong, K. Zhai, Y. Chai, D. Shang, D. D. Khalyavin, R. D. Johnson, D. P. Kozlenko, S. E. Kichanov, A. M. Abakumov, A. A. Tsirlin, L. Dubrovinsky, X. Xu, Z. Sheng, S. V. Ovsyannikov, and Y. Sun, Nature Commun. 9, 2996 (2018).
- [4] D. D. Khalyavin, R. D. Johnson, F. Orlandi, P. G. Radaelli, P. Manuel, and A. A. Belik, Science 369, 680 (2020).
- [5] D.D. Khalyavin, A.N. Salak, E.L. Fertman, O.V. Kotlyar, E. Eardley, N.M. Olekhovich, A.V. Pushkarev, Yu.V. Radyush, A.V. Fedorchenco, V.A. Desnenko, P. Manuel, L. Ding, E. Čížmár, and A. Feher, ChemComm. 55, 4683 (2019).

Dynamical Casimir Effect in Optomechanical systems: Fully Quantum and Non-Perturbative Description

S. Savasta

*University of Messina, Italy
ssavasta@unime.it*

This talk will provide a summary of some recent developments on the theory of the Dynamical Casimir Effect [1-4]. We studied this effect in optomechanical systems by using a fully quantum-mechanical and non-perturbative description of both the cavity field and the oscillating mirror [1]. Within this approach, we showed that the resonant generation of photons from the vacuum is determined by a ladder of mirror-field vacuum Rabi splittings. Moreover, we showed that vacuum emission can originate from the free evolution of an initial pure mechanical excited state, in analogy with the spontaneous emission from excited atoms [1,2]. This study also shows that a resonant production of photons out of the vacuum can be observed even for mechanical frequencies lower than the cavity-mode frequency [1]. We will also present results on the quantification of the entanglement between the oscillating mirror and the radiation produced by its motion in the vacuum field.

We also explored the dynamical Casimir effect under incoherent excitation of the mirror [2], and in the presence of a squeezed vacuum [4].

Finally, we will show how virtual photon pairs can mediate the coherent interaction of mechanical oscillators [3]. This process shows that the electromagnetic quantum vacuum can transfer mechanical energy somewhat like an ordinary fluid. Moreover, we showed that this system can also operate as a mechanical parametric down-converter even at very weak excitations.

- [1] V. Macrì, A. Ridolfo, O. Di Stefano, A.F. Kockum, F. Nori, S. Savasta, Phys. Rev. X 8, 011031 (2018).
- [2] A. Settineri, V. Macrì, L. Garziano, O. Di Stefano, F. Nori, S. Savasta, Phys. Rev. A 100, 022501 (2019).
- [3] O. Di Stefano, A. Settineri, V. Macrì, A. Ridolfo, R. Stassi, A.F. Kockum, S. Savasta, F. Nori, Phys. Rev. Lett. 122, 030402 (2019).
- [4] W. Qin, V. Macrì, A. Miranowicz, S. Savasta, F. Nori, Phys. Rev. A 100, 062501 (2019).

Nonlinear exciton drift in piezoelectric two-dimensional materials

V. Shahnazaryan¹, H. Rostami²

¹ Department of Physics, ITMO University,

49 Kronverksky pr, St. Petersburg, 197101, Russia

²Nordita, KTH Royal Institute of Technology and Stockholm University,

23 Roslagstullsbacken, Stockholm, SE-106 91, Sweden

vanikshahnazaryan@gmail.com

Noncentrosymmetric nature of single-layer transition metal dichalcogenides manifest itself in the finite piezoelectricity and valley - Zeeman coupling [1]. In turn, the giant piezoelectric effect leads to an enormous electric field, resulting in a built-in dipole moment of excitons. We

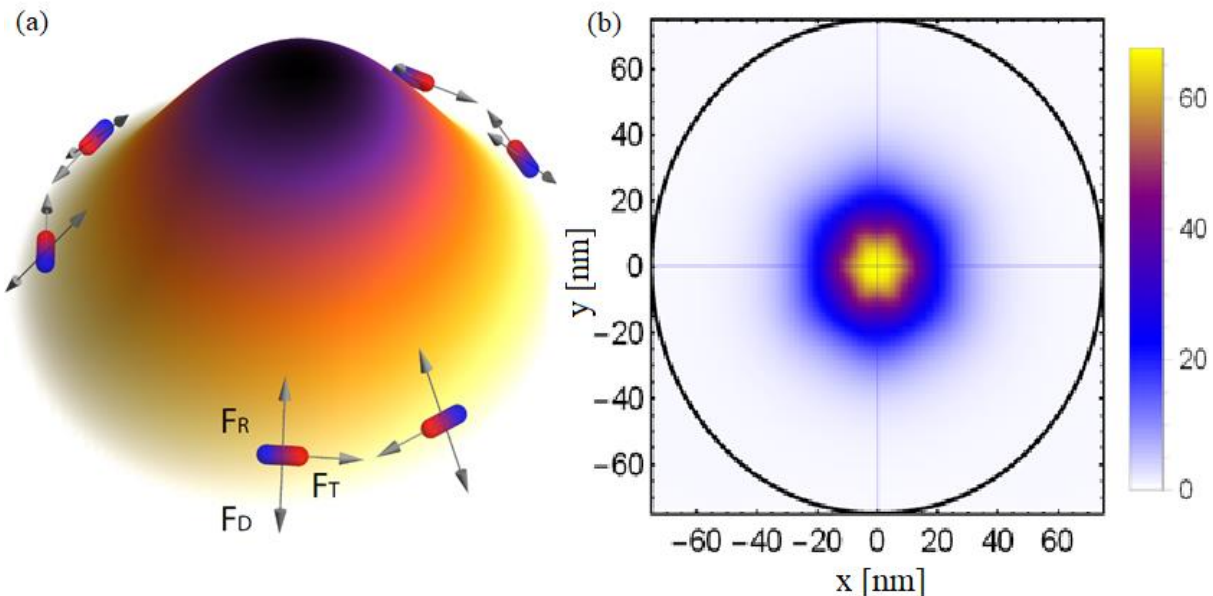


Fig. 1: (a) The sketch of SL-TMD nano-bubble. The strain-induced bandgap modulation gives rise to radial funneling force, which is partially compensated by the counteracting diffusive propagation. The piezoelectricity-induced dipolar interaction and the emergent pseudomagnetic field generate highly anisotropic forces, leading to spatially inhomogenous drift of excitons. (b) The snapshot of exciton density at $t = 20$ ps after initial evolution for temperature $T = 40$ K.

microscopically model nonlinear exciton transport in nano-bubble of single-layers of transition metal dichalcogenide (see Fig. 1 (a)). It is shown that the piezo-induced dipole-dipole interaction provides a novel channel for the nonlinear exciton transport distinct from the conventional isotropic funneling of excitons and leading to the formation of hexagon-shaped exciton droplet on top of a circularly symmetric nano-bubble, as shown in Fig. 1 (b). The effect is tunable via the bubble size dependence of the piezoelectric field $E_{\text{piezo}} \sim h_{\text{max}}^2/R^3$ with h_{max} and R being the bubble height and radius, respectively [2].

[1] W. Wu, L. Wang, Y. Li, F. Zhang, L. Lin, S. Niu, D. Chenet, X. Zhang, Y. Hao, T. F. Heinz, J. Hone and Z. L. Wang, Nature 514, 470–474 (2014).

[2] V. Shahnazaryan, and H. Rostami, arXiv: 2012.13730 (2020).

Study of the magnetoelectric effect in multiferroic ferrite-perovskite composite ceramics

V.V. Shvartsman

*Institute for Materials Science, University of Duisburg-Essen,
Universitätsstrasse 15, 45141 Essen, Germany
vladimir.shvartsman@uni-due.de*

Currently, multiferroic materials are considered as potential candidates for developing room temperature sensors for low magnetic fields, memory elements, electromagnetic energy harvesters, and cooling systems. In the multiferroics two ferroic order parameters of different nature: e.g. magnetization and ferroelectric polarization coexist. Of particular interest, is the coupling between these order parameters, the so called magnetoelectric (ME) effect. In single-phase multiferroics the ME effect is weak and usually occurs at cryogenic temperatures, which limits their applications. However, composite multiferroics show strong magnetoelectric effect at room temperature. Typically, the composite multiferroics combine separate ferroelectric and magnetic phases that are mechanically coupled. The applied magnetic field induces magnetostriction, which results in a mechanical stress at the interface to the ferroelectric phase. This stress will induce a change of polarization due to direct piezoelectric effect. In a similar way application of the electric field will result in change of the magnetization. The ME effect depends not only on properties the constituents, but also on microstructure (the type of connectivity, grain size, etc.) [1].

Here we report on study of the ME effect in several multiferroic composite systems. The CoFe_2O_4 - BaTiO_3 (CFO-BT) composite is a classic example that profits from the large magnetostriction of CFO, large piezoelectric coefficient of BT, and spinodal decomposition of this system, that allows to avoid chemical reaction between the constituents at high temperature ceramic sintering. The microstructure was controlled by the synthesis conditions. The sample prepared by conventional sintering shows a 0-3 connectivity with the coarse micron-size CFO grains distributed in the BT matrix. While, the sample sintered by spark plasma sintering consists on the nanosized BT grains distributed in the CFO matrix. The samples with different microstructure showed the different magnetoelectric effect [2].

The magnetoelectric coupling in the composites was improved by replacing BaTiO_3 with $(\text{Ba},\text{Ca})(\text{Ti},\text{Zr})\text{O}_3$ (BCZT) with the larger piezoelectric coefficient and by replacing of CFO with NiFe_2O_4 that has a large magnetic field derivative of magnetostriction. More than a twofold increase in the magnetoelectric effect was achieved in the NFO-BCZT composites in comparison with the CFO-BT composites [3].

Along with macroscopic measurements, the magnetoelectric effect was studied on meso- and microscopic scales. In particular, the displacement of the titanium ions of the BaTiO_3 phase under the action of a magnetic field was investigated by X-ray absorption spectroscopy. The spatial distribution of the ME effect depending on the distance to the interface with the ferrite phase was studied by piezoresponce force microscopy.

- [1] D. C. Lupascu, H. Wende, M. Etier, A. Nazrabi, I. Anusca, H. Trivedi, V. V. Shvartsman, J. Landers, S. Salamon, and C. Schmitz-Antoniak, GAMM-Mitt. 38, 25 (2015).
- [2] M. Etier, C. Schmitz-Antoniak, S. Salamon, H. Trivedi, Y. Gao, A. Nazrabi, J. Landers, D. Gautam, M. Winterer, D. Schmitz, H. Wende, V. V. Shvartsman, and D. C. Lupascu, Acta Mater. 90, 1 (2015).
- [3] M. Naveed-Ul-Haq, V. V. Shvartsman, H. Trivedi, S. Salamon, S. Webers, H. Wende, U. Hagemann, J. Schröder, and D. C. Lupascu, Acta Mater. 144, 305 (2018).

Features of the exciton self-trapping in molecular aggregates

A.V. Sorokin, I.I. Grankina, I.Yu. Ropakova, S.L. Yefimova

*Institute for Scintillation Materials of NAS of Ukraine,
60 Nauky Ave., Kharkiv, 61072, Ukraine
sorokin@isma.kharkov.ua*

Supramolecular high-ordered assemblies, called J-aggregates, possess a number of unique spectral properties, which distinctly differ from those of the individual molecules: a narrow absorption band, near-resonant fluorescence, high oscillator strength, giant third-order susceptibility, effective resonant energy migration, etc. Specificity of J-aggregates optical properties is governed by the electronic excitations delocalized over molecular chains and molecular (Frenkel) excitons formation due to translational symmetry and strong dipole-dipole interaction between molecules in the J-aggregate chain. One of the J-aggregate characteristic features is the narrow red-shifted exciton band, called J-band, which width is determined by the exciton coherence (or delocalization) length. Thus, J-aggregates are examples of molecular nanocrystals formed by cyanines, porphyrins, merocyanines, perylenes and other dyes. However, the exciton properties of J-aggregates often differ from those of typical molecular crystals. First of all, it is associated with the predominant one-dimensional J-aggregate geometry in solutions or two-dimensional geometry in films and on surfaces, while molecular crystals typically exhibit three-dimensional ordering. Another feature is a strong influence of significant configurational randomness of the J-aggregate environment leading to the exciton localization, which plays a very important role in the optical dynamics.

Unique spectral properties make J-aggregates excellent candidates for novel photonic materials especially in the form of thin films, particularly, polymer films. Indeed, while in solutions J-aggregates often possess low photostability, in polymer films their stability becomes much higher. However, J-aggregate formation in polymer films reveals also some drawbacks, such as low fluorescence quantum yield of formed J-aggregates. One of the possible reasons is exciton self-trapping in a more rigid environment. The exciton self-trapping appears when the excitons localize themselves in the self-induced potential well caused by the large lattice distortion under the condition of strong exciton-phonon coupling.

The feature of J-aggregates is a strong dependence of exciton-phonon coupling, and hence the self-trapping efficiency, on the exciton coherence length [1-3]. Indeed, it was demonstrated that the exciton-phonon coupling is less for the J-aggregates with larger the exciton coherence length [1]. Thus, if one will increase the exciton coherence length for J-aggregates it will lead to exciton-phonon coupling weakening and, hence, to the exciton self-trapping suppression, resulting to the J-aggregate fluorescence enhancement [4,5].

The present report is devoted to reviewing the features of the exciton self-trapping in J-aggregates depending on their formation conditions. Also the ways to control the self-trapping efficiency, and, hence, the fluorescence quantum yield, are shown.

- [1] Yu.V. Malyukin, A.V. Sorokin, V.P. Semynozhenko, Low Temp. Phys. 42, 429 (2016).
- [2] A.V. Sorokin, N.V. Pereverzev, I.I. Grankina, S.L. Yefimova, Yu.V. Malyukin, J. Phys. Chem. C, 119, 27865 (2015).
- [3] A.V. Sorokin, I.Yu. Ropakova, S. Wolter, R. Lange, I. Barke, S. Speller, S.L. Yefimova, Yu.V. Malyukin, S. Lochbrunner, J. Phys. Chem. C, 123, 9428 (2019).
- [4] G.Ya. Guralchuk, I.K. Katrunov, R.S. Grynyov, A.V. Sorokin, S.L. Yefimova, I.A. Borovoy, Yu.V. Malyukin, J. Phys. Chem. C, 112, 14762 (2008).
- [5] A.V. Sorokin, I.I. Grankina, I.I. Bespalova, A.V. Aslanov, S.L. Yefimova, Yu.V. Malyukin, J. Phys. Chem. C, 124, 10167 (2020).

The strain impact on ferromagnetic/graphene/ferroelectric nanostructures

M.V. Strikha^{1,2}, E.A. Eliseev³, A.N. Morozovska⁴

¹*Taras Shevchenko National University of Kyiv, Faculty of Radiophysics, Electronics and Computer Systems, Pr. Akademika Hlushkova 4g, 03022 Kyiv, Ukraine,*

²*V.Lashkariov Institute of Semiconductor Physics, National Academy of Sciences of Ukraine, Pr. Nauky 41, 03028 Kyiv, Ukraine*

³*Institute for Problems of Materials Science, National Academy of Sciences of Ukraine, Krjjanovskogo 3, 03142 Kyiv, Ukraine*

⁴*Institute of Physics, National Academy of Sciences of Ukraine, Pr. Nauky 46, 03028 Kyiv, Ukraine,
maksym.strikha@gmail.com*

We proposed a phenomenological model for the nanostructure "high temperature ferromagnetic insulator/ graphene/ ferroelectric film" (see Fig. 1) taking into account the shift of the Dirac point due to the proximity of ferromagnetic insulator and using the Landauer formula for the conductance of the graphene channel. Spin-polarized conductance was calculated with a special attention to the control of electric polarization in a multiaxial ferroelectric film by a misfit strain [1].

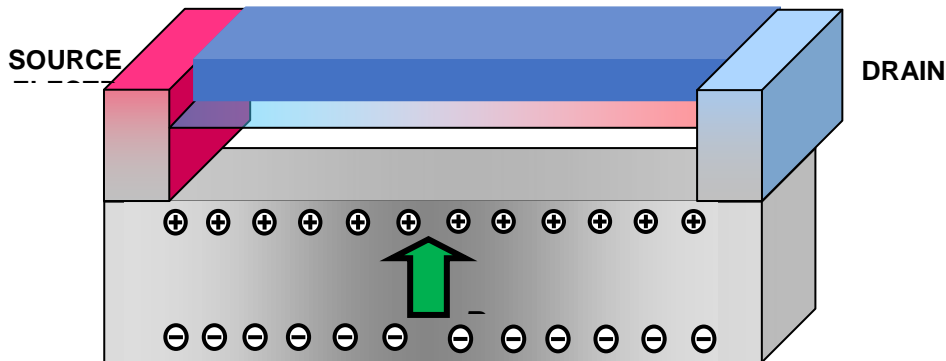


Fig. 1. Graphene single-layer placed between a single-domain ferromagnetic insulator and a polarized ferroelectric film. Adapted from Ref. [1].

The analytical expressions showing that the strain-dependent ferroelectric polarization governs the concentration of two-dimensional charge carriers and Fermi level in graphene in a self-consistent way was derived. It was shown that the graphene channel length should be shorter than an electron mean free path for spin polarization parallel with the one in the graphene channel modified by ferromagnetic insulator, and longer than an electron mean free path for spin polarization antiparallel with the one in graphene channel. However, because of long spin-flip length in a standard graphene-on-substrate, this restriction doesn't lead to ultra-short channels. Obtained results demonstrate the realistic opportunity to control the spin-polarized conductance of graphene by a misfit strain at room and higher temperatures in the nanostructures CoFeO₄/graphene/PZT and Y₃Fe₅O₁₂/graphene/PZT, and so open the possibilities for the applications of ferromagnetic/graphene/ferroelectric nanostructures as non-volatile spin filters and spin valves operating at room and higher temperatures.

A.N.M. work is supported by the National Research Foundation of Ukraine (Grant application 2020.02/0027).

[1] Eugene A. Eliseev, Anna N. Morozovska, and Maksym V. Strikha, Physical Review Applied 14, 024081 (2020).

Implementation of a simultaneous message-passing protocol using optical vortices

M. Szatkowski¹, J. Koechlin², J. Masajada¹, D. Lopez-Mago³

¹Wrocław University of Science and Technology, Department of Optics and Photonics,
Wybrzeże Wyspińskiego 27, 50-370 Wrocław, Poland

²University of Basel, Department of Physics, 4056 Basel, Switzerland

³Tecnológico de Monterrey, Escuela de Ingeniería y Ciencias, Ave. Eugenio Garza Sada 2501,
Monterrey, N.L. 64849, Mexico
mateusz.szatkowski@pwr.edu.pl

Beams carrying orbital angular momentum became an interesting solution for many application related to optical communication and information technologies. In this talk, the method to calculate similarities between two signals through Laguerre-Gaussian modes will be proposed.

Laguerre-Gaussian modes are generated by the Digital Micromirror Device (DMD), which simultaneously shape two separate beams, coming from the common laser source. To encode information, each of the Laguerre-Gaussian mode is shifted in phase, constructing signals that have to be compared. Polarization controlled SWAP gate exchanges information between two input signals, at the same time preventing them from being revealed. Detected intensity is proportional to the overlap of signals. Taking the advantage of a high frequency modulation offered by the DMD and integral nature of the used power meter, presented system is capable to directly provide the overlap factor represented as a single power value. Normalization procedure, implemented in the measurement itself, does not require further data post processing and offers an instant signal comparison without the access to encoded information.

This work, which uses classical light to realize a concept arising from the world of quanta, is another example of quantum-inspired analogy, easier to implement and offering more degrees of freedom. It could be applied directly in the classical world or serving as a prototype for quantum application.

Thermodynamic properties of coexisting phases of carbon tetrachloride on sublimation and melting lines

L.N. Yakub, O.S. Bodiuł

*Thermophysics Dept., Odessa National Academy of Food Technologies,
65039, Kanatnaya 112, Odessa, Ukraine
lydia.yakub@gmail.com*

Methane CH_4 , perfluoromethane CF_4 and carbon tetrachloride CCl_4 are the simplest representatives of a wide class of substances formed by molecules of tetrahedral symmetry. The increasing interest to these substances is due to the search for new energy-intensive molecular systems based on carbon materials suitable for storage and easy extraction of molecular hydrogen from them as fuel. CCl_4 (Freon R10) is one of the high-boiling substances. Its thermodynamic properties are well studied in the liquid phase and at the saturation line, but the amount of experimental data for the solid phase is limited.

The phase diagrams of methane, tetrafluoromethane, and carbon tetrachloride illustrate their complex structure and the presence of many high-pressure phases of these crystals. This work is devoted to study of the location of the melting line of CCl_4 on the phase diagram and to calculation of properties of coexisting phases of carbon tetrachloride at high pressure. We investigate the possibility of predicting the position of the melting line of carbon tetrachloride on the phase diagram, using separate equations of state for its solid and liquid phases in the framework of perturbation theory using a single small parameter;

In this study we consider exclusively phases I of solid CCl_4 , which are characterized by relatively free rotation of molecules.

In the study of thermodynamic properties of carbon tetrachloride in the high-pressure region we used the equation of state previously developed for methane [1] in the framework of the thermodynamic perturbation theory and the potential model of intermolecular interaction, in which the Lennard-Jones potential was supplemented by non-central octopol-octopol interaction of methane molecules. The exact expression of the octopol-octopol interaction of methane molecules obtained in [1] was used for analytical representation.

The equation of state for a fluid was also constructed within the framework of thermodynamic perturbation theory, including the basic system (the Lennard-Jones fluid) and the perturbation correction. For the basic Lennard-Jones system the equation of state proposed by Kolafa and Nezbeda [2] was chosen, which gives the best description of computer simulation data for the Lennard-Jones fluid.

We discuss the limits of applicability of the equations of state of the solid and liquid phases proposed earlier for methane to calculate the thermodynamic properties of its halide derivatives.

Possibilities of application of the Monte Carlo computer simulation as a tool for studying the properties of condensed phases of CCl_4 in the region of extreme state parameters are discussed and computer simulations of crystalline CCl_4 in the fcc phase from $T = 245$ K to $T = 320$ K along the melting line were performed.

- [1] L.N. Yakub, O.S. Bodiuł, Journal of Low Temperature Physics. 2017. Vol. 187. № 1. P. 33–42. DOI: <https://doi.org/10.1007/s10909-016-1721-7>
- [2] J. Kolafa, I. Nezbeda Fluid Phase Equilibria. 1994. Vol. 100. No. 1. DOI: 10.1016/0378-3812(94)80001-4

Magnetochiral effect of phonons

S. Zherlitsyn

*Hochfeld-Magnetlabor Dresden (HLD-EMFL), Helmholtz-Zentrum Dresden-Rossendorf, 01328 Dresden, Germany
s.zherlitsyn@hzdr.de*

The phonon magnetochiral effect is a nonreciprocal acoustic propagation arising due to the fundamental symmetry principles. Mirror symmetry breaking in chiral matters leads to natural optical or acoustic activity and time-reversal symmetry breaking by magnetic fields leads to magnetic optical or acoustic activity. When both symmetries are simultaneously broken, a nonreciprocal property appears - the magnetochiral effect.

We have observed the phonon magnetochiral effect in the chiral-lattice ferrimagnet Cu₂OSeO₃ below the magnetic ordering temperature $T_C \sim 58$ K [1]. Our high-resolution ultrasound experiments on this material have revealed that the sound velocity differs for parallel and antiparallel propagation with respect to the external magnetic field. The sign of the nonreciprocity depends on the chirality of the crystal in accordance with the selection rules of the magnetochiral effect. The nonreciprocity is enhanced nonlinearly towards higher ultrasound frequencies.

The underlying picture is that the acoustic phonons inherit the nonreciprocity from the asymmetric magnon excitations via a magnon-phonon band hybridization. This magnon-phonon hybridization results in a band repulsion or anticrossing, which deforms the linear dispersion of the phonons. For the origin of the magnon-phonon hybridization, we propose a chiral magnetoelastic coupling due to the modulation of the Dzyaloshinskii-Moriya interaction by shear strains. There is an overall agreement between the theory and experiment.

We acknowledge the support of the Hochfeld-Magnetlabor Dresden at HZDR, a member of the European Magnetic Field Laboratory (EMFL), and the Deutsche Forschungsgemeinschaft (DFG) through SFB 1143.

- [1] T. Nomura, X.-X. Zhang, S. Zherlitsyn, J. Wosnitza, Y. Tokura, N. Nagaosa, and S. Seki, Phys. Rev. Lett. 122, 145901 (2019).

Latest Advances in Theory of Logarithmic Fluids: Polycrystalline Metals and Superfluid Stars

K.G. Zloshchastiev

*Institute of Systems Science, Durban University of Technology, Durban 4000, South Africa
kostiantynz@dut.ac.za*

An up-to-date review of past, current and future studies of the logarithmic fluid hydrodynamic models is presented. We begin from a pedagogical introduction into a large class of condensate-like strongly-interacting materials and many-body systems, which allow description in terms of a single macroscopic function, at least effectively or in a leading-order approximation. Recently proposed statistical mechanics arguments [1] and previously known Madelung hydrodynamical presentation [2] reveal that the logarithmic nonlinearity occurs in equations describing such matter. From the viewpoint of classical fluid mechanics, the resulting equations describe in the simplest case the irrotational and isothermal flow of a two-phase barotropic compressible inviscid fluid with internal capillarity and surface tension [3]. We demonstrate the emergence of Hilbert space and spontaneous symmetry breaking in this class of fluids, which leads to a number of wave-mechanical and topological effects [4].

The applications of such fluids can be found in both classical and quantum physics. In quantum physics, such fluids can be used for describing strongly-interacting quantum fluids [5-9], including He II, a superfluid component of He-4 [8,9]. In classical realm's applications, one can show that the logarithmic fluid models can be used for describing various Korteweg-type materials, such as magmas in volcanic conduits [3,4]. Logarithmic nonlinearity can be used in hydrodynamic models of metals and alloys, which undergo liquid-solid or liquid-gas phase transitions. One of the predictions of the theory is a periodic pattern of density inhomogeneities occurring in the form of either bubbles (topological phase), or cells (non-topological phase). Such inhomogeneities are described by soliton solutions of the logarithmic wave equation, gaussons and kinks, in the vicinity of the liquid-solid phase transition. During the solidification process, these inhomogeneities become centers of nucleation. The theory thus predicts a Gaussian profile of material density inside such a cell, which should manifest in Gaussian-like profiles of microhardness inside a grain. We report experimental evidence of large-scale periodicity in the structure of grains in the ferrite in steel, copper, austenite in steel, and aluminium-magnesium alloy; and also Gaussian-like profiles of microhardness inside an averaged grain in these materials [10].

Yet another range of applications of the “logarithmic” matter can be found in relativistic astrophysics. One can demonstrate the existence of equilibria in self-gravitating logarithmic fluid, described by spherically symmetric nonsingular finite-mass asymptotically-flat solutions. Unlike other Bose liquid star models known to date, these equilibrium configurations are shown not to have scale bounds for their gravitational mass or size. Therefore, they can describe massive dense astronomical objects, such as bosonized superfluid stars or cores of neutron stars [11].

- [1] K.G. Zloshchastiev, *Z. Naturforsch. A* 73, 619 (2018).
- [2] Y.A. Rylov, *J. Math. Phys.* 40, 256 (1999).
- [3] S. De Martino, M. Falanga, C. Godano and G. Lauro, *Europhys. Lett.* 63, 472 (2003).
- [4] K.G. Zloshchastiev, *Europhys. Lett.* 122, 39001 (2018).
- [5] A. Avdeenkov and K.G. Zloshchastiev, *J. Phys. B: At. Mol. Opt. Phys.* 44, 195303 (2011).
- [6] B. Bouharia, *Mod. Phys. Lett. B* 29, 1450260 (2015).
- [7] K.G. Zloshchastiev, *Z. Naturforsch. A* 72, 677 (2017).
- [8] K.G. Zloshchastiev, *Eur. Phys. J. B* 85, 273 (2012).
- [9] T.C. Scott and K.G. Zloshchastiev, *Low Temp. Phys.* 45, 1231 (2019).
- [10] M. Kraiev, K. Domina, V. Kraieva and K. G. Zloshchastiev, *JPCS* 1416, 012020 (2019).
- [11] K.G. Zloshchastiev, *FNT* 47, 103 (2021).

Pressure-tuned magnetic interactions in a triangular-lattice quantum antiferromagnet

S. Zvyagin

*Dresden High Magnetic Field Laboratory (HLD)
Helmholtz-Zentrum Dresden Rossendorf (HZDR)
01328 Dresden, Germany
s.zvyagin@hzdr.de*

Quantum triangular-lattice antiferromagnets are important prototype systems to investigate numerous phenomena of the geometrical frustration in condensed matter. Apart from highly unusual magnetic properties, they possess a rich phase diagram (ranging from an unfrustrated square lattice to a quantum spin liquid), yet to be confirmed experimentally. One major obstacle in this area of research is the lack of materials with appropriate (ideally tuned) magnetic parameters.

Using Cs_2CuCl_4 as a model system, we demonstrate an alternative approach, where, instead of the chemical composition, the spin Hamiltonian is altered by hydrostatic pressure. The approach combines high-pressure electron spin resonance and r.f. susceptibility measurements, allowing us not only to quasicontinuously tune the exchange parameters, but also to accurately monitor them.

Our experiments indicate a substantial increase of the exchange coupling ratio from 0.3 to 0.42 at a pressure of 1.8 GPa, revealing a number of emergent fieldinduced phases.

[1] S.A. Zvyagin, D. Graf, T. Sakurai, S. Kimura, H. Nojiri, J. Wosnitza, H. Ohta, T. Ono, and H. Tanaka, Nat. Comm. 10, 1064 (2019).

Goos-Hänchen Effect and Brillouin Light Scattering

I.L. Lyubchanskii^{1,2}

¹*O.Galkin Donetsk Institute for Physics and Engineering NAS of Ukraine,
03028, Kyiv, Ukraine*

²*Faculty of Physics, V. N. Karazin Kharkiv National University,
61022, Kharkiv, Ukraine
ILyubchanskii@gmail.com*

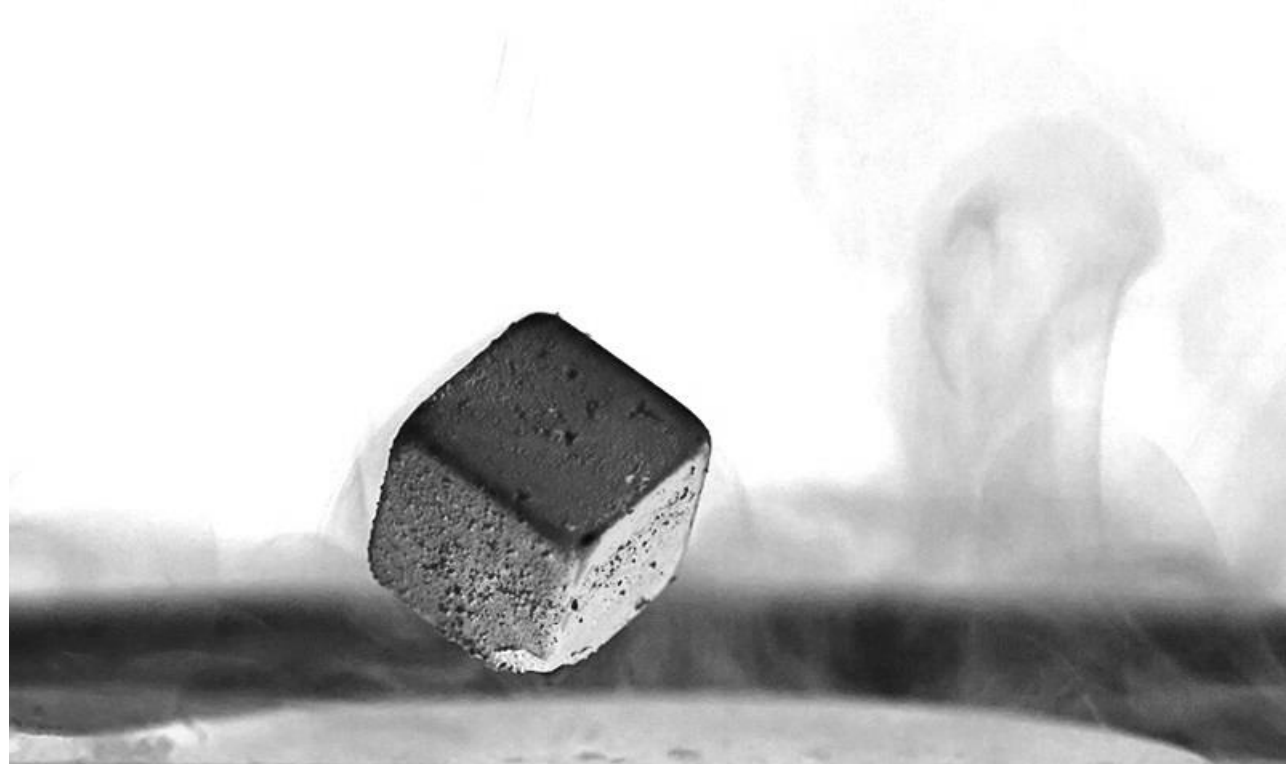
The effect of the lateral beam shift at the reflection of light from the interface between two media known as the Goos–Hänchen effect (GHE) was observed for the first time in a glass [1] when

The incidence angle of the light beam was close to the total internal reflection angle. The GHE has been studied in stationary cases when the incident and reflected beams were at the same frequencies.

In optically nonlinear media, the GH effect has been studied for materials with quadratic optical nonlinearity for three electromagnetic wave (EMW) interaction, i.e., for the second-harmonic generation [2,3]. It should be expected that it would be possible to observe the lateral shift in the case of three-wave interaction when one of these waves is an acoustic wave (AW). This type of coupling between the EMWs and AWs, which can be described via photoelastic interaction [4], leads to the well-known phenomenon of inelastic light scattering by sound (or acoustical phonons), i.e., Brillouin light scattering (BLS) [5]. In this case, a reflected wave at the frequency $\omega \pm \Omega$ will also be characterized by a lateral shift, where ω and Ω are the angular frequencies of the EMW and AW, respectively.

In this presentation, in the framework of the phenomenological description, the GHE at BLS by AWs will be presented. We investigate two possible ways (direct and cascade) to observe the GHE for both longitudinal and transversal AWs. In the direct case, the incident light wave with the frequency ω interacts with the AW with the frequency Ω , and the reflected EMW with the frequency $\omega \pm \Omega$ will undergo a lateral shift. In the cascading case, the incident light beam with the frequency ω is reflected from the interface, where the GHE takes place and, after that, the reflected EMW interacts with the AW, and the registered spatially shifted radiation will be at the frequency $\omega \pm \Omega$, as in the direct process [6]. Similar results for BLS by spin waves in the similar approach but with taking into account magneto-optical interaction will be presented too.

- [1] F. Goos and H. Hänchen, Ann. Phys. 436, 333 (1947).
- [2] H. Shih and N. Blombergen, Phys. Rev. A 3, 412 (1971).
- [3] V. J. Yallapragada, A. V. Gopal, and G. S. Agarwal, Opt. Express 21, 10878 (2013).
- [4] M. Born and E. Wolf, Foundations of Optics, 7th ed. (Cambridge University Press, 1999).
- [5] I. L. Fabelinskii, Molecular Scattering of Light (Plenum Press, 1968); translated from Russian (Nauka, 1965).
- [6] Y. Dadoenkova, N. Dadoenkova, M. Krawszik, and I. Lyubchanskii, Opt. Lett. 43, 3965 (2018).



ELECTRONIC PROPERTIES OF CONDUCTING AND SUPERCONDUCTING SYSTEMS

Fractal analysis of the critical state of the NbTi superconductor

**O.M. Chumak^{1,2}, V.V. Chabanenko¹, V.F. Rusakov³, O.I. Kuchuk¹, I. Abaloszewska²,
O. Abaloszew², A. Nabialek², R. Puźniak²**

¹*O.Galkin Donetsk Institute for Physics and Engineering, NAS of Ukraine,
46 Nauki Ave. 46, Kyiv, 03028 Ukraine.*

²*Institute of Physics, Polish Academy of Sciences, Al. Lotników 32/46, 02-668 Warsaw, Poland.*

³*Vasyl' Stus Donetsk National University, MOE, Ul. 600 Richcha 21, Vinnytsia, 21021 Ukraine.
vikchabanenko@gmail.com*

The Hausdorff dimension has experienced application in the characterization and comparison of highly rough structures. It is famous that the concept of Hausdorff dimension is applied as well to magnetic flux front (induction of the magnetic field) analysis in superconductors [1]. The critical state of a hard superconductor is formed by stochastic jumps of Abrikosov vortices (or vortex bundles) under the action of an external magnetic field. Magneto-optical imaging (Fig.1) and analysis of the magnetic flux front in the NbTi disk in an orthogonal magnetic field (H) revealed a rough penetration front. Its structure was studied in a field up to 600 Oe and in the temperature range (T) 5 ÷ 7 K. The position of the flux front, the boundary between the region where the flux entered and the Meissner state, was fixed. The shape of the flux front curves was analyzed by the Fast Fourier Transform (FFT) method. The constructed spectral function made it possible to obtain the roughness coefficients of the magnetic flux profile and the Hausdorff's dimension to characterize the critical state of the superconductor. Hausdorff fractal dimension at the flux front is about 1.5, which is close to the result for superconducting niobium [1]. The obtained values of the roughness coefficient are in the range of 0.435-0.480. With such roughness coefficient and for the fractal nature of the front, the system obeys the model of dynamic stochastic disorder [2].

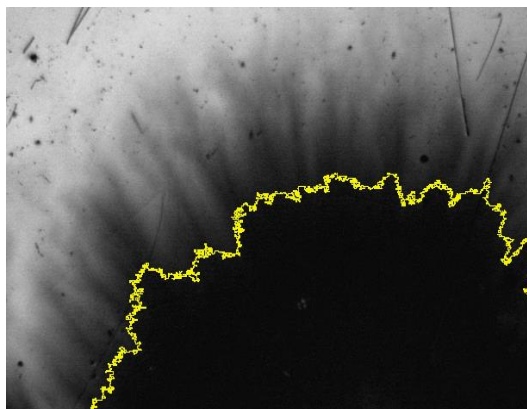


Fig.1. Magneto-optical images of flux penetration: 600 G, 6 K, NbTi disk

at different levels of induction bear the imprints of self-organized criticality in the vortex system. This can be a useful tool for studying the fractality of the dynamically formed critical state of hard superconductors. Such analysis method can also be used to improve the technology of manufacturing superconducting materials with increased stability of the critical state.

This technique was used to analyze the flux fronts after various methods of processing a superconductor: hydroextrusion and subsequent heat treatment. The analysis showed that the depth of penetration of the flux into the sample after annealing decreases significantly (approximately 4 times). This indicates an increase in the critical current density, which in turn confirms a change in the structure of the magnetic flux pinning. The difference in the roughness coefficients of the structures of the induction fronts, formed in the mode of shielding and the exit of the trapped magnetic flux, is also established.

The results show that not only the front of the magnetic flux at the Meissner level, but also the profiles imprints of self-organized criticality in the vortex system. This can be a useful tool for studying the fractality of the dynamically formed critical state of hard superconductors. Such analysis method can also be used to improve the technology of manufacturing superconducting materials with increased stability of the critical state.

- [1] V. K. Vlasko-Vlasov, U. Welp, V. Metlushko, and G. W. Crabtree. Phys. Rev. B. 69, 140504 (2004).
- [2] M. Kardar, G. Parisi, Y.-C. Zhang. Phys. Rev. Lett. 56, 889 (1986).
- [3] R. Surdeanu, R. J. Wijngaarden, E. Visser, J. M. Huijbregtse, J. H. Rector, B. Dam, and R. Griessen, Phys. Rev. Lett. 83, 2054 (1999).

Shift of the electronic bands in Fe(Se,Te) in the vicinity of the superconducting transition

Yu.V. Pustovit^{1,2}, D.P. Menesenko¹, A.A. Kordyuk²

¹*Taras Shevchenko National University of Kyiv,
64/13 Volodymyrska str., Kyiv, 01601, Ukraine*

²*Kyiv Academic University,
36 Academician Vernadsky Boulevard., Kyiv, 03142, Ukraine
jura.pustvit@gmail.com*

Fe(Se,Te) systems are interesting compounds among iron based superconductors due to puzzling physical properties and a variety of complex and competing electronic phases that coexist in such systems. In recent years these systems have got additional attention due to possible existence of topological non-trivial surface states in $\text{FeSe}_{0.55}\text{Te}_{0.45}$ [1].

Numerous articles [2,3] show existence of strong temperature induced shifts of the band structure in the center of Brillouin zone in a wide temperature range above superconducting transition. However, the changes of the band structure in the vicinity to the superconducting transition have not been well studied yet.

We have obtained ARPES spectra of the hole bands of $\text{Fe}_{1.05}\text{Se}_{0.84}\text{Te}_{0.16}$, using a photon energy of 21 eV, which corresponds to the Z point at the top of the Brillouin zone. To investigate the changes of the band structure in the vicinity to the superconducting transition, the ARPES data have been collected at the temperatures 4 K (below superconducting transition) and 20 K (above superconducting transition)[1]. To compare and single out the features that are characteristic for Fe(Se,Te), the ARPES spectra of FeSe (in the temperature range of 1.55 – 15.1 K) and $\text{Ba}(\text{Co},\text{Fe})_2\text{As}_2$ (in the temperature range of 1.1 – 25.1 K) have been obtained. To determine that FeSe undergoes superconducting transition and to estimate the value of the superconducting gap, the shift of the leading edge of energy distribution curves (EDC) have been used. It reveals the existence of the superconducting transition with the gap size approximately 3 meV that coincides with another investigations [4]. The strong downshift of both the hole-like bands (d_{yz} and d_{xz}) for $\text{Fe}_{1.05}\text{Se}_{0.84}\text{Te}_{0.16}$ with decreasing temperature have been revealed. The value of this shift is approximately 5 meV and its direction is opposite to the direction of the temperature-induced shift obtained for the temperature range from 20 K to 300 K. For the d_{xz} band of $\text{Ba}(\text{Co},\text{Fe})_2\text{As}_2$ and the d_{yz} band of FeSe the band shifts have not been observed.

This change may be a result of a complicated interplay of superconductivity and a physical mechanism that shifts the bands in the temperature range from 20 to 300 K.

- [1] P. Zhang et al., Science Vol. 360, Issue 6385, pp. 182-186 (2018).
- [2] L. C. Rhodes, M. D. Watson, A. A. Haghaghirad, M. Eschrig, and T. K. Kim, Phys. Rev. B 95, 195111 (2017).
- [3] Yu. V. Pustovit and A. A. Kordyuk, Low Temp. Phys. 45, 1381-1386 (2019).
- [4] Y. S. Kushnirenko et al., Phys. Rev. B 97, 180501(R) (2018).

Possibility for the anisotropic acoustic plasmons in LaH₁₀ and their role in enhancement of the critical temperature of superconducting transition

E.A. Pashitskii, V.I. Pentegov, A.V. Semenov

*Institute of Physics, NAS of Ukraine,
46 Nauki Ave., Kyiv, 03028, Ukraine
semenov@iop.kiev.ua*

Superconductivity at 250 K has been achieved recently in lanthanum decahydride under high (near 150 GPa) pressure [1,2]. Such nearly room-temperature superconductivity had been predicted previously for lanthanum and yttrium superhydrides at megabar pressures [3,4]. The phase with $T_c \sim 250$ K was attributed in [1,2] to the face-centered cubic (fcc) lattice structure with the stoichiometry LaH₁₀. For such compound, the first-principle calculations of the electron band structure and phonon spectra were performed [3,4] and very high values of electron-phonon coupling (EPC) constants and T_c were predicted within the Migdal – Eliashberg theory. It should be noted though, that values of about ~ 0.1 for the effective Coulomb potential were chosen in these calculations, which are negligibly small in comparison to the calculated EPC constants (2 – 2.5).

While the dominant role of the phonon mechanism of superconductivity in such compounds is evident due to the measured isotope effect with deuterium (on LaD₁₀) [2], the small values of the effective Coulomb constant chosen in theoretical calculations of the critical temperature deserve farther justification. We discuss here a possible role of the collective acoustic electronic excitations in the mechanism of the nearly room-temperature superconductivity in superhydrides at megabar pressures. We believe that the additional suppression of the Coulomb repulsion in superhydrides may be due to the appearance of additional acoustic plasmonic branches in their collective spectra as manifestation of the so called “plasmonic” mechanism of superconductivity [5,6]. In LaH₁₀ the conditions for such mechanism arise due to the hybridization of La 4f and H 1s states near the Fermi level in the vicinity of the *L*-point of the Brillouin zone (BZ) [3].

We propose an analytical model approximation for one of the resulting conducting bands obtained numerically in [3]. We generalize the Lindhard formula [7] for 3D polarization operator (PO) to the case of anisotropic uniaxial effective mass: $\varepsilon(\vec{p}) = \frac{p_\perp^2}{2m_\perp} \pm \frac{p_z^2}{2m_z}$; $p_\perp^2 = p_x^2 + p_y^2$, with $p=0$

in *L*-point, signs «+» and «-» for ellipsoid and one-sheeted hyperboloid of revolution, respectively. These shapes model the peculiarities of Fermi surface, such as “necks” and “lenses”, in the vicinities of eight *L*-points of the fcc BZ. Analytical estimates for PO as superposition of Fermi sphere and such segments, as well as numerical calculation of PO for the modeled band in the whole BZ show that in a certain range of directions in quasimomentum space an acoustic branch should appear in the spectrum of the collective electronic excitations in LaH₁₀. The contribution of these excitations to the suppression of the effective Coulomb constant is analyzed.

- [1] M. Somayazulu, M. Ahart, A. K. Mishra, Z. M. Geballe, M. Baldini, Y. Meng, V. V. Struzhkin, and R. J. Hemley, Phys. Rev. Lett. 122, 027001 (2019).
- [2] A. P. Drozdov, P. P. Kong, V. S. Minkov, et al., Nature 569, 528 (2019).
- [3] H. Liu, I. I. Naumov, R. Hoffmann, N. W. Ashcroft, and R. J. Hemley, Proc. Nat. Acad. Sci. USA 114, 6990 (2017).
- [4] H. Liu, I. I. Naumov, Z. M. Geballe, et al., Phys. Rev. B 98, 100102(R) (2018).
- [5] E. A. Pashitskii, JETP, 28, 1267 (1969).
- [6] E. A. Pashitskii, JETP, 76, 425 (1993).
- [7] J. Lindhard, Kgl. Danske Videnskab. Selskab, Math. Fys. Medd. 28.8 (1954).

The unusual microwave response of chalcogenide $\text{FeSe}_{1-x}\text{Te}_x$ film compared to other superconductors

Y. Wu¹, **A.A. Barannik**², **L. Sun**¹, **Y.-S. He**¹, **N.T. Cherpak**²

¹*Institute of Physics of Chinese Academy of Sciences, National Laboratory for Superconductivity, P.O.Box 603, Beijing, 100190, China*

²*O. Usikov Institute for Radiophysics and Electronics of NAS of Ukraine, 12 Acad. Proskura street, Kharkiv, 61085, Ukraine
wuyun@iphy.ac.cn*

The chalcogenide superconductor $\text{FeSe}_{1-x}\text{Te}_x$ is a presenter of FeSe compound family and one has a number of unusual physical features [1]. Recently, the unexpected feature was found on the temperature dependence of the microwave response of a thin $\text{FeSe}_{1-x}\text{Te}_x$ film in a hollow cavity excited with a H_{011} mode [2, 3].

It turned out that with a perpendicular orientation of the film relative to the microwave magnetic field at $T \leq T_c$ non-monotony on temperature dependence of the response was observed, which was absent in a parallel orientation. It was suggested that at $T < T_c$, the orientation of the magnetic field changes at the edge of the film. It was shown that in this case the effective surface resistance R_s^{eff} changes in such a way that nonmonotonicity may appear, since with a parallel field orientation, R_s^{eff} becomes smaller [2, 3]. This explanation assumes that the revealed feature may be observed in films of other type II superconductors.

Therefore, it becomes necessary to study the microwave response of films of other type II superconductors. In this work, we measured the microwave response of MgB_2 and $\text{DyBa}_2\text{Cu}_3\text{O}_{7-\delta}$ films using the same resonator with the same mode. And here the above mentioned response feature was not observed. The experiments with single crystals of chalcogenide $(\text{Li}_{0.8}\text{Fe}_{0.2})\text{OHFeSe}$ [4] and pnictide $\text{Ba}(\text{Fe}_{1-x}\text{Co}_x)_2\text{As}$ [5] did not reveal the effect of non-monotony observed in the $\text{FeSe}_{1-x}\text{Te}_x$ film also. Thus, we can say that the observed feature of microwave response takes place only in superconducting $\text{FeSe}_{1-x}\text{Te}_x$ films and the model proposed in [2, 3] to explain the discovered effect in $\text{FeSe}_{1-x}\text{Te}_x$ film requires revision [6].

- [1] T. Hanaguri, S. Niitaka, K. Kuroki, and H. Takagi, *Science*, 328, 474 (2010).
- [2] A.A. Barannik, N. T. Cherpak, Yun Wu, Sheng Luo, Yusheng He, M.S. Kharchenko, A. Porch, *Low Temp. Phys.* 40, 492 (2014).
- [3] A. A. Barannik, N. T. Cherpak, Y. He, L. Sun, X. Zhang, M.V. Vovnyuk, and Y. Wu, *Low Temp. Phys.* 44, 247 (2018).
- [4] A. A. Barannik, N. T. Cherpak, Y. Wu, X. Q. Zhang, J. Wang, X. L. Dong, L. Sun, and Y. S. He, *Journal of Physics: Conference Series*, 1559(1) (2020).
- [5] N. Cherpak, A. Barannik, Y. He, L. Sun, X. Zhang, P. C. Canfield, S. L. Bud'ko, M. A. Tanatar, and R. Prozorov, “Microwave surface impedance and complex conductivity of $\text{Ba}(\text{Fe}_{0.926}\text{Co}_{0.074})_2\text{As}_2$ single crystals”, unpublished.
- [6] N. Cherpak, O. Barannik, R. Prozorov, Liang Sun, M. Tanatar, Yun Wu, Yusheng He, IEEE Ukrainian Microwave Week (UkrMW). INSPEC Accession Number: 20136819 (2020).

Low field high-harmonic generation in $\text{Mo}_6\text{S}_6\text{I}_2$ Chevrel-phase superconductor

**I.R. Metskhvarishvili^{1,2}, B.G. Bendelian¹, G.N. Dgebuadze¹, G.R. Giorganashvili,
M.R. Metskhvarishvili², T.E. Lobzhanidze³**

¹*Ilia Vekua Sukhumi Institute of Physics and Technology, Laboratory of Cryogenic Technique and Technologies, Mindeli St. 7, 0186 Tbilisi, Georgia*

²*Georgian Technical University, Faculty of Informatics and Control Systems, Department of Microprocessor and Measurement Systems, Kostava St. 77, 0175 Tbilisi, Georgia*

³*Ivane Javakhishvili Tbilisi State University, Faculty of Exact and Natural Sciences, Department of Chemistry, Chavchavadze Ave. 3, 0179 Tbilisi, Georgia
bezhan20003@gmail.com*

High temperature polycrystalline superconductors are associated with the existence of superconductivity in each grain, whose parameters are similar to a bulk single crystal. Between the grains there are weak Josephson junctions, which determine the superconducting properties of the whole system. For the Josephson junctions in low fields, less than first critical field of the grains H_{c1} , a lot of irreversible and nonlinear phenomena are observed. These phenomena are characterized by the presence of high harmonics. In high temperature polycrystalline superconductors when ultraweak ac excitation field is immersed, only odd harmonic are generated. However, when dc magnetic field is applied along with the ac magnetic field, even harmonics are generated. The generation of higher harmonic components and nonlinearity of magnetization has been explained with critical state models.

The purpose of the present work is to study the high harmonics response of $\text{Mo}_6\text{S}_6\text{I}_2$ polycrystalline superconductor in ultra-weak magnetic fields in order to understand granularity nature of the Chevral phase polycrystalline superconductors. This choice was made because the ternary molybdenum chalcogenide, so called Chevral phase superconductors behave like the high temperature oxide superconductors. The Ginsburg-Landau parameter $\kappa \approx 100$ is large and the coherence length very short $\xi \approx 2-3$ nm. Inasmuch in Chevral phase superconductors ξ is of order of several angstroms, therefore there are grounds for expecting that for such values of ξ any, even a small, defect can act like a Josephson junction. Our experimental results have shown that, very weak ac magnetic fields of order of millioersteds do indeed penetrate into the $\text{Mo}_6\text{S}_6\text{I}_2$ polycrystalline superconductor and nonlinear magnetic response are analyzed in the frame work of Bean's critical state model.

This work was supported by Shota Rustaveli National Science Foundation of Georgia (SRNSFG), under GENIE project, grant number: CARYS-19-1832, Project title: Innovative Cryostat for Studying High-temperature Superconductors.

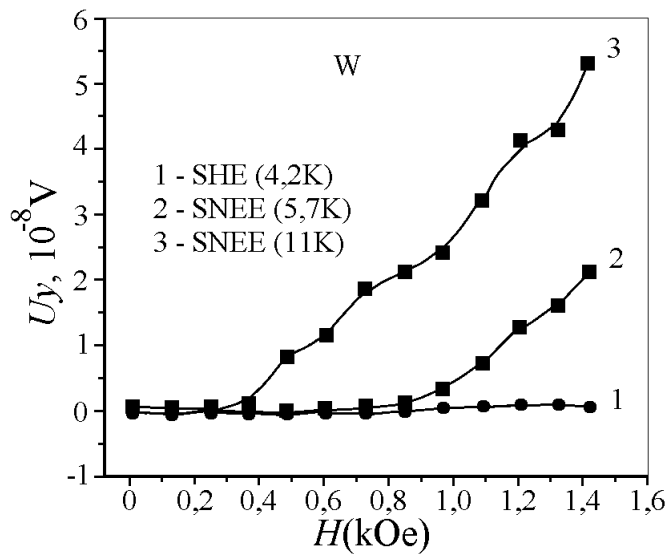
Spin Nernst effect in the platinum and tungsten samples

Yu.N. Chiang, M.O. Dzyuba

*B.Verkin Institute for Low Temperature Physics and Engineering of NAS of Ukraine,
47 Nauky Ave., Kharkiv, 61103, Ukraine
dzyuba@ilt.kharkov.ua*

The experimental observation of the spin Hall effect (SHE), for example [1], aroused great interest in the studies of the effects that are generating spin currents, since the last ones are capable to change the magnetization of the nanomagnets that can be used in memory elements and logical devices. The one of these effects, in addition to SHE, is the spin Nernst (-Ettingshausen) effect (SNEE), which was first observed by S.Meyer et al. in Pt thin film [2]. In contrast to SHE observed at the charge carriers drift caused by an electric field, in SNEE the charge drift is induced by a temperature gradient and, due to its diffusion nature, is not related to the sign of the charge carriers. The latter circumstance suggests that SHE and SNEE should be fundamentally different, especially for the metals with both negative and positive types of charge carriers.

We have studied SNEE in the macroscopic samples of the heavy metals of two types: with a predominantly negative type of the carriers (Pt) and with the carriers of both signs with equal concentration (W). It should be noted that the research of SNEE in tungsten was carried out for the first time. For the study, we used the previously proposed method with the use of the asymmetric samples, which makes it possible to study spin currents effects by electrical methods [3]. The results of the studies of the platinum samples are in qualitative agreement with early works [2], namely, both SHE and SNEE of comparable magnitude are observed. On the other hand, in tungsten SHE does not exceed the measurement error, while SNEE is significant. This can be explained by the fact that in a compensated metal, each electron k_y corresponds to a hole $-k_y$. Accordingly, their momentum-spin dynamics will be mirror-symmetric in an electric field, and the spin currents will be compensated. In the presence of a temperature gradient and, accordingly, a unidirectional drift of the electrons and the holes, their spin currents should be pairwise unidirectional, which contributes to the manifestation of SNEE, while the drift of the compensated carriers in an electric field does not lead to SHE, as shown in the figure.



The spin contributions to the Hall and Nernst- Ettingshausen effects in the high-purity tungsten.

- [1] Y. K. Kato, R. C. Myers, A. C. Gossard and D. D. Awschalom, Science 306, 1910(2004).
- [2] S. Meyer, Y.-T. Chen, S. Wimmer, et al., Nature Mater 16, 977–981 (2017).
- [3] Yu. N. Chiang and M. O. Dzyuba, EPL, 120, 17001 (2017).

Superconductivity in hole-doped Ge detected by Point-Contact Spectroscopy

N.V. Gamayunova¹, P. Szabó², J. Kačmarčík², P. Samuely², O.E. Kvintitskaya¹, L.V. Tyutrina¹, Yu.G. Naidyuk¹

¹*B.Verkin Institute for Low Temperature Physics and Engineering NASU, Kharkiv, Ukraine*

²*Centre of Low Temperature Physics, Institute of Experimental Physics SAS, Košice, Slovakia*

gamayunova@ilt.kharkov.ua

Superconductivity in the high-pressure metallic Si and Ge has been discovered more than 50 years ago with superconducting (SC) transitions $T_c=5.35$ K at 11.5 GPa and $T_c=6.7$ K at 12 GPa for Ge and Si respectively [1]. However, achieving superconductivity at ambient pressure was difficult enough. It required heavy doping beyond the metal-insulator transition for the carrier density in these materials to be sufficient to induce SC state at low temperatures. Moreover, Ge in a comparison with Si looks less promising for creating superconductivity in terms of the standard BCS model because of the lower Debye temperature [2]. But the predicted in [3] weak superconductivity in heavily hole-doped Ge at ambient pressure was observed in [2, 4, 5] and revealed $T_c = 0.45$ K, 0.5 K and 1.4 K in Ge doped by Al and Ga.

A few decades ago, degenerated Ge was studied by Yanson point-contact (PC) spectroscopy [6] to search for electron-phonon interaction function, which is responsible for superconductivity in the BCS theory. Some features associated with electron-phonon interaction was registered [7]. Here we report on the PC study of degenerated Ge with the concentration range of gallium impurities $2 \cdot 10^{17}$ — $2 \cdot 10^{18}$ cm³ [8]. Searching for SC state in doped Ge was reactivated by reporting the discovery of the superconductivity above 10 K in silicon PCs [9].

We performed the spectroscopic measurements in a liquid helium cryostat equipped with an insert for forming PCs. Before that the surfaces of Ge crystals were polished by sandpaper and cleaned by acetone at the room temperature. Then germanium PCs were created using the “needle-anvil” technique [6] by touching the sharpened PtIr wire ($\varnothing = 0.25$ mm) to the planes of the Ge crystals at helium temperature. The differential resistance spectra $dV/dI(V)$ of germanium PCs were recorded by sweeping the *dc* current I on which a small *ac* current i was superimposed using a standard lock-in technique at the temperature range 1.5–10 K and magnetic field up to 2 T.

As a result, we observed superconductivity in PCs based on p-type Ge. The SC features disappear above 6 K or above 1 T, what can be taken as the critical temperature and the critical magnetic field. The rare $dV/dI(V)$ spectra with Andreev-like double minimum structure for Ge PC were fitted within one-gap Blonder-Tinkham-Klapwijk model. The extracted SC gap demonstrate BCS-like behavior with high $2\Delta/k_B T_c$ ratio 10 ± 1 , which is 3 times higher as in conventional superconductors. Magnetic field suppresses Andreev reflection features, but the SC gap moderately decreases in magnetic field similarly as it was observed previously for type-II superconductors, including nickel borocarbide [10, 11] and iron based superconductors [12].

- [1] J. Wittig, Zeitschrift für Physik 195, 215 (1966).
- [2] T. Herrmannsdörfer, R. Skrotzki, V. Heera, et. al. Supercond. Sci. Technol. 23, 034007 (2010).
- [3] L. Boeri, J. Kortus, O.K. Anderson, J. Phys. Chem. Solids 67, 552 (2006).
- [4] T. Herrmannsdörfer, V. Heera, O. Ignatchik, et. al. Phys. Rev. Lett. 102, 217003 (2009).
- [5] S. Prucnal, V. Heera, R. Hübner, et. al., Phys. Rev. Materials 3, 054802 (2019).
- [6] Yu.G. Naidyuk and I.K. Yanson, Point-Contact Spectroscopy (New York: Springer, 2005).
- [7] Yu.G. Naidyuk, I.V. Koshkin, and A.A. Lysykh, Fiz. Nizk. Temp. 13, 103 (1987).
- [8] A.N. Ionov, I. S. Shlimak, Physics and technics of semiconductors 19, 1226 (1985).
- [9] A. Sirohi, S. Gayen, M. Aslam, G. Sheet, Appl. Phys. Lett. 113, 242601 (2018).
- [10] Yu.G. Naidyuk, O.E. Kvintitskaya, I.K. Yanson, et. al., Phys. Rev. B 76, 014520 (2007).
- [11] Yu.G. Naidyuk, O.E. Kvintitskaya, L.V. Tiutrina, et. al., Phys. Rev. B 84, 094516(2011).
- [12] Yu.G. Naidyuk, O.E. Kvintitskaya, N.V. Gamayunova, et. al. Phys. Rev. B 96, 094517 (2017).

The influence of magnetic field on phase dynamics of stacks of long Josephson junctions

A. Grib

*Physics Department, Kharkiv V. N. Karazin National University,
Svobody sq. 4, 61022, Kharkiv, Ukraine
alexander.gryb@googlemail.com*

It is known that the non-uniform distribution of critical currents along junctions causes the appearance of the movement of Josephson vortices along the junctions without applied magnetic field [1]. Due to the mixing of these excitations with Josephson generation, the so-called zero-field steps appear in the IV-characteristics of junctions at voltages which correspond to even Fiske steps [1]. In the stack of junctions, there is the interaction of individual junctions with each other due to the overlap of shielding persistent currents. As a result of this interaction, normal modes are formed in the stack. In the stack of two junctions there are only two such modes: the so called ‘in-phase mode’ and the ‘anti-phase mode’ which correspond to in-phase (or anti-phase) oscillations of voltages across junctions in the stack. Each (even) Fiske step in such a system is split to two steps which correspond to mentioned modes. The applied to such a system external magnetic field creates some dependence of critical currents along junctions which is quite different from the originally given spread of critical currents. Fiske steps can be formed now at voltages which correspond to frequencies of both odd and even geometrical resonances of the system. The aim of the present report is to state the change of Fiske steps and emission from junctions if magnetic field is applied to the stack with the original disorder of critical currents.

We modeled stacks of two Josephson junctions with the length of about three or four Josephson lengths of penetration of magnetic field. Distributions of critical currents along junctions have the Gaussian spread of about 0.1% on the average critical current. We calculated IV-characteristics and power of emission from stacks without applied magnetic field and with magnetic field. The method of calculations is described elsewhere [2]. The influence of magnetic field was expressed in normalized units of magnetic flux Φ/Φ_0 in the stack (here Φ_0 is the quantum of magnetic flux). Results of calculations can be qualitatively summarized as follows.

Without applied magnetic field ($\Phi = 0$) there are split even Fiske steps in the IV-curves of stacks. This means that there are only normal modes in the stack. Power of emission has maxima at steps which correspond to ‘in-phase modes’.

If there is the weak magnetic field ($\Phi \leq 0.2\Phi_0$), even Fiske steps which correspond to normal modes disappear and both even and odd Fiske steps which correspond to frequencies of Josephson generation of non-interacting junctions arise. This means that the normal modes are destroyed. There is some power of emission at these steps.

The following increase of the magnetic field lead to the appearance of both odd and even Fiske steps at voltages which correspond to normal modes of interacting junctions. Power of emission at these steps is very high.

In conclusion, we investigated phase dynamics of stack of two Josephson junctions with random distributions of critical currents in magnetic field. We found the region of magnetic fluxes penetrating the stack ($\Phi \leq 0.2\Phi_0$) in which normal modes are destroyed by magnetic field. This result is new and up to now is not described in the literature.

- [1] A. Barone, G. Paterno. Physics and applications of the Josephson effect. John Wiley & sons, NY, 1982.
- [2] A. Grib, S. Savich, R. Vovk, V. Shaternik, A. Shapovalov, P. Seidel, IEEE Trans. Appl. Supercond. 28, 1801106 (2018).

Magnetic transition in $\text{RuSr}_2(\text{Eu}_{1.5}\text{Ce}_{0.5})\text{Cu}_2\text{O}_{10-\delta}$ ceramic samples and VRH law

E.Yu. Beliayev, I.G. Mirzoev, V.A. Horielyi

B.Verkin Institute for Low Temperature Physics and Engineering of NAS of Ukraine,
47 Nauky Ave., Kharkiv, 61103, Ukraine
beliayev@ilt.kharkov.ua

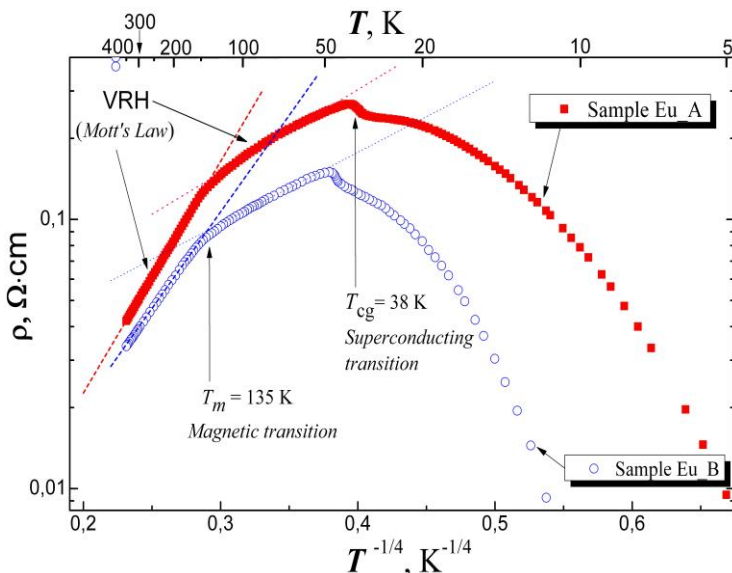


Fig. 1. VRH dependencies at $\text{AFM} \Rightarrow \text{WFM}$ transition.

temperatures near T_m , the $\rho(T)$ dependence plotted in Mott coordinates, exhibits a kink, after which in the intermediate temperature range $T = 50 \div 135$ K we again observe 3D Mott VRH behavior, but now with a changed slope. These Mott dependencies are clearly seen in Fig. 1. We assume that the above-mentioned decrease in the slope of the $\rho(T^{1/4})$ curve at temperature T_m and the corresponding decline in the Mott temperature T_0 is associated with an increase in ferromagnetic correlations and reinforcement of the magnetic ordering in the substance that leads to the alignment of electron spins in neighboring granules thereby making it easier for electrons to find a suitable state for jumping. Computer fitting for $\rho(T)$ curves, shown in Fig. 1 in the sections corresponding to the VRH conductivity, gives for the sample Eu_A the Mott temperature $T_0 = 153820$ K in AFM state and $T_0' = 2550$ K in WFM state. For the sample Eu_B, we have $T_0 = 74400$ K and $T_0' = 1385$ K, respectively. Such a decrease in Mott temperature (assuming the immutability of the density of states at the Fermi level $g(E_F)$) according to the formula $T_0 \propto 1/\{g(E_F) \cdot k_B \cdot a^3\}$ corresponds to an increase in the radius of localization of the charge carriers a after establishing the weak ferromagnetic ordering in $\sqrt[3]{T_0'/T_0} \approx 3.75 \div 3.9$ times. In pressed sintered powders, each granule usually has 4 nearest contacting neighbors. We believe that such a change in the slopes of $\rho \propto f(T^{1/4})$ dependencies and Mott's temperatures is associated with ferromagnetic correlations in the contacting grains and an increase in magnetic ordering. This leads to the alignment of the electron spins in the adjacent granules and thus facilitates the tunneling of charge carriers between them.

Studying the $\rho(T)$ behavior for two ruthenocuprate samples [1] with different oxygen content (Fig. 1), we note two regions of compliance with 3D Mott's variable range hopping (VRH) law $\rho \propto \exp\{(T_0/T)^{1/4}\}$. One region corresponds to the electron hopping between ruthenocuprate granules, when the intergranular substance is in the state of the AFM insulator (this law is well obeyed in the temperature interval from $T = 350$ K down to $T_m = 135$ K which, as is known from previously published magnetic studies, corresponds to the $\text{AFM} \Rightarrow \text{WFM}$ magnetic transition). Another region corresponds to the VRH hopping between the same granules, but now being in the WFM state. For

[1] E.Yu. Beliayev, Functional Materials, 23, No.2 (2016), p. 165-169.

The effect of hydrogen thermo diffusion on the superconducting properties of FeTe_{0.65}Se_{0.35} single crystals

S.I. Bondarenko¹, A.I. Prokhvatilov¹, R.Pužniak², J.Pietosa², A.A. Prokhorov³, V.V. Meleshko¹, V.P. Timofeev¹, V.P. Koverya¹, D.J. Gawryluk^{2,4}, A. Wiśniewski²

¹B.Verkin Institute for Low Temperature Physics and Engineering of NAS of Ukraine,
47 Nauky Ave., Kharkiv, 61103, Ukraine

²Institute of Physics of the Polish Academy of Sciences,
Aleja Lotników 32/46, PL-02668 Warsaw, Poland

³Institute of Physics of the Czech Academy of Sciences,
Na Slovance, 182 21 Praha 8, Czech Republic

⁴Laboratory for Scientific Developments and Novel Materials, Paul Scherrer Institute,
CH-5232 Villigen PSI, Switzerland
koverya@ilt.kharkov.ua

High-quality single crystals of FeTe_{0.65}Se_{0.35}, with the onset of superconducting state transition temperature (T_c) at about 14 K [1], have been hydrogenated for 10 hours at various temperatures, ranging from 20 to 250 °C [2].

It was shown that, molecular impurities do not change matrix symmetry, unless the material is not destroyed under hydrogenation at temperature of 250 °C. However, the tetragonal matrix becomes unstable and crystal symmetry is reduced for the material with hydrogen molecules dissociated already at temperature of 200 °C.

It was found that, the T_c onset is basically unchanged under hydrogenation until material is not destroyed. However, the bulk superconducting state transition temperature, taken at the middle of the transition, of about 12–13 K for the as-grown FeTe_{0.65}Se_{0.35} increases by 1–2 K to about 13–14 K and critical current density determined in magnetic field range of 0–70 kOe increases by 10–100 times as a result of hydrogenation at 200 °C for 10 h. Electron paramagnetic resonance studies confirmed higher value of the bulk T_c for hydrogenated crystals.

Obtained results indicate that, thermal diffusion of hydrogen leads to substantial structural changes, what significantly affects the superconducting state properties. It is caused by degeneration of crystallographic quality in hydrogenation process for specific crystal and not as a result of tailoring crystal growth conditions for various crystals, leading to the growth of the crystals with distinct crystallographic quality and thus with distinct superconducting state properties. Observed increase in the critical current density can be explained by the appearance of additional pinning centers due to significant mechanical stresses associated with the rearrangement of the crystal lattice after hydrogenation. Obtained results confirm that the inhomogeneous spatial distribution of ions in chalcogenides with nanoscale phase separation enhances the superconductivity in this system.

[1] A.G. Sivakov, S.I. Bondarenko, A.I. Prokhvatilov, V.P. Timofeev, A.S. Pokhila, V.P. Koverya, I.S. Dudar, S.I. Link, I.V. Legchenkova, A.N. Bludov, V.Yu. Monarkha, D.J. Gawryluk, J. Pietosa, M. Berkowski, R. Diduszko, R.Puzniak, A.Wisniewski, Supercond. Sci. Technol. 30, 015018 (2017).

[2] A.I. Prokhvatilov, V.V. Meleshko, S.I. Bondarenko, V.P. Koverya, A. Wiśniewski, Low Temp. Phys. 46, 181 (2020).

Josephson properties of phase-slip centers in narrow channels made of a bimetallic superconducting-normal film

A.G. Sivakov, S.O. Kruhlov, A.S. Pokhila

B.Verkin Institute for Low Temperature Physics and Engineering of NAS of Ukraine,
47 Nauky Ave., Kharkiv, 61103, Ukraine
kruhlov@ilt.kharkov.ua

The behavior of the current-voltage characteristics (CVC) of narrow channels made of tin films shunted by aluminum films is studied in microwave fields of various powers and frequencies. It is shown that the deposition of a normal metal on a narrow superconducting channel smooth out the jumps in the CVC associated with the appearance of individual phase-slip centers (PSC). In this case, in the resistive region above the critical current under the influence of microwave power, a series of Shapiro current steps appears on the CVC, completely repeating the behavior of the Josephson junction (Fig. 1). The critical currents of the Shapiro steps oscillate when the microwave power changes and the critical currents of the even and odd steps changes in antiphase (Fig. 2). This fact indicates that the current-phase dependence of the shunted channel differs from the sawtooth current-phase dependence of a conventional superconducting channel with a PSC. It should be noted that the voltage value of the Shapiro steps of the shunted channel does not correspond to the voltage following from the Josephson relation: $V \neq \frac{h}{2e} f$.

This work is supported by the NATO SPS Programme through grant No. G5796.

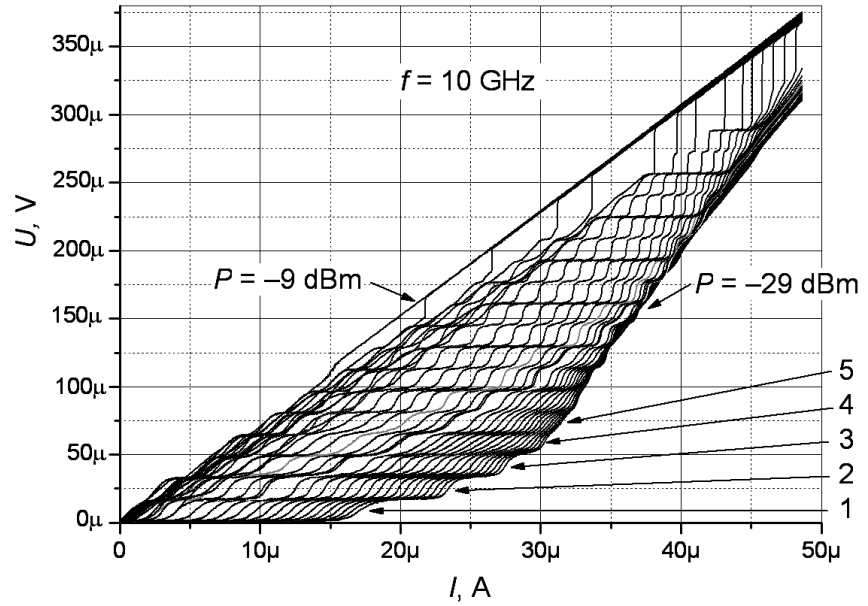


Fig. 1

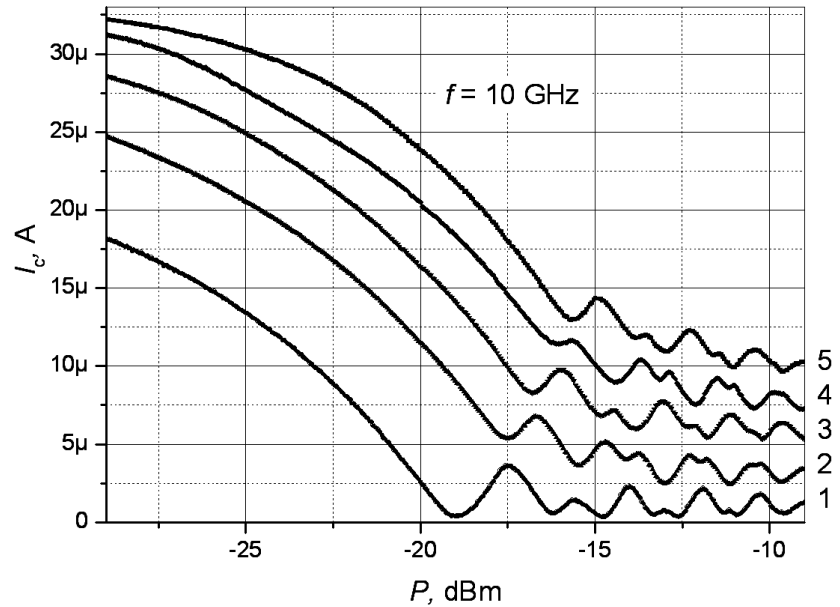


Fig. 2

Magnetic and structural properties of $\text{La}_{1-x}\text{Gd}_x\text{CoO}_3$ compounds

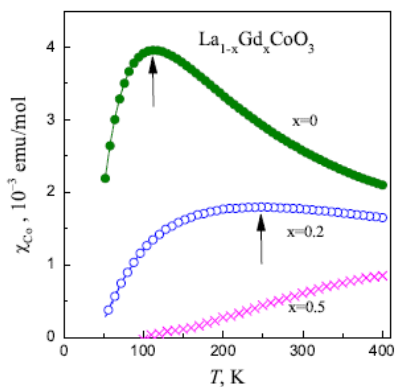
A.S. Panfilov¹, A.A. Lyogenkaya¹, G.E. Grechnev¹, V.A. Pashchenko¹, L.O. Vasylechko², V.M. Hreb², A.V. Kovalevsky³

¹*B. Verkin Institute for Low Temperature Physics and Engineering, National Academy of Sciences of Ukraine, 61103 Kharkov, Ukraine*

²*Lviv Polytechnic National University, 79013 Lviv, Ukraine*

³*Department of Materials and Ceramic Engineering, CICECO - Aveiro Institute of Materials, University of Aveiro, 3810-193 Aveiro, Portugal
alyogenkaya@gmail.com*

One of the effective methods for studying a phenomenon of the spin crossover of Co^{3+} ions in RCO_3 cobaltites is to explore the dependence of their magnetic susceptibility on temperature and the unit cell volume. Such studies for LaCoO_3 [1, 2] and for a number of RCO_3 compounds ($\text{R} = \text{Pr, Nd, Sm, Eu}$) [3] have revealed a strong increase under pressure of the energy difference between the ground and excited states of these compounds, which correspond to the non-magnetic low spin state ($\text{LS}, S=0$) and the magnetic state with either intermediate ($\text{IS}, S=1$) or high ($\text{HS}, S=2$) spin value of the Co^{3+} ions. The magnetic susceptibility studies for $\text{La}_{1-x}\text{R}_x\text{CoO}_3$ compounds ($\text{R} = \text{Pr, Nd, Sm, Eu, Gd}$) have provided some information on the behavior of Co^{3+} spin state under chemical pressure, which corresponds to a decrease in the unit cell volume when replacing the La^{3+} ions with the smaller R^{3+} ones. The main qualitative result of these studies is the observation of a shift of the characteristic maximum in the temperature dependence of the Co^{3+} ions magnetic susceptibility, χ_{Co} , towards higher temperatures and a simultaneous decrease in its magnitude (in figure).



Temperature dependencies of the Co^{3+} ions magnetic susceptibility χ_{Co} in compounds

dependence of the Co^{3+} spin state in these compounds on temperature and on decrease of the lattice volume under substituting La^{3+} with smaller Gd^{3+} ions. The results of analysis of the obtained experimental data in the framework of the two-level model are used to clarify a type of the spin state transition of Co^{3+} ions in $\text{La}_{1-x}\text{Gd}_x\text{CoO}_3$ compounds with different gadolinium content.

However, a quantitative estimation of χ_{Co} in $\text{La}_{1-x}\text{R}_x\text{CoO}_3$ systems is somewhat complicated by a large R^{3+} ions magnetism, which has to be carefully evaluated. It should be noted the similarity in sign and magnitude of the physical and chemical pressure effects on the excitation energy. Such similarity indicates a clear correlation between the spin state of cobalt ions and the lattice volume. To get more information on the relationship between the spin state of cobalt ions in RCO_3 compounds and their lattice parameters we have studied the structural and magnetic properties of $\text{La}_{1-x}\text{Gd}_x\text{CoO}_3$ compounds with $x = 0; 0.2; 0.5$ and 1.0 .

The aim of this work was to explore

[1] K. Asai, O. Yokokura, M. Suzuki, T. Naka, T. Matsumoto, H. Takahashi, N. Mori, K. Kohn, J. Phys. Soc. Jpn., 66 967 (1997).

[2] A.S. Panfilov, G.E. Grechnev, I.P. Zhuravleva, A.A. Lyogenkaya, V.A. Pashchenko, B.N. Savenko, D. Novoselov, D. Prabhakaran, I.O. Troyanchuk, Low Temp. Phys., 44 328 (2018).

[3] A.S. Panfilov, G.E. Grechnev, A.A. Lyogenkaya, V.A. Pashchenko, I.P. Zhuravleva, L.O. Vasylechko, V.M. Hreb, V.A. Turchenko, D. Novoselov, Phys. B: Cond. Mat., 553 80 (2019).

Magnetoresistive study of the excess conductivity in YBCO monolayers

E.V. Petrenko¹, L.V. Omelchenko¹, A.L. Solovjov¹, N.V. Shitov¹, K. Rogacki²

¹*B.Verkin Institute for Low Temperature Physics and Engineering of NAS of Ukraine,
47 Nauky Ave., Kharkiv, 61103, Ukraine*

²*Institute for Low Temperatures and Structure Research, Polish Academy of Sciences,
P.O. Box 1410, 50-950 Wroclaw, Poland
petrenko@ilt.kharkov.ua*

It is believed that understanding the mechanism of electron pairing in high-temperature superconductors (HTSC) will indicate the direction of synthesis of superconductors with a desired high T_c . For this, it is necessary to study the properties of HTSCs in the normal state, where the pseudogap is opened at $T^* \gg T_c$. Applying of an external magnetic field is one of the excellent methods to study superconducting fluctuations in HTSCs in the vicinity of critical temperature T_c .

From the literature, it is known that the orbital motion of the superconducting carriers is strongly suppressed when $\mathbf{H} \perp \mathbf{c}$ axis is applied. For this reason, only the Zeeman terms contribute to the fluctuation conductivity.

In our work, we have studied a high quality 100 nm-thick YBCO film with $T_c = 88.7$ K. The resistive measurements have been performed up to 8 T in $\mathbf{H} \parallel ab$ configuration in order to extract the pure Zeeman contributions to magneto-conductivity $\Delta\sigma_H$.

According to Aronov *et al.* [1], the contribution of the Zeeman effect on the Aslamazov-Larkin (ALZ) and Maki-Thompson (MTZ) terms reads as following:

$$\Delta\sigma_{ALZ} = -0.526 \frac{e^2}{\hbar d \varepsilon^2} \frac{1+\alpha}{(1+2\alpha)^{3/2}} \left[\frac{\omega_s}{4\pi k_B T_c} \right]^2 \quad (1)$$

and

$$\Delta\sigma_{MTZ} = -\frac{e^2}{16\hbar d \varepsilon} \left[\frac{1+\delta}{(1+2\delta)^{3/2}} - \frac{1+\delta+\delta/\alpha}{[(1+\delta/\alpha)(1+2\delta+\delta/\alpha)]^{3/2}} \right] \left[\frac{\omega_s \tau_\phi}{\hbar} \right]^2 \quad (2)$$

where $\omega_s = g\mu_B H$ is the Zeeman energy, g is the Lande g factor, μ_B is the Bohr magneton, τ_ϕ is the phase relaxation time, k_B is the Boltzmann constant, \hbar is the reduced Planck's constant, d is the length of the unit cell along the c -axis, α and δ are pairing and pair-breaking parameters, respectively, and ε is the reduced temperature.

It was shown that the found $\Delta\sigma_H$ is well described within the ALZ and MTZ approaches in magnetic fields starting only from 3 T. The clear crossover, observed at 91.7 K, retains up to 6 T, up to which the 2D-MTZ contribution still persists. With further increase of magnetic field, the magneto-conductivity shows exclusively ALZ behavior.

An additional analysis of the upper critical field within the Werthamer–Helfand–Hohenberg (WHH) theory [2] allowed us to determine corresponding coherence lengths in the ab -plane ($\xi_{ab} = 10.1$ Å) and along the c -axis ($\xi_c = 3.3$ Å) in a good agreement with the literature data [3].

- [1] A.G Aronov, S. Hikami and A.I. Larkin, Phys. Rev. Lett. 62, 965 (1989).
- [2] N.R. Werthamer, E. Helfand, and P.C. Hohenberg. Phys Rev. 147, 295 (1966).
- [3] J. Sugawara, H. Iwasaki, N. Kobayashi, H. Yamane, and T. Hirai, Phys Rev.B 46, 22 (1992).

Effect of MWCNT content on electrical properties of ternary PVDF/PANI/MWCNT nanocomposite at low temperature

R.M. Rudenko¹, O.O. Voitsihovska¹, V.M. Poroshin¹, M.V. Petrychuk², A.S. Nikolenko¹, N.A. Ogurtsov³, Yu.V. Noskov³, D.O. Sydorov³, A.A. Pud³

¹*Institute of Physics, NAS of Ukraine, 46 avenu Nauky, 03680, Kyiv, Ukraine*

²*Taras Shevchenko National University of Kyiv,*

4g avenu Academician Glushkov, 01133, Kyiv, Ukraine

³*V.P. Kukhar Institute of Bioorganic Chemistry and Petrochemistry, NAS of Ukraine,*

50 Kharkivske Shose, 02160, Kyiv, Ukraine

rudenko.romann@gmail.com

In this paper we present results of an investigation of effect of multi-walled carbon nanotubes (MWCNT) content on electrical properties of a new compression molded ternary nanocomposite films with conducting polymer of polyaniline (PANI) and dielectric matrix of polyvinylidene fluoride (PVDF). Based on the results of studies of electrical resistance in a wide temperature range of 4.2–300 K (Fig. 1 a), it was found that at low temperatures for studied ternary PVDF/PANI/MWCNT nanocomposites with 0–15 wt.% of MWCNT, electrical transport occurs due to the tunneling of charge carriers between localized states, in according to the mechanism of variable range hopping conductivity of $R \sim \exp[-(T_0/T)^{1/2}]$. It was found that the value of the characteristic temperature and the temperature range of variable range hopping conductivity depend on the content of MWCNTs. Increase in the MWCNT content in the nanocomposite films under study leads to decrease of characteristic temperature T_0 by two orders (Fig. 1 b). It should be noted that in the interval of 5–7.5 wt.% MWCNT content, the most pronounced changes occur, and T_0 decreases 17 times. At the same time, at 5–15 wt.% MWCNT content in ternary PVDF/PANI/MWCNT nanocomposites, the temperature range of the hopping conductivity narrows to 4.2–20 K. This fact, together with the behavior of T_0 , indicates strong qualitative changes in the conductive network, which occur when the MWCNT content is about 5 wt%. The presented results are in good agreement with the specific physicochemical interaction of the components in ternary PVDF/PANI/MWCNT nanocomposite revealed by us earlier [1].

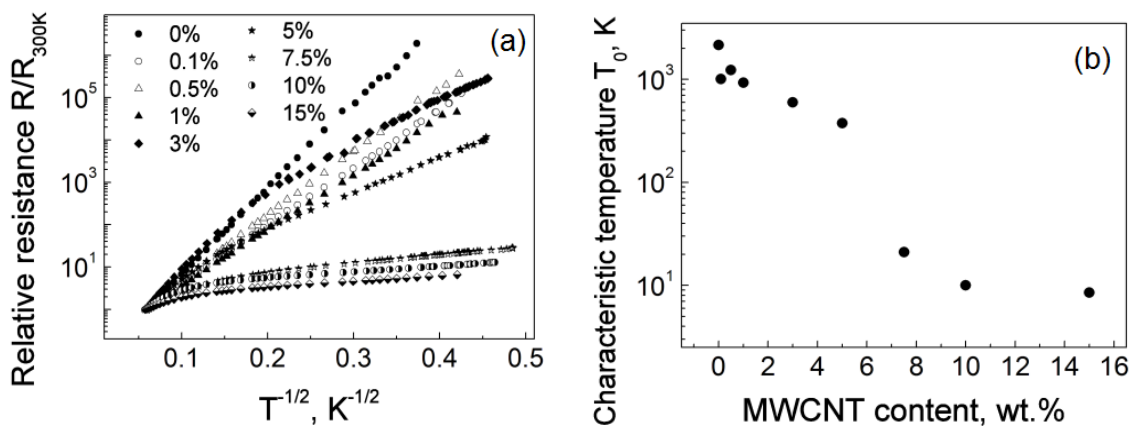


Fig. 1. Temperature dependences of relative resistance of ternary PVDF/PANI/MWCNT nanocomposite (a) and MWCNT content dependence of characteristic temperature T_0 (b).

- [1] R.M. Rudenko, O.O. Voitsihovska, V.M. Poroshin, M.V. Petrychuk, S.P. Pavlyuk, A.S. Nikolenko, N.A. Ogurtsov, Yu.V. Noskov, D.O. Sydorov, A.A. Pud, Composites Science and Technology, 198, 108284, (2020).

Electrical properties of molybdenum disulfide MoS₂ nanopowder

R.M. Rudenko, O.O. Voitsihovska, G.I. Dovbeshko, V.M. Poroshin

*Institute of Physics, NAS of Ukraine, 46 avenu Nauky, 03680, Kyiv, Ukraine
rudenko.romann@gmail.com*

Molybdenum disulfide MoS₂ is a very attractive material with the potential for multifunctional application [1-2]. The layered 2D structure of molybdenum disulfide is an inorganic analogue of graphene [3]. MoS₂ hold specific advantages over graphene, including the presence of a bandgap that is critical for electronic and optoelectronic devices. Integrating of semiconductor molybdenum with graphene opens up new possibilities for the development of next-generation, ultrathin, flexible, transparent, light emitting, light-harvesting and light-detecting devices.

This paper goal is to study the electrical properties of MoS₂ nanopowder in a wide temperature range. To understand the nature of the electrical transport in molybdenum disulfide nanopowder, temperature dependence of electrical resistance and current-voltage characteristics measurements were carried out in a wide temperature range of 60–300 K (Fig. 1) in the cryostat in a helium atmosphere. Current-voltage characteristics are symmetrical and linear, that indicates the ohmic regime of conductivity. Molybdenum disulfide MoS₂ nanopowder purchased from Aldrich-Sigma (N 804169) exhibits semiconducting behavior ($dR/dT < 0$). The analysis of the temperature dependence of the resistance indicates that thermally activated transport of charge carriers occurs in the temperature range of 200–300K. At temperatures below, hopping conduction is likely to be realized [3]. Thermal activation energy of the carriers E_a could be obtained using the Arrhenius plot $R \sim \exp(E_a/k_B T)$. For the studied MoS₂ nanopowder value of E_a is ~180 meV.

Acknowledgement. The work has received funding from the National Research Foundation of Ukraine (Grant application 2020.02/0027).

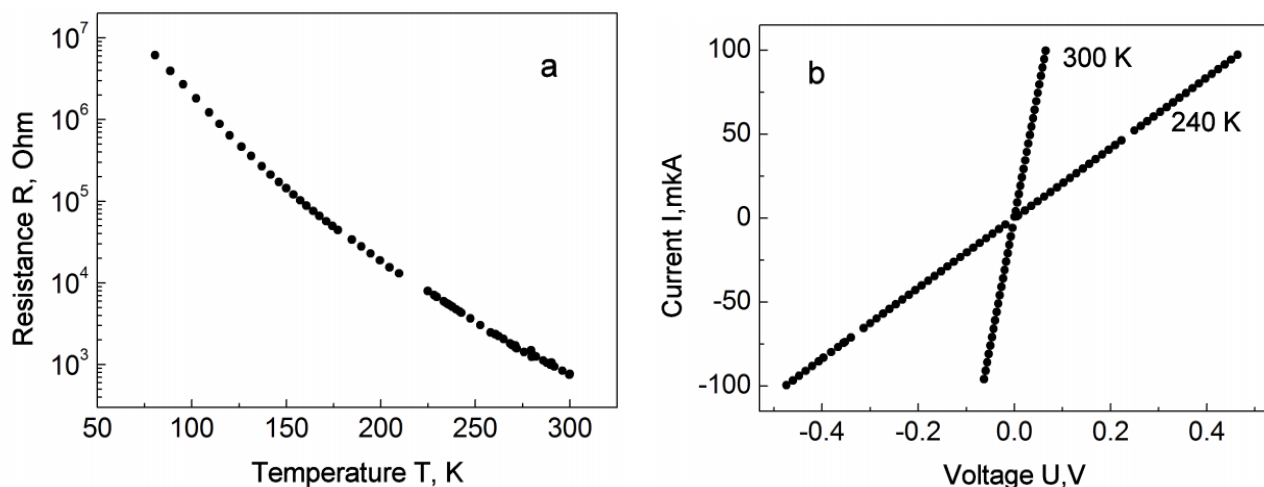


Figure. 1. Temperature dependences of resistance (a) and current-voltage characteristics (b) of molybdenum disulfide MoS₂ nanopowder.

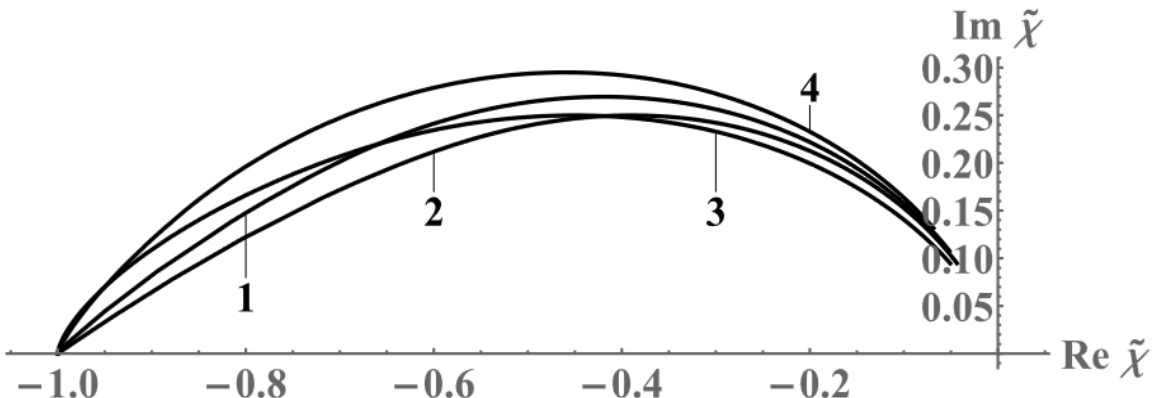
- [1] J.S. Kim, J. Kim, J. Zhao, S. Kim, J.H. Lee, Y. Jin, H. Choi, B.H. Moon, J.J. Bae, Y.H. Lee, S.C. Lim, ACS Nano 10, 2016, 7500.
- [2] M.D. Siao, W.C. Shen, R.S. Chen, Z.W. Chang, M.C. Shih, Y.P. Chiu, C.-M. Cheng, Nature Communications 9, 2018, 1442.
- [3] S. Mukherjee, S. Biswas, A. Ghorai, A. Midya, S. Das, S.K. Ray, J. Phys. Chem. C 122, 2018, 12502.

Generalized nonlinear magnetic susceptibility of superconductive disk in transverse AC field and its dependence on the pick-up coil size

A.V. Semenov

*Institute of Physics, NAS of Ukraine, 46 Nauky Ave., Kyiv, 03028, Ukraine
semenov@iop.kiev.ua*

Real and imaginary parts of the “generalized” (a pick-up coil size dependent) [1] nonlinear magnetic susceptibility $\tilde{\chi}(\alpha, h)$ are calculated for an arbitrary radii’s ratio $\alpha = r/R$ of the flat single-turn coil (r) and thin superconductive disk (R) (with thickness $d \ll R$) in the framework of the critical-state model at fundamental frequency. The results of the well-known Clem – Sanchez (CS) [2] critical-state model for nonlinear magnetic susceptibility $\chi(h)$ of the superconductive disk in transverse *ac* field with reduced amplitude h are reproduced in the limit $\alpha \rightarrow \infty$. It is shown that for a standard experimental situation (specimen inside magnetometer pick-up coil) the relative systematic error of the critical current J_c measurements is negligible (< 2%) for $\alpha > 2$, but tends to 25% while $\alpha \rightarrow 1$. On the other hand, in the case $\alpha < 1$ the generalized susceptibility’s dependence on h differs qualitatively from the CS one. It allows to pick two different points of $J_c(T)$ temperature dependence for each T run of measurement at fixed H_{ac} value (for the threshold of $\tilde{\chi}(\alpha, h)$ temperature T_0 and the maximum of $\tilde{\chi}''(\alpha, h)$ temperature T_m), rather than one point of $J_c(T_m)$ in the CS case. Series expansions of $\tilde{\chi}'(\alpha, h)$ and $\tilde{\chi}''(\alpha, h)$ were calculated for large reduced amplitude $h \gg 1$ and small amplitude $h \ll 1$ for $\alpha > 1$ (or small difference $\Delta h = h - h_0 \ll 1$ for $\alpha < 1$, where h_0 is the threshold amplitude). The amplitude parametric diagrams for generalized susceptibility are plotted for various α values.



Amplitude parametric diagrams for $\alpha \rightarrow \infty$ (1) (CS case), $\alpha = 1$ (2), $\alpha = 0.99$ (3) and $\alpha = 0.8$ (4).

- [1] A. A. Kalenyuk, G G. Kaminskyi, A. V. Semenov, V. O. Moskaliuk, and V. S. Flis, Metallofiz. Noveishie Tekhnol., 39, 441 (2017) (in Russian).
- [2] J. R. Clem and A. Sanchez, Phys. Rev. B 50, 9355 (1994).

Challenge in microwave study of unconventional superconductors in normal state and near the critical temperature

A.A. Barannik¹, S.A. Vitusevich², M.V. Vovnyuk¹, A.I. Shubnyi¹, S.K. Dukhnovskiy^{1,3}

¹*O. Usikov Institute for Radiophysics and Electronics of NAS of Ukraine,
12 Acad. Proskura street, Kharkiv, 61085, Ukraine*

²*Institute of Biological Information Processing (IBI-3): Bioelectronics, Forschungszentrum Juelich,
D-52425 Juelich, Germany*

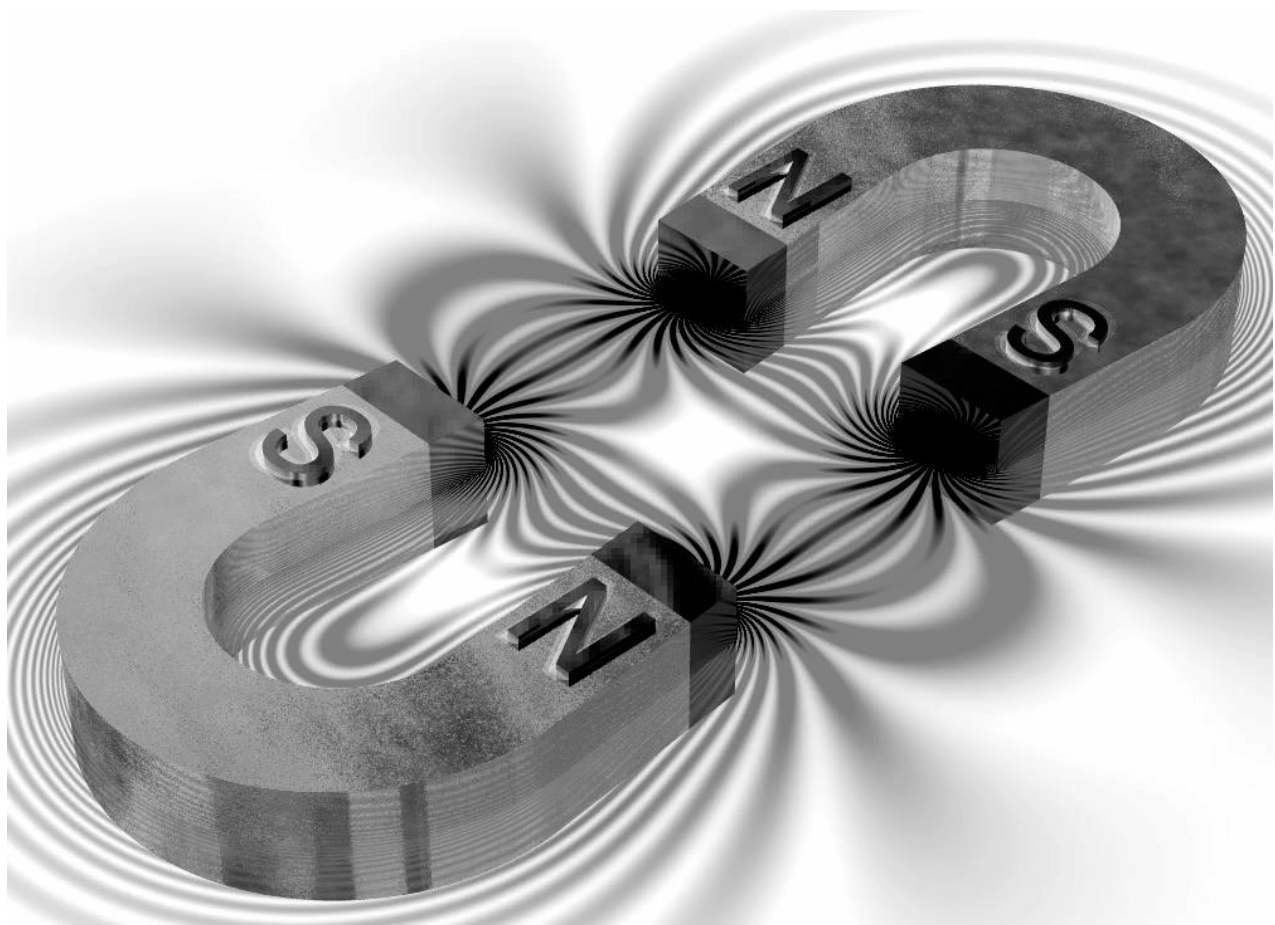
³*National University of Radioelectronics,
14 Nauky avenue, Kharkiv, 61000, Ukraine
maximus83onza@gmail.com*

In this work, we demonstrate the first results toward developing a technique for the study of unusual superconductors in the normal state and near the critical temperature, T_c , based on whispering gallery mode (WGM) sapphire resonators to analyze the material microwave surface impedance Z_s and, hence, the complex conductivity $\sigma = \sigma_1 - i\sigma_2$. The mentioned technique has been successfully used to study $\text{YBa}_2\text{Cu}_3\text{O}_{7-\delta}$ cuprate films [1] and $\text{Ba}(\text{Fe}_{1-x}\text{Co}_x)_2\text{As}$ pnictide single crystals [2] below the critical temperature.

This contribution is a continuation of work [3], in which the problem of measuring the surface impedance of superconductors in a normal state was analyzed. At temperatures when the superconductor is in a normal state and even in the vicinity of T_c (this is especially true for cuprates), the complexity of the problem solution is determined by the following facts: 1) the Q-factor of the WGM resonator is greatly reduced, which sharply reduces the accuracy and sensitivity of measurements of the response of the resonator with the sample; 2) already at $T \leq T_c$, the thickness of the superconducting films becomes relatively thin that the validity of using the impedance transformation relation for finding the intrinsic impedance Z_s is questioned to determine the complex conductivity σ [4].

Here we report the results of numerical simulation of several types of Ka-band sapphire WGM resonators, namely, cylindrical disk, truncated cone, and hemisphere resonators with conducting endplates (i.e. flat samples of superconductors), as well as resonators with a radial slot for studying small single crystals of superconductors. Preliminary results of measuring the microwave response of a WGM resonator with a $\text{YBa}_2\text{Cu}_3\text{O}_{7-\delta}$ quasi-single crystal in the normal state are presented and discussed.

- [1] A. A. Barannik, M. A. Tanatar, S. Vitusevich, V. Skresanov, P. C. Canfield, R. Prozorov, Phys. Rev. B, 87, 0144506 (2013).
- [2] N. T. Cherpak, A.A. Barannik, Yu. F. Filipov, Yu. V. Prokopenko, S. Vitusevich, IEEE Trans. on Appl. Supercond. 13, 3570, (2003).
- [3] A. Barannik, S. Vitusevich, A. Gubin, M. Vovnyuk, I. Protsenko, N. Cherpak, Telecommunications and Radioengineering, 78(17), 1559 (2019).
- [4] J. Krupka, J. Wosik, C. Jastrzebski, T. Ciuk, J. Mazierska, M. Zdroek, IEEE Trans. on Appl. Supercond. 23, 1501011 (2013).



MAGNETISM AND MAGNETIC MATERIALS

Magnetic Frustration in Insulating Jahn-Teller Manganite Crystals

L. Gonchar^{1,2}

¹*Ural State University of Railway Transport,*

66 Kolmogorov St., Yekaterinburg, 620034, Russia

²*Ural Federal University named after First President of Russia B.N. Yeltsin,*

19 Mira St., Yekaterinburg, 620002, Russia

l.e.gonchar@urfu.ru

The pseudoperovskite distorted manganite crystals $R_{1-x}A_xMnO_3$ (where R^{3+} is a rare earth ion or Bi^{3+} , A^{2+} is an alkaline earth ion, and x is a doping rate) are known as smart materials with strong correlation between crystalline, charge, orbital, and magnetic subsystems' orderings because of Jahn-Teller (JT) ions Mn^{3+} sublattice [1]. The influence of this correlation gives rise to low-dimensional, incommensurate and frustrated magnetic structures.

The dependence of magnetic properties upon R^{3+} ion is caused not only by size of the ion as was proposed earlier [2]. The bismuth manganites are considered to have multiferroic properties due to lone-pair s-electron of Bi^{3+} shell [3].

Magnetic frustration in these crystals has non-geometric origin. The superexchange interaction in different pair of magnetic manganese ions can be of different value or sign [4]. It depends upon orbital ordering which is formed in certain compound.

In current investigation, different insulating manganite compounds are theoretically studied. These compounds can have low-temperature magnetic structure without frustration, as $LaMnO_3$ and $La_{0.5}Ca_{0.5}MnO_3$ or have competing superexchange interaction as $BiMnO_3$ and $La_{0.33}Ca_{0.67}MnO_3$ [4].

The description of magnetic ordering is made in a way[4]. First, the experimental crystal structure is used to find the JT distortions and suppose the orbital structure. The non-local and non-linear terms in vibronic interaction can be taken into account. Second, within the framework of orbitally-dependent superexchange interaction the exchange parameters in manganese pairs are found. That stage of model affords to consider all possible magnetic arrangements. The final magnetic ordering is forming due to single-ion anisotropy, which also depends upon orbital states.

The model Hamiltonian of manganites' magnetic subsystem is [4]

$$\hat{H}_{mag} = \sum_{i>j} J_{ij}(\Theta_i, \Theta_j) (\mathbf{S}_i \cdot \mathbf{S}_j) + \sum_{i,\alpha,\beta} D_i^{\alpha,\beta}(\Theta_i) S_i^\alpha S_i^\beta, \quad (1)$$

where first sum is superexchange interaction, second one is single ion anisotropy. All terms are dependent upon total manganese spins \mathbf{S}_i , \mathbf{S}_j and orbital structure parameters Θ_i , Θ_j .

In the compounds under consideration, the role of orbital ordering in magnetic competition is emphasized. The conditions of ordered state's destruction are estimated. The ranges of orbital structure mixing angles to form frustrated or low-dimensional magnetic structures are determined.

The overdoped bismuth manganites as $Bi_{0.2}Ca_{0.8}MnO_3$ and $Bi_{0.31}Ca_{0.698}MnO_3$ have frustrated magnetic ordering like lanthanum compound $La_{0.33}Ca_{0.67}MnO_3$ [5]. The influence of non-linear and non-local terms of vibronic interaction [4] on orbital ordering and magnetic structure is discussed.

[1] N.G. Bebenin, R.I. Zainullina, V.V. Ustinov, Phys. Usp. 61, 719 (2018)

[2] E.O. Wollan, W.C. Koehler, Phys. Rev. 100 545 (1955).

[3] D.P. Kozlenko et al., Phys. Rev. B, 82, 014401 (2010); I.V. Solovyev, S.A. Nikolaev, Phys. Rev. B 90, 184425 (2014)

[4] L.E. Gonchar, JMMM 465, 661 (2018) & 513, 167248 (2020)

[5] S. Grenier et al., Phys. Rev. B 75, 085101 (2007)

Effect of Kink Scattering on their Confinement in Quasi One-Dimensional Magnetically Ordered Quantum Spin Systems

S.B. Rutkevich

*Bergische Universität Wuppertal,
Gaußstrasse 20, Wuppertal, 42119, Germany
rutkevich@uni-wuppertal.de*

The confinement phenomenon occurs when the constituents of a compound particle cannot be separated from each other and, therefore, cannot be observed directly. A prominent and, important, example in high-energy physics is the confinement of quarks in hadrons. Remarkable, confinement can also be realized in such condensed-matter systems, as quasi one-dimensional magnetically ordered crystals. In the recent decade, confinement of kink (spinon) topological magnetic excitations has been observed in many quasi one-dimensional ferro- and anti-ferromagnets [1, 2]. In analogy with high-energy physics, the two-kink bound states in such magnetic crystals in the confinement regime are often called “the mesons”. The experimentally observed “meson” energy spectra are usually compared with the results of numerical calculations based on the microscopic spin-chain Hamiltonian. Such direct numerical calculations exploiting DMRG or similar algorithms could hardly contribute to the qualitative understanding of the kink confinement phenomenon. Much more useful for the qualitative interpretation of the experimental data is the McCoy-Wu phenomenological theory [3], in which the two kinks confined in a “meson” are treated as quantum particles attracting one another with a long-range linear potential. Unfortunately, this simple theory contains phenomenological parameters, which relation with the parameters of the microscopic spin-chain Hamiltonian remains unclear.

In this report, I will describe the original analytical semi-heuristic method for calculation of the “meson” energy spectra in the confinement regime. Besides the transparent physical interpretation, this approach has several further advantages. In contrast to the McCoy-Wu theory, it can take into account the short-range interaction between kinks, which is encoded in the kink-kink scattering matrix in the deconfined phase. Further, the resulting analytic representations for the kink bound-state energies are expressed solely in terms of the parameters of the microscopic spin-chain Hamiltonian. Finally, the predicted by this method “meson” energy spectra in the massive antiferromagnetic XXZ spin chain in the presence of a weak staggered magnetic field [4] agree very well with the results of involved numerical calculations [2].

I will also describe on the example of the three-state Potts field theory, how the developed semi-heuristic method can be validated in the more sophisticated approach based on the Bethe-Salpeter equation.

This work was supported by Deutsche Forschungsgemeinschaft (DFG) via Grant BO 3401/7-1.

- [1] R. Coldea, D. A. Tennant, E. M. Wheeler, E. Wawrzynska, D. Prabhakaran, M. Telling, K. Habicht, P. Smeibidl, and K. Kiefer, Science 327, no. 5962, 177 (2010).
- [2] A. K. Bera, B. Lake, F. H. L. Essler, L. Vanderstraeten, C. Hubig, U. Schollwöck, A. T. M. N. Islam, A. Schneidewind, and D. L. Quintero-Castro, Phys. Rev. B 96, 054423 (2017).
- [3] B. M. McCoy, and T. T. Wu, Phys. Rev. D 18, 1259 (1978).
- [4] S. B. Rutkevich, EPL (Europhysics Letters) 121, 37001 (2018).

Magnetocaloric Effect in [Ni(fum)(phen)] – the Ferromagnetic Dimer with Spin 1

P. Danylchenko¹, V. Tkáč¹, A. Orendáčová¹, E. Čižmár¹, A. Uhrinová^{2,3}, M. Orendáč¹, R. Tarasenko¹

¹Institute of Physics, Faculty of Science, P.J. Šafárik University,
Park Angelinum 9, 041 54 Košice, Slovak Republic

²Institute of Chemistry, Faculty of Science, P.J. Šafárik University,
Moyzesova 11, 041 54 Košice, Slovak Republic

³Department of Chemistry, Biochemistry, and Biophysics, Institute of Pharmaceutical Chemistry,
University of Veterinary Medicine and Pharmacy,
Komenského 73, 04181 Košice, Slovakia
petro.danylchenko@student.upjs.sk

The title compound [Ni(fum)(phen)] (NIFUM) (*fum* = fumarato, *phen* = 1,10 -phenanthroline) crystallizes in the monoclinic structure, *P*2/c space group. The crystal structure exhibits two-dimensional character. The formed layers are built of Ni(II) dimers linked by bridging fumarato ligands. Both Ni(II) atoms are hexa-coordinated in the *cis*-NiO₄N₂ form. The layers are interconnected by π–π interactions operating between aromatic rings of the *phen* ligands. NIFUM has been previously identified as the array of antiferromagnetic *S* = 1 dimers with the easy-axis uniaxial magnetic anisotropy *D* comparable to the intradimer exchange coupling *J*, *D/J* ≈ 1 and *D/k_B* = 6 K [1]. Heat capacity measurements taken on NIFUM have shown the absence of any kind of magnetic phase transition down to 0.4 K in zero magnetic field. Magnetocaloric studies have been performed on powder sample NIFUM in the temperature range from 1.8 K to 44 K in magnetic fields up to 7 T using isothermal magnetization curves measured in a commercial Quantum Design SQUID magnetometer. Large conventional magnetocaloric effect (MCE) was found around 5.8 K (-Δ*S*_{max} = 8.2 J/(kg K) for 7 T). The analysis of magnetocaloric effect in NIFUM has shown that the temperature dependence of the isothermal entropy change under different magnetic fields is in good agreement with theoretical predictions for the *S* = 1 ferromagnetic dimer with *D/k_B* = -12 K, *E/k_B* = -3.5 K and intradimer exchange coupling *J/k_B* = 3 K. Theoretical analysis of MCE revealed that the presence of ferromagnetic coupling improves the MCE properties. Investigation of magnetocaloric properties of NIFUM suggests that the studied system can be considered as a good material for magnetic cooling at low temperatures.

This work was supported by the Slovak Research and Development Agency Project No. APVV-18-0197.

[1] J. Černák, A. Pavlová, A. Orendáčová, M. Kajňaková, J. Kuchár, Polyhedron 28, 2893 (2009).

Low Temperature Thermodynamics of the Finite Spin-1/2 XX Chain Decorated by Some Ising Impurities

O. Dzhennherov, E. Ezerskaya

*V.N. Karazin Kharkiv National University,
4 Svobody Sq., Kharkiv, 61022, Ukraine
adzhennherov@gmail.com*

Real low-dimensional magnetic structures always have some lattice distortions and impurities and the study of the effect of these structural defects on their thermodynamic characteristics has a big theoretical and practical interest. We proposed three exactly solvable spin models on the basis of the finite spin-1/2 XX chain: finite linear XX-chain decorated by two different Ising impurity spins S1 and S2 at arbitrary lattice sites, finite closed XX-chain (ring) with two different impurity spins S1 and S2, and XX chain with two different attached Ising “offshoots”. The spin-1/2 XX chain is a well-known example of an exactly solvable spin system [1, 2]. Jordan-Wigner transformation [1] reduces its Hamiltonian to the ideal gas of spinless fermions even for the chain with any defects. Proposed model Hamiltonians may give new information about the well-known broken-chain effect in real quasi-one-dimensional magnetic materials [3, 4].

For all the three proposed models the z-projections of the impurity spins are good quantum numbers. Therefore, these models are equivalent to the set of Hamiltonians of finite spin-1/2 XX chains with additional parameters $\sigma_i = -S_i, \dots, S_i$ ($i=1, 2$) which correspond to above impurities. We derive the exact dispersion relations for the stationary states with one inverted spin for all above models. The corresponding spectra consist of one quasi-continuous zone and several localized impurity levels. We obtained and analyzed the analytical inequalities for the values of the critical parameters of the models describing the appearance of local energy impurity levels above and below the quasi-continuous zone.

We also performed a numerical simulation of the field and the temperature dependences of the main thermodynamic characteristics. It is shown that the appearance of localized levels near impurities can effect significantly on the thermodynamic properties at low temperatures, leading to additional peculiarities in their field and temperature dependences. Zero temperature field dependence of the magnetization should have finite jumps associated with both quasi-continuous spectra and impurity levels. The remnants of these jumps are clearly visible at very low temperatures. The average values of the z-projection of the spins of the distorted bonds may decrease with the increasing of magnetic field for some values of model parameters. The temperature dependence of the specific heat capacity may show additional maxima at very low temperatures.

- [1] E. Lieb, T. Schultz, and D. Mattis, Ann. Phys. 16, 407 (1961).
- [2] A.A. Zvyagin, Quantum Theory of One-Dimensional Spin Systems, Cambridge Scientific Publishers, Cambridge, 2010. – 330 p.
- [3] A. Klumper and D.C. Johnston, Phys. Rev. Lett., 84, 4701 (2000).
- [4] Y. Liu, J.E. Drumheller and R.D. Willett, Phys. Rev., B52, 15327 (1995).

The Antiferromagnetic Phase Transition in the Lamellar Cu_{0.15}Fe_{0.85}PS₃ Semiconductor: Experiment and DFT Modeling

V. Pashchenko¹, O. Bludov¹, D. Baltrunas², K. Glukhov³, Yu. Vysochanskii³

¹B.Verkin Institute for Low Temperature Physics and Engineering of NAS of Ukraine,
47 Nauky Ave., Kharkiv, 61103, Ukraine

²Department of Nuclear Research Center for Physical Sciences and Technology Savanoriu, Ave.
231, Vilnius LT-02300, Lithuania

³Institute for Solid State Physics and Chemistry, Uzhhorod University, 46 Pidgirna Str.,
Uzhhorod, 88000, Ukraine
kglukhov@gmail.com

Relatively recently synthesized Cu_{0.15}Fe_{0.85}PS₃ crystal is barely investigated up to now [1]. Authors presenting the original experimental studies of the paramagnetic-antiferromagnetic phase transition through Moessbauer spectroscopy and measurements of temperature and field dependencies of magnetic susceptibility in the investigated material. The peculiar behavior of the magnetization-field dependence at low-temperature regions in this crystal stimulated our interest to study the origins of its ferromagnetic properties.

Also, the *ab initio* simulation of the features of electronic and lattice subsystems in the framework of electron density functional theory (DFT) as implemented in Quantum ESPRESSO code [2] is conducted. The peculiarities of spin ordering at low temperature as well as changes in interatomic interactions in the vicinity of the phase transition temperature ($T_c \approx 110$ K) (obtained in molecular dynamics run) are modeled and analyzed.

Calculated values of electric field gradient components and estimations of the total magnetic moment of the unit cell are in reasonable agreement with the measured experimental quantities.

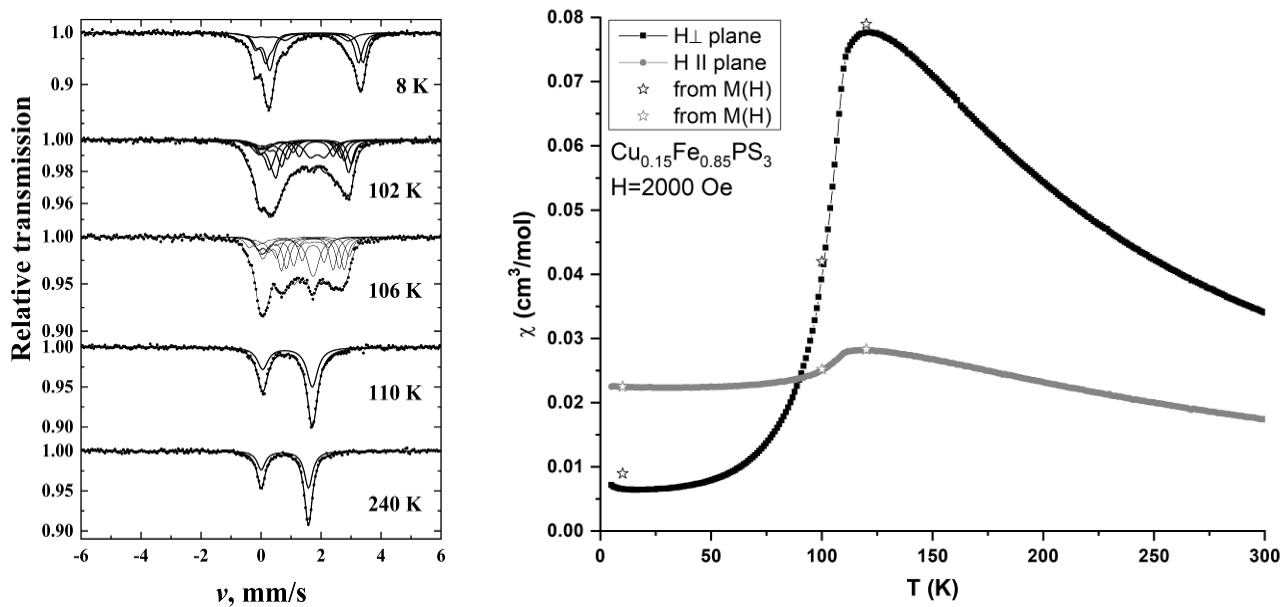


Fig. 1 (left) Mössbauer spectra of Cu_{0.15}Fe_{0.85}PS₃ measured at the indicated temperatures; (right) Temperature dependencies of magnetic susceptibility $\chi(T)$ of Cu_{0.15}Fe_{0.85}PS₃ single-crystal in a magnetic field of $H=2000$ Oe for two directions $H\perp$ plane and $H\parallel$ plane. By stars the values of magnetic susceptibility obtained from field dependencies $M(H)$ are denoted.

- [1] A. Dziaugys, J. Macutkevic, S. Svirskas, R. Juskenas, M. Wencka, J. Banys, S.F. Motria, Yu. Vysochanskii, Journal of Alloys and Compounds 650, 386 (2015).
[2] P. Giannozzi, S. Baroni, et al., J.Phys.: Condens.Matter 21, 395502 (2009).

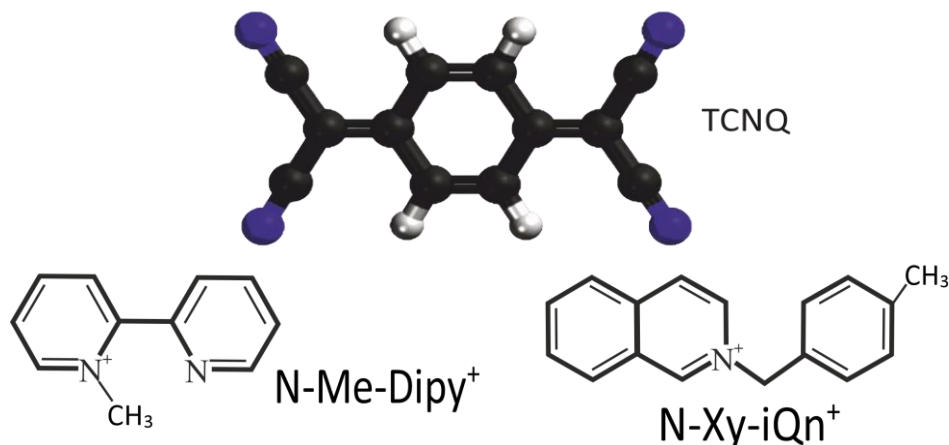
Antiferromagnetic Spin Chains Formed in Novel TCNQ-Based Organic Magnets

M. Holub¹, E. Čižmár¹, T.N. Starodub², A. Feher¹, V.A. Starodub²

¹*Institute of Physics, Faculty of Science, P. J. Šafárik University,
Park Angelinum 9, 041 54 Košice, Slovakia*

²*Institute of Chemistry, Jan Kochanowski University, 25-405 Kielce, Poland
mariia.holub@student.upjs.sk*

The work devoted to the study of two novel genuine organic anion-radical salts (ARS) $[\text{N-Me-Dipy}](\text{TCNQ})_2 \cdot \text{CH}_3\text{CN}$ (**1**) and $[\text{N-Xy-iQn}](\text{TCNQ})_2$ (**2**), where $\text{TCNQ} = 7,7,8,8$ -tetracyanoquinodimethane, N-Me-Dipy = N-methyl-2,2'-bipyridine, and N-Xy-iQn = N-(p-xylene)-isoquinoline, is presented.



In the past few decades molecular low-dimensional conducting materials have attracted much interest, in particular, electrical (conducting or semiconducting properties), magnetic and spectral. The uniqueness of ARS TCNQ is in a combination of electroconductivity and the ability to form magnetically ordered structures. Such structures are interesting primarily because, even though they do not have metal ions, and still exhibit magnetic properties in the role of the acceptor molecule.

The crystallographic data indicate the formation of $(\text{TCNQ})_2^{\bullet-}$ anion-radical π -dimers in the synthesized ARS carrying spin $S = 1/2$. The analysis of the TCNQ bond distances allowed the estimation of the charge distribution that suggests the formation of magnetic stacks along the crystallographic a -axis. Magnetic measurements of prepared ARS were performed in a temperature range from 1.8 to 350 K in magnetic fields up to 7 T using a SQUID magnetometer. Both studied ARS display an antiferromagnetic (AFM) behavior. A broad maximum in the temperature dependence of the susceptibility was observed at ~ 280 K for ARS **1** and described by a model of uniform spin chain with exchange interaction $J/k_B = -440$ K, which agrees with a uniform spacing of TCNQ π -dimers in the stacks. On the other hand, an exponential-like decrease of susceptibility with decreasing temperature for ARS **2** suggests strong spin chain dimerization due to the complicated stacking of TCNQ π -dimers along the a -axis. A model of AFM alternating bond (or dimerized chain) spin chain with $S = 1/2$ was used for the analysis. The energy gap in the excitation spectrum of the spin chain induced by dimerization was estimated from the analysis of susceptibility as $\Delta/k_B = 1322$ K with exchange interaction alternation parameter $\alpha = 0.195$. In both systems, low-temperature behavior is affected by a very small fraction (less than 2 %) of uncoupled or end-chain spins displaying simple paramagnetism.

This work was supported by projects VEGA 1/0426/19 and APVV-18-0197.

On the Spin-Wave Analysis of Narrow Graphene Nanoribbons with Periodically Embedded Impurities

E. Ezerskaya, A. Kabatova, V. Zaytseva

*V.N.Karazin Kharkiv national University,
4 Svobody Sqr., Kharkiv, 61122, Ukraine
kabatova.anna@ukr.net*

This work is devoted to the spin-wave analysis of the elementary excitation spectrum of the narrow graphene zig-zag nanoribbons with periodically embedded impurity atoms or distorted two-site links.

The linear spin-wave approximation (LSWA) permits to study the low-temperature properties of antiferromagnets and ferromagnets with two or more sublattices with the antiparallel spin orientation of the nearest neighbors. The application of Bose operators of creation and annihilation instead of the spin operators, proposed in Holstein–Primakov [1] in 1940, is still the powerful method for approximate investigations of such magnets.

The LSWA gives a fairly reliable estimate for ferromagnetically ordered states in solids (see, for example, [3, 4]). The influence of impurities on the magnetic properties of finite graphene nanoribbons was studied in [5]. In particular, the detailed analysis of the lowest energy spectrum was performed, and it was shown that this approximation leads to the gapless energy spectrum in zero magnetic field at any values of model parameters.

We investigate low energy part of the excitation spectrum for two models with different location of two impurity spins S_1 and S_2 per unit cell: (a) at top and bottom of each hexagon; (b) at top and valley of each hexagon; for two models with two-site impurity (one distorted link with spins S_1): (c) at each vertical connection of hexagons and (d) at one of the lateral sides of each hexagon. For all models, we derived the dispersion relations for the elementary excitations. Similar to [5], one should take only non-negative solutions for energies. It is shown that the solution $\epsilon = 0$ always exists at quasi-wave vector $k = 0$. This means that the LSWA energy spectrum is gapless for any values of site spins and coupling parameters. Due to the additional space symmetry of the model (c), the elementary excitations were obtained in analytical form. We also analyzed the long-wave limit for the lowest energies. For models (c) and (d) the corresponding dispersion laws are linear ($\sim |k|$). In the limit of small k the excitation energy spectra are quadratic ($\sim k^2$) for different values of impurity spins ($S_1 \neq S_2$) for the model (a) and for the model (b) with $2S \neq S_1 + S_2$ (for carbon atoms $S=1/2$). For model (a) with $S_1 = S_2$ and for model (b) with $2S = S_1 + S_2$ the corresponding dispersion laws are linear. Note that our analysis is valid also for graphene-like structures with any spins of the main nanoribbon structure S .

- [1] T. Holstein and H. Primakoff , Phys. Rev. 58 1098 (1940)
- [2] Л.И. Ахиезер, В.Г. Барьяхтар, С.В., Пелетминский, Спиновые волны (М.: Наука, 1967)
- [3] S.K. Pati, S. Ramasesha, D. Sen, Phys. Rev. B 55 (1997) 8894.
- [4] N.B. Ivanov, Phys. Rev. B 62 (2000) 3271.
- [5] V.O. Cherenovskii, V.V. Slavin, E.V. Ezerskaya, A.L. Tchougréeff, and R. Dronskowski, Crystals 9 251 (2019)

Giant Fourfold Magnetic Anisotropy in Nanotwinned NiMnGa Epitaxial Film

J. Kharlan¹, P. Bondarenko¹, A. Marinchenko², V. Golub¹

¹*Institute of Magnetism NAS of Ukraine and MES of Ukraine, Kyiv, Ukraine*

²*National Aviation University, Aerospace faculty, Kyiv, Ukraine*

julia-lia-a@ukr.net

The uniaxial magnetic anisotropy field value in 3d-metals based alloys can achieve thousands Oe, while the fourfold magnetic anisotropy field value usually doesn't exceeds several hundreds oersteds. Here we present experimental results of giant in-plane fourfold anisotropy, which is of about several kOe in NiMnGa alloy. These shape memory alloys usually undergo martensitic transformation, therefore the film twins because of the surface area conservation requirement when cooled. The magnetic anisotropy easy axes of twin variants are directed perpendicular to each other. The twin width can be comparable with exchange length . In this case magnetic moments of twin variants are coupled by exchange interaction on their borders [1].

Magnetic resonance measurements were obtained by the electron spin resonance and broadband FMR spectrometers (Fig.1). The resonance spectra at the temperature 160 K (in martensitic state) at frequency 9.87 GHz in perpendicular to the film plane external magnetic field has shown availability of two resonance peaks $H_{res1}=12.3$ kOe and $H_{res2}=9.3$ kOe. The ferromagnetic resonance with in-plane external magnetic field can be obtained only for four angles with interval 90° (Fig.2) with the equivalent spectra. This fact testifies about giant four-fold anisotropy in the system.

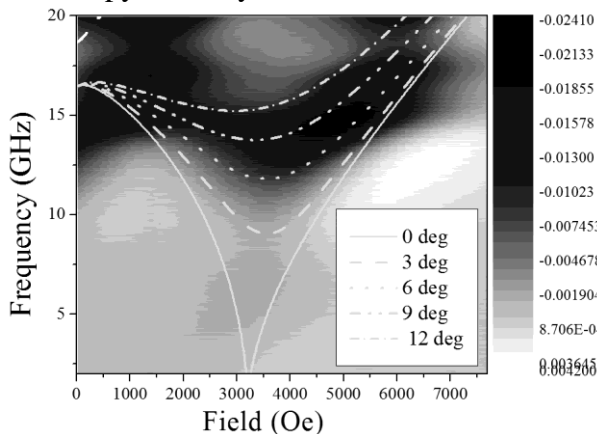


Fig. 1. Theoretical (lines) and experimental (dark areas) dependencies of resonance frequencies on external magnetic field. The lines shows one frequency branch calculated for external field directed at the angle 0° (bottom line), 3°, 9°, 12°(top line).

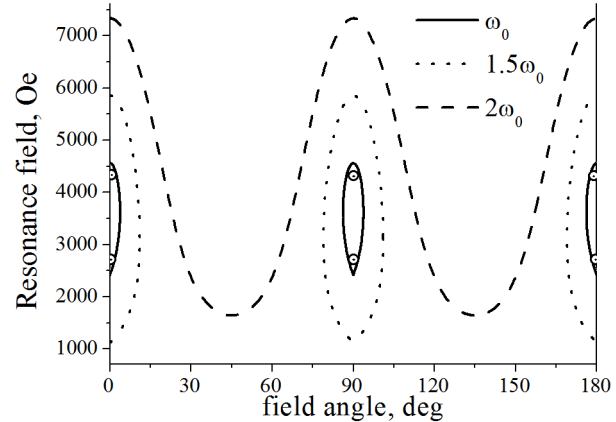


Fig.2. The experimental (circles) and theoretical (lines) angle dependencies of resonance field at the temperature 160 K. Solid line corresponds to the experimental frequency 9.87 GGz. Other lines correspond to larger frequencies.

We have shown that the giant fourfold anisotropy is implemented due to the ferromagnetic exchange between twin variants on their border and presence of large uniaxial anisotropy in each twin. Easy axes of uniaxial anisotropy in twin variants are in-plane and perpendicular to each other. If the exchange length is comparable with twin weight, competition of these interactions can results in fourfold anisotropy. Additional evidence of week ferromagnetic exchange on the twin borders is two resonance peaks in perpendicular magnetic field, which corresponds to common mode and antiphase oscillations of magnetic moments.

[1] V.O.Golub, V.A.Lvov, I.Aseguinolaza, O.Salyuk, D.Popadiuk., Y.Kharlan, V.A.Chernenko, Physical Review B, 95(2), 024422 (2017).

Hidden Magnetism of Superconducting Iron Chalcogenides

**V.D. Fil¹, D.V. Fil^{2,3}, G.A. Zvyagina¹, K.R. Zhekov¹, I.V. Bilych¹, D.A. Chareev^{4,5,6},
M.P. Kolodiazhnna¹, A.N. Bludov¹**

¹ *B. Verkin Institute for Low Temperature Physics and Engineering
 NAS of Ukraine, 47 Nauky Avenue, Kharkiv, 61103, Ukraine*

² *Institute for Single Crystals, NAS of Ukraine, 60 Nauky Avenue, Kharkiv, 61072, Ukraine*

³ *V.N. Karazin Kharkiv National University, 4 Svobody Square, Kharkiv, 61022, Ukraine*

⁴ *Institute of Experimental Mineralogy, RAS, Chernogolovka, 142432, Russia*

⁵ *National University of Science and Technology "MISiS", Moscow, 119049, Russia*

⁶ *Ural Federal University, Ekaterinburg, 620002, Russia*

m.kolodyajna@gmail.com

Acoustoelectric transformation in superconducting compositions of iron chalcogenide family $\text{FeSe}_{1-x}\text{S}_x$ ($x = 0, 0.075, 0.14$) was studied. In all samples, regardless of composition, the shear ultrasonic mode excites a linearly polarized electromagnetic field which magnetic component is collinear to the elastic displacement. The efficiency of the process increases rapidly (fig.1) at the temperatures of the structural transition (T_s).

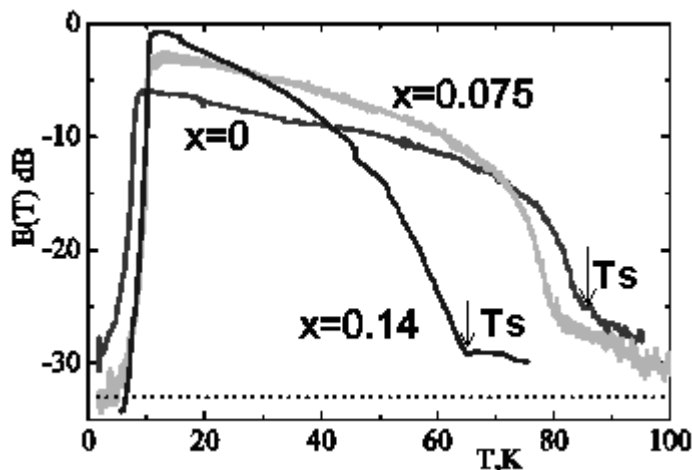


FIG. 1. Electromagnetic response to the shear deformation of $\text{FeSe}_{1-x}\text{S}_x$ single crystals at different values of x . The dotted line shows the approximate level of detection of the signal against the background noise.

Analysis shows that the piezomagnetism is the most acceptable explanation of the effect. We consider that in the absence of external perturbation the spins and orbital moments are oriented in such a way that the resulting magnetic moment is zero in each unit cell, and, due to the interaction, presumably through the lattice, a long-range order is established in the system at some temperature, i.e. elementary moments are oriented uniformly in each cell. In other words, a state of hidden magnetism emerges in the sample. External deformations lead to a partial uncompensation of magnetic moments, turning the sample into a weak ferromagnets. Within this concept pure iron selenide and sulfur-doped compositions up to $x \sim 0.14$ belong to systems with broken time-reversal symmetry. The effect exists under propagation of the sound wave along all major crystallographic directions. Symmetry consideration leads to the conclusion that the low-temperature phase (below the structural transition) belongs to the triclinic syngony.

Electric and Magnetic Properties of $\text{Fe}_{7-x}\text{A}_x\text{Se}_8$ Single Crystals

Y.T. Konopelnyk¹, M. Pękała², I. Radelytskyi¹, P. Iwanowski¹

¹*Institute of Physics, Polish Academy of Sciences, Warsaw, Poland*

²*Chemistry Department, Warsaw University, Warsaw, Poland*

konopelnyk@ifpan.edu.pl

Thermoelectric power, resistivity and magnetic measurements of $\text{Fe}_{7-x}\text{A}_x\text{Se}_8$ single crystals (where A = Ni) have been provided in fields up to 5 T and in the temperature range from 4 K to 500 K. The Fe_7Se_8 single crystal is ferrimagnetic metal with Néel temperature equal to 450 K and has NiAs-like structure with a large number of ordered vacancies. The single crystals of pure and Ni intercalated Fe_7Se_8 have been grown applying modified Bridgman's method. The spin reorientation transition (SRT) in pure Fe_7Se_8 precedes as a first-order phase transition at the temperature $T_{\text{SRT}} \approx 125$ K [1]. The intercalation with Ni affects both the T_N and T_{SRT} . Magnetic measurements show the decreasing of Fe_7Se_8 magnetization in crystals where Ni substitutes Fe.

Thermal variation of the electrical resistivity was measured by the four-probe method with temperature stabilization +/- 0.02 K. Resistivity is significantly higher than for a conventional metal and depends on the crystallographic direction. It was proposed hole-mechanism of conductivity in Fe_7Se_8 crystals. It was suggested the existence of interesting metal-semiconductor transition at the same temperature as the spin direction change occurs, which depends on Ni content. The explanation of this effect could be the iron vacancy existence [2]. Moreover, remarkable positive magnetoresistance is observed. The appearance of positive magnetoresistance in the crystals substituted with nickel is similar to that shown in [3]. The results suggest that the localization of 3d electron states on defect sites is responsible for the metal-semiconductor transition [2].

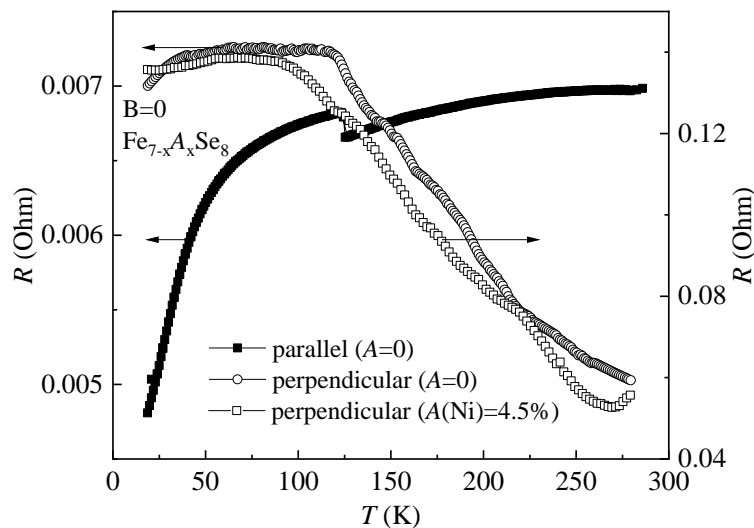


Fig. 15. The temperature dependence of the electrical resistance was measured along the a - axis (empty circles, empty squares) and along the c-axis (black squares) for $\text{Fe}_{7-x}\text{A}_x\text{Se}_8$.

This study was partly financed by the National Centre for Research and Development, Research Project no. PBS2/A5/36/2013

[1] I. Radelytskyi et al., J. Appl. Phys. 124, 143902 (2018).

[2] G. Li, B. Zhang, T. Baluyan, J. Rao, J. Wu, A. A. Novakova, P. Rudolf, G. R. Blake, R. A. de Groot, and T. T. M. Palstra, Inorg. Chem. 55, 12912 (2016).

[3] J. B. Sousa, J. F. D. Montenegro, J. M. Moreira, and M. E. Braga, J. Phys. F: Met. Phys., 12, 351 (1982).

Pressure Induced Modification of the Magnetic Properties of Triangular Antiferromagnet KFe(MoO₄)₂

D. Kamenskii^{1,2}, K. Kutko³, L. Prodan¹, T. Sakurai², H. Ohta²

¹*Experimental Physics V; Center for Electronic Correlations and Magnetism; Institute of Physics; University of Augsburg, 86159 Augsburg; Germany*

²*Molecular Photoscience Research Center; Kobe University; 657 – 8501 Kobe; Japan*

³*B.Verkin Institute for Low Temperature Physics and Engineering of NAS of Ukraine, 47 Nauky Ave., Kharkiv, 61103, Ukraine
kkutko@ilt.kharkov.ua*

In a last decade the intensive study of the triangular-lattice antiferromagnetic (TAF) compounds, reveal a rich variety of ground states, ranging from a gapless spin liquid to Neel order, depending on the exchange interactions there [1]. An externally applied pressure is capable to re-normalize exchange interactions, which leads to modification of the phase diagram and, even more, may induce new phases [2]. Here we study the pressure effect on magnetic properties of KFe(MoO₄)₂, where Fe³⁺ ions form a quasi-two-dimensional triangular magnetic structure [3]. Moreover KFe(MoO₄)₂ is ferroelastic material, which have structural domains, where the elastic stress on the domain walls may affected the exchange coupling between Fe³⁺ ions [4]. At room temperature, KFe(MoO₄)₂ exhibit a cascade of the hydrostatic pressure induced structural transitions at 0.25, 1.3 and 1.6 GPa, moreover, transitions at 0.25 and 1.6 GPa are irreversible [5].

The KFe(MoO₄)₂ single crystals were grown from flux by slow cooling [6]. The samples crystallizes as light green single crystals with the D³_{3d} space group ($a = 5.66 \text{ \AA}$ and $c = 7.12 \text{ \AA}$). Such a crystal of good optical quality was installed into the CuBe-pressure cell and load was applied at room temperature. This load corresponds to the hydrostatic pressure of about 1.5 GPa at room temperature and 1.3 GPa when the system is cooled to 4.2 K. After the system was warmed up and the pressure released, the sample changed color to the brown. Similar modification of the sample was reported in [4], which happened under pressure 1.6 GPa and heating up to 653 K. We found that such phase of sample remains stable after pressure released upon both a cooling down to 1.5 K and heating up to 500 K.

Here we report the magnetic properties of KFe(MoO₄)₂ in the pressure induced phase (β - phase) and compare it with the original compound (α - phase). The magnetization, magnetic susceptibility and heat capacity have been investigated between 1.5 and 300 K in the magnetic fields up to 7 T. We found that both modifications of the KFe(MoO₄)₂ crystal have the same (within our error bar) $T_N = 2.4 \text{ K}$ while the Curie temperature becomes higher in the β - phase. Thus, the enhanced spin-spin correlations in β -phase does not influence on the ordering temperature. It is can be possible due to a small coupling between the "TAF-planes", which dictates 3D ordering. We conclude that the lattice modification in KFe(MoO₄)₂ induced by irreversibly phase transition at 1.6 GPa mainly affects the exchange constants within a plane of triangles but not interplane interaction. This also reflects the hump in the specific heat at about 4 K.

- [1] R. Chen, H. Ju, H.-C. Jiang, O.A. Starykh, L. Balents, Phys. Rev. B 87, 165123 (2013).
- [2] S. A. Zvyagin, D. Graf, T. Sakurai, S. Kimura, H. Nojiri, J. Wosnitza, H. Ohta, T. Ono, H. Tanaka, Nat. Comm. 10, 1064 (2019).
- [3] A. I. Smirnov, L. E. Svistov, L. A. Prozorova et al., Phys. Rev. Lett 102, 037202 (2009).
- [4] A.I. Otko, N.M. Nesterenko, G.G. Krainyuk, A.E. Nosenko, Ferroelectrics 48, 143 (1983).
- [5] M. Maczka, A. Pietraszko, G. D. Saraiva et al., J. Phys.: Condens. Matter 17, 6285 (2005).
- [6] R. F. Klevtsova, P.V. Klevtsov, Kristallografiya 18, 953 (1970) (in Russian).

Temperature Evolution of Magneto-optic Spectra of YIG:Co as a Marker of Changes of Magnetic Anisotropy

E. Kychka², O.V. Miloslavskaya¹, Yu.M. Kharchenko¹, M.F. Kharchenko¹

¹*B.Verkin Institute for Low Temperature Physics and Engineering of NAS of Ukraine,
47 Nauky Ave., Kharkiv, 61103, Ukraine*

²*V.N.Karazin Kharkiv National University, Majdan Svobody 4, Kharkiv, 61022, Ukraine
olga.miloslav@gmail.com*

Cobalt-doped iron- yttrium garnet (YIG:Co) attracts attention as an object in which non-trivial temperature and photoinduced changes of magnetic and optical properties caused by spin reorientation are observed [1,2]. The interrelation of these properties extends the functional capabilities of cobalt-doped ferrimagnetic garnets as materials for sensitive elements in magnetic and magneto-optical devices, as well as components of photonic and plasmonic structures.

The temperature behavior of the magnetic field-induced dichroism of linearly polarized light in the YIG: Co film was investigated in the spectral range from 14000 to 20000 cm⁻¹ (500 - 714 nm). The 5.8 μm thick Y₂CaFe_{3.9}Co_{0.1}GeO₁₂ film was prepared on a transparent Gd₃Ga₅O₁₂ single crystal substrate with a (001) crystallographic plane. The light propagated along the normal to the film, $\mathbf{k} \parallel [001]$. The magnetic field with 8.8 kOe strength was applied in the plane of the sample along the direction of [100] crystallographic axis. In the 15000 - 16000 cm⁻¹ and 16000 - 19000 cm⁻¹ wavenumber regions the spectra had noticeable features, which varied differently with temperature increasing from 25 K to 100 K (see Fig.). The magnetic linear dichroism (MLD) values at lower wavenumbers dropped to almost zero, while in the higher wavenumber range it decreased by only 2 times. The MLD spectral bands of doped YIG:(Co,Ca) crystals are caused by electronic transitions at iron ions of crystalline matrix and at cobalt ions located in deformed octahedral and tetrahedral sites [3].

The temperature changes in dichroism originate from reorientation of Fe and Co spins in the YIG:Co crystals as a result of a change in orientation of easy magnetization axis from [001] to [110] crystallographic direction in the 20–150 K temperature interval [1]. The exchange energy between cobalt and iron ions is less than that between iron ones. The energy of single-ion anisotropy at cobalt sites is significantly greater than the anisotropy energy at iron positions. Due to competition of all interactions during spin-reorientation the temperature-dependent inhomogeneous magnetic structure may emerge. As a result, different temperature behavior of magnetic dichroism bands in different spectral regions is supposed to occur. In this work the attempt have been made to identify the observed MLD spectral features taking into account their temperature behavior.

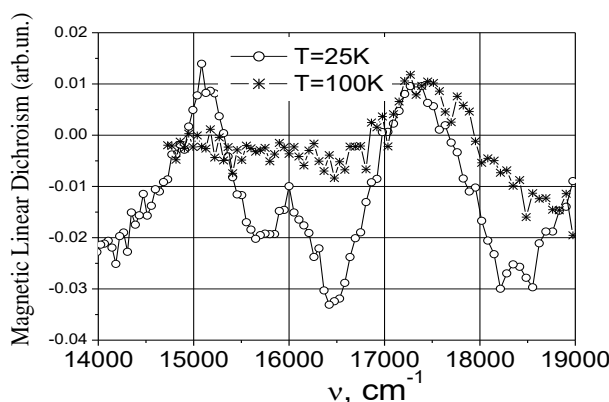


Fig. Magnetic linear dichroism spectra of YIG:Co film registered at $\mathbf{k} \parallel [001]$, $\mathbf{H} \parallel [100]$. $\mathbf{H} = 8.8$ kOe: open circles – $T = 25$ K, crosses – $T = 100$ K.

- [1] M.Tekielak, A.Stupakiewicz, A.Maziewski, J.M.Desvignes, J. Magn. Magn. Mater., 562 (2003)
- [2] A.A.Milner, N.F.Kharchenko, A.Maziewski, J.M.Desvignes, J. Magn. Magn. Mater. 2113 (1995).
- [3] Z. Simsa, J. Simsova, P. Gornert, A. Maziewski, Acta Ph. Pol. A76, 277 (1989)

The Study of Lattice Dynamics in Cu(en)₂SO₄ - the Low-Dimensional Heisenberg Quantum Antiferromagnet with Spin 1/2

O. Vinnik¹, L. Lederová¹, R. Tarasenko¹, L. Kotvytska¹, K. Zakut'anská², N. Tomašovičová², A. Orendáčová¹

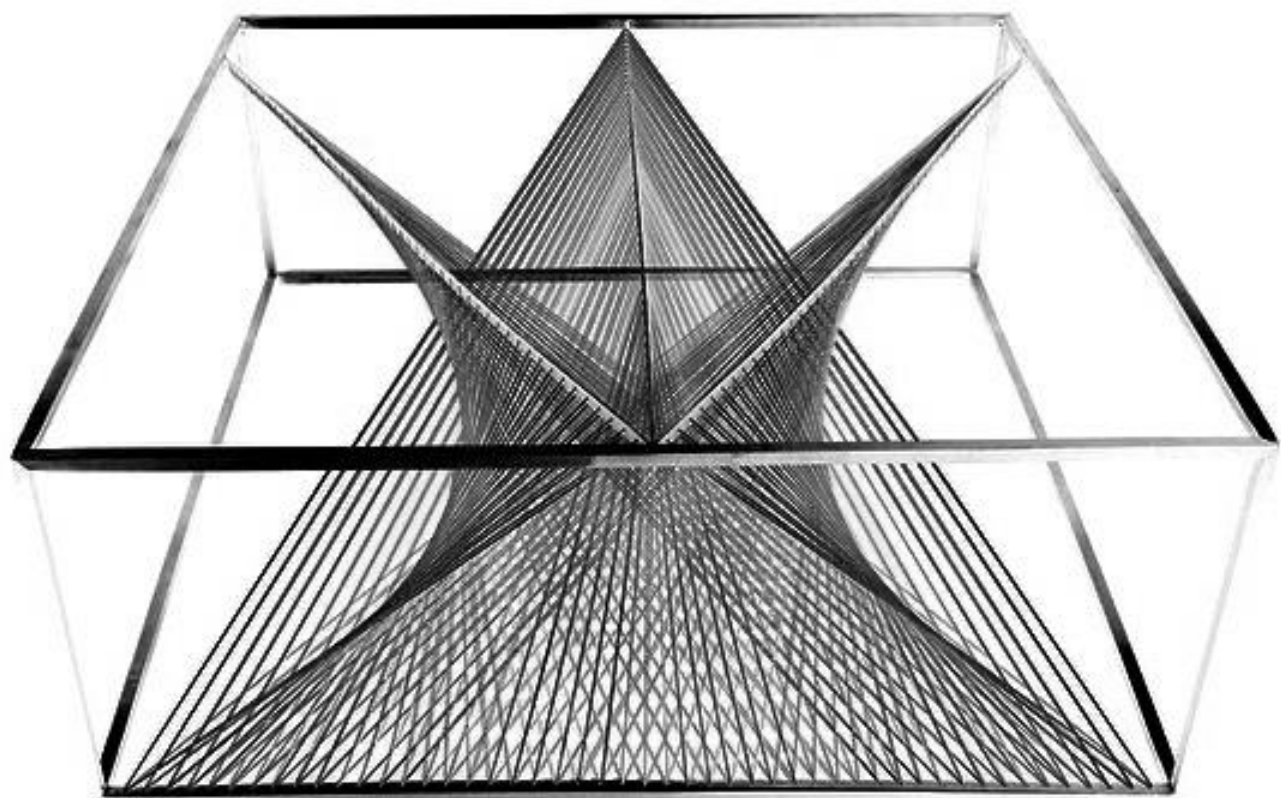
¹*Institute of Physics, P. J. Šafárik University, Park Angelinum 9, 04001 Košice, Slovakia*

²*Institute of Experimental Physics of SAS, Watsonova 47, 04001 Košice, Slovakia
olha.vinnik@student.upjs.sk*

Preliminary studies of magnetostructural correlations in Cu(en)₂SO₄ (en = ethylenediamine - C₂H₈N₂) revealed the presence of relatively strong exchange interaction [1]. It was shown that this organometallic compound based on Cu(II) ions with a quasi-one-dimensional polymer structure has a some kind of dimerization which prevents the ordering to the long-range magnetic state in zero magnetic field. The studies of polycrystalline sample revealed field induced magnetic phase transitions in magnetic fields above 7 T.

This work focuses on the lattice subsystem of the compound. The temperature dependence of the lattice specific heat was measured in the temperature range from 2 to 300 K in a zero magnetic field. In the data no specific heat anomalies were observed responsible for the structural phase transition. The analysis of the contribution of acoustic modes, described within the Debye approximation, with a Debye temperature $\Theta_D = 100$ K for the Cu(en)₂SO₄ sample was carried out. A deviation of the Debye model from the lattice specific heat was observed above 15 K. Also the contribution of optical modes to the total lattice specific heat was analyzed taking into account infrared active modes and Raman modes. The influence of acoustic and optical modes on the magnetic correlations of this system is discussed. The financial support of APVV-18-0197 is acknowledged.

[1] R. Tarasenko, PhD Thesis, P.J. Šafárik University, 2013.



OPTICS, PHOTONICS AND OPTICAL SPECTROSCOPY

Optical Response of Airplanes with Novel Coatings

L. Illyashenko

*Kharkiv National University of Radio Electronics,
14 Nauky Ave., Kharkiv, 61166, Ukraine
mila.illyashenko@gmail.com*

Cars, airplanes, and armors attract a lot of attention for scientists today. Novel coatings can bring them new features so that the strength of such structures became very high, and they are also able to resist crack propagation fractures and help dampen or dissipate energy within the material. Recently even living materials were developed, those have shown simultaneously exceptional strength, fracture resistance, and energy dissipation [1]. From another side, it can bring complications in device design to detect such an object with novel coating. To address this challenge, in this work the algorithm based on spectral spherical Galerkin method of Boundary Integral Equations (BIE) with singularity division and subtraction tricks powered by Fast Fourier Transform (FFT) was developed to solve the corresponding *Electromagnetic Transmission Problem* (ETP).

The second challenge is to detect several objects instead of one. Among others, airplanes are the most problematic. Their number increases. They connect our world, unite families, open our eyes to new horizons, perform repatriation flights, fly critical medical and other cargo around the world. While in the past it was possible to see in the best case one airplane in the sky, it is possible to observe two of them in the sky simultaneously now. This is why the problem of the interaction of the fields, scattered by several airplanes, is needed to be considered for future device design. In the past a scattering problem (SP) was solved numerically to design devices. Contrary to ETP, SP is based on assumption that the incident field from the source generates only the scattered field, while the transmitted field is almost zero, and therefore may become neglected. Due to this SP results in the matrix for System of Linear Algebraic Equations (SLAE), that is only $\frac{1}{4}$ of that obtained with ETP. However such benefits came with consequences. Neglecting by transmitted field in SP, leads to an increase of the scattered field. Thus, the result with SP is neither full nor correct. While mathematical models and numerical simulation algorithms are already well developed to solve SP on a single body [2, 3], it is needed to solve ETP for several interacting bodies with coatings. The above ideas are demonstrated with the generalized BIE method for ETP on several bodies.

The third challenge rises from the fact that the shape of the aircraft is too complicated [4] to be parametrized in such a way so that it may be used in conjunction with spectral BIE methods to get fast and accurate numerical results. In this work, the novel technique of surface representation that leads to fast numerics in addition to high accuracy was developed to bring new discoveries with application to homeland security and defense; target detection, recognition, and tracking; optical metrology and inspection; and geospatial informatics; surveillance; guidance systems; anomaly detection; leak detection; environmental monitoring; advanced driver-assistance systems and autonomous systems.

[1] An Xin, Yipin Su, Shengwei Feng, Minliang Yan, Kunhao Yu, Zhangzhengrong Feng, Kyung Hoon Lee, Lizhi Sun, Qiming Wang, Advanced materials, 2021, <https://doi.org/10.1002/adma.202006946>

[2] G.C. Hsiao, O. Steinbach, and W.L. Wendland, Boundary Element Methods: Foundation and Error Analysis, vol. Encyclopedia of Computational Mechanics, John Wiley & Sons, p. 62, 2018, doi: <https://doi.org/10.1002/9781119176817.ecm2007>.

[3] A. Nerukh, T. Benson, Non-Stationary Electromagnetics: An Integral Equations Approach, Jenny Stanford Publishing, p. 474, 2018, <https://doi.org/10.1201/9780429027734>

[4] O.P. Bruno and E. Garza, A Chebyshev-based rectangular-polar integral solver for scattering by general geometries described by non-overlapping patches, arXiv:1807.01813v1 (2018).

Simulation of elliptically polarized light propagation in turbid tissue-like scattering media with Monte Carlo method

I.V. Lopushenko¹, M. Borovkova¹, A. Bykov¹, I. Meglinski^{1,2}

¹*OPEM, ITEE, University of Oulu, P.O.Box 4500, FI-90014 Oulu, Finland*

²*College of Engineering and Physical Sciences, Aston University, B4 7ET Birmingham, UK
ivan.lopushenko@oulu.fi*

Nowadays numerous biomedical diagnostic applications feature usage of polarized light due to its unique optical properties [1,2]. Polarized light is usually employed as an efficient add-on to conventional imaging techniques, which allows to provide detailed insight on morphological structure of tissues [3,4]. It has been demonstrated that utilizing circularly polarized light has high potential for tissue characterization and cancer screening within Stokes-vector polarimetry [5,6].

Propagation of light through the turbid tissue-like scattering medium implies changes of both light intensity and polarization state due to many factors, including anisotropic scattering and internal reflections. By knowing the initial Stokes parameters and measuring the polarization state of the detected light, which is generally elliptic, it is therefore possible to study influence of each factor and to describe various types of malformations within biological tissues [7].

In order to provide accurate interpretation for the detected Stokes parameters, and in order to follow evolution of the polarization state of light within the biological tissue a computational modeling is required. Monte Carlo (MC) modeling approach allows to study light propagation in the random scattering medium via simulating a large number of photon trajectories ($\sim 10^9$), with the possibility of involving up to 10^3 scattering events along each trajectory. The cut-off tracing of the photon packet along trajectory is conducted according to the well-known Beer-Lambert-Bouguer law, whereas direction at each scattering event is defined via Henyey-Greenstein phase function. The modeling of light polarization is performed via assigning of two instantaneous components of the polarization vectors to each photon packet within Jones formalism, as introduced earlier [8,9].

Current study is devoted to the implementation of MC approach allowing simulation of the full set of Stokes parameters with account for such factors as phase shifts occurring due to light internal reflections inside the tissue and helicity flips occurring along the photon packet trajectory, which can significantly influence the resulting state of the light depolarization. The model is validated experimentally utilizing tissue-like phantoms with known optical properties, and we furtherly intend to apply it in order to study tissue samples influenced by various diseases, including cancer and Alzheimer.

- [1] V.T.Bachinskyi, O.Y.Wanchulyak, A.G.Ushenko, Y.A.Ushenko, A.V.Dubolazov, I. Meglinski, *Polarization Correlometry of Scattering Biological Tissues and Fluids* (Springer Briefs in Physics, Singapore, 2020)
- [2] I. Meglinski, L. Trifonyuk, V. Bachinsky, O. Vanchulyak, B. Bodnar, M. Sidor, O. Dubolazov, A. Ushenko, Y. Ushenko, I.V. Soltys, A. Bykov, B. Hogan, T. Novikova, *Shedding the Polarized Light on Biological Tissues* (Springer Briefs in Applied Science and Technology, Singapore, 2021)
- [3] V.A. Ushenko, B.T. Hogan, A. Dubolazov, A.V. Grechina, T.V. Boronikhina, M. Gorsky, A.G. Ushenko, Yu.O. Ushenko, A. Bykov, and I. Meglinski, *Sci. Rep.* 11, 3871 (2021)
- [4] V. Ushenko, B.T. Hogan, A. Dubolazov, G. Piavchenko, S.L. Kuznetsov, A.G. Ushenko, Yu.O. Ushenko, M. Gorsky, A. Bykov and I. Meglinski, *Sci. Rep.* 11, 5162 (2021)
- [5] C. Macdonald, I. Meglinski, *Laser Phys. Lett.* 8(4), 324–328 (2011)
- [6] D.Ivanov, V.Dremin, A.Bykov, E.Borisova, T.Genova, A.Popov, R.Ossikovski, T.Novikova, and I.Meglinski, *J. Biophoton.*, 13(8), e202000082 (2020).
- [7] M. Borovkova, A. Bykov, A. Popov, and I. Meglinski, *J. Biomed. Opt.* 25(5), 057001 (2020).
- [8] I. Meglinski, V.L. Kuzmin, D.Y. Churmakov, D.A. Greenhalgh, *Proc. Roy. Society A*, 461(2053), 43-53 (2005)
- [9] A. Doronin, C. Macdonald, and I. Meglinski, *J. Biomed. Opt.* 19(2), 025005 (2014).

Correlation Picture in Dicke Superradiance

S. Lyagushyn

*O. Honchar Dnipro National University, 72 Gagarin Ave., Dnipro, 49010, Ukraine
lyagush.new@gmail.com*

The Dicke's prediction of superfluorescence phenomena in systems of two-level atoms interacting via electromagnetic field played a great role both in theoretical and experimental investigations. Dicke superradiance remains the main idea for the coherent emission generation in the wavelength ranges where laser mechanism is inaccessible including a gamma radiation generator based on positronium. Some complicated conditions should be observed for the practical implementation of superradiance in crystals as well as in gaseous media. Particularly, low temperatures are used for experimental studies in this direction.

The mainstream in superradiance theory is passing to the description of "slow" subsystem of emitters. The method of eliminating boson variables (see [1]) provided the fast progress in the research of Dicke quasispin system self-organizing. But the questions of field states generated in such process were still in shadow. The way to solving them was opened by applying the Bogolyubov method of reduced description in the version developed by Peletminsky and Yatsenko [2] to the Dicke process. In Dnipro University the set of evolution equations for the Dicke model was obtained in the framework of such approach [3]. Field amplitudes and simultaneous binary correlation functions as well as energy density of the emitter subsystem are the reduced description parameters after averaging the operator equations in this case [4]. The general structure of equations for field parameters can be put down in brief as:

$$\partial_t \zeta_1 = i \sum_2 \mathbf{c}_{12} \zeta_2 + Q_1, \quad \partial_t (\zeta_1, \zeta_2) = i \sum_{1'} \mathbf{c}_{11'} (\zeta_1, \zeta_2) + i \sum_{2'} \mathbf{c}_{22'} (\zeta_1, \zeta_2) + (Q_1, \zeta_2) + (\zeta_1, Q_2)$$

$$\text{with } Q_\mu = Q_{in}(x), \quad Q_{1n}(x) = 0, \quad Q_{2n}(x) = 4\pi c \text{rot}_n P(x)$$

($P_n(x)$ – polarization density, \mathbf{c}_{12} – numerical matrix with differential operator) and the compact notations [5] are used

$$\zeta_\mu = \zeta_{in}(x), \quad \zeta_{1n}(x) = E_n^t(x), \quad \zeta_{2n}(x) = B_n(x), \quad (\zeta_\mu, \zeta_{\mu'}) = (\zeta_{in}(x), \zeta_{i'n'}(x')) = (\zeta_{in}^x \zeta_{i'n'}^{x'}) ;$$

$$\sum_\mu \dots = \sum_{in} \int_V dx \dots; \quad \zeta_s = \zeta_{\mu_s}, \quad \sum_s \dots = \sum_{\mu_s} \dots .$$

The set of kinetic equations can be analyzed numerically with using certain assumptions concerning the initial state of the system. It is necessary to use the ideas of macroscopic averaging of the field parameters and make some estimations for the interaction constants. In the applied formalism, we have no trouble with breaking the chain of equations, but must take into account material equations for this medium with integral forms for coefficients. The paper presents the results of the numerical simulation by dint of *Mathematica* program package. Several simplifications were used: the fixed polarization direction, neglect of edge effects. For any system volume shape, the exponential raise of correlation functions and the predominant role of the central zone were discovered.

- [1] N.N. Bogolyubov (Jr.) and A.S. Shumovsky, Superradiance (JINR, Dubna 1987, in Russian).
- [2] A.I. Akhiezer and S.V. Peletminsky, Methods of Statistical Physics (Pergamon Press, Oxford 1981).
- [3] S.F. Lyagushyn and A.I. Sokolovsky, Physics of Particles and Nuclei, 41(7), 1035 (2010).
- [4] S.F. Lyagushyn, A.I. Sokolovsky, and Yu.M. Salyuk, Problems of Atomic Science and Technology, Series: Nuclear Physics Investigations, 57, 235 (2012).
- [5] S.F. Lyagushyn, A.I. Sokolovsky, and S.A. Sokolovsky, Journal of Physics and Electronics, 27(2), 17 (2019).

Transverse Anderson Localization Versus Evanescent Waves Confinement

S.S. Melnyk¹, O.V. Usatenko¹, V.A. Yampol'skii^{1,2}

¹*A.Ya. Usikov Institute for Radiophysics and Electronics of NAS of Ukraine,*

12 Acad. Proskura Str., Kharkov, 61085, Ukraine

²*V.N. Karazin Kharkov National University, 4 Svobody Sq., Kharkov, 61077, Ukraine*

melnik.teor@gmail.com

In this paper, we study theoretically the transverse Anderson localization of light in the simplest geometry, where the wave propagates along the layers in the randomly inhomogeneous dielectric and evanesces in the direction across the layers, say, along the z -axis. Thus, we investigate the situation when there are simultaneously two reasons for the localization of the wave in the direction transverse to its propagation. The first reason is the usual evanescent wave confinement due to the large value of the wave vector, $q > \omega\sqrt{\varepsilon}/c$, where ω is the wave frequency, ε is the average value of the dielectric permittivity, $\langle \varepsilon(z) \rangle$, c is the speed of light in the vacuum. The second reason is the Anderson mechanism related to the randomness of the spatial distribution of $\varepsilon(z)$.

We solve the problem of p-polarized evanescent wave propagation in the randomly layered dielectric using the retarded-Green-function formalism in the Born approximation under conditions,

$$\kappa R_c \ll 1, \quad \kappa \gg (V_0^2 R_c)^{1/3}, \quad \kappa = \sqrt{q^2 - \frac{\omega^2 \varepsilon}{c^2}}.$$

Here R_c is the correlation radius of the random process $\varepsilon(z)$, κ is the inverse localization length for the evanescent wave, V_0 is the effective potential in the equation for the Green function. Then we apply the obtained result to two physical realizations of the evanescent waves.

The first problem is related to the so-called disturbed total internal reflection for the wave incident from an optically dense dielectric onto its boundary with the randomly inhomogeneous optically rare dielectric under conditions when the angle of incidence exceeds the limiting angle for the total internal reflection. It is known that, in this case, the wave penetrates into an optically rare medium in the form of evanescent wave which can tunnel into another optically dense dielectric located nearby. Contrary to expectations, the fluctuations of $\varepsilon(z)$ in rare medium lead not to a weakening, but to an increase in the coefficient of wave transmission through the optical tunneling barrier, in comparison with the case of a rare dielectric with constant dielectric permittivity ε . In other words, the Anderson mechanism does not enhance the localization of the evanescent wave with given q and ω in the z -direction, but weakens it.

The second solved problem is related to the propagation of surface plasmon-polaritons (SPPs). In this case, the Anderson mechanism changes the dispersion law for SPPs moving the dispersion curves away from the light line deep into the (q, ω) -plane. It is of interest that the occurrence depth for SPPs varies in different ways, depending on which of the quantities, q or ω , is fixed. If one keeps the wave frequency constant, then the fluctuations of $\varepsilon(z)$ result in decrease of the localization length, whereas the fluctuations have a weakening effect on the localization of SPPs with a fixed value of q .

Spectral properties of thiacarbocyanine J-aggregates depending on formation conditions

P. Pisklova, I. Ropakova, A. Sorokin, S. Yefimova

*Institute for Scintillation Materials of NAS of Ukraine,
60 Nauky Ave., Kharkiv, 61072, Ukraine
polinkapisklova@gmail.com*

Organic dye aggregation is of great importance due to aggregates properties and applications. For example, well-ordered aggregates, called J-aggregates, are characterized by a sharp and intense absorption band at a longer wavelength comparing with that of the monomer [1,2]. J-aggregates of cyanine dyes are formed in polar media above a certain critical concentration of the dye. Self-assembly of such supramolecular structures occurs mainly due to strong Van der Waals interactions arising from the high polarizability of organic chromophores containing chains of bound compounds [1,2]. Strong dipole-dipole interactions between the transition dipole moments of the dye monomers contribute to the propagation of electronic excitation in the aggregate of several hundred molecules in the form of the Frenkel exciton [1,2]. Collective excitation generates unique linear and nonlinear properties of J-aggregates, such as resonant fluorescence, exciton superradiation, and others.

In this work, the aim was to form J-aggregates of thiacarbocyanine (TCC) dye (the chemical structure is shown in Fig. 1) in aqueous solutions and polymer films, as well as to analyze the features of the aggregate spectral characteristics.

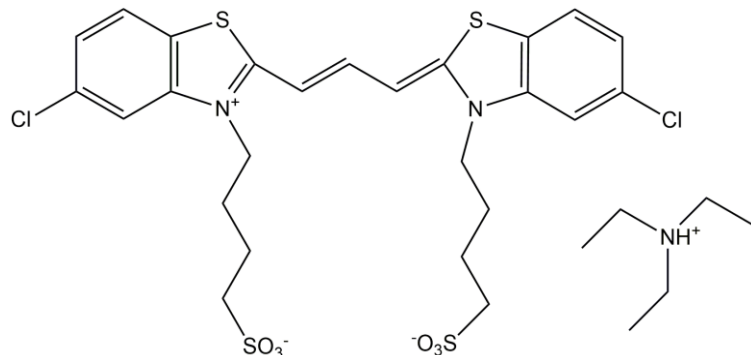


Fig 1. The structural formula of the dye TCC.

The interest in TCC J-aggregates is caused by the location of their excitonic band (J-band) in the red spectral region ($\lambda = 650$ nm), which is important for some applications. It should be noted, that the spectral properties for J-aggregates of some derivatives of the TCC dye are already described in the literature, especially that with meso-substituents (*meso*-TCC). So, special attention will be paid to the difference between TCC and *meso*-TCC J-aggregates.

- [1] A.V. Vannikov [et. al], Chem. Phys. 287, 261, (2003).
- [2] G. Busse [et. al], Phys. Chem. Phys. 6, 3309, (2004).
- [3] Hiroshi Yao [et. al], J. Phys. Chem. 111, №25, 7176, (2007).

Scattering of Surface Plasmon-Polaritons by a Segment of Metal-Dielectric Boundary with Randomly Fluctuating Impedance

Yu. Tarasov¹, O. Stadnyk^{1,2}

¹*O. Ya. Usikov Institute for Radiophysics and Electronics of NAS of Ukraine,*

12 Acad. Proskura Str., Kharkiv, 61085, Ukraine

²*Kharkiv National University of Radio Electronics,*

14 Nauky Ave., Kharkiv, 61166, Ukraine

tarasov@ire.kharkov.ua

The rapid development of nanotechnology has led to the relevance of the optics of surface electromagnetic waves and to the emergence of plasmonics, which studies the interaction of light with free electrons in noble metals [1]. Plasmon-polaritons (PPs) supported by the ideally flat homogeneous metal surfaces have a high degree of spatial localization and, thus, are promising for miniaturization of various optical devices. However, the miniaturization inevitably involves poorly controlled surface defects in the devices, which highly degrade their performance. Therefore, it is extremely important to consider in depth the scattering of surface PP (SPP) by in reality always existing surface inhomogeneities, in general of the impedance type.

Previous works on this topic were limited by either consideration of infinitely long 1D-random surfaces which support wave localization of Anderson type [2] or by the study of finite-size defects of regular rather than random structure (see, e.g., Refs. [3,4]). In the present study, we examine the case of SPP propagation as well as its out-of-surface luminescence due to surface imperfections of finite size and random character taken into account concurrently. To achieve this goal, we apply the field-theoretical method previously developed in Ref. [5] for the SPP single scattering, which now is modified so as to take rigorously into account the interference-nature localization achievable only within the framework of multiple scattering theory.

In the present work, we consider the propagation of TM polarized PP wave that hits the finite segment of metal-dielectric boundary with randomly varying surface impedance. The incident wave is assumed to partially back-reflect along the surface, partially penetrate through the imperfect segment, and partially radiate into free space. The integral equation is obtained, which describes the emitted wave as the radiation from a given source in the capacity of which is the irregular section of the metal-vacuum boundary. The solution to this equation connects the scattered field with the field of the incident SPP, which made it possible to calculate the scattering intensity as a function of the fluctuating impedance parameters (dispersion, correlation radius, length of the inhomogeneous segment) for different losses in the metal half-space. The scattered field intensity is expressed in terms of the pair correlation function of the impedance, which depends on the wave numbers of incident and scattered wave harmonics. Scattering effects at both weak and strong impedance fluctuations are interpreted in terms of Anderson localization of the SPP.

The novelty of the results obtained in this work is determined by the formulation of the problem (taking into account both scattered free electromagnetic waves and their Anderson-localized surface counterparts), by the approach to the solution (going beyond the limits of single scattering and using quantum-mechanical and field-theoretical methods in electromagnetic problems with random parameters), and by interpretation of the results in terms of scattering operator norm.

- [1] S. Enoch and N. Bonod (eds.), *Plasmonics - From Basics to Advanced Topics*, Springer Series in Optical Sciences (Springer, Berlin, 2012) Vol. 167.
- [2] V. Freilikher and I. Yurkevich, *Phys. Lett. A* 183, 247 (1993).
- [3] A. Yu. Nikitin, F. López-Tejeira, and L. Martín-Moreno, *Phys. Rev. B* 75, 035129 (2007).
- [4] J. Polanco, R. M. Fitzgerald, and A. A. Maradudin, *Phys. Rev. B* 87, 155417 (2013).
- [5] Yu. V. Tarasov, O. V. Usatenko, and D. A. Iakushev, *Low Temp. Phys.* 42, 685 (2016).

Surface Plasmon-Polaritons at Two-Dimensional Resonant Anisotropic Systems

O. Yermakov^{1,2}

¹*Department of Computer Physics, V. N. Karazin Kharkiv National University, 4 Svobody Square, Kharkiv, 61022, Ukraine*

²*Department of Physics and Engineering, ITMO University, Kronverksky Pr. 49, St. Petersburg, 197101, Russia
oe.yermakov@gmail.com*

Modern optical technologies require the miniaturization and planarization of the optical devices that leads to an urgent need for efficient control of localized light. In this aspect, surface electromagnetic waves on two-dimensional structures and materials attract a lot of attention, and can potentially become the main information carriers in planar data processing optical systems.

This work presents the results of theoretical and experimental studies and control of the properties (dispersion, polarization, field pattern, directivity, optical spin) of surface plasmon-polaritons localized at two-dimensional anisotropic resonant structures in the optical, near-infrared and microwave ranges.

Namely, we have developed the approach of an effective surface conductivity for the two-dimensional systems description in both far- and near-field [1]. We have theoretically studied the dispersion features of a novel type of surface waves at hyperbolic metasurfaces, well-known today as hyperbolic plasmon-polaritons [2,3]. Then, we make the classification of the possible polarization states of surface waves [4]. Particularly, we have demonstrated the possibility to control the direction of the optical spin angular momentum on demand due to the hybrid TE-TM polarization of hyperbolic plasmon-polaritons [5,6]. Besides, we have discovered the polarization degree of freedom for localized light by demonstrating the broadband TE-TM polarization degeneracy of surface waves [7]. The theoretical results have been confirmed experimentally in the microwave [8], near-infrared and optical [1,9] frequency ranges.

The results obtained open new opportunities for the flat-optics and photonic devices, optical data transfer and processing systems, opto-mechanics and sensing applications.

- [1] O.Y. Yermakov, D.V. Permyakov, F.V. Porubaev, P.A. Dmitriev, A.K. Samusev, I.V. Iorsh, R. Malureanu, A.V. Lavrinenko, and A.A. Bogdanov, *Sci. Rep.* 8, 14135 (2018).
- [2] O.Y. Yermakov, A.I. Ovcharenko, M. Song, A.A. Bogdanov, I.V. Iorsh, and Y.S. Kivshar, *Phys. Rev. B* 91(23), 235423 (2015).
- [3] J. S. Gomez-Diaz, M. Tymchenko, and A. Alù, *Phys. Rev. Lett.* 114(23), 233901 (2015).
- [4] O. Yermakov and A. Bogdanov, IEEE Ukrainian Microwave Week (UkrMW), 559 (2020).
- [5] O.Y. Yermakov, A.I. Ovcharenko, A.A. Bogdanov, I.V. Iorsh, K.Y. Bliokh, and Y.S. Kivshar, *Phys. Rev. B* 94(7), 075446 (2016).
- [6] O.Y. Yermakov, A.A. Bogdanov, I.V. Iorsh, K.Y. Bliokh, and Y.S. Kivshar, Proc. SPIE 10227, 1022703 (2017).
- [7] O.Y. Yermakov, A.A. Bogdanov, and A.V. Lavrinenko, *IEEE J. Sel. Top. Quantum Electron.* 25(3), 1 (2019).
- [8] O.Y. Yermakov, A.A. Hurshkainen, D.A. Dobrykh, P.V. Kapitanova, I.V. Iorsh, S.B. Glybovski, and A.A. Bogdanov, *Phys. Rev. B* 98(19), 195404 (2018).
- [9] A. Samusev, I. Mukhin, R. Malureanu, O. Takayama, D.V. Permyakov, I.S. Sinev, D. Baranov, O. Yermakov, I.V. Iorsh, A.A. Bogdanov and A.V. Lavrinenko, *Opt. Express* 25(26), 32631 (2017).

Photoelectric properties of heterostructures with GeSn thin films

S. Derenko, S. Kondratenko

*Taras Shevchenko National University of Kyiv, 64 Volodymyrs'ka St. 01601, Kyiv, Ukraine
serhii.derenko@knu.ua*

Germanium tin (GeSn) alloys are promising materials for use in various optoelectronic devices[1][2] and can be easily integrated onto Si-platforms.[3] The main advantages of future applications of the GeSn thin films are that at increasing tin reduces indirect and direct bandgap, and having crossover point at specific content. The main disadvantage of these structures is the presence of plenty of defects, significantly impacting optoelectronics property.[4] The description of the relationship between defects and alloys efficiency is a long-standing problem.

The photoconductivity mechanism and transport paths of photoexcited charge carriers in the GeSn/Ge/Si heterostructures was studied. The dark conductivity was studied as a function of temperature, which allowed to identify of the presence of deep levels at $\text{EV}+(100\div130)$ meV. We have established that point defects are the source of a band of electronic states and determine the photoconductivity response. The photocurrent dependencies on excitation intensity demonstrate that the main conduction occurs mainly through the Ge layer under low pumping and through the Si substrate under high one, since the GeSn top layer is much thinner has a much higher conductivity. This detailed understanding of the recombination processes is of critical importance for developing GeSn/Ge-based optoelectronic devices.

The optical and photoelectric properties of the Ge pin diodes with GeSn thin films in the space-charge region were studied at temperature range 10 K – 300 K. The structures show a photovoltage at 0.5 – 2.0 eV spectral range due to separation of charge carriers by potential barriers of 510 meV height. The impact of deep defect states on photoresponse was discussed.

- [1] Tran H et al., Study of GeSn mid-infrared photodetectors for high frequency applications. *Front. Mater.* 2019, 6, 278.
- [2] Elbaz A et al., Ultra-low-threshold continuous-wave and pulsed lasing in tensile-strained GeSn alloys. *Nat. Photon.* 2020, 14, 375–82.
- [3] Soref R Mid-infrared photonics in silicon and germanium. *Nat. Photonics* 2010, 4, 495–497.
- [4] Kondratenko S V et al., Photovoltage spectroscopy of direct and indirect bandgaps of strained $\text{Ge}_{1-x}\text{Sn}_x$ thin films on a $\text{Ge}/\text{Si}(001)$ substrate *Acta Mater.* 2019, 171, 40–7.

Impurity-based emitting centers of different types in doped molecular crystals: formation and spectral multiplicity

M.D. Curmei, V.I. Melnyk, G.V. Klishevich, T.V. Bezrodna, V.V. Nesprava, O.M. Roshchin

*Institute of Physics, NAS of Ukraine, 46 Nauki prosp., Kyiv 03028, Ukraine
curmei_nd@ukr.net*

Electronic spectra of the impurity-doped molecular crystals are characterized with a presence of the well-developed multiplet structure at low temperatures. Investigations of multiplet features allow to obtain information about types and properties of the impurity centers in crystals. Benzophenone and naphthalene crystals, and also their β -halogen derivatives (β -bromo-benzophenone and β -fluoro-naphthalene) have been chosen as objects for the study. The experiments have been carried out in the temperature range 4.2–50 K.

The multiplet structure in the absorption and luminescence spectra of these crystals has been explained by a use of symmetry properties of the free molecules and crystalline formations. The detail analysis of spectroscopic and polarization characteristics of absorption and luminescence for the molecular crystals of doped benzophenone and naphthalene allows to propose a model of impurity emitting centers, based on the consideration of interactions between translation-nonequivalent impurity molecules in a unit cell of the crystal.

When the impurity concentrations are small (less than 1 %wt.), the absorption and luminescence spectra at $T=4.2$ K possess doublet patterns with intervals between the doublet components of 96 cm^{-1} (doped naphthalene) and 102 cm^{-1} (doped benzophenone). These spectra are shown to be composed of two identical band series, induced by formation of two different centers, consisting of the impurity single molecules.

The growth of impurity concentration (over 1 %wt.) and temperature rise cause significant spectral changes. In the case of the benzophenone doped crystal, two broad bands D_1 и D_2 are observed in the long-wavelength side of doublet components; their intensity is much smaller than that of the doublet. Temperature increase up to 20 K results in the disappearance of the spectral doublet structure, and the further heating to $T=50$ K eliminates also the bands D_1 and D_2 . The impurity concentration increase in the naphthalene crystal results in appearance of the additional spectral structure in the polarized absorption spectra near the 0-0 bands of the single centers in a form of thin bands with similar intensity and different polarity. These structures are associated with a formation of impurity paired centers, consisting of the two resonantly interacting molecules. In some cases, the absorption spectra contain additional intense peaks in the high-frequency regions, relative to the 0-0 transition bands for each single center, and consisted of narrow-lined components. These spectral peaks are also explained by a formation of impurity paired centers, but here interactions between the molecules are not resonant. This work discusses the conditions, which cause formation of the resonant or nonresonant interactions between two impurity molecules in the molecular crystals.

Several types of the paired centers have been discovered for the different impurities at the concentrations over 1 %wt. Each center consists of two impurity molecules, located along crystallographic axes in the crystal unit cell. Since the molecules of centers do not satisfy any symmetry operation of a crystal, each molecule of the center absorbs independently. The proposed structure of paired centers describes quite well experimental results.

The idea of experimental determination for the space characteristics of wavetrains in the molecular crystals is also discussed; this is of great importance for understanding the physical nature of electron processes during light absorption in crystals.

Absolute cross sections of bremsstrahlung induced by 0.3–1 keV electron scattering by free xenon clusters

Yu.S. Doronin, A.A. Tkachenko, V.L. Vakula, G.V. Kamarchuk

*B.Verkin Institute for Low Temperature Physics and Engineering of NAS of Ukraine,
47 Nauky Ave., Kharkiv 61103, Ukraine
doronin@ilt.kharkov.ua*

Bremsstrahlung (BS) [1] arising from the scattering of electrons by atoms, molecules, or clusters is formed by two mechanisms. In one of the mechanisms, the emission of photons is caused by the incident electron when it is decelerated in the static field of the target particle (ordinary BS). In another method, continuous-spectrum photons are emitted by electrons of the target particle due to its dynamic polarization, namely polarization bremsstrahlung (PBS).

BS processes (including PBS) have been well studied using the scattering of intermediate-energy electrons by xenon atoms and clusters [2]. In particular, the absolute differential cross sections of BS were determined for the scattering of 0.6 keV electrons by Xe atoms [3], and a change in the PBS spectrum was found at the transition from atoms to clusters [2].

In this work, for the first time, the absolute differential cross sections of BS were experimentally measured by the bombardment of Xe clusters with electrons with energies of 0.3–1 keV. Additionally, the contribution of the polarization mechanism to the BS cross section is separated and the dependence of the BS cross section on the energy of the incident electron is established. Xenon clusters with an average size of 400 to 12000 atoms per cluster were obtained via the adiabatic expansion of a gas through a supersonic nozzle into a vacuum [2]. The size and number of interacting with electrons Xe clusters were measured according to the original approach [4]. The emission spectra of the Xe cluster jet were recorded in the 70–240 eV region with an X-ray spectrometer using a proportional counter.

The results obtained can be used for X-ray spectroscopy of clusters and for development of the theory of bremsstrahlung at low energies of interacting particles.

- [1] E.T. Verkhovtseva, E.V. Gnatchenko, B.A. Zon, A.A. Nekipelov, A.A. Tkachenko, Sov. Phys. JETP. 71, 443 (1990).
- [2] E.V. Gnatchenko, A.A. Tkachenko, V.N. Samovarov, A.N. Nechay, Phys. Rev. A. 82, 012702 (2010).
- [3] E.V. Gnatchenko, A.A. Tkachenko, A.N. Nechay, JETP Lett. 86, 292 (2007.)
- [4] Yu. S. Doronin, A. A. Tkachenko, V. L. Vakula, G. V. Kamarchuk, International Advanced Study Conference - CM<P 2020, p. 109 (2020).

Effect of annealing on optical properties of cadmium sulfide thin films

A. Kashuba¹, R. Guminilovych¹, H. Ilchuk¹, B. Andriyevsky², V. Kordan³, I. Semkiv¹, R. Petrus¹, T. Malyi³

¹*Lviv Polytechnic National University, 12 S. Bandera str., Lviv, 79013, Ukraine*

²*Koszalin University of Technology, 2 Sniadeckich str., Koszalin, 75-453, Poland*

³*Ivan Franko National University of Lviv, 8a Cyryl and Metody str., Lviv, 79005, Ukraine
Andrii.I.Kashuba@lpnu.ua*

Cadmium chalcogenides (CdX , with $X = \text{S}$, Se and Te) belong to a known $\text{A}^{\text{II}}\text{B}^{\text{VI}}$ group of crystals, which show a typical semiconductor behaviour. They are considered as very promising materials for various optoelectronic devices. In particular, CdTe has proven as a leading compound for manufacturing cost-effective second-generation photovoltaic devices. CdTe -based solar cells attract much attention of researchers, since CdTe is characterized by a direct forbidden gap with the bandwidth ~ 1.46 eV and a high absorbance (above 10^5 cm^{-1}) [1], which make it an excellent light-absorbing layer for solar cells. When forming high-efficiency p - CdTe -based heterojunctions for a window layer of solar batteries, cadmium sulphide (CdS) is mainly used [2–4]. It is characterized by a high absorbance and high photoconductivity in the visible region. This is due to the fact that CdS represents a direct-bandgap semiconductor, which reveals direct band-to-band optical transitions. Its bandgap at the room temperature is equal to ~ 2.42 eV. The electrical properties of CdS are characterized by the resistivity of about $10^6 \Omega \cdot \text{cm}$ and n -type conductivity.

CdS can be formed in either cubic or hexagonal phases, which depends mainly on the synthesis technique and growth parameters [5–8]. In the solar cells based on CdS/CdTe heterojunctions, the thickness of CdS layer is in the most cases equal to ~ 150 – 300 nm [9]. As a result, photogenerated charge carriers almost completely recombine inside a CdS film and generate no photocurrent. It is just the large absorption of the CdS film that causes no photocurrent in the structure. Therefore, it is desirable to use the CdS films with the thicknesses less than 100 nm in order to fabricate high-efficiency CdTe -based solar cells [9–11].

The results of experimental studies of the optical properties of CdS thin films annealed in an atmosphere of CdCl_2 are presented. The synthesis of CdS thin films was carried out by the chemical surface deposition method on a glass substrate. The quality of the obtained films was studied using X-ray diffraction, scanning electron microscopy and X-ray fluorescence spectroscopy. Optical transmission and reflection spectra were obtained experimentally. The dependence of the thickness of the thin films on the deposition time was established. The dependence of the bandgap on the film thickness is established.

- [1] N. Romeo, A. Bosio, R. Tedeschi, and V. Canevari, Mater. Chem. Phys. 66, 201 (2000).
- [2] B.M. Basola, and B. McCandless, J. Photon. Energy. 4, 040996 (2014).
- [3] N. Romeo, A. Bosio, V. Canevari, and A. Podesta, Sol. Energy. 77, 795 (2014).
- [4] N.R. Paudel, C. Xiao, and Y. Yan, J. Mater. Sci.: Mater. Electron. 25, 1991 (2014).
- [5] S.V. Averin, P.I. Kuznetsov, V.A. Zhitov, N.V. Alkeev, V.M. Kotov, L.Y. Zakharov, and N.B. Gladysheva, Techn. Phys. 57, 1514 (2012).
- [6] R.N. Bhattacharya, M.A. Contreras, B. Egaas, R.N. Noufi, A. Kanevce, and J.R. Sites, Appl. Phys. Lett. 89, 253503 (2006).
- [7] I.O. Oladeji, and L. Chow, Thin Solid Films. 474, 77 (2005).
- [8] W. Mahmood, J. Ali, I. Zahid, A. Thomas, and A. Haq, Optik. 158, 1558 (2018).
- [9] A. Bosio, N. Romeo, S. Mazzamuto, and V. Canevari, Progr. Cryst. Growth & Charact. Mater. 52, 247 (2006).
- [10] B.E. McCandless, and K.D. Dobson, Sol. Energy. 77, 839 (2004).
- [11] R.Yu. Petrus, H.A. Ilchuk, A.I. Kashuba, I.V. Semkiv, and E.O. Zmiovskaya, Opt. Spectrosc. 126, 220 (2019).

Effect of titanium doping on the structural and optical properties of spinel crystals

V. Gritsyna¹, V. Kobyakov¹, V. Hryshko¹, Yu. Kazarinov^{1,2}

¹*V.N. Karazin Kharkiv National University, 4, Svoboda Sq., Kharkiv, 61022 Ukraine*

²*NSC "Kharkov Institute of Physics and Technology", 1 Akademichna St., Kharkiv, 61108 Ukraine*

vtgritsyna@karazin.ua

Due to superior mechanical and thermal properties, also the wide spectral range of optical transparency, high resistance to corrosion and irradiation the magnesium aluminates spinel (MAS) crystals and ceramics are widely used for structural and optical applications. The optical properties of non-stoichiometric magnesium aluminates spinel crystals ($MgO \cdot 2.2Al_2O_3$) doped with titanium dioxide to concentration of 0.2 and 0.5 wt% grown by Verneuil method are investigated. The grown boles of dimensions of 10-20 mm in diameter and 20-50 mm in length have non-uniform coloration in bluish [1]. For investigation the boles were cut into slices of 1.5 mm in thickness along the direction of crystal growth and polished to optical finish.

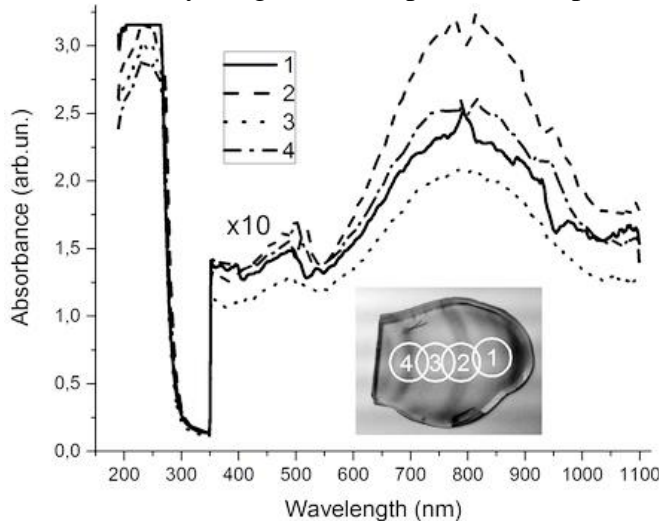


Fig. 1. Optical absorption spectra of $MgO \cdot 2.2Al_2O_3:Ti$ 0.2% at the indicated points

identify this band with the $Ti^{4+} + Fe^{2+} \rightarrow Ti^{4+} + Fe^{2+}$ charge transfer transition [2].

Photoluminescence and radio-luminescence excited with X-rays demonstrate the complex wide emission peak, which was deconvoluted in three different intensity bands. The main band at 490 nm was excited by photons at wavelength of 280 nm assigned to the charge transfer de-excitation of $Ti^{3+} 3d$ into the valence band hole created by band-to-band excitation [2]. As we noticed, the optical properties are very sensitive to UV- or daylight irradiation leading to deformation in shape the absorption and luminescence bands. Such behavior of MAS doped with Ti is consistent with transformation of optical band gap [3]. The formation of the electronic band structure of spinel crystals doped with different concentration of titanium and its modification at annealing to different temperature will be discussed.

The structural properties of experimental samples were investigated measuring variation of the lattice parameter along the direction of growth and across diameter of boles. Therefore, the variation of lattice parameter and crystal molar composition was obtained. Also along the bole the relative concentration of impurity ions of Ti, Cr, Mn, and Fe was measured using X-ray fluorescent analyzer KRAB-3UM. As-grown crystals demonstrate two absorption bands at about 800 and 470 nm and in UV range a strong absorption edge arising from 300 nm (see Fig. 1.). Strong absorption in the UV range 200-300 nm has two slightly resolved bands at 215 and 260 nm and band at 280 nm for deeply colored spots. The correlation of the band intensity at 800 nm to impurity iron concentration allows us to

- [1] V.T. Gritsyna, Yu.G. Kazarinov, V.A. Kobyakov and L.A. Lytvynov. Acta Phys. Polonica A 133, 774, (2018).
- [2] A. Jouini, A. Yoshikawa, A. Brenier, T. Fukuda, and G. Boulon, Phys. Stat. Sol. C4, No. 3, 1380 (2007).
- [3] K. Izumi, S. Miyazaki, S. Yoshida, T. Mizokawa, E. Hanamura. Phys. Rev. B 76, 075111 (2007).

IR spectrometric studies of recondensates CCl_4 obtained by the method of cryomatrix isolation.

E. Korshikov, D. Sokolov, A. Nurmukan, D. Zhaxybekov

*Al-Farabi Kazakh National University, Institute of Experimental and Theoretical Physics,
Al-Farabi ave. 71/23, Almaty 050040, Kazakhstan
e.s.korshikov@physics.kz*

The processes of formation and properties of thin films of cryovacuum condensates are the subject of versatile research throughout the more than 100-year period of intensive development of low-temperature physics and cryogenic technologies, developed on the basis of the obtained fundamental knowledge. [1]

The processes of heat and mass transfer, which include: condensation, sublimation and recondensation of gases at low and ultra-low temperatures, are an integral part, both in cryogenic-vacuum equipment, and are constantly implemented in the natural conditions of space. So, a significant part of the substance on cryogenic surfaces, surfaces of space objects is in a condensed state. Under the influence of external factors, phase transformations are carried out in them. In this case, one of the components can evaporate, which will lead to the recondensation of the remaining component. As a result, a new phase is formed, the properties of which will depend on the cluster composition of the recondensed gas and on the surface temperature. A similar process can also be implemented in cryogenic equipment. [2]

Our research presents the results of studies of cryoprecipitation processes of a two-component mixture of a matrix gas (nitrogen, argon) with a test substance (freon CCl_4) in various concentration ratios. The task of determining the relationship between the conditions of cryoprecipitation (substrate temperature, pressure of the gas phase and its concentration) and the properties of the resulting cryocondensed film (refractive index, density, reflectivity in the IR range) has been experimentally performed.

The results were obtained using several experimental methods:

1) The method of two-beam laser interferometry to determine the growth rate, the thickness of the cryocondensed film and its refractive index;

2) IR spectrometric method for determining the state of samples of cryovacuum condensates based on the analysis of the absorption amplitudes and the position of the bands corresponding to the characteristic vibrations of the studied molecules in the unbound state;

3) Thermal desorption method for alternative determination of the temperature of structural-phase transformations.

Thus, the main purpose of the research was to study the formation and evolution of the properties of thin films of recondensates of CCl_4 freon molecules formed as a result of structural-phase transformations and relaxation processes in solid solutions of the investigated substances at low and ultra-low temperatures.

The objects of research were Freon CCl_4 recondensates obtained by the method of gas-phase condensation with a matrix gas in various concentration ratios with nitrogen and argon.

[1] Drobyshev A., Strzhemechny Yu., Aldiyarov A., Korshikov E., Kurnosov V., Sokolov D., Journal of Low Temperature Physics. 187, 71 (2017).

[2] Aldiyarov, A., Nurmukan, A., Sokolov, D., Korshikov, E., Applied Surface Science, 507, 144857, (2020).

Features of light absorption by a model molecular aggregate

I.Yu. Ropakova¹, A.A. Zvyagin^{2,3}

¹*Institute for Scintillation Materials of NAS of Ukraine,
60 Nauky Ave., Kharkiv, 61072, Ukraine*

²*B.Verkin Institute for Low Temperature Physics and Engineering of NAS of Ukraine,
47 Nauky Ave., Kharkiv, 61103, Ukraine*

³*Max-Planck für Physik komplexer Systeme,
38 Noethnitzer Str., Dresden D-01187, Germany
adelma@ukr.net*

Low-dimensional optical materials, such as quantum wells and wires, and organic systems, such as conjugated polymers, photosynthesized complexes of plants and bacteria, and molecular aggregates, have been intensively studied in recent years. Interest in them is associated with their special optical properties: fast transmission of electromagnetic energy, strong (with the ability to change color) optical absorption, the possibility of optical switching and photoluminescence. Light in such molecular systems is collectively absorbed by many molecules, and their optical properties exhibit collective coherent behavior.

Aggregates of organic molecules are supramolecular complexes with strong interactions between electronic transitions. The so-called Jaggregates⁴ exhibit a long-wavelength shift (whereas for H-aggregates, a hypsochromic, i.e., short-wave shift is characteristic) and many aggregates are characterized by a narrowing of the spectral absorption band, the J-band (H-band). This occurs, e.g., for cyanine dyes with a strong intermolecular interaction of the dipole nature.

Unlike aggregates with the J-band, the H-band absorption line is usually highly affected by vibrations; it is wider than the J-band and comparable in magnitude to the bandwidth of the monomers forming the aggregate. Some substances, e.g., PIC (pseudoisocyanine), can exhibit both J and H-bands upon aggregation. As a result of the complex contribution of vibrations, the study of light absorption in H-band systems is difficult, and there is much less publications (as compared to the case of J-aggregates) addressing the optical properties of H-aggregates.

The purpose of this work is to study theoretically the effect of randomly distributed H-aggregate impurities in chains of J-aggregates on the absorption spectra of such quantum molecular complexes. In the present work, based on the exact quantum-mechanical solution of the model problem, it is shown that in the ground state, even a small degree of disorder of the H-aggregate impurities in the J-aggregate chain leads to a significant weakening of the intensity of the J-absorption band (along with the appearance of the H-band). A further increase in the degree of disorder of the impurities does not lead to a substantial rearrangement of the absorption spectrum of the system. However, in the case of complete disorder, there is no absorption.

X-ray luminescence spectra of the undoped ZnTe crystal

M. Rudko¹, V. Kapustianyk¹, V. Mykhailyk²

¹Ivan Franko Lviv National University, 50 Dragomanova St., Lviv 79000, Ukraine

²Diamond Light Source, Harwell Campus, Didcot, OX11 0DE, UK

rudko_mykola@ukr.net

ZnTe is representative of the zinc chalcohenide family that may offer a unique opportunity for experimental searches for rare events such as neutrinoless double beta decay (0vDBD).

In this work we report the results of studies of the X-ray luminescence spectra of the undoped ZnTe crystal, measured when cooled to 10 K. The spectra are displayed in Fig. The luminescence band with the maximum at 575 nm (2.15 eV) starts to appear when the temperature reduces to below 140 K. Further cooling of the sample leads to a gradual increase of the emission intensity.

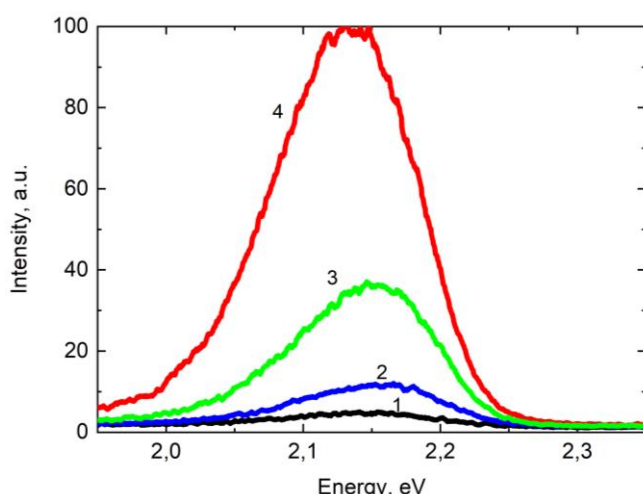


Fig. X-ray luminescence spectra of undoped ZnTe monitored at T=120 K (1) 80 K (2), 40 K (3) and 10 K (4).

radiative decay. It has been shown that the cation sublattice of zinc chalcohenides has lower stability and hence higher propensity for defect formation [5]. Indeed, due to a higher evaporation rate of zinc at elevated temperature the most common type of native defect in ZnTe is a Zn vacancy (V_{Zn}) [6]. A Zn vacancy can act as double acceptor with ionisation energies of 0.05 and 0.14 eV [1]. At high-energy excitation, electrons are promoted to the conduction band, creating holes in the valence band of the crystal. Then the holes are trapped by Zn vacancies while thermalised electrons can be captured by shallow levels of the charge compensating sites associated with either donor type impurities or intrinsic defects. The holes recombine with the electrons from these sites, resulting in a broad emission band with characteristic bimolecular decay kinetics. This type of emission complexes is regarded as efficient centres of radiative recombination in zinc chalcohenides and responsible for their high scintillation light yield [7].

- [1] S. Tanimizu, Y. Otomo, Phys. Rev. Lett. 20, 745 (1967).
- [2] Y.-M. Yu et al., J. Appl. Phys. 90, 807 (2001).
- [3] G. Shigaura et al., J. Cryst. Grow. 301-302, 297 (2007).
- [4] C. Chen et al., Funct. Mater. 43, 879 (2014).
- [5] K. M. Lee, L. S. Dang and J. D. Watkins, Sol. St. Commun. 35, 5127 (1980).
- [6] W. R. Woody, J. M. Meese, Appl. Phys. 47 3640 (1976)
- [7] B. Grynyov, V. Ryzhikov, J. K. Kim, M. Jae, Scintillatior Crystals, Radiation Detectors and Instruments on Their Base (Kharkiv, 2004).

The nature of the intrinsic emission of undoped ZnTe has been studied in details for decades. The current common opinion is that the sharp emission lines, which observed at low temperatures just below the band gap ($E_g=2.4$ eV), are due to free excitons and excitons bound to shallow traps. The broad luminescence band observed in the 2.1–2.3 eV region are attributed to the radiative recombination of the donor-acceptor pairs that localised at the impurities or defects [1–4]. Similar to other semiconductors, the physical processes that involve transitions of carriers across the band gap in ZnTe are strongly influenced by intrinsic defects and impurities. They form different centres with energy levels within the band gap of the crystal that in turn may drastically affect the

Photoluminescence of Ag_8SnSe_6 argyrodite

I. Semkiv¹, H. Ilchuk¹, M. Pawłowski², N. Kashuba¹

¹*Lviv Polytechnic National University, 12 S. Bandera, Lviv, 79013, Ukraine*

²*Warsaw University of Technology, 75 Koszykowa, 00-662 Warszawa, Poland*

Semkiv.Igor.5@gmail.com

The Ag_8SnSe_6 compound ingot was prepared by direct melting of a stoichiometric mixture of Ag, Sn and Se of high purity grade in a sealed (10^{-5} Torr) silica ampoule.

The photoluminescence spectra of the Ag_8SnSe_6 samples were measured at different levels of excitation and temperature (between 15 K and 60 K, up to the evanescence of the photoluminescence signal). At low temperatures, the spectra of the sample are dominated by a peak located at 0.85 eV. A second peak at 0.95 eV is also visible in the spectrum. All of the results relating to the peak at 0.85 eV are consistent.

The blue shift of the spectra with increasing excitation, increasing temperature and the increase in the amplitude with excitation suggest that this peak is associated with donor-acceptor recombination.

Based on temperature-dependent photoluminescence and transmission measurements, the ionization energies of the defects involved in the transition are estimated at 44 meV and 72 meV for the shallower and deeper levels, respectively. The maximum of the second peak at 0.95 eV is very close to the value of the band gap expected at low temperatures; this peak can therefore be associated with a transition between the conduction and valence bands or their tails. At room temperature, based on transmission measurements, the band gap was estimated to be 0.84 eV.

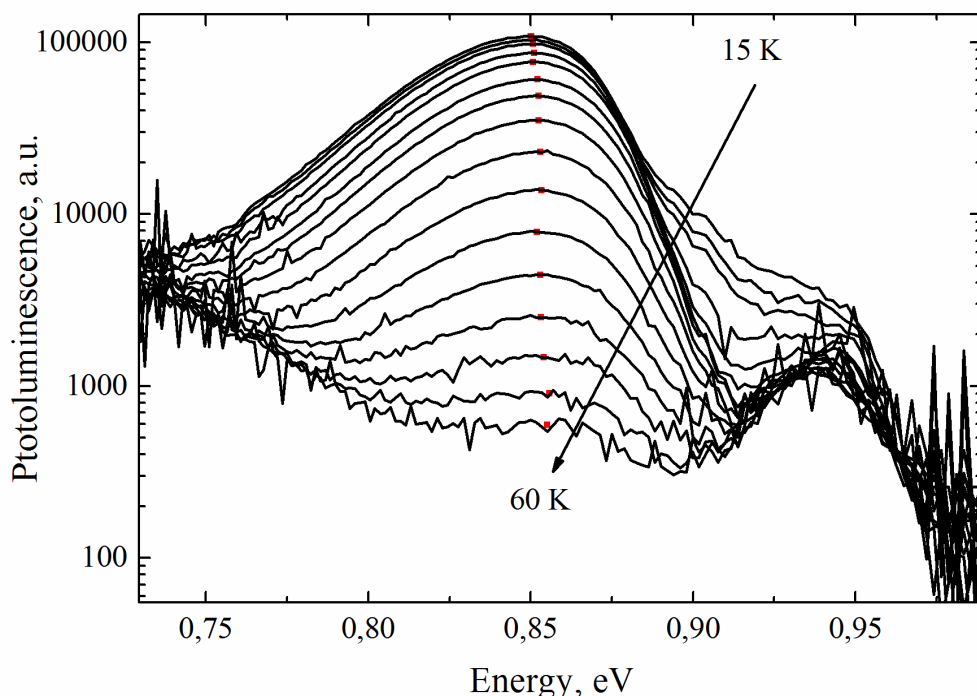


Fig. 1. Temperature dependence photoluminescence spectra of Ag_8SnSe_6 measured under the laser excitation of 64 mW

Single-photon switch controlled by an artificial atom in an engineered electromagnetic environment

E.V. Stolyarov

*Institute of Physics of the National Academy of Sciences of Ukraine,
pr. Nauky 46, Kyiv 03028, Ukraine
eugenestolyarov@gmail.com*

Propagating photon is a promising candidate for the role of a “flying” qubit – a transmitter of a quantum state within a quantum network [1]. The latter is built of nodes, where quantum information is processed, which are interconnected by quantum channels represented by optical waveguides. Rapid and accurate control of photon transport in waveguides is essential for the operation of quantum networks. Thus, one requires devices for the efficient manipulation of the photons flow in optical waveguides, such as photonic switches and routers [2,3], photonic diodes [4], and transistors [5].

In this report, we theoretically demonstrate a realistic scheme of an efficient switch for single photons based on a waveguide QED system. The proposed switch is controlled by a state of a qubit. The latter is formed by the pair of the lowest levels of a ladder-configuration three-level system (qutrit) coupled to a single-mode resonator. The resonator-qutrit system act as an active (switching) component in the considered scheme. The active element is embedded into an engineered electromagnetic environment featuring a band gap on a frequency of the control qubit leading to pronounced inhibition of the Purcell relaxation of the qubit [6]. The engineered electromagnetic environment is realized by a chain of resonators with the nearest-neighbor coupling [7]. The proposed scheme does not require the continuous classical drive to switch the system between the reflective and transmissive states. In this setup, one needs only short classical control pulses for manipulation of the qubit state.

We discuss the potential implementation of the proposed switch on the microwave circuit QED architecture [8]. The resonator chain is composed of an odd number of capacitively coupled coplanar waveguide resonators. The terminal resonators are coupled to microwave transmission lines serving as input and output ports. The central resonator in the chain is coupled to a transmon artificial atom [9]. This type of superconducting artificial atoms features a ladder-type structure of energy levels and offers tunable couplings and high coherence times.

The single-photon transport in the system is treated fully quantum-mechanically. We use a quantity called a *switching contrast* as a measure of the efficiency of the proposed switch. It is determined as a difference of probabilities of a photon transmission when the control qubit is prepared in its ground and excited state, correspondingly. The dependence of the switching contrast on the parameters of the system is studied in detail. We show that high contrasts can be achieved for the parameters typical for the superconducting circuit QED setups.

- [1] T. E. Northup and R. Blatt, Nat. Photonics 8, 356 (2014); H. J. Kimble, Nature (London) 453, 1023 (2008).
- [2] L. Zhou, Z. R. Gong, Y.-x. Liu, C. P. Sun, and F. Nori, Phys. Rev. Lett. 101, 100501 (2008).
- [3] L. Zhou, L.-P. Yang, Y. Li, and C. P. Sun, Phys. Rev. Lett. 111, 103604 (2013).
- [4] D. Roy, Phys. Rev. B 81, 155117 (2010).
- [5] D. E. Chang, A. S. Sørensen, E. A. Demler, and M. D. Lukin, Nat. Phys. 3, 807 (2007); L. Neumeier, M. Leib, and M. J. Hartmann, Phys. Rev. Lett. 111, 063601 (2013).
- [6] E. Yablonovitch, Phys. Rev. Lett. 58, 2059 (1987); S. John and J. Wang, *ibid.* 64, 2418 (1990).
- [7] P. Longo, P. Schmitteckert, K. Busch, Phys. Rev. A 83, 063828 (2011).
- [8] X. Gu, A. F. Kockum, A. Miranowicz, Y. xi Liu, and F. Nori, Phys. Rep. 718–719, 1 (2017).
- [9] J. Koch, *et al.*, Phys. Rev. A 76, 042319 (2007).

New opportunities of the optical investigation of distant scattering objects

V.M. Tkachuk

*Yuriy Fedkovych Chernivtsi National University, Kotsyubynsky 2
58012, Chernivtsi, Ukraine
vlad040495@gmail.com*

The work is devoted to the study of optical field structure obtained by scattering of laser radiation on a rough surface. In purpose of field singularities diagnostics, carbon nanoparticles are used, which act as a field probe due to the following advantages: high lightfastness, high solubility in water, bright luminescence at a wavelength of 530 nm and minimal absorption at a wavelength of 633 nm [1]. The scheme of model experiment is proposed (Fig. 1), which allows to study the motion of carbon nanoparticles in a speckle field. Under the influence of optical forces (gradient, scattering and absorbing forces), carbon nanoparticles move in a speckle field, being captured by optical vortices [2]. It is shown that the number and concentration of nanoparticles differ in the regions of minimum intensity (with and without singularities).

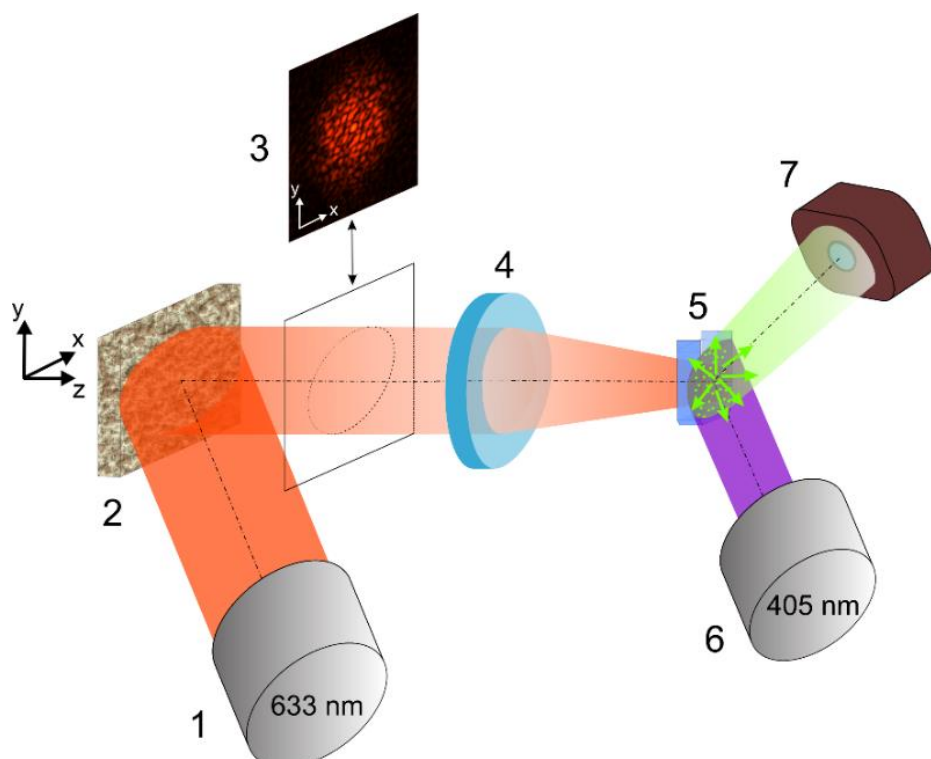
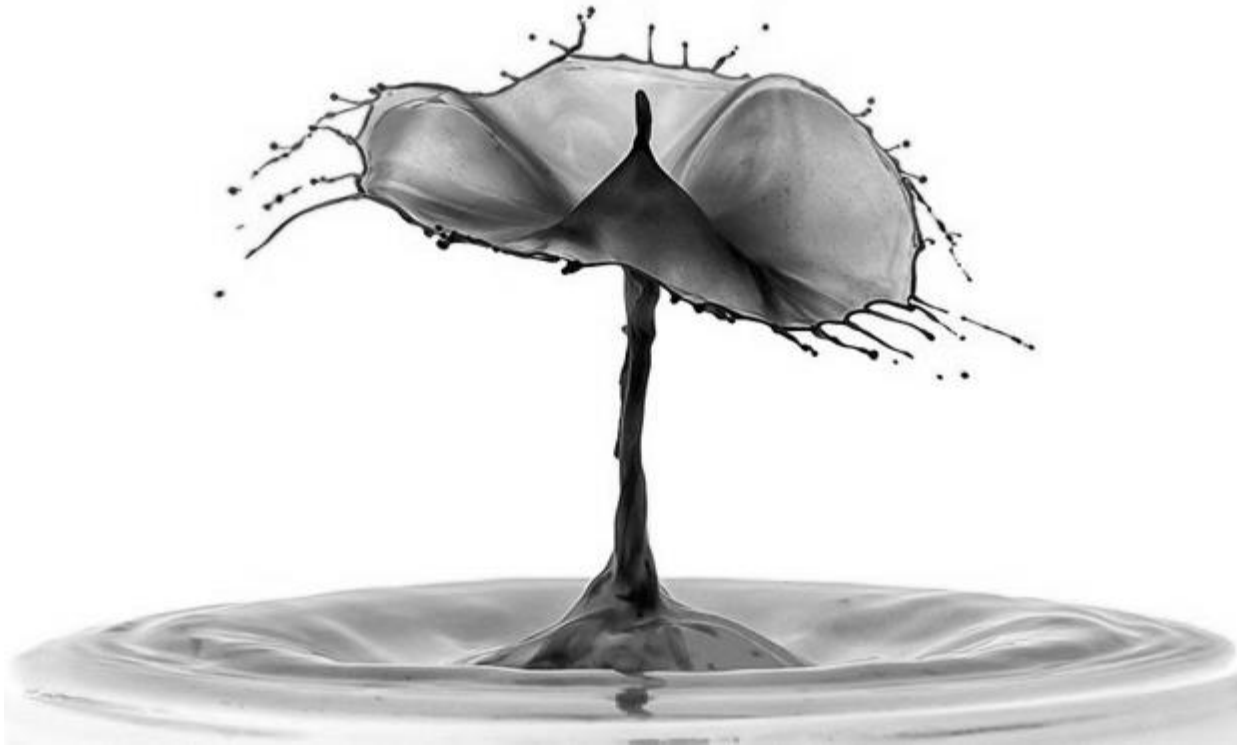


Fig. 1. Model scheme of the experiment: 1 – He-Ne laser, 2 – the studied scattering object with roughness; 3 – speckle-field, 4 – objective, 5 – cuvette with carbon nanoparticles suspended in water, 6 – semiconductor laser, 7 – CCD camera

The possibility of reproducing the optical field and obtaining information about the amplitude and phase of the studied object has been demonstrated.

[1] P.P.Maksimiyak, C.Y Zenkova., V.M. Tkachuk, Physics and Chemistry of Solid State 21(1), 13 (2020).

[2] O.V. Angelsky, C.Yu. Zenkova, S.G. Hanson, D.I. Ivansky, V.M. Tkachuk, and Jun Zheng, Opt. Express 29, 916 (2021)



QUANTUM LIQUIDS AND QUANTUM CRYSTALS, CRYOCRYSTALS

Second sound resonances in superfluid ^3He - ^4He mixtures

T.G. Vikhtinskaya, N.O. Herashchenko, K.E. Nemchenko

*V. N. Karazin Kharkiv National University,
4 Svobody Sq., Kharkiv, 61022, Ukraine
n.gerashchenko@karazin.ua*

The study of resonant excitation of second sound waves in superfluid ^3He - ^4He mixtures is carried out. The main aim of this work is to study temperature and temperature oscillations to determine the conditions under which oscillations of a solid wall excite the second sound in superfluid helium and to calculate the contributions of these processes to the formation of resonances during oscillations of closed tuning forks.

The use of an oscillating quartz tuning fork in pure superfluid helium and the superfluid mixtures of helium isotopes has become one of the most productive methods of studying transport phenomena over the past ten years [1, 2]. In these experiments, many interesting and unusual phenomena were discovered, including, for example, the existence of second sound resonances [3]. In Ref. [3], the results of experiments with an oscillating quartz chamber immersed in a superfluid ^3He – ^4He solution with concentrations up to 15% ^3He are presented.

In this mixture, the quartz tuning forks can cause the emission of not only the first sound but also the second sound [4, 5] and heatwave [6]. The point is that heat transfer in a superfluid ^3He – ^4He solution has many unusual features. One of them is that concentration and temperature excitations relax both in the second sound wave and in a dissipative diffusion wave [7, 8]. The purpose of this work is to find out under what conditions the oscillations of a solid wall excite the first and second sounds, generate a dissipative wave, and determine the contributions of these processes to the damping of the quartz tuning fork oscillations.

To solve this problem, a coupled system was considered – liquid helium and an oscillator, which is stimulated by a tuning fork located in a closed tube filled with helium. The solution of these equations allows to consider the generation of concentration and temperature oscillations in standing waves of the first and second sounds and a thermal wave by vibrating walls [4] in superfluid solutions of ^3He – ^4He with any concentration of ^3He [9]. In particular, the possibility of the creation of second sound resonances and the influence of the thermal dissipative wave [5–8] on these resonances are considered.

As the result, the efficiency of second sound radiation as a function of the concentration of the solution, and the possible effect of this radiation on the damping of vibrations of the tuning fork, which is observed in experiments and has not yet been explained theoretically are explained.

- [1] D.I. Bradley, M. Človečko, S.N. Fisher, D. Garg, E. Guise, R.P. Haley, O. Kolosov, G.R. Pickett, V. Tsepelin, D. Schmoranzer, and S. Skrbek, Phys. Rev. B 85, 014501 (2012).
- [2] D. Schmoranzer, M.J. Jackson, V. Tsepelin, M. Poole, A.J. Woods, M. Človečko, and L. Skrbek, Phys. Rev. B 94, 214503 (2016)
- [3] A. Salmela, J. Tuoriniemi, and J. Rysti, J. Low Temp. Phys. 162, 678 (2011)
- [4] Э.Я. Рудавский, И.А. Сербин, ЖЭТФ 51, 1930 (1966).
- [5]. K. Nemchenko, S. Rogova, and T. Vikhtinskaya, Low Temp. Phys. 44, 1358 (2018).
- [6]. K. Nemchenko and S. Rogova, J. Low Temp. Phys. 150, 187 (2008).
- [7]. K. Nemchenko and S. Rogova, J. Mod. Phys. Lett. B 26, 1 (2012).
- [8]. K. Nemchenko, S. Rogova, and T. Vikhtinskaya, J. Low Temp. Phys. 187, 324 (2017).
- [9] V. Bakhvalova, V. Chagovets, I. Gritsenko, and A.G. Sheshin, J. Low Temp. Phys. 187, 413 (2017).

Magnetoelectric Properties of Quantized Vortices and Vortex Rings

A.M. Konstantinov, S.I. Shevchenko

*B.Verkin Institute for Low Temperature Physics and Engineering of NAS of Ukraine,
47 Nauky Ave., Kharkiv, 61103, Ukraine
akonstantinov@ilt.kharkov.ua*

In the recent works [1-2] it was predicted that a heat flux induced by the temperature gradient in superfluid helium that is placed in a magnetic field generates an electric field (thermomagnetic effect). However, the cited works did not take into account the possibility of quantized vortices and vortex rings generation in the system. The influence of such vortex formations on the thermomagnetic effect can be significant near the transition temperature (thermally activated vortices) or at sufficiently large temperature gradients (turbulent vortices).

In this report, we consider the magnetoelectric properties of rectilinear vortex pairs (superfluid film) and vortex rings (bulk sample of a superfluid system). It is shown that in the presence of an external magnetic field \mathbf{H} the vortex pair and the vortex ring acquire a dipole moment \mathbf{d} , which has the form

$$\mathbf{d} = \frac{\alpha}{Mc} [\mathbf{p} \times \mathbf{H}]$$

where \mathbf{p} is momentum of the pair or of the ring, α and M are polarizability and mass of a helium atom respectively, c – the velocity of light in a vacuum. Using the BKT theory for a two-dimensional system and its generalization for a three-dimensional case (see, for example, [3]), it was found that in the presence of relative motion of the normal and superfluid components, thermally activated vortex formations will lead to additional polarization of the system in the predicted in [1] thermomagnetic effect. It is shown that this additional polarization does not qualitatively change the predicted effect.

- [1] S. I. Shevchenko and A. M. Konstantinov, JETP Letters, 109, 790 (2019).
- [2] S. I. Shevchenko and A. M. Konstantinov, Low Temp. Phys. 46, 48 (2020).
- [3] Gary A. Willams, Phys. Rev. Lett. 59, 1926 (1987).

NMR investigation phases of ^3He adsorbed on MCM-41 one-dimensional nanotubes

N.P. Mikhin, S.S. Sokolov

*B.Verkin Institute for Low Temperature Physics and Engineering of NAS of Ukraine,
47 Nauky Ave., Kharkiv, 61103, Ukraine
mikhin@ilt.kharkov.ua*

The pulsed nuclear magnetic resonance technique was used to study diffusion processes [1-3] in ^3He adsorbed by the SiO_2 nanostructured material MCM-41 (Mobile Crystalline Material-41). The material contained bundles of nanotubes with internal cylindrical channels 2.5 nm in diameter. It was found that there are three different diffusion processes in the ^3He system, in which the diffusion coefficients D differ by an orders of magnitude. It was also found that two diffusion coefficients depend on the value of diffusion time, that is a characteristic feature of restricted diffusion. It is shown that the sizes of limitations of diffusive times correspond to the real sizes of nanotubes[4]. Spin diffusion in the first 1,5 monolayers of ^3He is characteristic of the solid hcp phase.

The nuclear magnetization of ^3He adsorbed by MCM-41 was also investigated using the pulsed NMR. The amplitude of the spin-echo signal was measured in the experiment after two probe rf-pulses, applied to the system. The obtained temperature dependence of the echo signal amplitude for various ^3He coatings is described by a uniform dependence corresponding to the Curie law. It is shown that the values of the echo signal amplitude obtained in the experiment coincide with the calculated value of the corresponding amplitude due to the nuclear magnetization that arises in the system of nuclear spins of ^3He placed in an external magnetic field, so the temperature of adsorbed ^3He corresponds to the temperature of the experimental cell.

- [1] E. Hahn, Phys. Rev. 80, 580 (1950).
- [2] H.Y. Carr, E.M. Purcell, Phys. Rev. 94, 630, (1954).
- [3] D.E. Woessner , J. Chem. Phys. 34, 2057 (1961).
- [4] A. Birchenko, N. Mikhin, E. Rudavskii, Ya. Sopel'nik, Low Temp. Phys.(rus) 45, 1462, (2019)

Desorption of excited H^{*} atoms from free clusters Ar/CH₄ and solid Ar doped with CH₄

**Yu.S. Doronin, V.L. Vakula, G.V. Kamarchuk, A.A. Tkachenko, I.V. Khyzhniy,
S.A. Uyutnov, M.A. Bludov, E.V. Savchenko**

*B.Verkin Institute for Low Temperature Physics and Engineering of NAS of Ukraine,
47 Nauky Ave., Kharkiv, 61103, Ukraine
elena.savchenko@gmail.com*

CH₄ and CH₄-containing systems as important constituents of Interstellar Medium and Solar System have been widely studied by astrophysicists (see e.g. [1, 2] and references therein). Studies of matrix-isolated CH₄ are not so numerous. For the excitation of methane isolated in the matrix with an electron or ion beam, when the radiation-induced processes are determined by energy transfer, the choice of the matrix is of decisive importance. As it was shown in [3] an Ar matrix is of special interest because electronic excitations of the matrix – free and self-trapped excitons, fall into the range of CH₄ absorption. This results in efficient CH₄ dissociation. The main channels of the CH₄ dissociation yield H, CH₃, CH₂, CH and H₂ species. H atoms in the ground state trapped in the lattice were detected in [3, 4]. Moreover, there was detected desorption of excited H atoms – emission of the Ly – α line. However, a mechanism of this phenomenon was not discussed.

To get more insight into desorption processes we performed comparative studies of this desorption from two systems – free clusters Ar/CH₄ and CH₄-doped Ar matrices. Pure and doped Ar clusters were generated in a supersonic jet. The temperature and size of the clusters were taken from the study on electron diffraction of pure Ar clusters. Solid doped matrices were grown on the Cu substrate at LHe temperature. In experiments with clusters and with solid matrices electrons of close energy were used. The emission spectra were measured in the VUV range, and their transformation caused by an admixture of CH₄ was investigated.

Pure Ar clusters of a middle size (1500 at/cl) emit the well-known emission of self-trapped excitons related to the bound-free ${}^1,{}^3\Sigma_u^+ \rightarrow {}^1\Sigma_g^+$ transitions of the molecular dimer Ar₂^{*}. Clusters of this size emit also the band stemmed from charged complexes (Ar₄⁺)^{*}. Doping of clusters with 0.1 % CH₄ resulted in complete quenching of the Ar₂^{*} and (Ar₄⁺)^{*} bands and appearance of the Ly – α line, demonstrating desorption of excited H atoms, which was observed by the cluster's group (Yu.S. Doronin, V.L. Vakula, G.V. Kamarchuk, A.A. Tkachenko) for the first time.

The most intense intrinsic emission of Ar matrix was the Ar₂^{*} band which was quenched by doping with CH₄ as its concentration increased from 0.1 to 10 %. The Ly – α emission line was detected in the second order of spectra. The relative intensity of the desorbing H atoms varied monotonically with the methane concentration. It grew linearly with an increase in CH₄ content.

Two scenarios of the excited H atoms desorption are discussed via holes and excitons. Because ionization potential of Ar exceeds that of CH₄ efficient charge transfer with CH₄⁺ formation proceeds. Deprotonation to the matrix results in H⁺ formation followed by its radiative recombination with electron (H⁺ + e → H^{**} → H^{*} → hν). The second scenario involves excitons. Taking into account that the n=3 level of H atom coincides with the exciton band n=1 Γ 3/2 a direct population of the n=3 H level is possible followed by relaxation to the n=2 level and the Ly – α emission.

- [1] F. A. Vasconcelos, S. Pilling, W. R. M. Rocha, H. Rothard, and P. Boduch, *Astrophys. J.* 850, 174 (2017).
- [2] M. J. Abplanalp, B. M. Jones and R. I. Kaiser, *Phys. Chem. Chem. Phys.* 20, 543 (2018).
- [3] E. Savchenko, I. V. Khyzhniy, S. A. Uyutnov, M. A. Bludov, and V. E. Bondybey, *J. Mol. Structure.* 1221, 128803 (2020).
- [4] I. V. Khyzhniy, S. A. Uyutnov, M. Bludov, E. V. Savchenko and V. E. Bondybey, *Fiz. Nizk. Temp.* 45, 843 (2019) [*Low Temp. Phys.* 45, 721 (2019)].

Radiolysis of Pyridine-Water-Ices by swift Ions

P. Ada Bibang¹, A.N. Agnihotri^{1,2}, P. Boduch¹, A. Domaracka¹, Z. Kanuchova³, H. Rothard¹

¹*Centre de Recherche sur les Ions, les Matériaux et la Photonique,
Normandie Univ, ENSICAEN, UNICAEN, CEA, CNRS, CIMAP, 14000 Caen, France*

²*now at: Indian Institute of Technology Delhi, India*

³*Astronomical Institute of the Slovak Academy of Science,
059 60 Tatranska Lomnica, Slovak Republic
rothard@ganil.fr*

We have studied the radiolysis of the complex organic molecule pyridine. Pure pyridine (C_5H_5N) and mixed pyridine-water ices ($T = 12$ K) were irradiated with swift ions at two beam lines (SME: 650 MeV Zn^{26+} , ARIBE: 90 keV O^{6+}) of the GANIL facility (Caen, France). The evolution of the IR absorption lines of pyridine in the ices was measured as a function of projectile fluence with a FTIR spectrometer in CIMAP's CASIMIR device. From the exponential decrease of the peak intensities, destruction cross sections of pyridine were calculated in pure and mixed ices. Also, the appearance of radiolytic products was followed by in-situ infrared absorption.

The destruction cross sections as a function of electronic energy loss follow a power law. A pronounced dependence on the pyridine concentration (the percentage of pyridine in H_2O) was found: the destruction cross sections are significantly higher for small concentration. The water environment significantly modifies the radiation resistance of the initial complex organic molecules: it enhances radiosensitivity and destruction of pyridine, with implications for radiobiology and astrochemistry.

Acknowledgements. We thank the staff of CIMAP and GANIL and among them all in particular T. Been, C. Feierstein, T. Madi, J.M. Ramillon, F. Ropars, P. Rousseau, P. Voivenel, L. Maunoury and our collaborators B. Augé, C. Desfrançois, F. Lecomte, B. Manil, R. Martinez, Gabriel S.V. Muniz and N. Nieuwjaer. We gratefully acknowledge funding from INSERM-INCa (Grant BIORAD), Région Normandie Fonds Européen de Développement Régional - FEDER Programmation 2014-2020, and a Ph. D. grant from Région Normandie RIN 2018. The infrastructure of GANIL (Grand Accélérateur National d'Ions Lours, Caen, France) was used to do the research presented here. The research of Z. K. was supported by ENSAR2-Access-TNA GANIL and VEGA – the Slovak Grant Agency for Science (grant No. 2/0023/18).

- [1] Prudence C. J. Ada Bibang, Aditya N. Agnihotri, Basile Augé, Philippe Boduch, Charles Desfrançois, Alicja Domaracka, Frédéric Lecomte, Bruno Manil, Rafael Martinez, Gabriel S.V. Muniz, Nicolas Nieuwjaer, Hermann Rothard, Low Temp. Phys. 45, 590 (2019).
- [2] Prudence C. J. Ada Bibang, Aditya N. Agnihotri, Philippe Boduch, Alicja Domaracka, Zuzana Kanuchova, and Hermann Rothard, European Physical Journal D, (2021).

Low-temperature features in heat capacity of complex molecular crystals

Yu.V. Horbatenko, O.A. Korolyuk, A.I. Krivchikov, O.O. Romantsova

*B.Verkin Institute for Low Temperature Physics and Engineering of NAS of Ukraine
47 Nauky Ave., Kharkiv, 61103, Ukraine
horbatenko@ilt.kharkov.ua*

The aim of this study was to explain the nature of the low-temperature feature in the heat capacity for complex crystals. We was carried out normalization and analysis for low-temperature heat capacity data of complex molecular crystals in particular polycyclic crystals such as benzophenone (BP), bromo-substituted benzophenone (2, 3, 4-bromobenzophenone, BrBP), p-polyphenyls, liquid crystalline compounds, metal organic compounds and powders. The normalization was as follows: the excess heat capacity, which is defined as the excess over the Debye contribution observed in the C_p/T^3 from T coordinates, was normalized to ΔC_{\max} , and the temperature was normalized to T_{\max} . The normalized data of the low-temperature heat capacity for cyclic orientationally ordered deuterated thiophene [1] were compared with someone for atomic crystalline argon.

It was shown that the characteristic features in the low-temperature heat capacity which is associated with the avoid crossing of the acoustic and low-energy optical modes in the case of complex crystals it is a similar to Van-Hove singularity which take place in ordered crystals, and its also the same as a boson peak in glasses. So observed features in the low-temperature heat capacity for complex molecular crystals are due to the topology of density of states of vibrational modes.

[1] Y. Miyazaki, M. Nakano, A.I. Krivchikov, O.A. Koroyuk, J.F. Gebbia, C. Cazorla, and J.L. Tamarit "Low-temperature heat capacity anomalies in ordered and disordered phases of normal and deuterated thiophene", The Journal of Physical Chemistry Letters (to be published, 2021).

Mean squared displacement of molecules in the low-temperature phase of solid Nitrogen

L.A. Alekseeva¹, E.S. Syrkin¹, D.E. Hurova¹, N.A. Aksanova^{1,2}, N.N. Galtsov¹

¹*B.Verkin Institute for Low Temperature Physics and Engineering of NAS of Ukraine,
47 Nauky Ave., Kharkiv, 61103, Ukraine*

²*Ukrainian State University of Railway Transport, Feuerbach Square 7, Kharkiv, 61050, Ukraine
hurova@ilt.kharkov.ua*

The peculiarity of solid nitrogen is that it is a molecular crystal, in which the interaction between molecules is much less than the interaction between atoms inside the molecule[1].

A first-order phase transition has observed in solid nitrogen at T=35,6 K, accompanied by a jump in the volume. The phase transition from a hexagonal ($P6_3/mmc$) to simple cubic ($Pa3$) lattice is a result of both due to shear transformations in the lattice and for the orientation of linear nitrogen molecules along the spatial diagonals ($<111>$ directions) of the cube.

In [2, 3], the behavior of the orientation order parameter in the low-temperature phase of solid nitrogen have been experimentally obtained by NQR (nuclear quadrupole resonance) spectroscopy and from X-ray diffraction data. However, there are currently no experimental data on the displacement of nitrogen molecule from own site for the crystal lattice.

In this work, the temperature dependences of mean square displacement of linear molecules from the lattice site were found using experimental X-ray diffraction data.

Mean squared displacement from the equilibrium position have been calculated using Debye-temperature of solid nitrogen, sounds velocity of low-temperature phase of N_2 [1] and based on theoretical data [4].Our calculations results and experimentally obtained data has strongly correlate.

- [1] V.G. Manzhelii, A.I. Prokhvatilov, V.G. Gavrilko, and A.P. Isakina, Structure and Thermodynamic Properties of Cryocrystals, Begell House, Inc., New York (1996).
- [2] J. R. Brookeman, M. M. McEnnan, and T. A. Scott, Solid Nitrogen: A Nuclear Quadrupole Resonance Study, Phys. Rev., 4, (1971).
- [3] N.N. Galtsov, O.A. Klenova, and M.A. Strzhemechny, Fiz. Nizk. Temp. 29, 517 (2002) [Low Temp. Phys. 29, 365 (2002)].
- [4] V.I. Peresada and E.S. Syrkin, Surface Science 54 (1976).

V(T) Phase diagrams of the Fluoroethanes

V.V. Sagan, V.A. Konstantinov, A.V. Karachevtseva

*B.Verkin Institute for Low Temperature Physics and Engineering of NAS of Ukraine,
47 Nauky Ave., Kharkiv, 61103, Ukraine
zvonareva@ilt.kharkov.ua*

In this work, based on the literature and experimental data obtained directly from the experiment, phase V(T) diagrams were plotted for ethane hydrofluorocarbons. The following representatives of this class of substances, which belong to a large group of so-called «plastic» crystals, were selected as objects of research: hexafluoroethane - $\text{CF}_3\text{-CF}_3$ [1], 1,1,2,2 - tetrafluoroethane - $\text{CF}_2\text{H-CF}_2\text{H}$ (freon R-134a) and 1,1-difluoroethane - $\text{CHF}_2\text{-CH}_3$ (freon R-152a) [2].

The isochoric thermal conductivity of HFCs was investigated on samples of different molar volumes in the temperature range from 70 K and up to melting. Samples were grown at various pressures from 30 to 120 MPa. The purity of freons was not worth than 99%.

A distinctive feature of freons of the ethane series is the presence in them of a wide range of phases that differ in the nature of translational, orientational, and conformational ordering. In particular, a high-temperature phase transition into dynamically orientationally disordered (DOD) – «plastic», bcc symmetry ($Im\bar{3}m$) with $Z=2$ molecules per cell, phase. At the same time, this phase has a high plasticity, and its melting occurs at anomalously low values of enthalpy and entropy. Violation of the orientational order is possible for most of these compounds due to the «pseudospherical» shape of the molecules.

The importance of constructing these diagrams is that they provide complete information about the presence and number of phases, regions of coexistence of phases, phase transitions, and also show that, if the conditions of isochoricity ($V=\text{const}$) are met, the region of existence of the DOD phase increases and the temperature shifts melting to the region of higher temperatures with an increase in the density of the sample under study.

- [1] V.A. Konstantinov, V.P. Revyakin and V.V. Sagan, Low Temp. Phys.33, 1048 (2007).
- [2] V.A.Konstantinov, A.I.Krivchikov, A.V.Karachevtseva, V.V.Sagan, Solid State Communications. V.329, 114241 (2021).

Thermal activation heat transfer in dynamically disordered phases of molecular crystals

A.V. Karachevtseva, V.A.Konstantinov, A.I. Krivchikov, V.V. Sagan

*B.Verkin Institute for Low Temperature Physics and Engineering of NAS of Ukraine,
47 Nauky Ave., Kharkiv, 61103, Ukraine
zvonaryova@ilt.kharkov.ua*

The intensive development of the physics of disordered state leads to reconsidering crystalline state concepts. A wide range of practical applications characterizes such disordered states of molecular crystals. One of the most sensitive tools for studying the nature and character of disorder in solids is isochoric thermal conductivity. This method make possible to obtain the dependence of thermal conductivity on temperature for samples with various densities at constant volume.

This work is dedicated to experimental investigation of isochoric thermal conductivity of a molecular crystal of 1,1-difluoroethane (Freon F-152a). Isochoric thermal conductivity was studied for three samples with different molar volumes ($V_m = 49.2, 50.25$, and $51.5 \text{ cm}^3/\text{mole}$) in a dynamically oriented disordered phase.

The thermal conductivity increased with temperature, similar to how it occurs in amorphous and glass-like substances above the plateau area. It is found that this behavior can be described by a thermo-activation mechanism with constant activation energy and density-dependent pre-exponential factor.

The Bridgman coefficient , which characterizes the degree of dependence on the molar volume is determined by the coefficient, is 6.0 ± 0.5 was found from experimental data.

Moreover, a comparison is made with thermal conductivity of other representatives of ethane series freons: F-112, F-113 [1], F-116 [2] and SF₆ [3].It has been found that the thermal conductivity of a number of other molecular crystals with a random disordered orientation can be described in a similar manner.

- [1] Jezowski A., Strzhemechny M. A., Krivchikov A. I., Pyshkin O. S., Romantsova O. O., Korolyuk O. A., Zloba D. I., Horbatenko Yu. V., Filatova A, AIP Advances. 9, 015121 (2019).
- [2] Konstantinov V.A., Revyakin V.P., Sagan V.V., Low Temp. Phys. 33, 1048 (2007).
- [3] Konstantinov V.A., Manzhelii V.G., Smirnov S.A., Sov. J. Low Temp. Phys. 18, 902 (1992).

Radiation-induced non-stationary processes in solid Ar doped with CH₄

I.V. Khyzhniy, E.V. Savchenko, S.A. Uyutnov, M.A. Bludov

*B.Verkin Institute for Low Temperature Physics and Engineering of NAS of Ukraine,
47 Nauky Ave., Kharkiv, 61103, Ukraine
elenasavchenko@gmail.com*

Excitation-induced processes in solid CH₄ are of special interest in various fields of science. Methane is the simplest compound among the hydrocarbon family and its relationship to prebiotic chemistry was discussed in [1]. Being an important constituent of Interstellar Medium and Solar System solid methane and methane-containing systems have attracted considerable attention of astrophysical and matrix-isolation communities for years [2]. Radiation effects in methane-doped Ar matrix were investigated when excited by an electron beam in [3,4]. The motivation for these studies was the behavior of solid methane under neutron flux. Despite high efficiency of the conversion of short wavelength neutrons to long wavelength ones its application encounters some difficulties. It turned out that a neutron flux can cause spontaneous release of accumulated energy and rapid heating followed by hydrogen expansion and moderator destruction.

Nonstationary processes in the Ar matrix doped with CH₄ were studied with a focus on the behavior of radiolysis products – H atoms and CH radicals. Samples of 25 μm thickness were irradiated with 1.5 keV electron beam. It has been shown that because of the small penetration depth of electrons the bulk of the matrix is excited preferentially by photons with an energy of 9.8 eV, the most intense emission band of the matrix (excitons self-trapped into the configuration of Ar₂^{*}), in other words “internal photolysis” occurs. The spectrally resolved emission of H atoms and CH radicals, along with the total yield of desorbing particles, were monitored in a correlated manner under the concurrent action of photons and external heating. These dependences, called nonstationary luminescence (NsL) and nonstationary desorption (NsD), were compared with the measured yield of thermally stimulated exoelectron emission (TSEE), that enabled us to reveal the appearance of the CH radical in the neutralization reaction CH₃⁺ + e⁻ → CH₃^{*} followed by dissociation of CH₃^{*}. Thus, the CH radical was assumed to be a signature of the CH₃^{*} species. The antibate behavior of the CH NsL and the NsD in the temperature range 37 – 43 K, where diffusion in the Ar matrix occurs, was interpreted as a result of the recombination of CH₃ radicals with the formation of C₂H₆ and the energy release spent for desorption. Self- oscillations (with τ of about 10 s) of increasing amplitude were detected, indicating self-oscillating processes in the bulk of the Ar matrix doped with CH₄. Measurements were performed in the concentration range 1% - 10%. The data obtained provide the support to the assumed mechanism of the explosive desorption of solid methane based on thermally activated diffusion and recombination of CH₃ radicals.

- [1] K. Kobayashi, W.D. Geppert, N. Carrasco, N.G. Holm, O. Mousis, M.E. Palumbo, J.H. Waite, N. Watanabe, and L.M. Ziurys, *Astrobiology* 17, 786 (2017).
- [2] R. N. Clark, R. Carlson, W. Grundy, K. Noll, Observed Ices in the Solar System, in: M. S. Gudipati, J. Castillo-Rogez (Eds.). *The Science of Solar System Ices; Astrophysics and Space Science Library*: Springer, New York, Vol. 356, p. 3, (2012).
- [3] I. V. Khyzhniy, S. A. Uyutnov, M. A. Bludov, E. V. Savchenko and V. E. Bondybey, *Fiz. Nizk. Temp.*, 45, 843 (2019) [*Low Temp. Phys.* 45, 721 (2019)].
- [4] E. Savchenko, I. Khyzhniy, S. Uyutnov, M. Bludov, and V. Bondybey, *Nucl. Instrum. Meth. B* 469, 37 (2020).

Vibrations Localized on Defects in One-Dimensional Atomic Structures Adsorbed on Bundles of Carbon Nanotubes

E.V. Manzhelii, S.B. Feodosyev

*B.Verkin Institute for Low Temperature Physics and Engineering of NAS of Ukraine,
47 Nauky Ave., Kharkiv, 61103, Ukraine
emanzhelii@ilt.kharkov.ua*

In many cases, one-dimensional models give possibility to obtain analytical expressions for the physical quasi-particle spectra and for the physical quantities determined by these spectra. The instability of one-dimensional structures (the divergence of their rms atomic displacements) is conditioned by the inverse root feature of the phonon densities of states at zero frequency [1]. Placing a one-dimensional chain on any substrate eliminates the instability. The unique opportunity to create extended atomic chains is to use nanotubes (the so-called nanobundles) as substrates.

Because of the interaction of the atoms of the adsorbed chain with the atoms of carbon nanotubes, the distance between the atoms of the chain does not coincide with the equilibrium distance r_0 corresponding to the minimum of the potential of interatomic interaction of the adsorbed atoms [2]. In the case $r < r_0$ the non-central interaction parameter, which determines the width of the spectrum of transverse vibrations, is negative.

Naturally, the adsorption of linear atomic chains on the surface of carbon nanobundles induces numerous defects in the structures of these chains. The presence of defects and the absence of a threshold for the formation of discrete vibrational levels give rise to localized states, both above and below the band of the quasi-continuous spectrum of the chain. We have shown that defects such as local changes in the distances between atoms in the linear chains adsorbed on the surface of carbon nanobundles often form localized states in the phonon spectrum of the chains with frequencies both above and below the quasi-continuous band[3-5]. For the basic characteristics of localized states (their frequencies, intensities, and attenuation) induced by such a defect, we have obtained simple analytical expressions both for $r < r_0$ and for $r > r_0$. This makes it possible to obtain localized oscillations with given frequencies, changing the parameters of defects and of the chains themselves (for example, pressure). The inversion of these formulas allows one to find the parameters of defects by experimentally measured frequencies of localized discrete levels.

- [1] L.D. Landau, JETP 7, 627 (1937).
- [2] M. Bienfait, P. Zeppenfeld, N. Dupont-Pavlovsky, M. Muris, M. Johnson, T. Wilson, M. De Pies, O.E. Vilches, Physica B, 350, e423 (2004).
- [3] S.B. Feodosyev, I.A. Gospodarev, E.V. Manzhelii, V.A. Sirenko, E.S. Syrkin, Low Temp. Phys., 45, 763 (2019).
- [4] E.V. Manzhelii, S.B. Feodosyev, I.A. Gospodarev, Low Temp. Phys .45, 355 (2019).
- [5] E.V. Manzhelii, JLTP 187, 105 (2017).

Based on cluster model analysis of the orientational order in CO-Ar alloys

N.S. Mysko-Krutik, A.O. Solodovnik

*B.Verkin Institute for Low Temperature Physics and Engineering of NAS of Ukraine,
47 Nauky Ave., Kharkiv, 61103, Ukraine
misko@ilt.kharkov.ua*

Binary cryocrystal solutions are of considerable interest for many reasons [1,2]. One of them is the possibility to compare experimental results with theoretical predictions. In molecular cryocrystals the contribution of the non-central component of interparticle interaction forces due to multipole moments of molecules is rather appreciable. This component determines the character of the orientational ordering of particles at low temperatures. An anisotropic interaction between molecules may be changed by the introduction of spherically symmetric inert gas atoms in the lattice of molecular crystal. There is the correlation between a degree of orientational order in the matrix and the character of the concentration dependence of the lattice parameter of the solutions.

Using the transmission electron diffraction technique we studied the structure CO-Ar cryoalloys with the aim to understand how the introduction of Ar atoms affects the orientational order of the CO molecules [3]. Information about orientational order can be obtained from analysis of the intensity of diffraction peaks. Samples were prepared *in situ* by depositing gaseous mixtures on substrate film. Measurements were made at temperature from 6K to the Ar sublimation temperature. The deposition regime was chosen in order to obtain random distributions of impurity.

The concentration dependence of the lattice parameter and the experimental intensity of superstructure lines are measured at T=20K. The dependence of the intensity was used to determine the orientational order factor. It was shown that degree of orientational disordering of CO molecules increases with the increase of Ar atom in the matrix. The behaviour of the lattice parameters and orientational order factor were analyzed within a cluster approach, which accounts three mechanism of the interaction of argon clusters with their CO environments. The distortion mechanisms related with the presence of cluster in CO-Ar cryosolutions are examined.

- [1] B. I. Verkin and A. F. Prihotko, Cryocrystals (Naukova dumka, Kiev, 1983).
- [2] V.G. Manzhelii, Yu.A. Freiman, Physics of cryocrystals, (New York: AIP Press, 1997).
- [3] A. Solodovnik, N.S. Mysko-Krutik, Low Temperature Physics 45, 545 (2019).

Nanostructured phases in Ar-Kr condensed mixtures

A.O. Solodovnik, N.S. Mysko-Krutik

*B.Verkin Institute for Low Temperature Physics and Engineering of NAS of Ukraine,
47 Nauky Ave., Kharkiv, 61103, Ukraine
misko@ilt.kharkov.ua*

Rare gas cryoalloys are ideal model systems for studying basic crystal growth problems in real mixed crystals [1].

The paper presents an electron diffraction investigation of Ar-Kr deposits. In our method there is the possibility to vary in controlled way quenching conditions [2]. One preparation procedure gave regular solutions with lattice parameters close to those dictated by Vegard's rule. In another case the gas mixture quenching temperature was close to the sub-liquid nitrogen level (sub-Ln). The samples were grown *in situ* by condensation gaseous mixtures on Al or C substrate at T=6K and T=20K.

The structure characteristics of Ar-Kr solid mixtures prepared in two different manners have been studied. Analysis of the concentration dependence of lattice parameters, the intensity of diffraction peaks and their shapes has been done. Based on obtained information may be summarized as follows. The morphology of Ar-Kr deposits dependents on the preparation procedure. Kr-rich sub-Ln condensates contained a *fcc* enriched krypton phase and a dispersed argon phase. The morphology of the Ar-based sub-Ln deposits was a mixture of two crystalline phases (*fcc* Ar-Kr solution and *hcp* phase of pure Ar). We believe that these states are analogs of gel-like media. It is shown that cooling gas mixture favours clustering of solute atoms prior to nucleation. Prenucleation cluster concept is confirmed by the character of annealing process in obtained samples.

- [1] M.L. Klein and J.A. Venables (eds.), Rare Gas Solids, (Academic Press, London, (1976) Vol. 1; (1977) Vol. 2).
- [2] A.A. Solodovnik and V.V. Danchuk Low Temperature Physics 29, 788 (2003) [Fiz Nizk Temp 29, 1041 (2003)].
- [3] A. Solodovnik, N.S. Mysko-Krutik, Low Temperature Physics 45, 545 (2019) [Fiz Nizk Temp 45, 637 (2019)].

The Structure and Collective Vibrations of Electronic Systems Consisting of Several Chains

V. Syvokon, E. Sokolova, S. Sokolov

*B.Verkin Institute for Low Temperature Physics and Engineering of NAS of Ukraine,
47 Nauky Ave., Kharkiv, 61103, Ukraine
esokolova@ilt.kharkov.ua*

The aim of this work is to determine the details of the evolution of a low-dimensional system of electrons over liquid helium and the conditions for the occurrence of linear charge configurations.

The authors simulated the behavior of an electronic system that forms structures consisting of several lines of charges in the presence of a confining potential across the system of particles. A system of surface electrons over liquid helium is considered as a real system corresponding to the performed studies. The parameters of the arising configurations of charges consisting of two, three and four lines, were determined. Moreover, in the latter case, two configurations of the system were investigated - one with the same distance between the lines, and the second of the "double zigzag" type with a variable distance.

A Fourier analysis of the mean values of the coordinates of particles along and across the system was carried out. The values of the characteristic frequencies of their oscillations in the long-wavelength limit were found. The results were compared with the theoretical calculation of the dispersion law for collective plasma modes caused by the Coulomb interaction between the particles of the system. The good agreement was found between the results of both methods. The dispersion law was obtained from the compatibility condition of the equations of motion for small displacements of electrons from the equilibrium positions.

In contrast to earlier studies [1, 2], where the main attention was paid to long-wave oscillations, the results obtained in this work are applicable in the entire range of wave numbers corresponding to the first Brillouin zone of the quasicrystalline approximation.

It was shown that the dispersion law of plasma oscillations depends significantly on the number of charge lines and differs in the case of two possible configurations of a system consisting of four lines.

- [1] V. E. Syvokon, S. S. Sokolov, Low Temp. Phys. 41, 858 (2015).
- [2] S. S. Sokolov and V. E. Syvokon, J. Low Temp. Phys. 187, 427 (2017).

Viscosity measurement of superfluid solutions ^3He - ^4He using a quartz tuning fork

V.A. Vrakina¹, S.S. Kapuza¹, V.K. Chagovets^{1,2}

¹*B.Verkin Institute for Low Temperature Physics and Engineering of NAS of Ukraine,
47 Nauky Ave., Kharkiv, 61103, Ukraine*

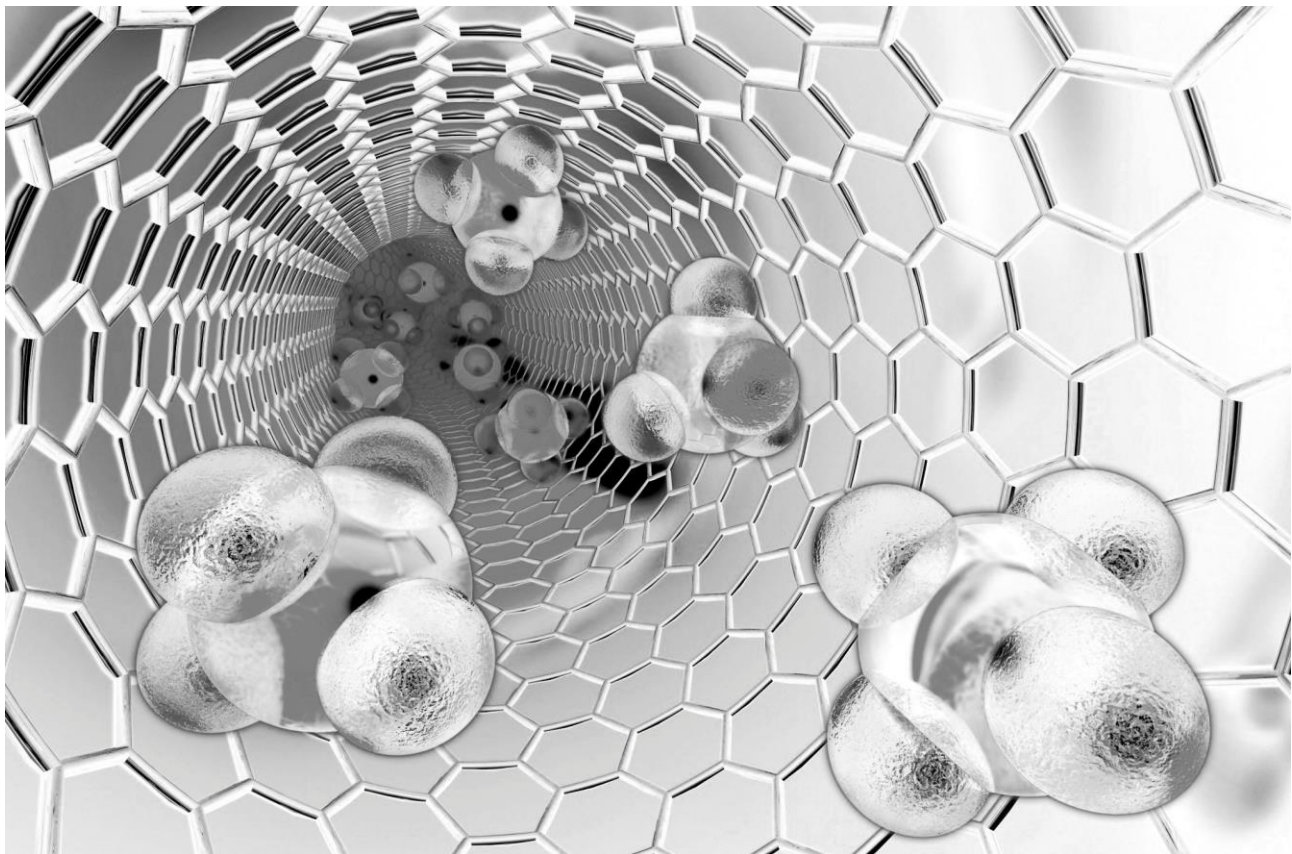
²*V.N. Karazin Kharkiv National University, Svobody Sq. 4, Kharkiv, 61022, Ukraine
verikvrakina@rambler.ru*

Viscosity studies have an important role in understanding the nature of superfluid helium and building of a two-fluid model of He II. In a superfluid state, liquid helium exhibits a vanishingly low viscosity when flowing through narrow capillaries, and on the other hand, when extraneous particles move in a liquid, a finite viscosity appears due to the normal component of He II. Landau and Khalatnikov [1] created the kinetic theory of superfluid helium and showed that the viscosity of the normal component is associated with the processes of interaction of elementary excitations - phonons and rotons.

According to Zharkov's consideration [2], the viscosity of ^3He - ^4He solutions consists of three parts: viscosity due to the transfer of momentum by rotons η_r , viscosity due to the transfer of momentum by phonons η_{ph} , and viscosity due to the transfer of momentum by impurities η_i - impurity viscosity. Experimental studies of the viscosity of ^3He - ^4He solutions were carried out using two "classical" methods: the oscillating disk method [3] and flow through a capillary [4]. However, both methods in this case have several features associated with the specificity of liquid helium and require considering the corrections.

At present, the method of an oscillating quartz tuning fork, which has a Q-factor about $\sim 10^6$ and provides high sensitivity of measurements in a wide temperature range, is widely used to study the properties of superfluid liquids. In [5], this method was used to measure the viscosity of liquid ^4He in the hydrodynamic and ballistic regions. In this work, using the amplitude-frequency characteristics of the tuning fork, the viscosity of concentrated ^3He - ^4He solutions was measured in the temperature range 0.3–2.3 K. It has been experimentally shown that in concentrated ^3He - ^4He solutions, in contrast to He II, at low frequencies of phonon and impurity vibrations, a hydrodynamic regime is realized in the entire temperature range.

- [1] L.D. Landau, I.M. Khalatnikov, JETP 19, 637, 709, (1949).
- [2] V.N. Zharkov, JETP 33, 929 (1957).
- [3] J.G. Dash, R.D. Taylor, Phys. Rev. 107, 1228 (1957).
- [4] F.A. Staas, K.W. Taconis, K. Fokkens, Physica 26, 669 (1960).
- [5] A.A. Zadorozhko, E.Ya. Rudavskii, V.K. Chagovets, G.A. Sheshin, Yu.A. Kitsenko, LTP 35, 134 (2009).



NANOPHYSICS AND NANOTECHNOLOGIES

Structural Models for the Diffraction Analysis of Various Carbon Honeycombs

D.G. Diachenko, N.V. Krainyukova

*B.Verkin Institute for Low Temperature Physics and Engineering of NAS of Ukraine,
47 Nauky Ave., Kharkiv, 61103, Ukraine
dyachenko@ilt.kharkov.ua*

Carbon honeycomb (CH) is a novel carbon cellular material first reported in [1]. Walls in these structures are formed from single graphitic sheets (or simply graphene). A unique property of these objects to soak and keep inside large amounts of gases was already confirmed in experiments [1-4]. High sorption levels become possible given the very high surface area where adsorption may occur. It is about twice higher as compared with graphene and carbon nanotubes, which are currently the most popular objects in similar studies, because in CHs both sides of graphene sheets are open for adsorption in contrast to only one side in graphene and nanotubes.

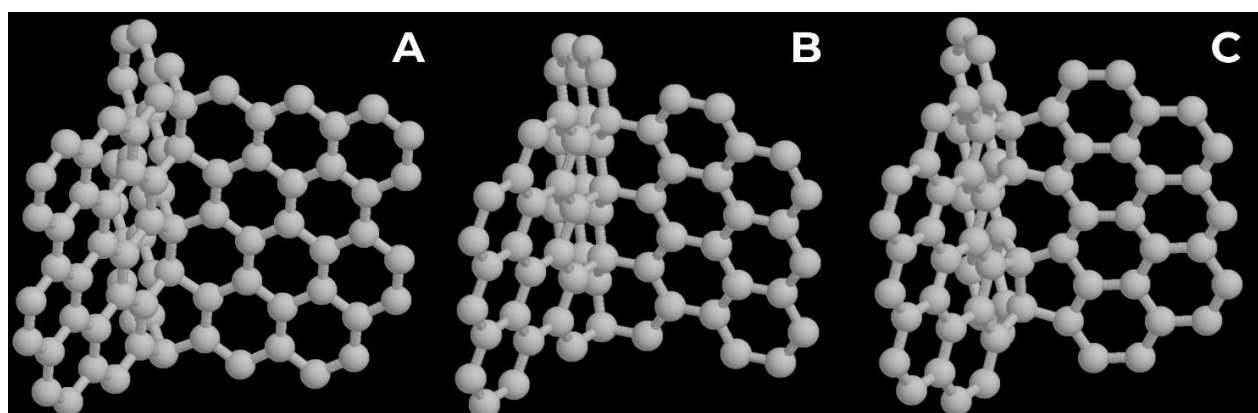


Fig. 1. Carbon 3D architecture formed by intersectional collision of graphene patches.

Three different approaches of honeycomb wall orientations and junction lines between walls were proposed in 2005 [5] (Fig. 1). The structures A, B and C have the only sp^3 bonds along the junction lines between the walls. However, in the A and C models one of four bonds is oriented along the walls' junction line, and three others are placed symmetrically within the wall graphene-like planes. In this case we have the hexagonal symmetry about the axis directed along the honeycombs' cell axis. But in the B case all the bonds are located in the walls' planes and the hexagonal symmetry is broken, owing to the different angles between walls as well as to the walls' widths. The A as well as the C structures have all the angle 120° between the walls, unlike the B, in which one angle between walls is equal to the angle between bonds, i.e. 109.5° , while two others are the same and equal to 125.25° . Cell wall widths are also variable, therefore we have additionally many variants allowing for different cell wall widths.

In summary all the structures have to be distinguished in the diffraction patterns. In the proposed report we analyze the diffractograms calculated for these three types of structures with different cell sizes and compare them with experiment.

- [1] N.V. Krainyukova and E.N. Zubarev, Phys. Rev. Lett. 116, 055501 (2016).
- [2] N.V. Krainyukova, J. Low Temp. Phys. 187, 90 (2017).
- [3] N.V. Krainyukova, Y.S. Bogdanov, and B. Kuchta, Low Temp. Phys. 45, 325 (2019).
- [4] N.V. Krainyukova, B. Kuchta, L. Firlej, and P. Pfeifer, Low Temp. Phys. 46, N3 (2020).
- [5] T. Kawai, S. Okada, Y. Miyamoto, and A. Oshiyama, Phys. Rev. B 72, 035428 (2005).

Research of impact of presence of vitamins B2, B3, and C on calcium oxalate monohydrate crystallization processes in simulated body fluid

M. Dryhailo¹, Yu. Taranets²

¹*V. N. Karazin Kharkiv National University,
4 Svoboda Sq., Kharkiv, 61000, Ukraine*

²*Institute for Single Crystals of the National Academy of Sciences of Ukraine
60 Nauky Ave., Kharkiv, 61000, Ukraine*

Urolithiasis is one of the most common diseases of human urinal tract. Crystals of mineral origin have the propensities for renal calculi, or kidney stones formation. The reviewed example of these crystals is calcium oxalate monohydrate $\text{CaC}_2\text{O}_4 \cdot \text{H}_2\text{O}$ (COM) [1]. Nowadays the crystallization of COM under influence of various compounds that come to human organism with food is not fully studied and analyzed. Scientists are interested in impact on crystallization COM of amino acids, food supplements, and especially vitamins [2].

The main purpose of this work is modelling COM crystallization processes in simulated body fluid with presence of water-soluble vitamins B₂, B₃, and C and examining their influence on the nucleation processes, morphology, and size of COM crystals. The temperature during the experiments was 37°C, pH = 5.8, and I = 0.15 (NaCl).

The structure and the phase composition of the synthesized calcium oxalate precipitates were determined using the methods of X-ray phase analysis and IR spectroscopy. The morphology of the crystals was examined applying scanning electron microscopy. The crystallization kinetics for the model COM solutions was studied by measuring the solution turbidity.

[1] Rez. P., What does the crystallography of stones tell us about their formation?, Urolithiasis 45(1), 11-18 (2017).

[2] Taranets Y. V. et al., Effect of amino acids and B-group vitamins on nucleation of calcium oxalate monohydrate crystals, Journal of Crystal Growth 531, 125368 (2020).

Phonon models of thermal conductivity of nanosized structures

T.V. Medintseva, K.E. Nemchenko, T.G. Vikhtinskaya

*V. N. Karazin Kharkiv National University,
4 Svobody Sq., Kharkiv, 61022, Ukraine
n.gerashchenko@karazin.ua*

In the paper we consider the problem of thermal conductivity of two-dimensional nanostructures – nanoribbons – in the temperature range, when the interaction between phonons can be neglected [1, 2]. In this ballistic mode, heat fluxes can be limited only by the interaction of phonons with the sample boundaries [3, 4]. The existing mechanisms of interaction of phonons with the boundaries of samples and their influence on the thermal conductivity of bodies are studied. A model of phonon heat transfer in two-dimensional structures in ballistic mode has been developed. A number of types of interaction with boundaries in two-dimensional samples are considered: absorption at the boundary, finite number of reflections, absorption inside the sample on defects, impurities, etc. The explicit expressions for the thermal conductivity in these cases are derived. Interpolation relations are obtained, which generalize the existing expressions for the thermal conductivity in the case of mirror and diffuse reflection from the walls. Conditions for conducting new experiments to test the models proposed in the thesis are proposed.

A rectangular two-dimensional strip of the width W and the length L was considered as the object of study. For the phonon system of this sample, one type of polarization and the ratio of isotropic energy and momentum were considered. As the heat sources, heat tanks of infinite heat capacity with given temperatures were considered: hot with temperature T_h and cold with temperature T_c , which are in thermal contact with the ends of the sample. It is assumed that these tanks provide a constant temperature on these sides. In this case, the heat flux radiated by these walls will be determined by the law of radiation of an absolutely black body.

Then, an effective coefficient of thermal conductivity was introduced as a coefficient of proportionality between the heat flux density and the ratio of the temperature difference to the length of the sample. The coefficient of thermal conductivity is presented in the form that is common for phonon systems [5]:

$$\kappa_{\text{eff}} = \frac{1}{2} C_s V_{\text{eff}} \Lambda_p. \quad (1)$$

As a result, the following result was obtained for the effective mean free path:

$$\Lambda_p = \frac{2}{\pi} \frac{1+p}{1-p + W(1+p)/2L} \frac{WL}{\sqrt{W^2 + L^2} + L}. \quad (2)$$

This result can be used over the entire range of p value of phonon absorption probability in the boundary and the W/L ratio of the width and length of the sample.

- [1] Aymeric Ramiere, Sebastian Volz and Jay Amrit, Geometrical tuning of thermal phonon spectrum in nanoribbons, *J. Phys. D: Appl. Phys.* 49 (2016) 115306 (8pp).
- [2] H. B. G. Casimir, Note on the conduction of heat in crystals, *Physica* V, no 6, 1938.
- [3] Tom Klitsner, J. E. VanCleave, Henry E. Fischer, and R. O. Pohl, Phonon radiative heat transfer and surface scattering, *Physical Review B* Volume 38, Number 11, 1988-I.
- [4] Humphrey J. Maris, Heat flow in nanostructures in the Casimir regime, *Phys. Rev. B* 85, 054304 (2012).
- [5] Jay Amrit, Konstantin Nemchenko, and Tatiana Vikhtinskaya, Effect of diffuse phonon boundary scattering on heat flow *J. Appl. Phys.* 129, 085105 (2021).

Fundamental description of Wannier qubits in semiconductor

K. Pomorski^{1,2}

¹*Cracow University of Technology, Faculty of Computer Science and Telecommunications, ul.
Warszawska 24, 31-155 Krakow, Poland*

²*Quantum Hardware Systems, ul. Babickiego 10 m 195, 94-056 Lodz, Poland
kdvpomorski@gmail.com*

Current implementation of CMOS quantum computer relies on the usage of Wannier qubits [1-6]. Justification of tight-binding model [7-9] basing on Schroedinger formalism for various topologies of position-based semiconductor qubits is presented in this work. Simplistic tightbinding model allows for description of single-electron devices at large integration scale [11-13]. However it is due to the fact that tight-binding model omits the integro-differential equations that arise from electron-electron interaction in Schroedinger model [10]. Two approaches are given in derivation of tight-binding model from Schroedinger equation. First approach is conducted by usage of Green functions obtained from Schroedinger equation. Second approach is given by usage of Taylor expansion applied to Schroedinger equation. The obtained results can be extended for the case of many interacting position-based qubits with more than one electron and can be applied to 2 and 3 dimensional model.

- [1].K.K.Likharev, Single-Electron Devices and Their Applications, Published in Proc. IEEE, vol. 87 (1999)
- [2].T.Fujisawa, T. Hayashi, HD Cheong, YH Jeong, and Y. Hirayama. Rotation and phase-shift operations for a charge qubit in a double quantum dot. Physica E: Low-dimensional Systems and Nanostructures, 21(2-4):10461052 (2004).
- [3].K.D.Petersson, J. R. Petta, H. Lu, and A. C. Gossard. Quantum coherence in a one-electron semiconductor charge qubit. Phys. Rev. Lett., 105:246804 (2010).
- [4].D.Leipold, Controlled Rabi Oscillations as foundation for entangled quantum aperture logic, Seminar at UC Berkley Quantum Labs (2018)
- [5].P.Giouvanlis, E.Blokhina, K.Pomorski, D.R.Leipold, R.B.Staszewski, Modeling of Semiconductor Electrostatic Qubits Realized Through Coupled Quantum Dots, IEEE Access (2019)
- [6].K.Pomorski, P.Giouvanlis, E.Blokhina, D.Leipold, P.Peczkowski, R.B.Staszewski, From two types of electrostatic position-dependent semiconductor qubits to quantum universal gates and hybrid semiconductorsuperconducting quantum computer, Proc. SPIE 11054 (2019)
- [7].H.Q.Xu, Method of calculations for electron transport in multiterminal quantum systems based on realspace lattice models. Phys. Rev. B, 66:165305 (2002).
- [8].K.Pomorski, P.Giouvanlis, E.Blokhina, D.Leipold, R.B.Staszewski, Analytic view on Coupled SingleElectron Lines, Semiconductor Science and Technology, Vol.34, No.12 (2019)
- [9].K.Pomorski, R.B.Staszewski, Analytical Solutions for N-Electron Interacting System Confined in Graph of Coupled Electrostatic Semiconductor and Superconducting Quantum Dots in TightBinding Model with Focus on Quantum Information Processing, Arxiv:1907.03180v3 (2019)
- [10].B.Szafran, Paired electron motion in interacting chains of quantum dots, Physical Review B, Vol. 101, 075306 (2020)
- [11].K.D.Pomorski,P.Peczkowski, R.B.Staszewski, Analytical solutions for N interacting electron system confined in graph of coupled electrostatic semiconductor and superconducting quantum dots in tight-binding model, Cryogenics, Vol-109 (2020)
- [12]. K.Pomorski, Arxiv:2001.02513, 1912.01205v1, 2012.09923 (2019-2021).
- [13].K.Pomorski,R.Staszewski, Towards quantum internet and non-local communication in position-based qubits, AIP Conference Proceedings 2241, 020030 (2020)

On the problem of charge transfer and phototransfer in nonregular condensed media

G.D. Tatishvili, T.A Marsagishvili, M.N. Matchavariani

*Iv. Javakhishvili Tbilisi State University, R. Agladze Institute of Inorganic Chemistry and Electrochemistry, 11 Mindeli str., Tbilisi, 0186, Georgia
tatigia@yahoo.com*

A very large number of publications are devoted to the study of the problem of charge transfer in nonregular condensed medium, in which, depending on the specific conditions of the problem, various approaches are used [1 - 7]. For solving problems on the proposed topic, the most suitable apparatus is the apparatus of the temperature Green's functions [8].

The paper deals with the issues of optical spectroscopy of nonregular condensed media with charge transfer between impurity centers. The objective of the study is to develop a method for analyzing the optical absorption curve of light by a system and calculate the kinetic parameters of the charge transfer process between impurities in such media.

In the approximation of uncoupling of the Green's functions of the operators of fluctuations of the polarization of a condensed medium, the processes of electron transition both on impurity particles and between particles are considered.

The kinetics of charge transfer and phototransfer processes in nonregular condensed systems is studied taking into account the interaction of intramolecular vibrations of impurity particles with fluctuations in the polarization of the condensed medium.

A general scheme for calculating the kinetic parameters of the charge phototransfer process from the shape of the light absorption curve by the systems under study is presented.

Model functions are proposed to describe the Green's functions of the polarization operators of a medium at finite temperatures. The use of these model functions allows numerical calculations of the kinetic parameters of the charge transfer and phototransfer processes in nonregular condensed medium.

- [1] Catherine E. Housecroft, and A. G. Sharpe, Outer Sphere Mechanism. Inorganic Chemistry. (Harlow, England: Pearson Prentice Hall, 2008).
- [2] Alan K. Brisdon, UV-Visible Spectroscopy. Inorganic Spectroscopic Methods. (Oxford: Oxford UP, 1998).
- [3] Russell S. Drago, Effect of Solvent Polarity on Charge-Transfer Spectra. Physical Methods for Chemists. (Ft. Worth: Saunders College Pub., 1992).
- [4] Gary L. Miessler, and Donald A. Tarr, Coordination Chemistry III: Electronic Spectra. Inorganic Chemistry. (Upper Saddle River, NJ: Pearson Education, 2004).
- [5] R.R. Dogonadze, A.M. Kuznetsov, T.A. Marsagishvili, *Electrochimica Acta*, 25, 1, (1980).
- [6] T.A. Marsagishvili, G.D. Tatishvili. *Russian Journal of Electrochemistry*, 29,10, (1993).
- [7] T.A. Marsagishvili. *Journal of Electroanal. Chem.*, 450, 47, (1998).
- [8] T. A. Marsagishvili, M. N. Machavariani, G. D. Tatishvili. *Eur. Chem. Bull.*, 3, 127 (2013).

A New Method for Real-Time Selective Detection in Complex Gas Mixtures Using Yanson Point Contacts

V. Vakula¹, A. Pospelov², V. Belan¹, D. Harbuz^{1,2}, L. Kamarchuk³, Yu. Volkova³, G. Kamarchuk¹

¹*B.Verkin Institute for Low Temperature Physics and Engineering of NAS of Ukraine,
47 Nauky Ave., Kharkiv, 61103, Ukraine*

²*National Technical University “Kharkiv Polytechnic Institute”,
2 Kyrpychov Str., Kharkiv, 61002, Ukraine*

³*SI “Institute for Children and Adolescents Health Care” of NAMS of Ukraine,
52-A Yuvileinyi Ave., Kharkiv, 61153, Ukraine
vakula@ilt.kharkov.ua*

We propose a new method for selective detection in complex gas mixtures using nanosensors based on Yanson point contacts. The unique properties of Yanson point contacts make it possible to obtain a rich spectrum-like response to the action of various gaseous mixtures, including very complex ones. This spectrum-like signal, which has no analogue for traditional sensors using the principle of registration of variation in electric conductance, is a unique quantum “fingerprint” of the analyzed gaseous medium and contains information about all of its components.

To demonstrate the efficiency of the proposed approach we applied it to one of the most complex gas mixtures – the human breath – which contains over 2000 components and is a promising medium for noninvasive diagnosis of various physiological states of the human body [1]. Two important hormones – serotonin (the hormone of happiness) and cortisol (the hormone of stress) – were chosen as the substances to be detected in the human body. It was shown that these hormones leave their traces in the human breath which impact the response signal (the breath profile) of the point-contact nanosensor. A new correlation technique was developed and successfully applied to analyze the breath profiles of the patients and find in real time (within a few minutes) the concentration of the hormones in the patients’ blood. The hormone concentrations found using the point-contact breath test are shown to be in good agreement with the concentrations determined by means of traditional medical techniques.

The obtained results provide another demonstration that nanosystems consisting of Yanson point-contacts can effectively interact with the components of complex gaseous media. This interaction includes adsorption of the gas molecules on the surface of the point contacts, transfer of the excess energy of non-equilibrium electrons accelerated by the electric field concentrated in the point contact to the adsorbed molecules, and desorption of the molecules from the surface of the point contact when the transferred energy is sufficient for that. Different molecules are characterized by different energy parameters which are reflected in the processes of their adsorption and desorption and shape the point-contact profile of the gaseous medium. Our new method allows one to quickly and effectively decipher the traces left by the molecules in the gas profile.

The new method can be used in various areas of science and technology, with medicine being one of the top priorities. When applied to detect such complex biological compounds as those related to serotonin and cortisol markers in the human breath, it allows one to rapidly and accurately estimate the emotional state of the human organism, its stress level, and promptly and adequately react to it. Our new approach can be used in express medical diagnosis as well as in real-time studies of the human emotional states, which can be important, for example, in preventing terrorist attacks.

[1] I.Kushch, N. Korenev, L. Kamarchuk, A. Pospelov, A. Kravchenko, L. Bajenov, M. Kabulov, A. Amann, G. Kamarchuk, J. Breath Res. 9, 047111 (2015).

Base Pressure Effect on Electrical Properties of Chromium Nanofilms

S.L. Udachan¹, N.H. Ayachit¹, L.A Udachan², S. Siddanna³, S.S. Kolkundi⁴, S. Ramya⁵

¹*Dept of Physics, Rani Channamma University, Belagavi-591156, Karnataka, India.*

²*S. S. Tegnoor Degree College, Kalaburagi-585105, Karnataka, India*

³*Dept of PG Studies & Research in Physics, Kuvempu University Jnanasahyadri, Shankaraghatta-577451, Shimoga, Karnataka, India*

⁴*Government First Grade College, Shahapur-585223, Yadgir, Karnataka, India*

⁵*Shree Sangam Vidya Mandir, Kalaburagi-585104, Karnataka, India*

shivaudachan8@gmail.com

The morphology and electrical characteristics of deposited films mainly depend upon the base pressure during the deposition. If the base pressure is high, the deposited films may have more impurities compared to that deposited at low pressure. This leads to high resistivity of the films deposited at higher pressures compared to that deposited at lower pressures. Naturally the conduction electron mean free path in films will be reduced due to the scattering of electrons from impurities. Therefore, the conduction electron mean free path for the film grown at lower deposition pressure will be higher compared to that grown at higher deposition pressure

We have successfully grown chromium films in the thickness range (3.5-70) nm onto cleaned glass substrate. The electrical resistivity of films was measured by the standard four probe method. It is observed that the resistivity increases with increasing base pressure [1,2], because of the incorporation of defects during the film growth. The electrical resistivity data was analyzed in the frame of Fuchs-Sondheimer (F-S) and Mayadas-Shatzkes (M-S) theories. It was found, that the electrical resistivity and electron mean free path are strongly depend on base pressure in the samples. Electrical variables are governed by the proper control of deposition parameter such as base pressure.

[1] F. Bouaraba, M.S. Belkaid , S. Lamri, Journal of Nano and Electronic Physics, 10 04001-05 (2018).

[2] G. S. Frankel et al, Journal of The Electrochemical Society, 161 C195-200 (2014).

Influence of the Aharonov-Bohm Effect on the Eigenmodes Spectra of a Semiconductor Nanotube With a Dielectric Filling

Yu. Averkov^{1,2}, Yu. Prokopenko^{1,3}, V. Yakovenko¹

¹*O. Usikov Institute for Radiophysics and Electronics of NAS of Ukraine,
12 Acad. Proskura St., Kharkiv, 61085, Ukraine*

²*V. Karazin Kharkiv National University, 4 Svobody Sq., Kharkiv, 61022, Ukraine*

³*Kharkiv National University of Radio Electronics, 14 Nauky Ave., Kharkiv, 61166, Ukraine
yuriyaverkov@gmail.com*

In the present work, the spectra of electromagnetic eigenmodes of a structure consisting of a semiconductor nanotube filled with a nonmagnetic dielectric are theoretically investigated. This structure is placed in a constant magnetic field parallel to the nanotube axis. The walls of the nanotube are assumed to be infinitely thin. In order to derive the dispersion equation for the eigenmodes in the structure under consideration, it is necessary to satisfy certain boundary conditions on the nanotube surface. These conditions are as follows. First, the tangential components of the electric field of the eigenmodes are continuous. Second, the azimuthal component of the magnetic field and the radial component of the electric displacement vector of the eigenmodes are discontinuous because of the surface current along the nanotube.

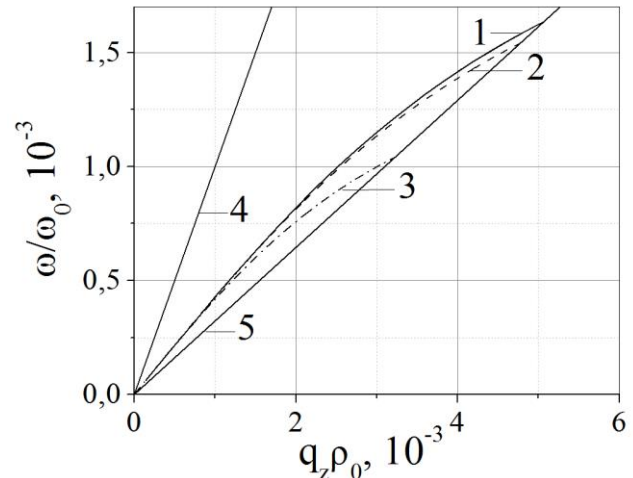
We carry out a numerical analysis of the structure with the use of the following parameters: the material of the cylinder is polikor with the dielectric constant $\varepsilon = 9.6$, the radius of the cylinder is $\rho_0 = 2$ nm, the material of the nanotube is

semiconductor InSb with the equilibrium surface density of charge carriers $N = 10^{13} \text{ cm}^{-2}$. In the figure, curves 1 – 3 correspond to the waveguide eigenmodes of the structure with the azimuthal mode index $n = 10$ and the radial mode index $s = 1$, lines 4 and 5 represent the light lines in vacuum and the dielectric cylinder, respectively, $\omega_0 = c/\rho_0$ (where c is the velocity of light in vacuum). Curve 1 corresponds to the value of the azimuthal quantum number of the nanotube electrons $m = 0$ and the number of magnetic flux quanta inside the nanotube $\phi = 0$, curve 2 is for $m = 0$ and $\phi = 1$, curve 3 is for $m = 0$ and $\phi = 2$.

Note that in the dispersion equation the quantities m and ϕ appear in the combination $(m + \phi)^2$. As seen from the figure, the dispersion curves of plasma eigenmodes have the ending points of the spectra on the light line in the dielectric. These points shift towards lower frequencies as the number of magnetic flux quanta inside the nanotube increases. For a given value of m there is a maximum possible number of quanta ϕ_{\max} , for which the existence of the plasma eigenmodes is possible. The dependence of the spectra on the number of magnetic flux quanta inside the nanotube may be considered as one of the manifestations of the Aharonov-Bohm effect [1].

We gratefully acknowledge support from the National Research Foundation of Ukraine, Project No. 2020.02/0149 “Quantum phenomena in the interaction of electromagnetic waves with solid-state nanostructures”.

[1] H. Batelaan, A. Tonomura, Physics Today. 62, 38 (2009).



Influence of grinding and oxidation of carbon nanotubes on their heat capacity

M.S. Barabashko¹, D. Szewczyk², M.I. Bagatskii¹, V.V. Sumarokov¹, A. Jeżowski², V.L. Kuznetsov^{3,4}, S.I. Moseenkov³, A.N. Ponomarev⁶

¹*B. Verkin Institute for Low Temperature Physics and Engineering, NASU,
47 Nauka Ave., 61103 Kharkov, Ukraine*

²*W. Trzebiatowski Institute of Low Temperature and Structure Research,
PAS, P.O. Box 1410, 50-950 Wrocław, Poland*

³*Boreskov Institute of Catalysis, 5 Lavrentiev Ave., 630090 Novosibirsk, Russia*

⁴*National Research Tomsk State University, 36 Lenin Ave., 634050 Tomsk, Russia*

⁵*National Research Tomsk Polytechnic University, 30 Lenin Ave., 634050 Tomsk, Russia*

⁶*Institute of Strength Physics and Materials Science of SB RAS,
2/4 Academicheskii Ave., 634055 Tomsk, Russia
barabaschko@ilt.kharkov.ua*

The temperature dependences of the specific heat of MWCNTs $C(T)$ undergo changes in dimensionality from 1D at room temperatures to 3D at helium temperatures [1]. In this work, we investigated the effect of defects that appear after grinding and oxidation of MWCNTs on the character of the $C(T)$. For this, we measured the specific heat of MWCNTs with an outer diameter of 7 to 18 nm, prepared from the original nanotubes [1] by two methods: grinding and grinding-oxidation, in the temperature range from 1.8 to 275 K.

Significant effects are found: large changes are observed both in the magnitude of the heat capacity and in the dimensionality of the $C(T)$ curves. The nature of the temperature dependences of the heat capacity of milled MWCNTs of different diameters is fundamentally different. Although, as a result of grinding, the ratio of the length of the tubes to their diameter decreased from thousands to several tens, this did not affect the linear dimensionality of the specific heat curves of all MWCNTs in the high-temperature region. Below 140 K, the effect of grinding and grinding-oxidation on the manifestation of the dimensionality of the system is ambiguous. The effect of grinding MWCNT Ø7.2 nm is opposite to the case of Ø18 nm. Grinding the original tubes Ø7.2 nm leads to a decrease in their heat capacity in the temperature range from 100 to 3 K and an increase below 3 K. Whereas, the heat capacity of the milled nanotubes Ø18 nm significantly increased compared to the initial tubes below 200 K. Dimensional effects of 2D and 3D behavior on the $C(T)$ curves of the milled MWCNTs Ø18 nm are preserved. An explanation for the observed features is proposed. The effect of grinding and grinding-oxidation on the $C(T)$ curve of Ø9.4 nm MWCNTs is intermediate between the cases of Ø7.2 and 18 nm MWCNTs.

Oxidation preceding the grinding process leads to an increase in the specific heat of MWCNTs relative to the initial nanotubes below 140 K. When oxidized MWCNTs are ground, their physical properties change radically, in particular, oxygen-containing groups are formed, as well as the parameters and the number of other defects. Oxygen-containing functional groups formed on the surface areas of tubes Ø7.2 nm with topological defects prevent the formation of quasi-bundles.

[1] V.V. Sumarokov, A. Jeżowski, D. Szewczyk, M.I. Bagatski, M.S. Barabashko, A.N. Ponomarev, V.L. Kuznetsov, S.I. Moseenkov, *Low Temp. Phys.* 45, 347 (2019).

Preparation of colloidal aqueous solution of C₆₀ fullerene by the sublimation method

**R.M. Basnukaeva, A.V. Dolbin, N.A. Vinnikov, A.M. Plohotnichenko, V.B. Esel'son,
V.G. Gavrilko, S.V. Cherednychenko**

*B.Verkin Institute for Low Temperature Physics and Engineering of NAS of Ukraine,
47 Nauky Ave., Kharkiv, 61103, Ukraine
basnukaeva@ilt.kharkov.ua*

Water-soluble derivatives of light fullerenes have unique biological activity and they are used as anticancer, neuroprotective, antiviral drugs, have antioxidant and antibacterial activity. However, their application for solving specific practical problems is difficult due to the almost complete absence of solubility of C₆₀ fullerenes in water. In this work, we propose a simple method for preparing colloidal aqueous solutions of C₆₀ fullerenes.

We have obtained a solid mixture of fullerene molecules and water molecules by the method of vacuum sublimation of C₆₀ fullerene followed by condensation together with water vapor on a surface cooled to -50 °C. The condensation of fullerene and water vapors was accompanied by the formation of a solid phase in the form of white flakes, which, when warmed to room temperature, turned into a yellowish jelly-like liquid. The optical studies conducted by us using an ultraviolet (UV) spectrometer showed that the resulting liquid is a stable colloidal aqueous solution of C₆₀ molecules. The figure shows the absorption spectra of the pure C₆₀ film deposited on a sapphire substrate (1) and an aqueous colloidal solution of C₆₀ (2).

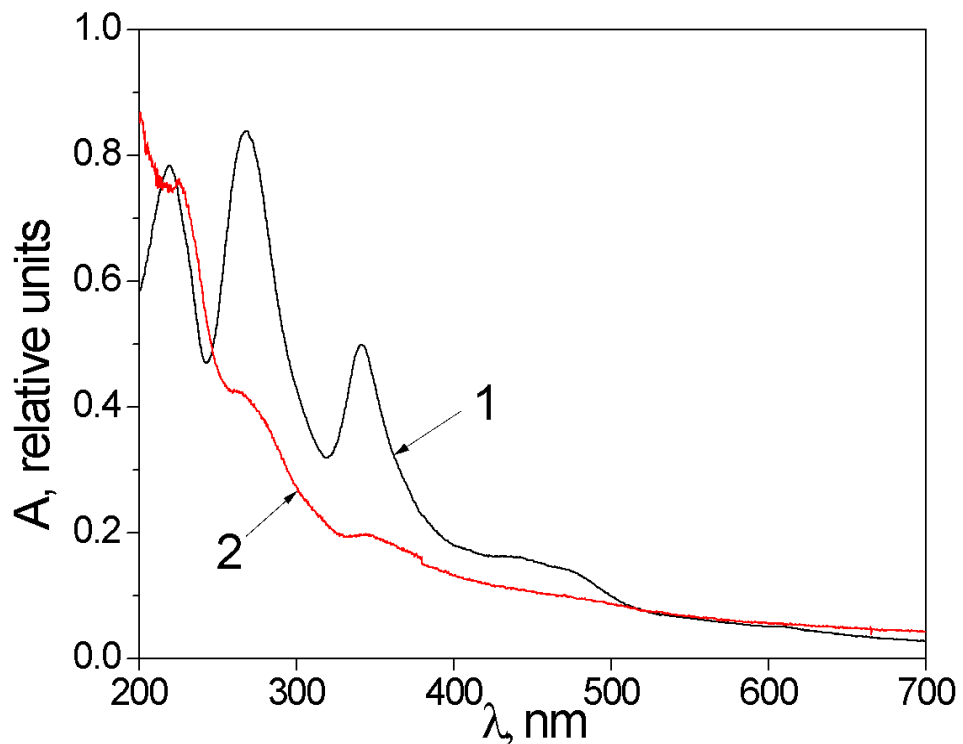


Fig. 1. Optical absorption spectra of the investigated samples: 1 – C₆₀ films, 2 – aqueous colloidal solution of C₆₀

Analysis of energy spectrum of tunable superconducting flux qubit intended for single microwave photon counting

A.P. Boichenko¹, O.G. Turutanov¹, V.Yu. Lyakhno¹, A.A. Soroka², V.I. Shnyrkov³

¹*B.Verkin Institute for Low Temperature Physics and Engineering of NAS of Ukraine,
47 Nauky Ave., Kharkiv, 61103, Ukraine*

²*National Science Center “Kharkiv Institute of Physics and Technology”,
Akhiezer Institute for Theoretical Physics, 1 Akademicheskaya Str., Kharkiv 61108, Ukraine*

³*Kyiv Academic University, 36 Acad. Vernadsky Blvd, Kyiv 03142, Ukraine
turutanov@ilt.kharkov.ua*

Single-photon detection technique has variety of applications in optical range including fiber-optic communication, medical imaging, quantum information science, quantum encryption etc. [1]. However, some applications (superconducting quantum computer, qubit state read-out, quantum radar, etc.) are naturally associated with microwave frequency range (~ 10 GHz). The detection in this range is much more difficult task since the microwave photon energy is by 4-5 orders of magnitude lower in comparison with optical range. This requires brand-new measurement methods using resonant photon absorption in quantum systems with discrete energy spectrum such as current-biased Josephson junction [2].

In [3-4] we proposed a scheme for frequency-tuned microwave photon counter based on a flux qubit whose discrete energy spectrum can be modified *in situ* by an external magnetic flux and critical current of the Josephson junction designed as a small dc SQUID loop. The approach is similar to [5] but uses other read-out circuit with non-hysteretic ultra-high frequency SQUID.

In present work we analyze (by numerical solving of the stationary Schrödinger equation) the changes in the qubit spectrum due to variations of the external flux (potential tilt) and the Josephson energy (barrier height) from the point of view of resonant frequency shift, inter-well tunneling probability and different detection protocols. Important role of inner and environment dissipation in the photon detection is discussed.

This work is supported by the NATO SPS Programme through grant No. G5796 and National Academy of Sciences of Ukraine under grant 0117U002291.

- [1] Robert H. Hadfield, Single-photon detectors for optical quantum information applications, *Nature Photon.* 3, 696 (2009).
- [2] Y.-F. Chen, D. Hover, S. Sendelbach, L. Maurer, S.T. Merkel, E.J. Pritchett, F.K. Wilhelm, and R. McDermott, *Phys. Rev. Lett.* 107, 217401 (2011).
- [3] V. I. Shnyrkov, Wu Yangcao, O. G. Turutanov, V. Yu. Lyakhno, A. A. Soroka. Scheme for Flux-Qubit-Based Microwave Single-Photon Counter with Weak Continuous Measurement, *Proc. 2020 IEEE Ukrainian Microwave Week*, vol. 3 MSMW-2020, 737-742.
- [4] V.I. Shnyrkov, Wu Yangcao, A.A. Soroka, O.G. Turutanov, V.Yu. Lyakhno. Frequency-tuned microwave photon counter based on a superconductive quantum interferometer, *Low Temp. Phys.* 44, 213 (2018).
- [5] K. Inomata, Zh. Lin, K. Koshino, W. D. Oliver, J.-Sh. Tsai, Ts. Yamamoto, Y. Nakamura, *Nat. Commun.* 7, 12303 (2016).

Graphene-based nanocomposite adhesive compounds

**S.V. Cherednychenko, A.V. Dolbin, N.A. Vinnikov, V.B. Esel'son, V.G. Gavrilko,
R.M. Basnukaeva, N.V. Isaev, P.A. Zabrodin**

*B.Verkin Institute for Low Temperature Physics and Engineering
of the National Academy of Sciences of Ukraine
bjiactep@icloud.com*

Currently, the priority in the development of aerospace parts designs belongs to polymer composite materials, combined and adhesive compounds. Their bearing capacity, reliability, and service life significantly depend on the quality of bonding of structures made of polymeric composite materials. We have developed a general concept and the scientific and technological approach to the creation of nanocomposite adhesive mixtures, which are based on graphene – the strongest two-dimensional carbon material. During the curing of nanocomposite mixtures, graphene particles were diffused into the compound, which allowed to obtain the adhesive seam thickness of no more than 10 μm . Since the average linear size of graphene flakes was about 10-15 μm , this technique of forming the adhesive seam provided the spatial ordering of graphene particles with respect to the plane of the adhesive joint. Scanning electron microscopy, X-ray diffraction, and mechanical tests have shown that the polymerization of thin layers of nanocomposite adhesive compounds under conditions of application of uniaxial pressure up to 1 MPa leads to the ordering of graphene planes in the composite layer and increases the strength of adhesive compounds. The created adhesive mixtures also combine such properties as good adhesion, high mechanical shear strength, a wide range of application temperatures, absence of brittleness, minimal shrinkage during curing. Gluing techniques, requirements for adhesive joints and their test modes were developed in close cooperation with State Enterprise "Antonov", where the industrial application of the created nanocomposites is expected.

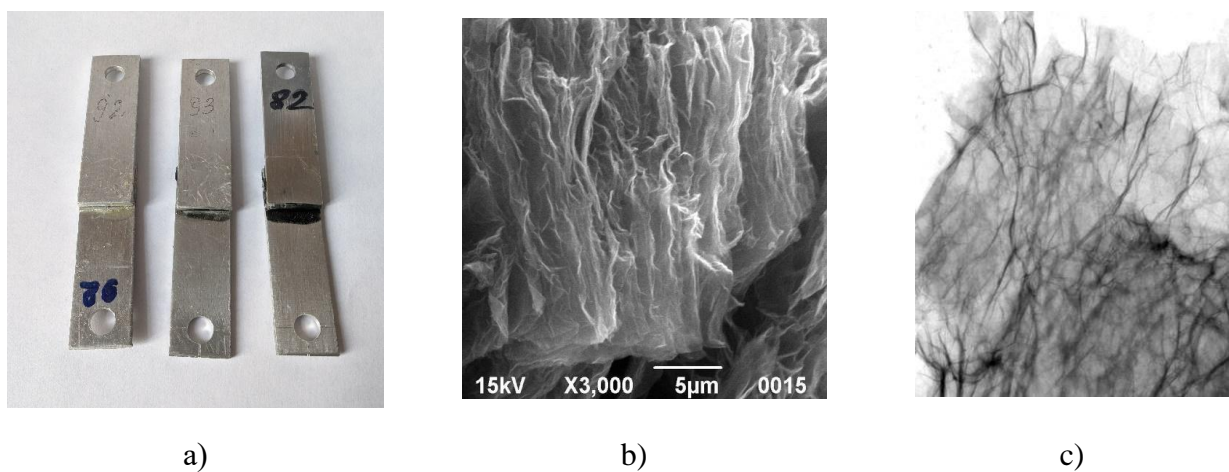


Fig. 1. Samples of adhesive joints for shear tests (a). Images of ordered graphene planes obtained by scanning (b) and transparent (c) microscopy.

Study of the mechanism of the cyclic switchover effect for quantum sensing with dendritic Yanson point contacts

A.O. Herus¹, A.V. Savytskyi¹, A.P. Pospelov², Yu.S. Doronin¹, V.L. Vakula¹, G.V. Kamarchuk¹

¹*B. Verkin Institute for Low Temperature Physics & Engineering of NASU,
47 Nauky Ave., Kharkiv, 61103, Ukraine*

²*National Technical University “KhPI”, 21 Kyrpychov Str., Kharkiv, 61002, Ukraine
gerus@ilt.kharkov.ua*

In the modern world, the development of nanotechnology stimulates discovery of new research methods that allow us to study the nature of physical phenomena at the atomic level and may become the basis of advanced technologies of the future. One of such methods is quantum sensing which uses the simple tool of Yanson point contacts and the properties of quantum systems. Thanks to the unique basic characteristics of Yanson point contacts, it has become possible to obtain energy portraits of quantum systems and easily analyse them.

The studies carried out in the recent years have unequivocally demonstrated that the Yanson point contact [1, 2] placed in an ion-conducting medium can be viewed as an electrochemical gapless electrode system (GES) [3]. One of the characteristic features of GES behaviour is transfer of charge along two parallel branches corresponding to the electronic and ionic conduction channels. One of the most interesting results of this process is the point-contact cyclic switchover effect [3]. The cyclic processes of synthesis and dissolution of dendritic point contacts occur in accordance with the quantum shell effect and are characterized by a number of features which explicitly demonstrate the quantum properties of Yanson point contacts. This makes it possible to apply the innovative operation principle of the new class of selective quantum sensing elements to the analysis of liquid and gaseous media [3].

The purpose of this study is to reveal the peculiarities of the processes occurring in dendritic Yanson point contacts during the cyclic switchover effect and providing the ground for the realization of selective quantum detection mechanism and of the enhanced sensitivity of point-contact sensors to liquid and gaseous analytes. The object of the study was dendritic copper Yanson point contacts [3]. The contacts were produced using a modified “needle-anvil” technique. The dendritic point contact was formed in an electric field generated by a stabilized d.c. source. The present report analyses the experimental data on the dynamics of electric conductance and lifetime of dendritic Yanson point contacts. A mathematical model is proposed for the anode destruction of copper point contacts during the cyclic switchover process. It is shown that a GES in an electric field functions as a system with a positive feedback, which determines the dynamics of the point-contact resistance variation in an ion-conducting medium. Taking into account the key influence of the Faraday processes on the mechanism of the nanostructure destruction, we find a correlation between the duration of the anode reaction and the linear dimensions of the conduction channel.

A comparative analysis of the calculated and measured times of interruption of the direct conduction of Yanson point contacts suggests an enhanced chemical activity of the conduction channel surface of these nanostructures. This peculiarity of dendritic point contacts may be due to the size effect and the presence of a fresh metallic solid surface at the interface. The approaches and results of the present research can be used for development of selective quantum sensors based on point-contact nanostructures.

- [1] Naidyuk Yu.G. and Yanson I.K.: Point-contact spectroscopy. New York: Springer. 300 (2005).
- [2] Pospelov A.P., Pilipenko A. I., Kamarchuk G.V., Fisun V.V., Yanson I. K., and Faulques E., J. Phys. Chem. C, 119(1): p. 632-639 (2015).
- [3] Kamarchuk G.V., Pospelov A.P., Savytskyi A.V., Herus A.O., Doronin Yu.S., Vakula V.L., Faulques E., SN Applied Sciences. 1:244 (2019).

Small orthovanadate nanocrystals with controlled redox-activity

K.O. Hubenko, S.L. Yefimova, P.O. Maksimchuk, N.S. Kavok, V.K. Klochkov

*Institute for Scintillation Materials of NAS of Ukraine,
60 Nauky Ave., Kharkiv, 61072, Ukraine
gubenko@isma.kharkov.ua*

Nanocrystals, which promote generation of reactive oxygen species (ROS) and stimulate the onset of oxidative stress responsible for the development of a variety of adverse conditions, are of great prospect for various nanomedicine applications. ROS generation in semiconducting nanocrystals is a complex process, the efficiency of which is governed by both nanocrystals characteristics (size, morphology, etc.) and external conditions, such as type of irradiation. On the other hand, in nanocrystals characterized by high amount of structural defects, for instance, oxygen vacancies (V_O) in oxide nanocrystals, such defects could serve as traps for charge carriers and are responsible for ROS production in nanocrystals even without UV irradiation (in the dark). In our previous works, we have shown that $GdYVO_4:Eu^{3+}$ nanocrystals exhibit photo-catalytic activity (ROS production) at both UV-light irradiation [1, 2] and in the dark condition [3].

In this work, we report controlled redox-activity of small ($d=2$ nm) $GdYVO_4:Eu^{3+}$ nanocrystals in aqueous solutions and biological environment. It has been revealed that depending on pre-treatment conditions (exposure to UV light or storage in the darkness), the same nanocrystals exhibit pro- or antioxidant properties.

Pro-/antioxidant activity in aqueous solutions was evaluated by UV-vis spectroscopy by the ascorbic acid (AA) oxidation test, and hydroxyl radical ($\cdot OH$) generation analysis. Lipid oxidation under the effect of nanocrystals have been also analyzed.

Multi-functional $GdYVO_4:Eu^{3+}$ nanocrystals with controlled redox-activity are assumed to be a new theranostic agent in radiotherapy.

- [1] S.L. Yefimova, P.O. Maksimchuk, V.V. Seminko, N.S. Kavok, V.K. Klochkov, K.A. Hubenko, A.V. Sorokin, I.Yu. Kurilchenko, Yu.V. Malyukin, J. Phys. Chem. C., 123, 15323 (2019).
- [2] K. Hubenko, S. Yefimova, T. Tkacheva, P. Maksimchuk, I. Borovoy, V. Klochkov, N. Kavok, O. Opolonin, Yu. Malyukin, Nanosc. Res. Lett., 13, 101 (2018).
- [3] P. O. Maksimchuk, S. L. Yefimova, K. O. Hubenko, V. V. Omelaeva, N. S. Kavok, V. K. Klochkov, A. V. Sorokin, Y. V. Malyukin. Phys. Chem. C., 124, 3843 (2020).

Electron diffraction diagnostics of N₂-Kr binary cluster beams

O. P. Konotop, O.G. Danylchenko

*B.Verkin Institute for Low Temperature Physics and Engineering of NAS of Ukraine,
47 Nauky Ave., Kharkiv, 61103, Ukraine
konotop@ilt.kharkov.ua*

Free clusters of inert and simplest molecular gases are created by the method of adiabatic gas expansion into vacuum through a supersonic nozzle. When the gas is cooled and condenses in the jet, heat exchange between the gas and the external environment is practically absent, and the further growth of free clusters is not affected by the properties of the substrate, in contrast to other methods for producing clusters. In such cluster beams, it is possible to study cluster effects in the most "pure" form, including those associated with a change in the size of nanoaggregations.

If a binary gas mixture is set to the nozzle inlet, then, depending on the composition of the mixture, its initial temperature T_0 and pressure P_0 , either homogeneous clusters of one of the components or heterogeneous aggregations can be formed in the jet. In previous works [1, 2], our attention was devoted to the diagnostics of binary cluster beams for systems with unlimited solubility of components: Ar-Kr, Kr-Xe, and N₂-Ar. On the contrary, the N₂-Kr system, according to the literature data for bulk samples [3] and thin films [4], is characterized by limited solubility with the formation of two-phase regions.

The purpose of this work is to study the features of cluster growth in an N₂-Kr gas mixture which adiabatically expands into vacuum through a supersonic nozzle. In particular, the dependence of the size and structure of clusters on the initial concentration of krypton in the gas mixture and the temperature of the mixture at the nozzle inlet was investigated.

Electron diffraction data were obtained for the concentration of krypton in the initial gas mixture of 0.5 at.%, 1 at.% and 6 at.%, for two gas temperatures T_0 at the nozzle inlet (100 K and 120 K), and by varying the initial gas pressure P_0 in the range of 0.1-0.6 MPa. The average sizes of the formed clusters varied from 1×10^3 to 2×10^4 molecules per cluster.

It was found that, at krypton concentrations in the gas of 0.5 at.% and 0.1 at.% for both studied temperatures T_0 , the phase composition of mixed clusters slightly differs from the composition of pure N₂ clusters formed under identical conditions. In both cases, the clusters have a mixed fcc-hcp structure, and the addition of krypton leads only to an increase in the fraction of the fcc phase relative to the hcp one. At these krypton gas concentrations, the sizes of mixed clusters and pure nitrogen clusters are practically the same, which indicates that the N₂-Kr system, in contrast to the Ar-Kr one, does not exhibit heterogeneous intensification of cluster growth.

At $T_0 = 120$ K and an increase in the krypton gas concentration to 6 at.%, a sharp decrease in mean cluster size was observed, and their structure with an increase in P_0 transforms as follows: icosahedral \rightarrow fcc with stacking faults \rightarrow fcc+hcp. Such transformation is inherent in pure clusters of inert gases, which indicates the formation of only homogeneous krypton clusters in a binary N₂-Kr jet. In this case, nitrogen molecules act as a buffer gas. Spectroscopic studies are planned to confirm this assumption..

- [1] O.G. Danylchenko, S.I. Kovalenko, O.P. Konotop, V.N. Samovarov, J. Clust. Sci. 26, 863 (2015).
- [2] O.G. Danylchenko, S.I. Kovalenko, O.P. Konotop, V.N. Samovarov, Low Temp. Phys. 41, 637 (2015).
- [3] A.I. Prokhvatilov, L.D. Yantsevich, Sov. J. Low Temp. Phys. 10, 270 (1984).
- [4] A.A. Solodovnik, N.S. Mysko-Krutik, Low Temp. Phys. 45, 1296 (2019).

Gold-Fullerene Heterojunctions for Thermoelectricity

V. Kozachenko, V. Shmid, A. Podolian, A. Nadtochiy, O. Korotchenkov

*Taras Shevchenko National University of Kyiv,
64/13 Volodymyrska Street, 01601 Kyiv, Ukraine
olegk@univ.kiev.ua*

Effective thermoelectrics with high heat to electrical energy conversion efficiency in terms of the figure-of-merit (ZT) value implies high Seebeck coefficient and high electrical conductivity combined with low thermal conductivity. It is well known that usage of nanostructuring thermoelectric materials offers a suitable means for achieving this purpose, which enables manipulation of both the electron and phonon transport and leads to improved thermoelectric performance [1]. Therefore, there have been numerous attempts to reduce the thermal conductivity employing various composites, such as the ones with the fullerene C₆₀ [2, 3].

Here we show that by embedding fullerene nanoparticles in a gold matrix allows to effectively control the phonon- and electron-transport properties and achieve the Seebeck coefficient comparable to that observed in other nanocomposites with C₆₀.

A 10-nm gold film showing an island structure was thermally deposited onto a mica foil. The fullerene film having a thickness of 50 nm was then deposited yielding a C₆₀ film/Au nanoparticle composite layer mounted on the mica substrate. A representative temperature dependent Seebeck coefficient is shown in Fig. 1. At about 300K, the Seebeck coefficient is $\approx 6 \mu\text{V/K}$, roughly two times greater than in the sample without C₆₀.

The current through C₆₀/metal junctions can be controlled by properly selecting the metal electrode material for energy level alignment based upon its work function. Here, a C₆₀/Au is used in the composite and the charge transport properties are addressed by the surface photovoltage (SPV), as exemplified in the inset of Fig. 1.

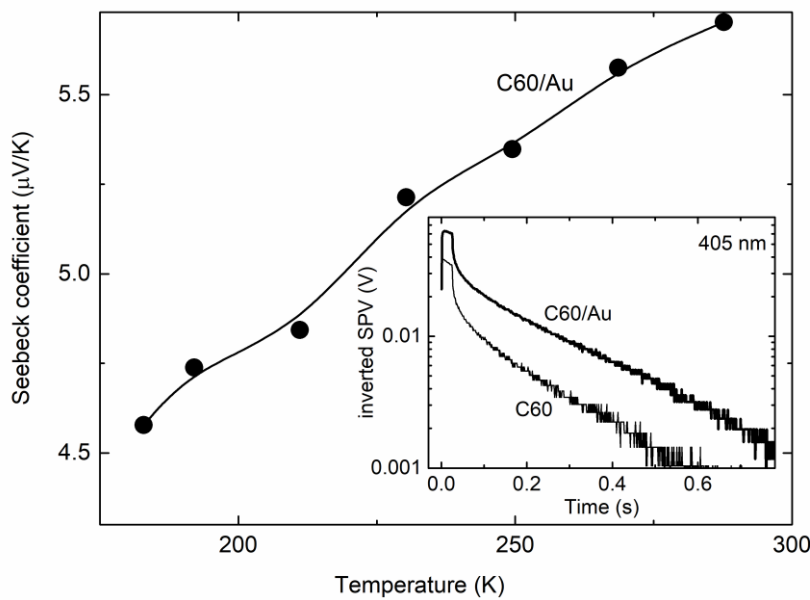


Fig. 1. Temperature dependent Seebeck coefficient of C₆₀ film/Au nanoparticle composite layer. Inset: SPV decays of C₆₀ film and C₆₀ film/Au nanoparticle composite layer.

- [1] M.S. Dresselhaus, G. Chen, M.Y. Tang, R. Yang, H. Lee, D. Wang, Z. Ren, J.-P. Fleurial, and P. Gogna, *Adv. Mater.* 19, 1043 (2007).
- [2] S.K. Yee, J.A. Malen, A. Majumdar, and R.A. Segalman, *Nano Lett.* 11, 4089 (2011).
- [3] D. Olaya, C.-C. Tseng, W.-H. Chang, W.-P. Hsieh, L.-J. Li, Z.-Y. Juang, and Y. Hernández, *FlatChem.* 14, 100089 (2019).

Size oscillations of the frequency of surface plasmons in metal nanowires with an elliptical cross section

A. Korotun¹, A. Babich²

¹National University "Zaporizhzhia Politechnic", 64 Zhukovsky Str., Zaporizhzhya, 69063, Ukraine

²Max Planck Institute for Solid State Research, 1 Heisenbergstraße, Stuttgart, 70569, Germany

andko@zntu.edu.ua

The plasmonic properties of metallic nanowires are extensively studied both theoretically and experimentally. This is due to the widespread use of metal 1D structures as optical antennas, probes for near-field optical microscopy, as well as components of lasers, biosensors, and other devices. The modern stage of development of nanotechnologies allows to obtain the wires with different cross-section shapes. Mechanical strain-induced effects may form the elliptical cross-section of the nanowires. It is well-known, the size quantization effects appear in nanowires with a diameter less than 5 nm. It was studied in Ref. [1], these effects result in specific frequency dispersion laws of the surface plasmon peaks strongly depending on the nanowire diametre. Nevertheless, the strain-induce effects causing their elliptical cross-sections on the surface plasmon resonances in the metallic nanowires.

In the case of 1D systems, surface plasmon resonances satisfy the condition:

$$\text{Re}\tau_{xx}(\omega_{sp}) = -\tau_m, \quad (1)$$

where τ_m is the dielectric constant of the environment; ω_{sp} is the frequency of the surface plasmons.

Taking into account the quantum size effects, the diagonal component of the dielectric tensor can be written in the form [1]:

$$\text{Re}\tau_{xx}(\omega_{sp}) = 1 - \frac{k_p^4}{k_{\omega_{sp}}^4} \left\{ 1 + \frac{k_\tau^2 (k_{\omega_{sp}}^2 + k_\tau^2)}{k_{\omega_{sp}}^4 + k_\tau^4} S(\omega_{sp}, \rho_0) \right\}. \quad (2)$$

Here $k_p^2 \equiv 2m_e\omega_p/\hbar$, ω_p is the frequency of the bulk plasmons; $k_\tau^2 \equiv 2m_e/\hbar\tau$, τ is the relaxation time; $k_{\omega_{sp}}^2 \equiv 2m_e\omega_{sp}/\hbar$, and

$$S(\omega_{sp}, \rho_0) \equiv \frac{2}{Nm_e} \sum_{i,j} f_{mnp} k_{mn}^2 C_{mn}^2 \left\{ \mathcal{F}_{(-)} + \mathcal{F}_{(+)} \right\}; \quad (3)$$

$$\mathcal{F}_{(\mp)} = \frac{\left(k_{mn}^2 - k_{m\mp 1, n'}^2 \right) \left\{ \left(k_{mn}^2 - k_{m\mp 1, n'}^2 \right)^2 - 3k_{\omega_{sp}}^4 + k_\tau^4 \right\}}{\left[\left(k_{mn}^2 - k_{m\mp 1, n'}^2 \right)^2 - k_{\omega_{sp}}^4 + k_\tau^4 \right]^2 + 4k_{\omega_{sp}}^4 k_\tau^4} \mathcal{J}_{(\mp)}^2, \quad \mathcal{J}_{(\mp)} \equiv C_{m\mp 1, n} \int_0^{\rho_0} I_{m\mp 1}(k_{m\mp 1, n'} \rho) I_{m\mp 1}(k_{mn} \rho) \rho d\rho;$$

f_{mnp} is the step function; $C_{mn} = \sqrt{2}/\rho_0 |I'_m(k_{mn} \rho_0)|$; $I_m(\xi)$ is the Bessel function of the m -th order; numbers k_{mn} are the roots of the equation [2]

$$(1 + \varepsilon m) I_m(k_{mn} \rho_0) - \varepsilon k_{mn} \rho_0 I_{m+1}(k_{mn} \rho_0) = 0, \quad (4)$$

where $\rho_0 = (a+b)/2$ is the effective radius of the elliptical cross-section, a and b are the elliptical semi-major and semi-minor axes, respectively; ε is the eccentricity of the wire. Thus, in the case of metal nanowires with an elliptical cross section with a low eccentricity, the SPR frequency changes due to a change in the energy spectrum of electrons.

[1] A.V. Korotun, A.A. Koval', Phys. Met. Metallogr. 120, 621 (2019).

[1] A.V. Korotun, Phys. Sol. St. 56, 1245 (2014).

Softening of the Metastable Bi-43wt.%Sn Eutectic under Repeated Loading in the Region of Microplasticity

V. Korshak

V. N. Karazin Kharkiv National University, 4 Svobody Sq., Kharkiv, 61022, Ukraine
vera.korshak@gmail.com

The nature of the physical processes that cause the superplasticity of polycrystalline materials is still not fully clarified. It is generally believed that eutectic alloys exhibit structural superplasticity, that is, the appearance of the effect is not associated with phase nonequilibrium and the course of structural-phase transformations in them under deformation conditions. However, earlier studies have established that the crystallization of the eutectic Bi-43wt.%Sn alloy investigated in this work under conditions that ensure the manifestation of its superplastic properties is nonequilibrium. The phase state of the alloy is characterized by an excess of the relative proportion of α (Sn)-phase, a solid solution of bismuth in tin, compared with the state in equilibrium not only at the room temperature but also at the eutectic temperature.

The report presents the results of the study of the microplastic deformation effect on the strength characteristics of the investigated alloy. The experiments were carried out in the mode of active loading at room temperature, at which the alloy exhibits superplastic properties. The deformation of the specimens was determined using strain gauge measurements. After another loading, the specimens were kept for a certain time in the unloaded state and then deformed again. The experiments were carried out on samples compressed on a hydraulic press at $\approx 70\%$ immediately after casting and then aged for 12 days.

The obtained dependences of the stress σ on the value of deformation ε are shown in Fig. 1.

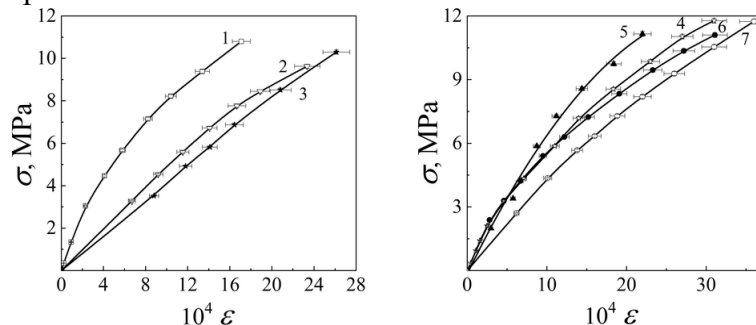


Fig. 1. The dependence of stress σ on deformation ε of the initial (1) and repeatedly deformed after unloading samples of Bi-43wt.%Sn alloy with the duration of exposure between the next and previous loads: $2 \div 1 - 3$, $3 \div 2 - 4$, $4 \div 3 - 17$ days; $5 \div 4 - 50$ min; $6 \div 5 - 53$, $7 \div 6 - 17$ days. The residual deformation is $3.2 \cdot 10^{-4}$, $5.8 \cdot 10^{-4}$, $5.3 \cdot 10^{-4}$, $19.0 \cdot 10^{-4}$, 0 , $8.8 \cdot 10^{-4}$ for curves 2 – 7, respectively.

We observe the effect of alloy softening under repeated loading, in contrast to the strengthening of metallic materials usually found under similar test conditions. In all cases, after unloading, significant inverse inelastic deformation of specimens is observed, which indicates the presence of significant internal stresses in the material exceeding the yield stress at room temperature.

Considering the obtained data on the metastable phase state, which is formed in conditions of nonequilibrium crystallization of the studied alloy [1], we conclude that the alloy softening is caused by the relaxation of internal stresses and the course of the initial stages of the decay of supersaturated solid solutions stimulated by the external mechanical extensional stress.

[1] V. F. Korshak, P. V. Mateychenko, and Yu. A. Shapovalov, The Physics of Metals and Metallography 115, 1249 (2014).

Low-temperature magnetoresistance of multiwall carbon nanotubes with perfect structure

T. Len¹, I. Ovsienko¹, I. Mirzoiev², E. Beliayev², V. Andrievskii², D. Gnida³, L. Matzui¹, V. Heraskevych¹

¹*Taras Shevchenko National University of Kyiv, Department of Physics, Kyiv, Ukraine*

²*B.Verkin Institute for Low Temperature Physics and Engineering of NASU, Kharkiv, Ukraine*

³*Institute of Low Temperature and Structure Research PAS, Wroclaw, Poland*

talen148@gmail.com

The work presents the results of investigations of magnetoresistance of multiwall carbon nanotubes (MWCNTs) with perfect structure. The MWCNTs have been prepared by the method of the catalytic decomposition of a hydrocarbon in the presence of a nickel catalyst. According to the X-Ray diffraction data for obtained MWCNTs, the distance d_{002} between neighboring layers is 0.340 nm, the crystallite size does not exceed 30 nm. For measuring the electrical resistance, the bulk specimens in the form of rectangular parallelepipeds 2 mm × 3.5 mm × 15 mm have been made of MWCNTs powder by cold pressing using polyvinyl acetate as a binder. The mass fraction of polyvinyl acetate in the dry specimen was 25 %. The transverse magnetoresistance measurements (the magnetic field was perpendicular to the current through specimen) have been carried out in the temperature interval 2 – 293 K and magnetic fields up to 8 T.

Fig.1 presents the dependence of magnetoresistance $\Delta R/R$ for the bulk MWCNTs specimen on magnetic field B in the temperature range from 2 K up to 200 K.

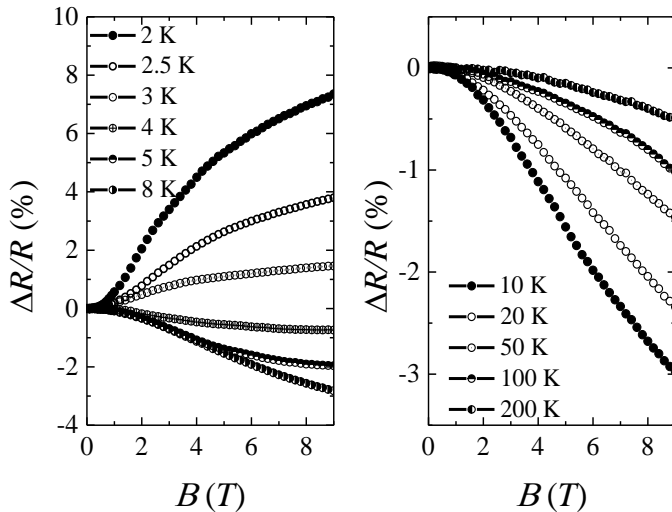


Fig.1. Dependence $\Delta R/R(B)$ for the bulk MWCNTs specimen.

As can be seen from Fig.1, the dependence of magnetoresistance on magnetic field at different temperatures is rather complex. There is a change in the sign of magnetoresistance. At temperatures below 4 K, the magnetoresistance is positive, while in the temperature range from 4 K to 200 K, the magnetoresistance is negative. A quadratic dependence of relative conductivity on magnetic fields can be seen in the low magnetic fields domain. However, with the magnetic field increasing, a logarithmic dependence of relative conductivity on the magnetic field arises.

So we believe that for MWCNTs with perfect structure, in the low-temperature domain, the behavior of conductivity in magnetic fields can be described in terms of weak electron localization and electron-electron interaction for 2D-systems [1]. In the framework of these models, using the obtained experimental data on the field and temperature dependencies of magnetoresistance, the values of the Fermi energy (E_F) and the interaction constant (G), as well as the exact form for the temperature dependence of the electron wave function phase relaxation time (τ_ϕ) can be determined. We found that the phase relaxation time of wave function changes with temperature according to the expression $\tau_\phi = 3.6 \cdot 10^{-12} \times T^{-1.12}$. Thus, the temperature dependence of the phase relaxation time for MWCNTs is steeper compared to the temperature dependence of this parameter for fine-crystalline graphite, for which this dependence has the form $\tau_\phi \propto A^*/T$, where A^* is a constant.

[1] Altshuler B.L., Khmel'nitzkii D., Larkin A.I., Lee P.A. Phys.Rev.B, **22**, 5142 (1980).

Gate-controlled Electroluminescence in a Molecular Photodiode

V.O. Leonov, E.G. Petrov, Ye.V. Shevchenko

*Bogolyubov Institute for Theoretical Physics of NAS of Ukraine,
14-b Metrolohichna str., Kyiv, 03143, Ukraine
leogluck@gmail.com*

A molecular photodiode is a nanoscale molecular junction that contains an interior fluorophore center (F) linked to nanoelectrodes 1 and 2 via organic or inorganic isolating spacers ($^1\text{F}_2$ system). At a certain voltage bias, the energy of electrons, transporting through the $^1\text{F}_2$ -system can be converted into the energy of light quanta. Physically, this process is similar to what happens in organic light-emitting diodes. The difference is that the fluorophore is located in a nanoscale volume, where, due to the formation of plasmons, the emission of photons can be noticeably enhanced. It was previously shown that the efficiency of electroluminescence is largely determined by the kinetics of electron transitions between the neutral and charged states of the molecule–fluorophore [1, 2].

Using a nonequilibrium density matrix method, the role of the gate voltage in regulating the electroluminescence of a molecular photodiode with asymmetric localization of electron density on the highest occupied (HOMO) and lowest unoccupied molecular orbitals (LUMO) of a photochromic molecule was considered [3,4]. It was shown that, as in the case of a transistor, the gate voltage can have a significant effect on the formation of electroluminescence when one of the orbital energies is outside the gap between the biased Fermi levels of the electrodes.

The role of the gate voltage is to change the position of the energy levels of the orbitals until both HOMO and LUMO fall into the transmission gap and thus provide a resonant mechanism for the formation of electroluminescence [5]. This allows electroluminescence to be turned on at a lower bias voltage than when electroluminescence is turned on at zero gate voltage.

The appearance of polarity is associated with the switching on and off of the resonant electron hopping between the conducting states of the electrodes and molecular orbitals localized at different distances from the electrode surfaces [4, 5].

- [1] E. G. Petrov, V. O. Leonov, Ye. V. Shevchenko, JETP Letters, 105, No. 2: 89 (2017).
- [2] E. G. Petrov, V. O. Leonov, Ye. V. Shevchenko, JETP, 125, No. 5: 856 (2017).
- [3] V.O. Leonov, Ye.V. Shevchenko, E. G. Petrov, Nanosystems, Nanomaterials, Nanotechnologies, 18, № 2, p. 227–240 (2020).
- [4] E. Petrov, V. Leonov, Y. Shevchenko, V. Snitsarev, Modern Phys. Lett. B, 2040063 (2020)
- [5] E.G. Petrov, V.V. Gorbach, A.V. Ragulya, A. Lyubchik, S. Lyubchik, J. Chem. Phys. 153, 084105 (2020).

High-frequency quantum interferometry for a double-quantum dot

M.P. Liul¹, A.I. Ryzhov¹, S.N. Shevchenko^{1,2}

¹*B.Verkin Institute for Low Temperature Physics and Engineering of NASU, Kharkiv, Ukraine*

²*V.N. Karazin Kharkiv National University, Kharkiv, Ukraine*

maximliul@gmail.com

The area of quantum computations becomes more and more popular nowadays. The main building block of quantum computers is a qubit. Qubit is any two-level system (TLS), which can occupy two possible quantum states: atom, nuclear or electron spin, photon, quantum dot and so on. Most of such objects are very well studied experimentally as well as theoretically. One of the strongest tools for describing a TLS is the Landau-Zener-Stückelberg-Majorana interferometry. It was applied for studying many systems. On the other hand, from the practical point of view, it can be interesting to expand this approach on multilevel systems. We explore a four-level system, proposed by the authors of Ref. [1]. The object of our analysis is a single-electron double quantum dot (DQD), created by using silicon-insulator technology [2].

Any multilevel system can be studied, using several different methods: solving the Lindblad Master equation or a system of rate equations [3]. Both of these methods were successfully applied for describing many quantum systems. In the current research we use the rate equations formalism. The methodology is the following:

1)Finding a Hamiltonian of the system and building the plot of corresponding energy levels.

The obtained energy levels of the system are plotted in Fig. 1.

2)Writing and solving the system of rate equations. The solutions are probabilities of a certain energy level occupation. In general it is possible to get probabilities as a function of time, or in other words, to look at the system dynamics. But we are interested in the stationary case, i.e. we want to understand the time-averaged behavior of the system.

3)Building the interferograms. The obtained probabilities are functions of excitation amplitude and energy detuning, so varying these two values we can plot the interferograms which describe the system behavior.

Comparing the obtained theoretical with experimental results [1] and, as a result, establishing a correspondence between the theoretical characteristics and the technical parameters of the system.

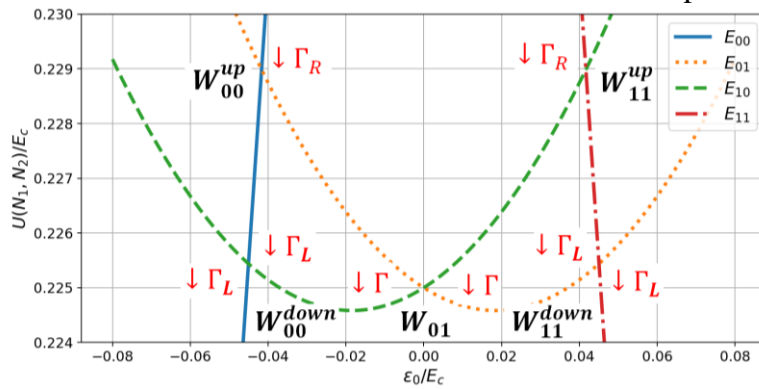


Fig. 1. The DQD energy levels as functions of energy detuning ε_0 . Energy E_{NIN2} corresponds to the state with N_1 excess electrons on the left and N_2 excess electrons on the right QD. $\Gamma_{L(R)}$ and W_{ij} are relaxations and relaxation rates respectively (for more details see Ref. [3]).

Acknowledgments: This research is sponsored by the Army Research Office and is accomplished under Grant Number W911NF-20-1-0261.

[1] A. Chatterjee, et al. Phys. Rev. B 97, 045405 (2018).

[2] B. Voisin, et al., Nano Lett. 14, 2094 (2014).

[3] D. M. Berns, et al., Phys.Rev. Lett. 97, 150502 (2006).

Effect of defects on polarization switching in CuInP₂S₆ crystals

D. Gal, H. Ban, A. Haysak, A. Molnar

*Department of the Physics of Semiconductors, Uzhhorod National University
54 Voloshina Str., Uzhhorod, 88000, Ukraine
alexander.molnar@uzhnu.edu.ua*

Over the past few years many studies have been devoted to using CuInP₂S₆ as an active element of a ferroelectric storage cell [1]. The investigation of the properties of CuInP₂S₆ crystals has shown that the samples have a branched domain structure (Fig. 1) and a wide boundary of the stability of the ferroelectric phase. Domains have different sizes in the range of 0.2-3 microns. The phase of the piezoelectric response changes to the opposite (π) on the domain walls, which confirms the orientation of the polarization perpendicular to the plane. Moreover, the re-polarized regions remain stable at a layer thickness of 3-4 nm, which allows for the creation of ferroelectric cells of ultrahigh-density memory [1].

Our studies show a significant difference in the domain structure of CuInP₂S₆ crystals obtained from the gas phase, from the melt, and enriched by Cu and In. The technology of obtaining the single crystals, as well as deviations from stoichiometry, significantly affect the defectiveness of their structure, which leads to the formation of a strongly different domain structure and also significantly affects the switching processes in CuInP₂S₆ crystals (Fig. 2).

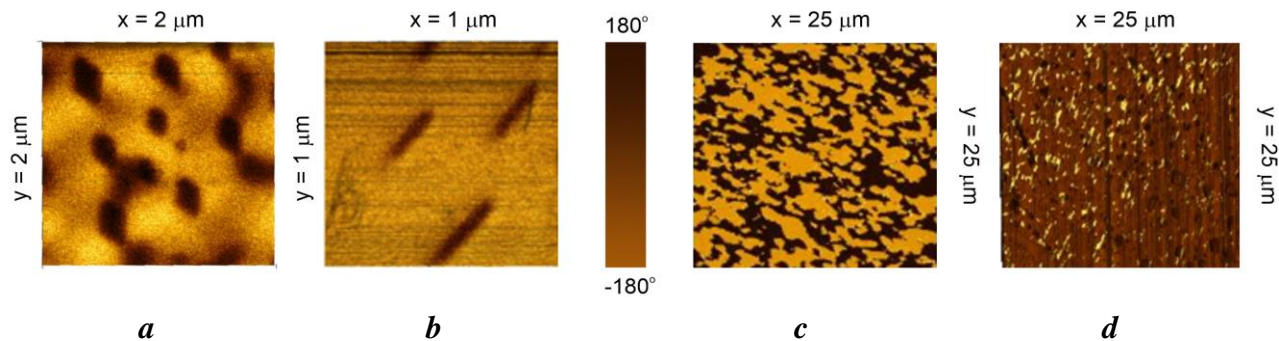


Fig. 1. Domain structure of CuInP₂S₆ crystals at room temperature. *a* – sample obtained from the gas phase, *b* - crystal obtained from the melt by the Bridgeman-Stockbarger method, *c* - CuInP₂S₆ + CuS₂ (copper enriched), *d* - CuInP₂S₆ + In₂S (indium enriched).

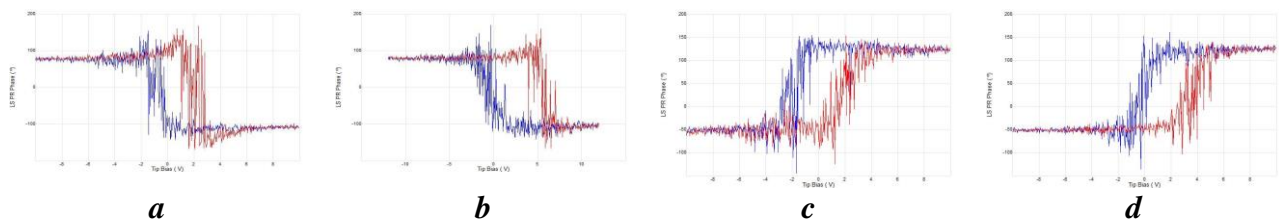


Fig. 2. Phase loops of CuInP₂S₆ crystals at room temperature. *a* – sample obtained from the gas phase, *b* - crystal obtained from the melt by the Bridgeman-Stockbarger method, *c* - CuInP₂S₆ + CuS₂, *d* - CuInP₂S₆ + In₂S.

Based on the data obtained, we can conclude that for practical use it is more appropriate to use crystals obtained from the gas phase and enriched by Cu, in which the switched areas remain more stable and there are practically no internal electric fields that lead to the displacement of the polarization loops (Fig. 2,b,d).

[1] F.Liu, L.You, K.L.Seyler, X.Li, P.Yu, J.Lin, X.Wang, J.Zhou, H.Wang, H.He, S.T.Pantelides, W.Zhou, P.Sharma, X.Xu, P.M.Ajayan, J.Wang, Z.Liu, Nature Communications 7, 12357 (2016).

Split of surface plasmon resonance in metal nanodisks with a small aspect ratio

N. Pavlishche¹, A. Korotun¹, V. Kurbatsky¹, I. Titov²

¹*National University "Zaporizhzhia Politechnic", 64 Zhukovsky Str., Zaporizhzhya, 69063, Ukraine*

²*UAD Systems, 84 Alexandrovska Str., Zaporizhzhya, 69002, Ukraine*

andko@zntu.edu.ua

As is known, the unique optical properties of metal nanoparticles are due to collective electronic excitations, called surface plasmon resonance (SPR). The properties of such plasmons strongly depend on the geometric shape of the nanoparticles. At the same time, if surface plasmons in spherical and rod objects have been studied quite fully, then a rather complex structure of plasmon modes has been experimentally found in metal nanodisks [1], which has not yet received its explanation. It should be noted that this issue is of great practical importance, since lattices of metal nanodisks are used to enhance the effective absorption of sunlight in the latest generation solar cells. Thus, the problem of determining the frequencies of surface plasmon resonances in a metal nanodisc is urgent.

Consider a metal nanodisk with a diameter D and height H in a medium with a dielectric constant ϵ_m . In this case, the frequencies of surface plasmons are determined by the relations

$$\omega_{sp}^{\perp(\parallel)} = \sqrt{\frac{\omega_p^2 \mathcal{L}_{\perp(\parallel)}}{(1 - \mathcal{L}_{\perp(\parallel)})\epsilon_m + \mathcal{L}_{\perp(\parallel)}\epsilon^\infty}} - (\gamma_{eff}^{\perp(\parallel)})^2, \quad (1)$$

where ω_p is the frequency of bulk plasmons; ϵ^∞ is the contribution of the ionic core to the dielectric permittivity of the metal; $\mathcal{L}_{\perp(\parallel)}$ is depolarization coefficients determined by the ratios $\mathcal{L}_\perp = \pi\mu/4$, $\mathcal{L}_\parallel = 1 - \frac{\pi\mu}{2}$; $\mu = H/D$; $\gamma_{eff}^{\perp(\parallel)}$ is the effective transverse (longitudinal) relaxation rate, which in the case of a disk is defined as

$$\gamma_{eff}^{\perp} = \gamma_{bulk}, \quad \gamma_{eff}^{\parallel} = \gamma_{bulk} + \frac{\mathcal{K}_\parallel}{(\omega_{sp}^{\parallel})^2}, \quad (2)$$

γ_{bulk} is the relaxation rate in 3D metal;

$$\mathcal{K}_\parallel = \frac{1}{2} \omega_p^2 \frac{v_F}{H} \left(\frac{1}{\mu} \right) \left\{ \frac{9}{4} \left(1 + (\epsilon_m - 2) \frac{\pi}{2} \mu \right) + \frac{V}{2\sqrt{\epsilon^\infty \epsilon_m}} \left(\frac{\omega_p}{c} \right)^3 \left(1 + \left(\frac{\epsilon_m}{2\epsilon^\infty} - 1 \right) \frac{\pi}{2} \mu \right) \right\}, \quad (3)$$

v_F is the Fermi velocity of electrons; V is the volume of the nanodisc; c is the velocity of light.

In the case when the aspect ratio is small $\mu \ll 1$, we obtain the following expression for the SPR frequency splitting

$$\Delta\omega_{sp}(\mu) = - \left(\frac{\pi \omega_p^2}{4 \epsilon_m} \mu - \gamma_{bulk}^2 \right)^{\frac{1}{2}} + \chi^{\frac{1}{2}} \left(1 - \frac{\gamma_{bulk} \mathcal{K}_\parallel}{\chi^2} \right) \left\{ 1 - \frac{\pi \omega_p^2 \epsilon_m}{\epsilon^\infty \chi} \left[\frac{1}{4} + \frac{\gamma_{bulk} \mathcal{K}_\parallel}{\chi^2 - \gamma_{bulk} \mathcal{K}_\parallel} \right] \mu \right\}, \quad (4)$$

$$\chi \equiv \frac{\omega_p^2}{\epsilon_m} - \gamma_{bulk}^2.$$

The results of calculations of the size dependence of the SPR re-splitting showed that as the aspect ratio increases, the splitting decreases, and, therefore, the peaks will merge.

- [1] H. Wang, X. Wang, C. Yan, H. Zhao, J. Zhang, C. Santschi, and O.J.F. Martin, ACS Nano. 11, 4419 (2017).

Electron tunneling through graphene-based double-barrier structure

V. Sakhnyuk, A. Shutovskyi, O. Zamurujeva, S. Fedosov

*Lesya Ukrainka Volyn National University, 13 Voli Ave., 43000 Lutsk, Ukraine
theoryva@gmail.com*

For the electrons that are incident on the potential barrier in graphene, there are the following values of the angles of incidence, for which the coefficient of passage is equal to one. For electrons with the normal incidence barrier is completely transparent regardless of its height and width. Such an effect for relativistic electrons has long been known as the "Klein's paradox" [1,2] and is associated with the preservation of pseudopsin.

We investigated the symmetric double-barrier structure of rectangular shape determined by the function $V(x) = V_0[H(-x - a)H(x + a + d) + H(x - a)H(-x + a + d)]$, there $H(x)$ – Heaviside step function. A massless two-dimensional Dirac equation with potential $V(x)$ was solved to analyze the tunneling of electrons through such a potential barrier.

The main results of the study:

- 1) A new formula for the dependence of the coefficient of transparency of a symmetric double-potential rectangular barrier on its parameters and on the angle of incidence of electrons has been obtained;
- 2) Conditions which must satisfy the angles with 100% probability of tunneling of electrons through the barrier have been found;
- 3) Angles of incidence at which the probability of a tunneling is equal to one have been found from the analysis of the conditions of resonance tunneling for certain values of the barrier parameters. It is shown that with the decrease in the barrier height, the number of resonance angles increases, and the maxima become more acute.

[1] O. Klein, Z. Phys. 53, 157 (1929).

[2] M. I. Katsnelson, K. S. Novoselov, A. K. Geim, Nat. Phys. 2, 620 (2006).

New scintillation materials based on perovskite nanocrystals with intensive photoluminescence

T.V. Skrypnyk, I.I. Bespalova, A.V. Sorokin, S.L. Yefimova

*Institute for Scintillation Materials NAS of Ukraine, 61072, 60 Nauky ave., Kharkiv, Ukraine
skrypnyk_tamara@isma.kharkov.ua*

In the last few years, interest in halide perovskite nanocrystals with the general formula CsPbX_3 (where X is Cl, Br or I), which can be obtained both in the form of powders and in the form of transparent colloidal solutions, has rapidly increased.

Due to the quantum-dimensional effect, such nanocrystals have a fast nanosecond luminescence of free excitons, the quantum yield of which can reach 90%. Another feature of such nanocrystals is that replacing anions in the Cl/Br/I series leads to the band gap changes, resulting in a sequential shift of the edges of the absorption spectra and luminescence maxima from the blue to red regions [1, 2].

This allows to vary their optical properties in a wide spectral range. Such unique properties of CsPbX_3 nanocrystals, as well as their high effective atomic number ($Z_{\text{eff}} = 62 \div 66$), allow us to consider them as scintillation materials.

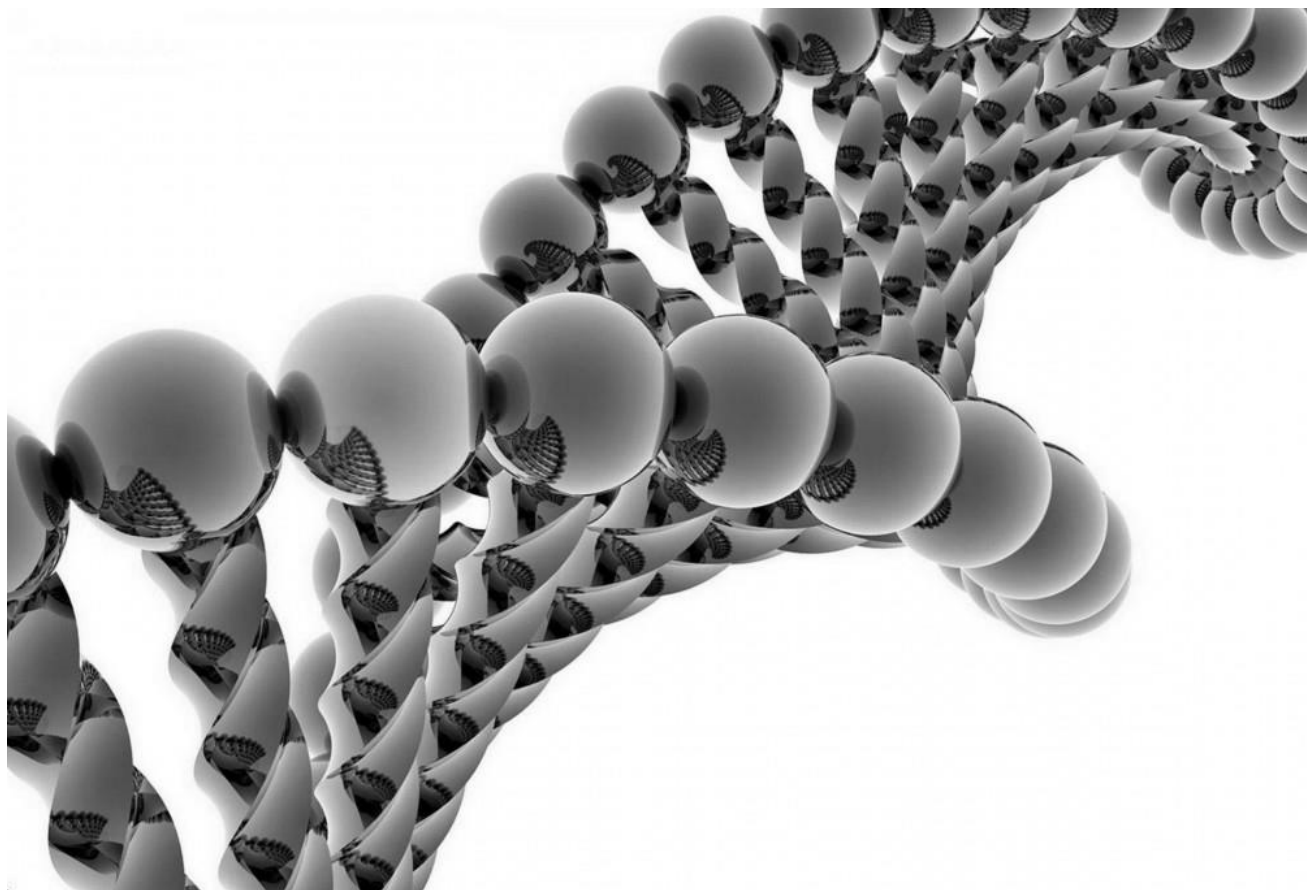
But toxicity and instability of Pb-based perovskite materials are preventing their commercial implementation [3]. Therefore, our goal is to develop new lead-free compounds.

Colloidal perovskite CsPbX_3 nanocrystals and lead-free perovskite nanocrystals of different compositions were obtained by LARP-strategy and their luminescent and scintillation performances were determined and compared.

[1] L. Protesescu, S. Yakunin, M.I. Bodnarchuk, F. Krieg, R. Caputo, C.H. Hendon, R.X. Yang, A. Walsh, M.V Kovalenko, Nanocrystals of Cesium Lead Halide Perovskites (CsPbX_3 , X = Cl, Br, and I): Novel Optoelectronic Materials Showing Bright Emission with Wide Color Gamut, *Nano Lett.* 15 (2015) 3692-3696.

[2] M.V. Kovalenko, L. Protesescu, M.I. Bodnarchuk, Properties and potential optoelectronic applications of lead halide perovskite nanocrystals, *Science*. 358 (2017) 745-750.

[3] R. Wang, J. Wang, S. Tan, Y. Duan, Z. Wang, Y. Yang Opportunities and Challenges of Lead-Free Perovskite Optoelectronic Devices. *Trends in Chemistry*. 2019.



BIOPHYSICS AND PHYSICS OF MACROMOLECULES

Melatonin determination in the human organism by a breath test

D.O. Harbuz¹, A.P. Pospelov², V.I. Belan¹, V.A. Gudimenko¹, V.L. Vakula¹, L.V. Kamarchuk³, Y.V. Volkova³, G.V. Kamarchuk¹

¹*B.Verkin Institute for Low Temperature Physics and Engineering of NAS of Ukraine,
47 Nauky Ave., Kharkiv, 61103, Ukraine*

²*National Technical University “Kharkiv Polytechnic Institute”,
2 Kyrpychov Str., Kharkiv, 61002, Ukraine*

³*SI “Institute for Children and Adolescents Health Care” of NAMS of Ukraine,
52-A Yuvileinyi Ave., Kharkiv, 61153, Ukraine
zeyxes@gmail.com*

Nowadays, gas nanosensorics is a rapidly developing area of research. Despite the advantages nanoscale objects have over bulk sensors such as a much higher sensitivity and a much shorter response time, they are not without drawbacks. The low reproducibility of the production of complex nanostructures in the manufacture of sensors, a long relaxation time after exposure to a gas agent and unstable baselines are among them [1].

An important area of application of gas nanosensors is human breath analysis. Breath contains a lot of components, some of which are products of human metabolism and carry information about the state of the body. Currently, such sensors allow detecting a lung cancer in the early stages and the presence of carcinogenic strains of *Helicobacter pylori* bacterium in the body [2].

One of the interesting and important tasks for modern research is the determination of various hormones in the human organism. This work is devoted to the detection of melatonin in the human body.

Melatonin is one of the key hormones in the human body. It is a product of pineal gland secretion that affects many physiological functions of the body. Melatonin acts as a photoregulator of circadian biorhythms, and all endogenous rhythms of the body are subordinated to its effect [3]. Despite the variety of the methods for its determination, they all are not without drawbacks. The main one is the impossibility of viewing a large number of samples with a sufficient speed.

We used multistructures of Yanson point contacts based on Cu-TCNQ compound as breath sensors. To obtain the samples, an original technology of combined electrochemical synthesis was used, which made it possible to obtain sensors with an integrated power supply. The breath gas of 20 volunteers, who were patients treated at SI “Institute for Children and Adolescents Health Care” of NAMS of Ukraine, was used as the test substance. To adjust the point-contact sensor matrix and verify the breath test, the fluorometric method was used to determine the content of melatonin in the urine of the patients.

The results of the study suggest that the problem of noninvasive determination of melatonin concentration in the human body can be successfully solved by using breath tests based on Yanson point contacts. Employment of scientific and technological achievements of the past and of the present combined with mathematical tools makes it possible to successfully solve a number of problems which cannot be solved or present significant difficulties when approached with other methods. Many years ago, Yanson point-contact spectroscopy offered unique possibilities for solving scientific and technological problems of the time. Now, more than 40 years later, Yanson point contacts are used in new cross-disciplinary areas of research.

- [1] G. Di Francia, B. Alfano, and V. La Ferrara, *J. Sensors*, 2009, 1 (2009).
- [2] I. Kushch, N. Korenev, L. Kamarchuk, A. Pospelov, A. Kravchenko, L. Bajenov, M. Kabulov, A. Amann, and G. Kamarchuk, *J. Breath Res.* 9, 047109 (2015).
- [3] A.Y. Bespyatykh, V.Ya. Brodskiy, O.V. Burlakova, V.A. Golichenkov, L.A. Voznesenskaya, D.B. Kolesnikov, A.Yu. Molchanov, and S.I. Rapoport, *Melatonin: theory and practice* (Medpraktika-M, Moscow 2009).

The limitations of DFT tight-binding approximation and their role in conformational analysis of DNA constituents

O.S. Husak, T.Yu. Nikolaienko

*Faculty of Physics of Taras Shevchenko National University of Kyiv, 64/13 Volodymyrska Str.,
Kyiv, 01601, Ukraine
olhahus@gmail.com*

Obtaining complete conformer ensembles of model DNA monomers can help in expanding the present understanding of the conformational variability in DNA regions with apurinic/apirimidinic (AP) sites [1]. Typically, experimental methods [2, 3] available for studying individual nucleotides don't provide complete information about the conformational properties of these objects, because only a few energetically most-stable conformations are observed in experiments. On the other hand, the methods of computational quantum mechanics make it possible to analyze all possible conformations of molecules. However, large conformational capacity of biomolecules as large as DNA monomer units makes traditional high-level computational *ab initio* techniques resource-consuming. In the variety of molecular modeling approaches available nowadays, the density-functional based tight-binding (DFTB) method is unique in combining the clear hierarchy of physically sound approximations with high computational efficiency [4], thus being ideal for treating the systems of hundreds of atoms in a reasonable time. Yet, the impact of the involved approximations on the results of conformational analysis has not been studied so far in details.

In the present contribution, we report inaccuracies peculiar to DFTB semiempirical methods of GFN-xTB family [5] in geometry optimization of 1',2'-dideoxyribofuranose-5'-phosphate molecule (IUPAC name: [(2R,3S)-3-hydroxyxolan-2-yl)methyl dihydrogen phosphate]. This molecule is the sugar-phosphate residue of isolated 2'-deoxyribonucleotides and can be considered as a model for AP-site defected regions of DNA strands. We demonstrate the existence of systematic biases in conformers obtained by xTB methods relative to more accurate non-empirical quantum-chemical methods and discuss the possible implications.

- [1] Т. Ю. Ніколаєнко, Л. А. Булавін, Д. М. Говорун, О. О. Мисюра, Ukr.Biochem.J. 2011, 83.
- [2] Lindahl T., Nyberg B., Biochemistry. 1972, 11, N 19.
- [3] Schärer O. D., Jiricny J., BioEssays. 2001, Vol 23, P. 270–281.
- [4] J. Cuny, N. Tarrat, F. Spiegelman, A. Huguenot, M. Rapacioli. Journal of Physics: Condensed Matter (2018), Vol. 30, p. 303001.
- [5] C. Bannwarth, E. Caldeweyher, S. Ehlert, A. Hansen, P. Pracht, J. Seibert, S. Spicher, S. Grimme, WIREs: Computational Molecular Science(2020) 11(18)

Permittivity characterization of aqueous solutions of biological active substances

K.S. Kuznetsova¹, V.A. Pashynska^{1,2}, Z.E. Eremenko¹, O.I. Shubniy¹, A.V. Martunov³

¹*O. Usikov Institute for Radiophysics and Electronics of the NAS of Ukraine,
12, Ac. Proskura str., Kharkiv, 61085, Ukraine*

²*B. Verkin Institute for Low Temperature Physics and Engineering of NAS of Ukraine,
47 Nauky Ave., Kharkiv, 61103, Ukraine*

³*Mechnikov Institute of Microbiology and Immunology National Academy of Medical
Sciences of Ukraine, 14-16 Pushkinskaya St., Kharkiv, 61057, Ukraine
vlada.pashynska@gmail.com*

The problem of pollution of environment and, in particular, environmental water sources by organic pollutants from food, pharmaceutical, chemical industries and agricultural production is one of the most urgent ecological problems all over the world. Understanding the importance of development of robust and non-invasive methods of ecological control of water samples, we propose to use for this purpose a dynamic control method based on microwave dielectrometry of aqueous solutions of organic substances. Such a method and unique dielectrometry with appropriate software was developed and designed in Usykov IRE NASU [1]. In the current study we applied and adapt the method and device developed to investigate the complex permittivity (CP) of model aqueous solutions of representatives of different classes of organic compounds such as ethanol, protein albumin, antibiotic levofloxacin and some others. The adapted method is based on determining the dielectric parameters (real ϵ' and image ϵ'' parts of CP of water solutions of biological compounds) of aqueous solutions of organic compounds in the millimetre range of electromagnetic wavelengths. The aqueous ethanol solutions of different concentrations in the range of 0-40% were measured and the obtained data on ϵ' and ϵ'' dependence from ethanol concentration is in a good agreement with the classical literature data [2], obtained on frequency range from 0.1 to 89 GHz. Further, the aqueous solutions of albumin of concentration 0÷5% were examined. The data on ϵ' and ϵ'' dependence from the solutions concentration demonstrated that the CP of water solutions of albumin are sensitive to the low protein concentration that is important for our method application for testing of the waste water of food or pharmaceutical industries. We also studied the influence of addition of salt (10% of sodium chloride) into the protein solution on the CP of the solution studied. The ϵ' and ϵ'' of albumin solutions with 10% NaCl differ from the values of ϵ' and ϵ'' of aqueous solutions of albumin with the same protein concentration and testify that salt presence in the solution changes the amount of free water in the solution. The proposed device is working well to detect the change in free water part in water solutions of glucose, antibiotics gentamicin and penicillin and experimental results showed the maximum changes of ϵ' and ϵ'' are at small concentrations of biological active substances. The dependencies of ϵ' and ϵ'' on glucose concentration in water are close to linear character that is very suitable for express-test measurements. At the last stage of the study we tested the antibiotic levofloxacin solutions of 0-5mg/ml concentrations range and determined the permittivity values of the antibiotic solutions comparing with the pure water and dynamics of the change of the parameter with the concentration increasing. Thus, the results of our study demonstrate that CP of aqueous solutions of different classes of organic compounds including proteins and antibiotics can be considered as a base physical parameter to define the part of free water in of aqueous solutions.

[1] Z.E. Eremenko, K.S. Kuznetsova, N.I. Sklyar, A.V. Martynov. Measuring complex permittivity of high-loss liquids. Chapter to the book entitled “Dielectric Materials and Applications”, published by Nova Science (of the USA) Publication Date: May 2019, 371 pages, pp.41-75.

[2] T. Sato, R. Buchner. Dielectric Relaxation Processes in Ethanol/Water Mixtures J. Phys. Chem. A 2004, 108, 5007-5015.

Detection of carbon monoxide in exhaled air

D. Velyhotskyi, A. Mysiura

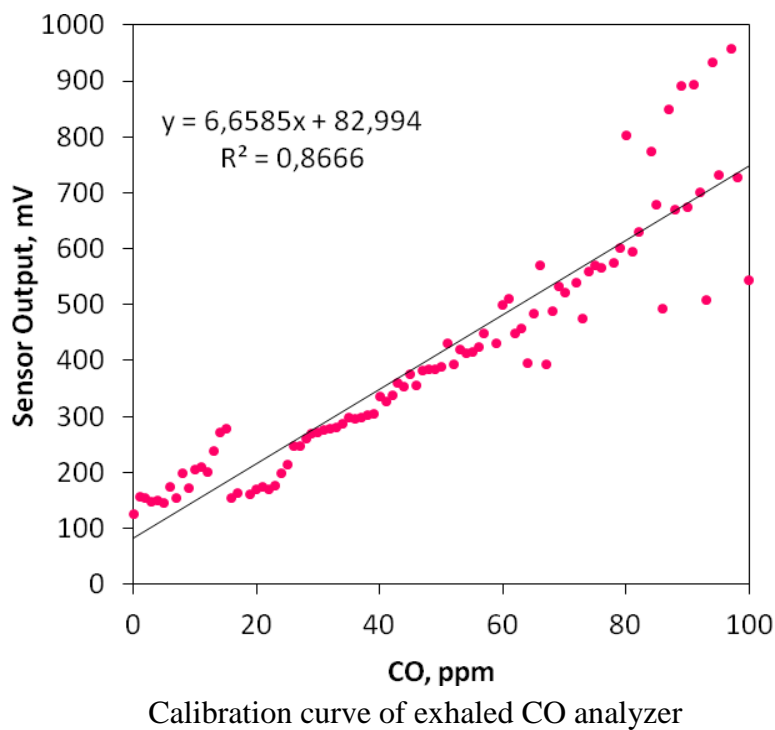
*Institute of Applied Problems of Physics & Biophysics, NAS of Ukraine,
3 V. Stepanchenka St., Kyiv, 03142, Ukraine
velyhotskyi@nas.gov.ua*

Carbon monoxide (CO) due to its properties is a toxic substance. During respiration, CO penetrates rapidly through the alveolar-capillary membrane into the blood and binds to hemoglobin (Hb), forming a carboxyhemoglobin (COHb) fraction. As a result of COHb formation, oxygen delivery to tissues decreases, hypoxia (oxygen starvation) increases, which negatively affects the activity of other human organs – heart, lungs, brain, etc. The COHb level begins to increase at low CO concentrations in the air and The World Health Organization suggests that levels greater than 6 ppm are potentially toxic over a longer period of time [1].

In this paper, we present a developed prototype of analyzer for exhaled CO detection. The design of the CO analyzer consists of sensor, a printed circuit board and a display which are placed in one case. The analyzer is controlled by software. An electrochemical sensor TGS5042 [2] manufactured by Figaro was used for CO detection. Additionally, an electrical circuit and software have been developed to register the sensor output signal to achieve the required sensitivity to low CO concentrations.

The CO analyzer was characterized by conducting a series of measurements under exposure to CO. Figure shows the calibration curve of the exhaled CO analyzer. The correlation coefficient $R^2 = 0.87$ indicates a satisfactory linearity of the dependence of the analyzer output signal with the actual CO value in the range 0-100 ppm.

The developed analyzer is a part of the health monitor [3] for definition of other physiological indicators of the person. The health monitor is designed to detect signs of poisoning by toxic substances during fires.



- [1] J. Rose and L. Wang, Amer. Journ. Respir. Critic. Care Med. 5, 596 (2017).
- [2] Figaro Inc., «Technical Information for TGS5042», Dec. 2007.
- [3] Д.В. Велигоцький та Н.В. Стельмак, Віс-к КрНУ «Інформ. с-ми і тех-гii». 72, 71 (2012).

Thermodynamic model to dielectric parameters of erythrocytes: effect of temperature

L.V. Batyuk¹, N.N. Kizilova²

¹*Kharkiv National Medical University, 4 Nauky Ave., Kharkiv, 61022, Ukraine*

²*Warsaw University of Technology, Pl. Politechniki 1, Warsaw, 00661, Poland*

lv.batyuk@knmu.edu.ua

Thermodynamic models play a crucial role for describe the loss of intracellular water from human erythrocytes at temperature below 5~2°C and hydration of the erythrocyte membrane. The performed calculations which are based on the extrapolation of data obtained by UHF-dielectrometry method in the study of the dielectric properties of erythrocytes and erythrocytes membranes of healthy donors and sick patients with neurological and oncological diseases showed that temperature is an important factor controlling the interaction between the water and membrane of the cell [1,2]. The Debye's model has been generalized for a medium with a set of relaxation phenomena at different scales with different relaxation times $\{\tau_j\}_{j=1}^N$ in the form [3]:

$$\varepsilon^*(\omega) = \varepsilon_\infty + (\varepsilon_0 - \varepsilon_\infty) \int_0^\infty \frac{\zeta(\tau)}{1+i\omega\tau} d\tau$$

where $\zeta(t)$ is the memory function that describes the non-Markovian relaxation process. The data are analyzed together with static permittivity values. By using the single-shell model, reliable values of erythrocyte internal conductivity and permittivity have been obtained. Also, the reported values of the membrane capacitance per unit surface [4] were found to be in a good agreement with those of the solvent-free cellular membranes. Therefore, the measurement data of the ε' and ε'' values can be used for computations of the following parameters:

1) from Debye's model: the dielectric loss coefficient $\delta = a \tan(\varepsilon''/\varepsilon')$; the dielectric relaxation frequency of water $f_d = f(\varepsilon' - \varepsilon_\infty)/\varepsilon''$ in the solution/suspension, where f is the frequency of the external field; the activation energy of dipole relaxation ΔF of the water molecules in studied systems $\Delta F = RT \ln\left(\frac{RT}{hN}\tau\right)$, where τ is the time of dielectric relaxation; for

different cells and tissues in healthy and impaired states. These factors include the probability of initiation of transmembrane defects at temperature below 5~2°C, which reduce the resistance of cells to temperature effects. As the temperature decreases, the membrane conductivity becomes absorption rate-limited and, in effect, shuts off the probability of closure of defects on the membrane surface, which contributes to the decrease of cell resistance.

2) from the single-shell model: dielectric permittivity ε_m , ε_{in} of the membrane and the internal matter (cytoplasm, free and bound water) separately, provided the values σ_m , σ_{in} and the membrane thickness h are known from other measurements/experiments;

3) from the non-equilibrium thermodynamic model with single relaxation time: phenomenological and state coefficients of the model, and entropy production.

- [1] L. Batyuk and N. Kizilova, AS Cancer Biology 4, 3, (2020).
- [2] L.V. Batyuk, N.M. Kizilova, Bulletin of Taras Shevchenko National University of Kyiv (Series: Physics & Mathematics). 4, (2017).
- [3] A. Pérez-Madrid, L.C. Lapas and J. M. Rubí, Z. Naturforsch. 72, 2 (2017).
- [4] K. Asami, Y. Takahashi and S. Takashima, Biochim. Biophys. Acta 1010, (1989).

Binding of proflavin to poly(ethylene glycol): investigation by spectroscopic methods

Iu. Blyzniuk, E. Dukhopelnykov, E. Bereznyak, N. Gladkovskaya

*O. Ya. Usikov Institute for Radiophysics and Electronics of NAS of Ukraine, 12 Akad. Proskury Str., Kharkiv, 61085, Ukraine
j.n.blyzniuk@gmail.com*

One of the important aspects of modern pharmacotherapy is the targeted delivery of drugs in complexes with nanoparticles. It allows to increase the drug's selectivity and reduce the side effects of chemotherapy. A significant step is selecting coatings for nanoparticles, which are linkers between the nanoparticle surface and the drugs. Optimization of the nanoparticles loading by a drug requires estimating the binding parameters between the linker and the drugs.

The promising coatings are various polymer compounds *e.g.* polyethylene glycol (PEG) [1, 2]. At the initial stages of research, it is convenient to use the drugs with a simple molecular structure. We used mutagen proflavin (3,6-diaminoacridine hydrochloride, PF) which has strong antibacterial and antiviral properties [3]. The binding of polyethylene glycol with proflavin is investigated using spectroscopic techniques.

The infrared (IR) spectra of PEG, PF-PEG mixture and dried PF solution were obtained. IR spectra were analyzed in two spectral ranges: the 1550-1620 cm⁻¹ region of deformation vibrations of proflavin N-H-groups and the 1200-1000 cm⁻¹ range of stretching vibrations of the poly(ethylene glycol) C-O-C-group. High-frequency shift of δ(N-H)-groups of proflavin and low-frequency shift of ν(C-O-C)-group of the poly(ethylene glycol) indicate the formation of hydrogen bonds in the PF-PEG complex.

The spectrophotometric titration experiment for the PF-PEG system in the range $\lambda=330-550$ nm was carried out. The full set of experimental spectra were analyzed by the MCR-ALS algorithm (multivariate curve resolution with alternating least squares). It enables to obtain the spectra of three absorbing particles: free proflavin ($\lambda_{\max} = 445$ nm) and two PF-PEG complexes ($\lambda_{\max} = 454$ nm and $\lambda_{\max} = 466$ nm). The concentrations of free and bound PF were calculated at different concentration ratios of the reacting components. The Langmuir equation considering the two types of complexes formation was applied for approximating the experimental binding isotherms. It allows obtaining the binding parameters in PF-PEG systems. The optimal values of the binding constants are 2×10^4 and 4×10^6 M⁻¹.

Conclusion: The interaction of proflavin with poly(ethylene glycol) has been investigated using VIS and IR spectroscopy methods. The results demonstrate that PF binds to PEG via hydrogen bonds in two ways with sufficiently different binding constants.

- [1] Anisha A. D'souza and Ranjita Shegokar, Polyethylene glycol (PEG): A versatile polymer for pharmaceutical applications, Expert Opinion on Drug Delivery (2016).
- [2] K. Knop, R. Hoogenboom, D. Fischer and U. Schubert, Poly(ethylene glycol) in Drug Delivery: Pros and Cons as Well as Potential Alternatives. Angewandte Chemie International Edition, 49, 6288-6308 (2010).
- [3] D. Sabolova, P. Kristian, M. Kozurkova, Proflavine/acriflavine derivatives with versatile biological activities. J Appl Toxicol. 40: 64– 71, (2020).

Assessment of the degree of BSA denaturation in solutions with AlCl_3 and FeCl_3 by the parameters of film textures

**D. Glibitskiy¹, O. Gorobchenko², O. Nikolov², T. Cheipesh³, T. Dzhimieva^{3,4}, I. Zaitseva^{5,6},
A. Zibarov⁶, A. Roshal⁶, M. Semenov¹, G. Glibitskiy¹**

¹*Department of biological physics, O.Ya. Usikov Institute for Radiophysics and Electronics,
NAS of Ukraine, Kharkiv, 61085, Ukraine*

²*Department of molecular and medical biophysics, School of radiophysics, biomedical electronics
and computer systems, V.N. Karazin Kharkiv National University, 4 Svobody Sq., Kharkiv, 61022,
Ukraine*

³*Chemical faculty, V.N. Karazin Kharkiv National University, 4 Svobody Sq., Kharkiv, 61022,
Ukraine*

⁴*V.N. Karazin Kharkiv National University, 4 Svobody Sq., Kharkiv, 61022, Ukraine*

⁵*O.M. Beketov National University of Urban Economy, Kharkiv, 61002, Ukraine*

⁶*Institute for Chemistry, V.N. Karazin Kharkiv National University, 4 Svobody Sq., Kharkiv, 61022,
Ukraine
dima.glib@gmail.com*

When assessing the nativity of biopolymers in solutions, various methods are employed, including those based on the analysis of spectrophotometric data. However, in some cases, the influence of chemical and physical factors on the properties of biopolymers complicates the analysis of the obtained data. For example, a decrease in pH leads to a partial precipitation of the protein in the solution, due to a change in the surface potential of the biopolymer. One of the techniques for assessing the degree of influence of biologically active substances on the changes in biopolymer structure and properties is the method of analysis of textures on films obtained from dried solutions of biopolymers.

Earlier [1], data were obtained on the correspondence of thermal denaturation of bovine serum albumin (BSA) to changes in the parameters of textures on the film. We also studied the effect of different concentrations of AlCl_3 and FeCl_3 (from 0.1 to 0.8 mmol/l) on the change in texture parameters. Although binding of these salts to BSA affects the processes of charge regulation [2], this effect is comparatively small and the change in pH still plays the primary role in protein destabilization.

Comparison of the film textures obtained from BSA solutions subjected to heat treatment with the textures of BSA solutions containing Al^{+3} or Fe^{+3} showed that the effect of 10-minute heating at 70°C (level of denaturation is approximately 57% [3]) leads to the same changes in the parameters of textures as the effect of Al^{+3} and Fe^{+3} ions at concentrations of 0.2 mmol/l and 0.4 mmol/l, respectively. Exposure to the temperature of 85°C for 10 min (level of denaturation is approximately 98% [3]) leads to the same texture changes as 0.4 mmol/l Fe^{+3} and 0.7 mmol/l Al^{+3} .

Thus, the method of film texture analysis can be used to assess the degree of denaturation of biopolymers for various factors resulting in denaturation.

- [1] G. Glibitskiy, D. Glibitskiy, O. Gorobchenko, O. Nikolov, A. Roshal, M. Semenov, A. Gasan. *Nanoscale Res. Lett.* 10(1). Article ID 155 (2015)
- [2] F. Roosen-Runge, B. Heck, F. Zhang, O. Kohlbacher, F. Schreiber. *J. Phys. Chem. B* 117(18), 5777 (2013)
- [3] K. Aoki, K. Hiramatsu, K. Kimura, S. Kaneshina, Y. Nakamura, K. Sato. *Bull. Inst. Chem. Res.* 47(4), 274 (1969)

Protein Condensation in Solution in the Presence of Vitamin B₁

T.O. Hushcha, M.S. Mykula, A.I. Vovk

*V.P. Kukhar Institute of Bioorganic Chemistry and Petrochemistry of NAS of Ukraine,
1 Murmanska str., Kyiv, 02094, Ukraine
hushcha@bpci.kiev.ua*

Recent years have seen increased interest in biomolecular condensates. This class of membraneless organelles is formed through liquid–liquid phase separation (LLPS) driven by the aggregation of proteins, nucleic acids and other biomolecules. Precipitation can facilitate the assembly of multicomponent complexes for biochemical processes, however, the resulting condensation of intrinsically disordered proteins can cause amyloidization and neurodegenerative diseases (Alzheimer's, Parkinson's, Huntington's), myopathy, cancer. Therefore, fine regulation of condensation process is essential. Cells capable of regulating phase separation by means of changes in solvent conditions, such as salt concentration, pH and temperature, as well as protein or RNA concentrations. Binding vitamin ligand also can influence protein aggregation.

Vitamin B₁ (thiamine) is of particular interest due to its vital role in transformations of neural cells. It is significant that neurodegenerative disorders and classic deficiency of vitamin B₁ have a number of common signs involving amyloid substance deposit. From publications on this topic one can conclude that interactions with proteins are at the heart of neurological activity of thiamine. However, molecular mechanisms of these interactions are far from clear.

In this paper we report on how different ionic forms of thiamine can be employed to regulate the interactions and associated phase behavior of protein. We investigate colloid properties of negatively charged globular protein, albumin from human (HSA) and bovine (BSA) serum, in solutions at different pH and in the presence of thiamine hydrochloride.

Using viscosity measurements we find that interaction of HSA with thiamine shifts the protein isoelectric point towards alkaline pH range. The shift implies existence of the specific localized binding, in contrast to the usual electrostatic interaction, between thiamine cations and negatively charged protein residues.

Using spectrofluorimetry we detect quenching of BSA intrinsic fluorescence upon adding thiamine. The quenching efficiency exhibits maximum at pH around isoelectric point (as determined by the viscosity measurements mentioned before) of the thiamine–bound protein. We suggest that primary cause for the fluorescence quenching is the ligand–assisted decrease in solubility and subsequent aggregation of the protein into droplets, which scatter light, and consequently the protein sample appears turbid to fluorometer.

Using uv-visible spectroscopy we monitor turbidity of a series of BSA samples with various thiamine concentrations. We find that the protein condensation occurs only in solutions with thiamine content between two critical concentrations. The findings can imply that tightly bound ligand cations cause neutralization and inversion of the protein charge, as well as condensation of the protein and redissolution of precipitates.

Using temperature dependent uv-visible spectroscopy we observe phase separation LLPS of the ligand–protein solutions upon heating above transition temperature. We show that transition temperature is high for monovalent cations of thiamine, while it is something weaker for divalent cations and monovalent anions of thiamine. The lower the transition temperature, the higher the interprotein attraction induced by ligand. Our observations suggest that the introduction of substituents that change the ratio between different ionic forms into the thiamine molecule can be a sensitive tool for adjusting protein condensation in solution.

Protein phase behavior in solutions with sodium chloride

T.O. Hushcha, A.I. Vovk

*V.P. Kukhar Institute of Bioorganic Chemistry and Petrochemistry of NAS of Ukraine,
1 Murmanska str., Kyiv, 02094, Ukraine
hushcha@bpci.kiev.ua*

Solubility of proteins is conditioned by many factors, such as temperature, pH, salt concentration, valency of added ions. All these factors can effectively control the protein–protein interactions in solutions and assist crystallization. The aggregates, gels, or liquid-liquid phase separation (LLPS) are usually observed during the process of protein crystallization. The origin of such precipitates, similarly to those observed in various other colloid systems, can be interpreted in terms of well defined phase transition. As such, a comprehensive characterization of protein condensation behavior is not only one that crucial to our understanding of protein crystallization but also one that we expect to shed more light on the mechanisms of protein condensation-related diseases, as well as drug delivery and the genesis of membrane-less organelles.

Protein condensation in salt solutions has been intensively studied in the past decade. In particular, it has been found that multivalent metal cations may cause a short-range attraction between the protein molecules resulting in a variety of phenomena, such as crystallization, cluster formation and dissolution, and LLPS. However, these phenomena have not been detected in solutions with monovalent cations. So far, the exact interaction mechanisms between monovalent ions and proteins are poorly understood.

In this paper we report on the experimental study of the colloid properties of protein solution as functions of salt concentration. Our goal was to explore, how the interactions between charged side chains of the protein and monovalent metal counterions can control the protein condensation. We focused on the characterization of density, shear viscosity and optical turbidity of human serum albumin (HSA) in aqueous solutions with sodium chloride (NaCl). The measurements were performed with high precision in broad ranges of temperatures and salt concentrations that enabled us to discover anomalous phase behavior of the studied protein solutions. We found that the isotherms of both density and shear viscosity demonstrate non-monotonic dependence on NaCl concentration. Density reached its highest point and shear viscosity did its lowest one at the same molar ratio [NaCl]/[HSA] close to physiological conditions. Using measured properties, we estimated the changes of the apparent protein sizes upon adding NaCl. The calculations yield that partial molar volume of HSA, as determined by the density measurements, maximize at the molar ratio [NaCl]/[HSA] mentioned before. By this the HSA hydrodynamic volume, as determined by the viscosity measurements, minimize at this concentration conditions. Both results indicate the decrease of HSA solvation layer and might be due to protein aggregation induced by NaCl. Using UV-visible spectroscopy we monitored the turbidity of HSA samples with various content of NaCl. We determined the transition from homogeneous to phase separated states of the solutions upon heating. By this the transition temperature was found to be dependent on the concentration of NaCl. The observed phenomena imply tight local binding of Na^+ counterions to charged side chains and subsequent concentration dependent neutralization and overcompensation of the protein surface charge.

The findings indicate that monovalent metal ions quite similarly to multivalent ones may modulate protein-protein interactions inducing the formation and dissolution of protein clusters and a rich variety of protein condensed phase states.

Peculiarities of interaction of short double-stranded polynucleotide poly(A:U) with graphene: molecular dynamics simulation

M.V. Karachevtsev

*B.Verkin Institute for Low Temperature Physics and Engineering of NAS of Ukraine,
47 Nauky Ave., Kharkiv, 61103, Ukraine
mkarachevtsev@ilt.kharkov.ua*

In the past decade the interactions between DNA/RNA and graphene-based nanomaterials have been a focus of many investigations, as these nanosystems show great promise in both fundamental study and in application area. Graphene-based nanomaterials demonstrate unique physical and chemical properties that open a wide spectrum of their possible using in various fields. Integrating graphene with biopolymers results in the formation of unique multifunctional nanoplates which have potential applications in nanomedicine. These applications include a visualization of different tissues, drug delivery, and treatment of diseases. To apply these nanobiohybrids to nanomedicine a comprehensive and reliable information on the interactions between double stranded nucleic acid and graphene is needed. This research is complicated as double-stranded nucleic acids and their synthetic analogues consist of different structural units (nucleotides) that interact in different ways with each nanosystem.

The main purpose of this work is to analyze the noncovalent interaction between double-stranded RNA oligonucleotides, formed by adenylic and uridylic nucleotides, and graphene employing molecular dynamics method. We considered two oligonucleotides: (rA)₁₅:(rU)₁₅ duplex and relatively longer (rA)₃₀:(rU)₃₀ one. Our simulations showed that the adsorption of duplex (rA)₁₅:(rU)₁₅ or (rA)₃₀:(rU)₃₀ on graphene starts with the interaction between π -systems of graphene and base pairs located at a duplex tails. For (rA)₁₅:(rU)₁₅ two possible initial arrangements of relatively longer (rA)₁₅:(rU)₁₅ duplex on the graphene surface (a perpendicular and parallel orientations) were simulated. It occurs that the starting binding of the short duplex (rA)₁₅:(rU)₁₅ with graphene does not depend on the initial orientation of the duplex relative to graphene, as a rigid construction of the duplex facilitates the short duplex flipping to the perpendicular orientation. The simulation also demonstrates that this ordered structure of the duplex is unzipped with time. In contrast to this behavior of short duplex, the relatively long duplex (rA)₃₀:(rU)₃₀ keeps a parallel arrangement along the graphene surface. Unzipped base pairs at the both tails of (rA)₃₀:(rU)₃₀ provide the stable arrangement of the duplex on graphene. Base pairs of the long duplex hidden inside do not have an opportunity for direct contact with the graphene surface and this steric limitation hampers the polymer unzipping. Thus, the simulation indicates that the interaction of duplex with graphene depends on its length: the short duplex always acquires the perpendicular orientation relative to graphene with following unzipping while the long duplex can maintain the double-stranded structure in the parallel orientation although with a structural disturbance. The interaction energy between stacked adenine and graphene in water environment prevails over the same energy for uracil (-16 vs -12 kcal/mol). This prevalence in the interaction energy keeps for their nucleotides ~ -27 and ~ -23 kcal/mol for binding of rA and rU nucleotide with graphene in water environment, respectively.

The results of the study on the binding of double-stranded RNA to graphene presented here provide a deeper understanding of the mechanism of the interaction of double-stranded DNA/RNA with the carbon surface and may help in the elaboration of new nanoscaffold for gene delivery in cells as well as sensitive and selective biosensors.

Interaction of organic cations with graphene oxide

**M.V. Kosevich, O.A. Boryak, A.M. Plokhotnichenko, V.S. Shekovsky, V.G. Zobnina,
V.V. Orlov, V.A. Karachevtsev**

*¹B.Verkin Institute for Low Temperature Physics and Engineering of NAS of Ukraine,
47 Nauky Ave., Kharkiv, 61103, Ukraine
mvkosevich@ilt.kharkov.ua*

Diversified applications of such neoteric nanomaterial as graphene oxide (GO) in drug delivery, antimicrobial and antiviral therapy, ecological purification are based on its intermolecular interactions with organic and inorganic compounds. Such interactions are facilitated by electrostatic attraction of electronegative oxygen-containing groups of GO to positively charged moieties of organic and biomolecules. The aim of the present work was to check whether the structure of organic cations influences the GO-cation interactions.

Two types of organic salts were selected for this purpose: methylene blue (MB) dye having planar heterocyclic cation and bisquaternary ammonium salt decamethoxinum (Dec) containing flexible $(\text{CH}_2)_{10}$ chain between two alkylammonium groups. Significant difference in the effect of the two compounds on aqueous suspension of GO was revealed. Dec, as well as some linear polyamines, caused gelation of GO dispersion resulting in formation of brownish dense clot. The effect of the MB showed pronounced dependence on MB concentration, which ranged from tiny flakes formation and sedimentation to preservation of stable turbid suspension. The result of simultaneous application of both Dec and MB was qualitatively different and consisted in flocculation resulting in efficient liquid purification from all components of the initial suspension.

These results mean that the coulombic interaction between the cations and GO is only the tool for attraction of the components, while the difference in 3D structures of (GO+Dec) and (GO+MB) composites is determined by the distinctions in the structure of Dec and MB cations. Obviously, two quaternary ammonium groups of Dec dication can form salt bridges with $-\text{COO}^-$ anionic moieties of GO, thus arranging GO flakes into a chaotic mesh.

The observed effects were characterized quantitatively by UV-vis spectroscopy. For high concentrations of MB in (GO+MB) system the bands corresponding to MB adsorption on GO surface in the form of dimers and trimers were recorded. Neutralization of negative charge of GO by MB cations caused destruction of GO dispersion and sedimentation of $\text{MB}_n\text{-GO}$ complexes. At low MB concentrations MB cations were adsorbed in the monomer form, which was evidenced by characteristic bands in UV-vis spectra. In this case MB-GO complexes retained partial negative charge and thus preserved their solubility in the form of water suspension. For Dec the exponential dependence of its adsorption on GO was established. For (GO+Dec+MB) ternary system, the recession of all spectral lines practically to the baseline pointed to the withdrawal of all components from the supernatant as the result of flocculation.

In relation to a problem of GO applications in drug delivery, a possibility of varied types of interaction of GO with different cationic functional groups of biomolecules is to be thoroughly analyzed. In particular, relatively strong electrostatic binding of medicinal compounds containing quaternary alkylammonium groups with GO is expected, while in the living organisms biomolecules possessing alkylammonium functional groups may be able to trap GO flakes. Composite of GO with Dec as an approved antimicrobial agent may be recommended for production of GO-based functional hydrogels. The effects accompanying formation of the GO composite (GO+Dec+MB) with two cationic additives may be accounted in development of functional GO-based materials destined for water purification.

The research was supported by the Grant N 0120U100157 of the National Academy of Sciences of Ukraine.

Interaction of mixture of amino acids with graphene oxide probed by mass spectrometry

M.V. Kosevich, O.A. Boryak, V.V. Orlov

*B.Verkin Institute for Low Temperature Physics and Engineering of NAS of Ukraine,
47 Nauky Ave., Kharkiv, 61103, Ukraine
mvkosevich@ilt.kharkov.ua*

Study of interactions of graphene oxide (GO) as 2-D nanomaterial with amino acids as components of proteins is of interest in the framework of both nanomaterial-biomolecules complexation and drug delivery problems.

The aim of the present work was probing interactions of a set of amino acids with GO by means of fast atom bombardment (FAB) mass spectrometry. To evaluate the effect of various types of amino acids, an equimolar mixture of four representatives: cysteine (Cys, mw 122), histidine (His, mw 156), phenylalanine (Phe, mw 166), tryptophan (Trp, mw 205) was added to aqueous suspension of GO. Addition of the mixture, as well as of individual amino acids, caused rather rapid coagulation of GO homogeneous dispersion and formation of visible tiny dark flakes (Fig. 1c). The effect was observed starting from total amino acids concentration of 10^{-4} M.

For FAB mass spectrometric measurements the above water dispersion was mixed with glycerol matrix in 1:1 volume ratio and subjected to analysis immediately. The resulting FAB mass spectra (Fig. 1a) contained the peaks of four amino acids in the protonated form. Obtaining of concentration dependences was hampered by the fact that the reliable signals were obtained only at amino acids concentration higher than 10^{-3} M; however, time dependences (Fig. 1a,b) were monitored. Noticeable growth of His \cdot H $^+$ peak relative intensity with time was observed, which may be connected with more efficient His release from the composite as compared to other components. More rapid exhaustion of glycerol matrix in the presence of GO nanomaterial as compared to neat glycerol was observed. As a consequence, the concentration of all amino acids in the liquid phase increased, which was reflected in the increase of the corresponding ion abundances.

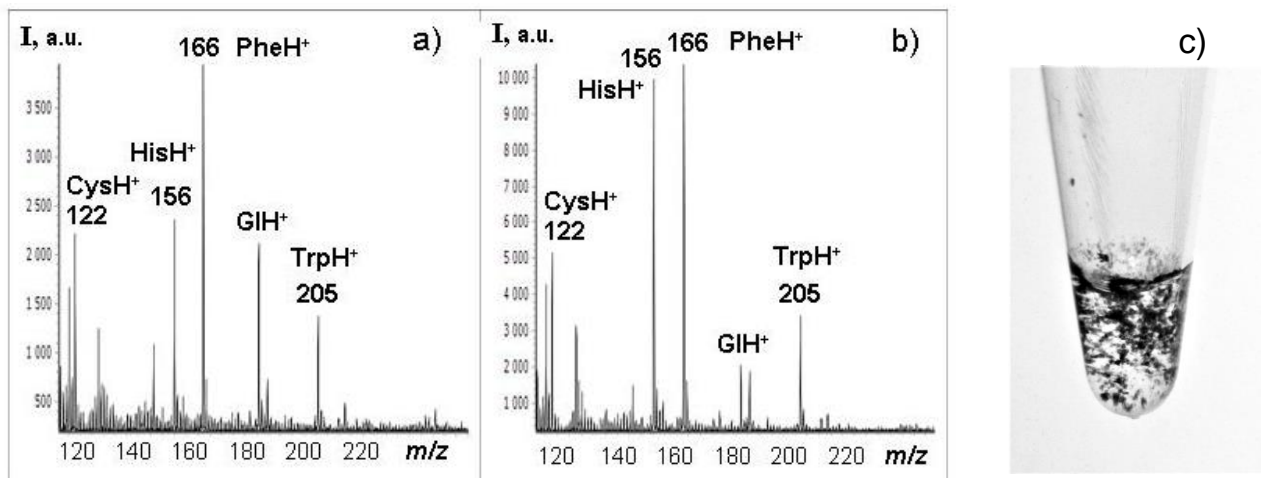


Fig. 1. FAB mass spectra of aqueous dispersion of GO with four amino acids Cys, His, Phe, Trp mixed with glycerol matrix. The spectra are recorded for just prepared mixture (a) and with 15 minutes interval (b). The appearance of (GO+Cys+His+Phe+Trp) aqueous dispersion (c).

The results obtained at the level of amino acids may be of interest for further investigations of GO interactions with peptides and proteins.

The research was supported by the Grant N 0120U100157 of the National Academy of Sciences of Ukraine.

The charge ordering of the heavy doped organic crystals

E.S. Syrkin¹, V.A. Lykah², E.N. Trotskii³

¹ *B.Verkin Institute for Low Temperature Physics and Engineering of NAS of Ukraine,
47 Nauky Ave., Kharkiv, 61103, Ukraine*

² *National Technical University 'Kharkiv Polytechnic Institute', 2 Kyrpychova str., Kharkiv, 61002,
Ukraine*

³ *V.N. Karazin Kharkiv National University, 4 Svobody Sq., Kharkiv, 61022, Ukraine
lykahva@yahoo.com*

The simple model that can describe structure and charge ordering in complex doped organic crystals is proposed. We consider the quasione-dimensional model of pure BEDT-TTF (Bisethylenedithiolo-tetrathiafulvalene) crystal with chains (stacks) of flat molecules [1]. In the heavy doped crystal, small dopant molecules or metal atoms fill every space between large BEDT-TTF molecules in the initial chain. In the real crystal, the picture of the dopants arrangement is much more complicated. The interaction between all molecules is described by the Lennard-Jones potential. It is shown that the small dopant molecules are in the double-well molecular potential along the chain. It is shown that in the case of the electrically neutral molecules at low temperatures there is a fluctuating structural ordering: the small molecules group in pairs near a large molecule, the lattice period in the fluctuation domain doubles. The structure of the boundary between the fluctuation domains is defined. In the case of the molecules charged due to different electronegativity of BEDT-TTF and the dopants, correction to long-range electric dipole interaction makes the system essentially three-dimensional, there is ferroelectric ordering in a chain (a domain in Fig.1) and antiferroelectric one (opposite electric dipole moments in Fig.2) between the chains. Structure of the charge domains and domain boundaries is described.

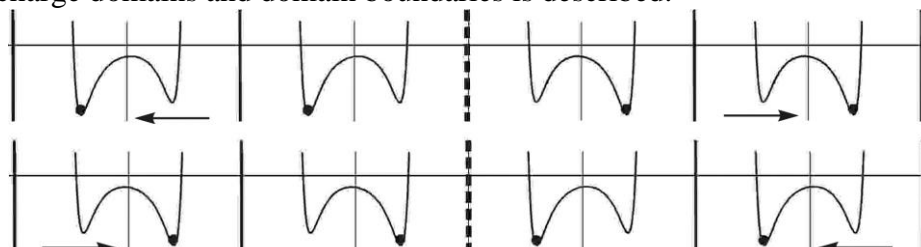


Figure 1. Charge ordering state in the molecular chain with the charge-ordered small dopant (metals). Two domains and two possible domain boundaries (dotted line) are shown. Arrows show electric dipole moments.

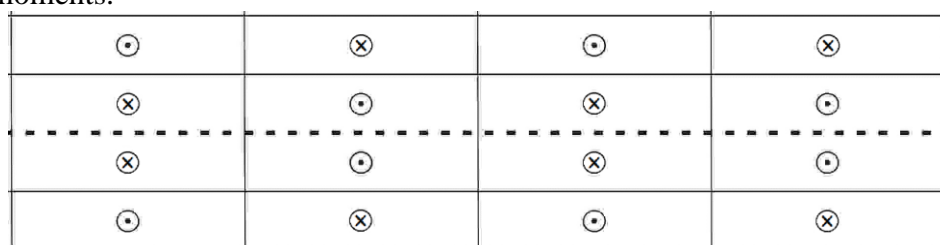


Figure 2. Transverse cross-section of the parallel chains (stacks) in the charge ordered crystal. The rectangles correspond to the BEDT-TTF molecules with real size proportion [2]. The chess packaging of the dipoles' orientation, arrows in Fig. 1, is shown; up (dot) and down (cross) vectors are shown in the chains. One of two possible domain boundaries is shown by dotted line.

[1] F. Kagawa & H. Oike, Adv. Mater. 29, N25, 1601979 (2017).

[2] Y. Misaki, Sci. Technol. Adv. Mater. 10, N2, 024301 (2009).

Molecular dynamics simulation of eosin Y and methylene blue aggregates in a water-ion environment

K.V. Miroshnychenko¹, A.V. Shestopalova^{1,2}

¹*O.Ya. Usikov Institute for Radiophysics and Electronics of NAS of Ukraine,
12 Ac. Proskura st., Kharkiv, 61085, Ukraine*

²*V.N. Karazin Kharkiv National University, 4 Svoboda Sq., Kharkiv, 61022, Ukraine
kateryna.miroshnychenko@gmail.com*

The organic dyes eosin Y (EOS) and methylene blue (MB) are widely used in industry, microscopy, and analytical chemistry. Since these dyes have different absorption ranges, they can be used as competitive ligands in binding assays but the heteroassociation of dyes should be taken into account. The complexation of dyes in a natural water environment can be studied at an atomic detail using modern computer simulation methods.

In this study, the aggregates of EOS and MB were investigated by the molecular dynamics simulation method with explicit water and ions. Four systems were studied: EOS-EOS homodimer, EOS-MB heterodimer, EOS-MB-EOS trimer, and a system consisting of randomly placed 100 EOS and 1 MB molecules in a water-ion environment. The geometries of EOS and MB were optimized in ORCA4.0.1 at B3LYP/ma-def2-SVP and B3LYP/def2-SVP levels, respectively. The initial structures of dimers and trimer were built by the molecular docking method in Autodock Vina. The molecular dynamics simulations were performed in AMBER18 package using gaff2 force field for ligands and SPC/E water model. Na⁺ ions were used as counterions. For each system, a 500 ns production molecular dynamics trajectory was obtained. The most probable structures of complexes were determined by cluster analysis of trajectories.

The homodimer EOS-EOS was stable during the molecular dynamics simulation: one main cluster was obtained, in which xanthene rings were stacked antiparallel with benzene rings pointing into opposite directions. For EOS-MB heterodimer, two main clusters were observed. Both parallel and antiparallel stacking of the xanthene ring of EOS and the phenothiazine ring of MB were possible. In the trajectory of EOS-MB-EOS sandwich trimer, there were two types of complexes: the external xanthene rings were either parallel or antiparallel to each other. During the molecular dynamics simulation of 100 EOS-1MB system, most EOS molecules formed dimers but EOS aggregates of higher order (ternary and quaternary complexes) were also observed. Around MB, the aggregates containing up to 9 EOS molecules were formed, but the maximum stack consisted of three molecules (2 EOS and 1 MB).

The results of the simulation indicate that the formation of different types of aggregates is possible between the EOS and MB in a water-ion environment. These aggregates should be considered upon the simultaneous use of two dyes.

PVA nanofibers containing Ag nanoparticles formed by ultrasonication

V.A. Karachevtsev, A.M. Plokhotnichenko

B.Verkin Institute for Low Temperature Physics and Engineering of NAS of Ukraine,
47 Nauky Ave., Kharkiv, 61103, Ukraine
plokhotnichenko@ilt.kharkov

One of the most promising applications of nanomaterials is preparation of the polymer nanocomposites, in which nanoparticles are incorporated into polymer matrix. In particular polymers are excellent host matrix for different metallic nanoparticles such as silver nanoparticles (AgNPs). It is well known that AgNPs exhibit unique antimicrobial efficiency against a broadspectrum of organisms such as bacteria, and viruses. For last two decades electrospinning has gained considerable attention among researchers who elaborates wound dressing bionanomaterials for biomedicine, fabricate different implants materials or scaffolds in tissue engineering.

In this work, we present the fabrication of nanofibers using electrospinning of polyvinylalcohol (PVA) in which AgNPs were incorporated. The synthesis of the AgNPs occurred from the polymer-encapsulated AgNO_3 precursor material in water with a reduction by an ultrasonication treatment. In this experiment, we used the tip sonication method (4 W, 44 kHz) with the treatment duration up to 90 minutes. Ratio of AgNO_3 :PVA preliminary concentrations in aqueous solutions was 6:80 mg/ml. Absorption spectra of AgNO_3 :PVA aqueous solutions were exploited for the control of the appearance of AgNPs in the suspension, which is characterized by the plasmon band in the violent region. Fig. 1a demonstrates appearance of this band with maximum at around 430-435 nm. From this figure can see that the band intensity enhances with duration of the sonication. Our estimation of AgNPs size from the UV spectrum gave 5-50 nm. Scanning electron microscopy (SEM) image showed relatively uniform and bead-free fibers with smooth surfaces (Fig. 1b). The fibers presented in this Figure have 200-250 nm in diameter. The optimized electrospinning process parameters for producing the solid and continuous PVA:AgNPs nanofibers were 0.25 mL/h feeding rate using a syringe pumping, 15 kV applied voltage, and 7 cm spinneret-to-collector distance.

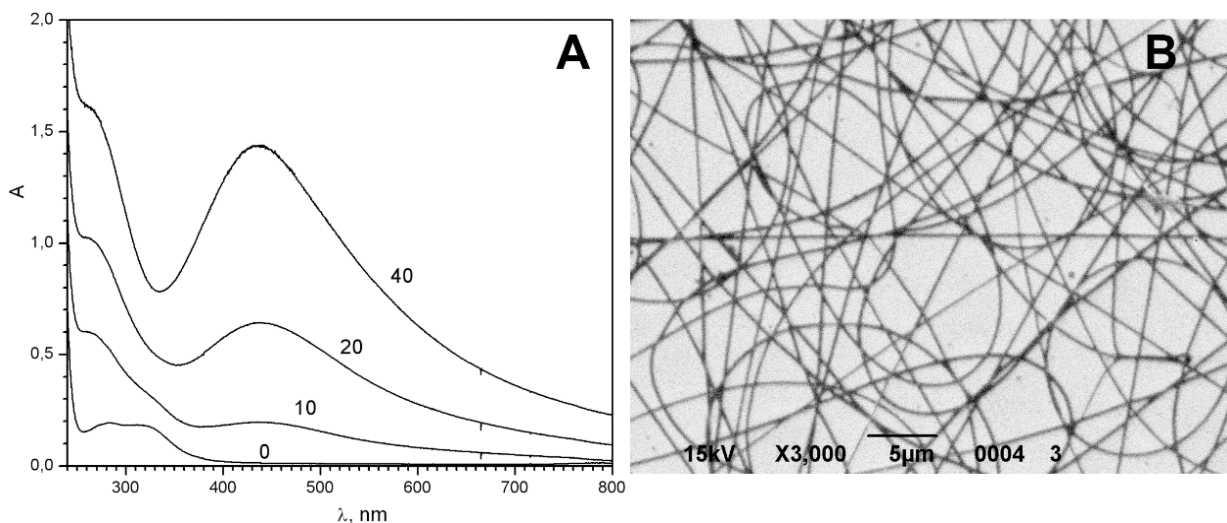


Fig.1. (a) UV-visible absorption spectra of PVA:AgNPs suspensions obtained after different ultrasonication times indicated above the each spectrum (in minutes); (b) SEM images of fabricated PVA:AgNPs nanofibers

This observation indicates that the sonication provides a simple method to obtain different sizes of AgNPs in polymer matrix exploiting for nanoparticle growth and as stabilizing agent, that prevent them from aggregating. Fabricated nanofibers possess effective antimicrobial function and can be used in biomedical area to treatment of different microbial infections.

Förster resonance energy transfer in insulin amyloid fibrils doped by Thioflavin T and novel cyanine dyes

M. Shchuka¹, O. Zhytniakivska¹, A. Kurutos², U. Tarabara¹, K. Vus¹, V. Trusova¹, G. Gorbenko¹

¹*Department of Medical Physics and Biomedical Nanotechnologies, V.N. Karazin Kharkiv National University, 4 Svobody Sq., Kharkiv 61022, Ukraine*

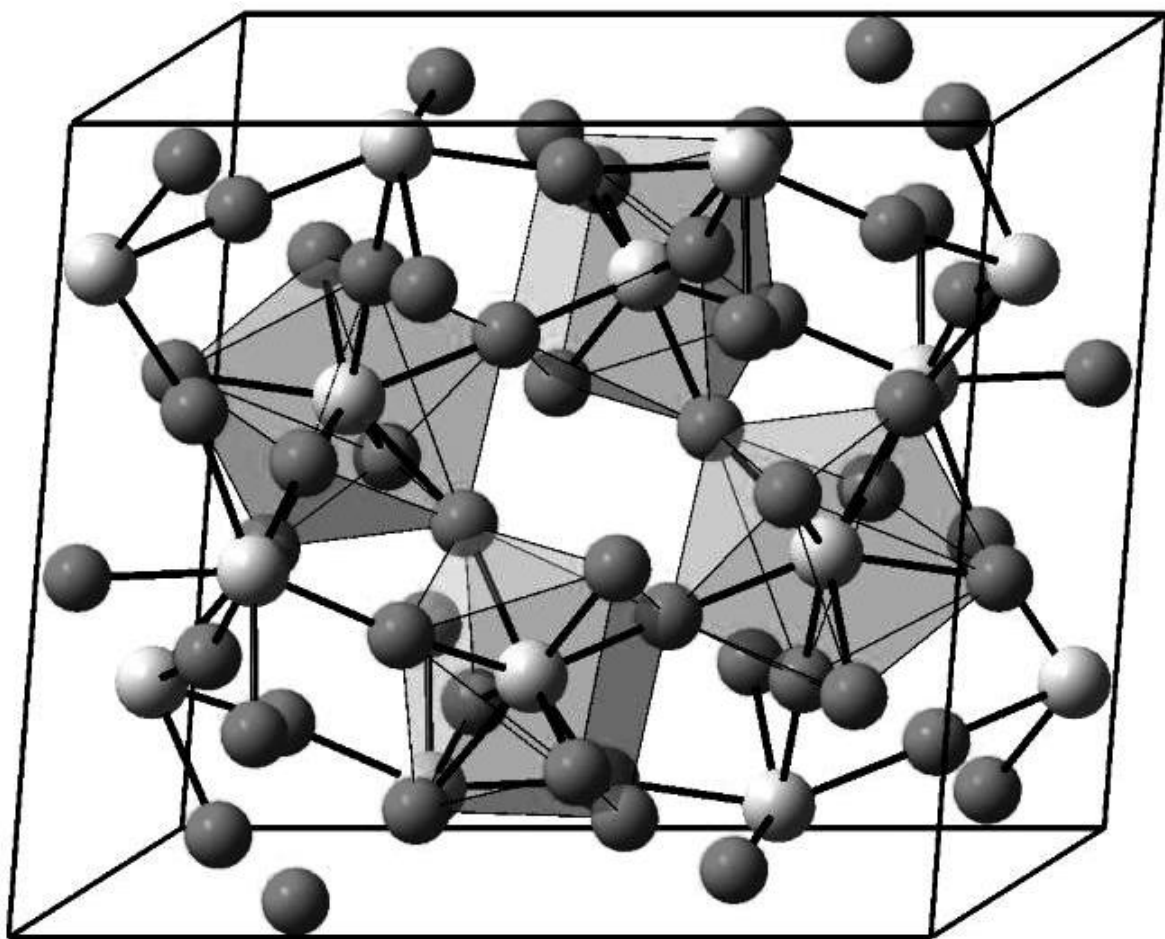
²*Institute of Organic Chemistry with Centre of Phytochemistry, Bulgarian Academy of Sciences, Acad. G. Bonchev str., bl. 9, 1113 Sofia, Bulgaria
mikhail.shchuka@gmail.com*

Förster resonance energy transfer (FRET) is currently widely used for the structural characterization of biological macromolecules and their assemblies, as well as for devising the FRET-based nanosensors. In the present study the FRET between the benzothiazole dye Thioflavin T (ThT) and novel cyanine dyes (referred here as AK3-1, AK3-3, AK3-5, AK3-7, AK3-8 and AK3-11) was employed for detection of the particular class of protein aggregates, amyloid fibrils. In the FRET measurements, the appropriate amounts of the stock solution of cyanine dyes in DMSO were added to the ThT-protein mixtures containing either fibrillar or non-fibrillized insulin and incubated for 5 minutes. The fluorescence spectra were recorded under varying concentrations of cyanines from 460 to 800 nm at the excitation wavelength 440 nm. The addition of cyanines to the ThT-fibrillar insulin mixtures resulted in the intensity decrease at the ThT emission maximum coupled with the appearance of the emission maximum at ~ 670 nm (the intensity of this band was found to depend on the chemical structure of the cyanine dye and its concentration). At the same time, no energy transfer from ThT to cyanines was observed in the presence of the non-fibrillized insulin. By measuring the quenching of ThT fluorescence under varying concentrations of cyanine dyes the efficiency of energy transfer was determined. For the ThT-cyanine donor-acceptor pairs the efficiencies of energy transfer calculated for the fibrillar insulin at the maximum acceptor concentration (1.3 μ M) were found to be 82%, 96%, 87%, 95%, 74% and 49 % for AK3-1, AK3-3, AK3-5, AK3-7, AK3-8 and AK3-11, respectively. Taken into account that for the trimethine cyanines under study (except AK3-11) the dye dimerization and aggregation on the amyloid matrix prevails over the fibril binding of the monomeric dye species and that the lowest energy transfer efficiency was observed for the ThT-AK3-11 pair, we assumed that the energy is transferred from ThT to the dye aggregates. To obtain the quantitative estimates for the donor-acceptor separation, the FRET data were analyzed in terms of the classical expression for the distance dependence of FRET efficiency. The critical distance of energy transfer (R_0), the overlap integral between the donor emission and acceptor absorption spectra (J) and the possible limits for the donor-acceptor distance (R) at different values of the orientation factor κ^2 are presented in Table 1. The obtained distance estimates appeared to be in good agreement with the insulin amyloid fibril geometry.

Table 1. FRET parameters derived for the donor-acceptor pairs

Donor-acceptor pair	R_0 , nm	J , $M^{-1}cm^{-1}nm^4$	R , nm*			
			$\kappa^2 = 0.01$	$\kappa^2 = 0.67$	$\kappa^2 = 1$	$\kappa^2 = 4$
ThT-AK3-1	3.8	4.38×10^{15}	1.4	2.9	3.9	3.1
ThT-AK3-3	3.7	3.75×10^{15}	1.1	2.1	2.9	2.3
ThT-AK3-5	3.6	3.49×10^{15}	1.3	2.7	3.6	2.8
ThT-AK3-7	3.4	2.75×10^{15}	1.1	2.2	3.0	2.3
ThT-AK3-8	3.8	4.23×10^{15}	1.6	3.1	4.2	3.3
ThT-AK3-11	3.8	4.26×10^{15}	1.9	3.7	4.9	4.0

To summarize, the present study has demonstrated that ThT-cyanine dye chromophore systems can be employed for the identification and characterization of amyloid fibrils.



MATERIALS SCIENCE

Hydrogen storage properties, structural analysis, elastic and electronic properties of K_2PdH_4

S. Al¹, C. Kurkcu²

¹*Department of Environmental Protection Technologies, Vocational School, Izmir Democracy University, 35140, Izmir, Turkey*

²*Department of Electronics and Automation, Kırşehir Ahi Evran University, Kırşehir, Turkey
selgin.al@idu.edu.tr*

Density functional theory is adopted to study phase transitions, structural, elastic, and electronic properties of hydrogen storage K_2PdH_4 thoroughly. Perdew-Burke-Ernzerhof, generalised gradient approximation (PBE-GGA) is utilized for the exchange correlation potential. The package of SIESTA is used to carry out the calculations. Firstly, structural evolution of K_2PdH_4 is investigated under high pressure along with the hydrogen storage properties. Gravimetric hydrogen density and hydrogen desorption temperature of K_2PdH_4 is computed. According to high pressure investigations, a phase transition from I4mmm tetragonal structure to Immm orthorhombic structure is observed at 20 GPa. Subsequently, the density of states and electronic band structures are obtained for each phase. Mechanical stabilities of each phase are investigated. Elastic constants and Born stability criteria are used to evaluate mechanical stabilities which are also correlated the material's failure. Mechanical properties of solid state hydrogen storage materials are crucial in terms of handling the material especially for portable applications. Bonding properties, ductile and brittle behaviour of K_2PdH_4 for each phase are examined using Cauchy pressure, Poisson's ratio, Pugh's criteria, Bulk and Shear modulus in details.

Phase transitions, elastic and electronic properties of hydrogen storage Na_2PdH_4

S. Al¹, C. Kurkcu²

¹*Department of Environmental Protection Technologies, Vocational School, Izmir Democracy University, 35140, Izmir, Turkey*

²*Department of Electronics and Automation, Kırşehir Ahi Evran University, Kırşehir, Turkey
selgin.al@idu.edu.tr*

Hydrogen can be absorbed by some materials at specific pressures and temperatures. This is extremely important in terms of creating carbon free and sustainable society. Hydrides are good candidates to fulfil these aims. Electronic and magnetic properties of hydrides are investigated. This study considers Na_2PdH_4 as a solid storage of hydrogen. Hydrogen is highly soluble in palladium and can be stored in large amount at ambient conditions. The structural evolution, electronic and elastic properties of Na_2PdH_4 has been investigated by means of density functional theory. The package of SIESTA is used with the generalized gradient approximation (GGA) for the exchange-correlation functional and norm-conserving Troullier-Martins pseudopotentials. High pressure computations have been carried out to reveal phase transitions. Na_2PdH_4 is transformed from I_4/mmm tetragonal structure to $Immm$ orthorhombic structure at 100 GPa. The electronic band structures and density of states are obtained for both phases. Mechanical stabilities are analysed using elastic constants. Moreover, several parameters such as Young modulus, Shear modulus and B/G ratios are obtained and discussed.

Lattice softening at the electric field and pressure-induced Mott insulator to metal transitions

D. Babich, L. Cario, B. Corraze, C. Adda, J. Tranchant, M.- P. Besland, J.-Y. Mévellec, P. Bertoncini, B. Humbert, E .Janod

*Institut des Matériaux Jean Rouxel, Université de Nantes – CNRS, 44322 Nantes, France
Etienne.Janod@cnrs-imn.fr*

Mott insulators are a class of strongly correlated materials with emergent properties important for modern electronics applications^[1]. The key property for potential application is the Mott insulator to metal transition (IMT). This IMT appears at equilibrium by submitting Mott insulators to various external perturbations such as pressure or electronic doping. However, the breakthrough concerning applications comes from recent discoveries showing the possibility of inducing out-of-equilibrium Mott IMTs thanks to light or electrical pulses which generate highly excited electronic states. On the theoretical side, the full description of Mott IMTs is a long-standing problem. At equilibrium, the evolution of most of the electronic properties at the Mott IMT can be well captured by the Hubbard Hamiltonian, a purely electronic model ignoring the response of the lattice.[2,3]. Conversely the description of out-of-equilibrium Mott IMTs is still a major theoretical challenge because of complex many-body effects and constitutes a very active field of research at present [4].

The paradigmatic example of Mott insulator is the $(V_{1-x}Cr_x)_2O_3$ system. In this compound, an IMT can be induced at equilibrium by physical or chemical pressure and out-of-equilibrium by strong electronic excitation [5,6]. We have recently demonstrated that a local lattice contraction accompanies the out-of-equilibrium Mott IMT caused by an electric field [7], which is reminiscent of $\approx 1\%$ volume drop observed at the Mott IMT observed at equilibrium under pressure [6].

During the talk, we will present Raman studies on $(V_{1-x}Cr_x)_2O_3$, showing that, despite the lattice contraction, the Mott IMT is associated to a softening of elastic constants, both at equilibrium (chemical or physical pressure-induced IMT) and out-of-equilibrium (E-field-induced IMT). These results show that the minimal model to fully describe the Mott IMT in solids is a Hubbard model on a compressible lattice. Most importantly, this work also illustrates how the degree of the electronic delocalization can control the lattice stiffness in strongly correlated systems, [7,8] both at and out-of thermodynamic equilibrium.

- [1] E. Janod et al., *Adv. Funct. Mater.* 2015, 25, 6287.
- [2] V. I. Anisimov, J. Zaanen, O. K. Andersen, *Phys. Rev. B* 1991, 44, 943.
- [3] J. Hubbard, *Proceedings of the Royal Society of London A: Mathematical, Physical and Engineering Sciences* 1964, 281, 401
- [4] Aoki et al, *Reviews of Modern Physics*, 2014, Vol. 86, Iss. 2
- [5] M. Querré et al., *Thin Solid Films* 2016, 617, Part B, 56.
- [6] D. B. McWhan, J. P. Remeika, *Phys. Rev. B* 1970, 2, 3734.
- [6] D. Babich et al., submitted to *Nature Commun.* (2021).
- [7] S. Populoh, P. Wzietek, R. Gohier, P. Metcalf, *Phys. Rev. B* 2011, 84, 075158.
- [8] I. Leonov, V. I. Anisimov, D. Vollhardt, *Phys. Rev. B* 2015, 91, 195115.

Hemispherical microwave X-band Fabry-Perot resonator for determining in wide band of dielectric parameters of solid materials

A. Breslavets¹, Z. Eremenko¹, O. Voitovich¹, G. Rudnev¹, Zhu Gang², Li Rong²

¹*O.Ya. Usikov Institute for Radiophysics and Electronics of NAS of Ukraine,
12 Ac. Proskura St., Kharkiv, 61000, Ukraine*

²*Anhui Huadong Photoelectric Technology Institute, Ltd Wuhu, China
zoya.eremenko@gmail.com*

Low loss dielectric materials are widely used in microwave circuit components. Knowing the exact complex permittivity values of solid dielectrics is essentially needed for accurate design of passive and active microwave devices. There are many microwave resonant and waveguide methods for measuring dielectric parameters of solid materials at microwaves. Open resonator (OR) techniques are well known and common, because they provide an accurate measurement of the dielectric properties of low loss materials at microwaves. Fabry-Perot ORs with semispherical mirrors have a very high Q factor in comparison with cavity resonators at the same frequencies, since they use large confocal concave mirrors to form a field maximum region in the form of a Gaussian beam with a bouncing ball effect [1-2].

A computer simulation of the OR was carried out using the CST Microwave Studio 2019 program. We found an original solution to the problem of determining the dielectric constant of samples of solid materials in a given range from 1.5 to 20 units using an OR with maximum resonance frequency sensitivity for small samples (50×5 mm). The diameter of the OR spherical mirror is 167 mm, its depth is 50 mm, the diameter of the flat mirror is 50 mm.

It was found that for an X-band (7 - 12 GHz) OR with a working mode of TEM_{005} (where indices are azimuthal, radial and axial ones) the frequency range of the working mode in the presence of different dielectrics (in a given range of variation of the dielectric constant) placed in the OR is quite wide – approximately 1.4 GHz. This indicates a high resolution of measurements of the dielectric constant of various solid dielectric materials. At the same time, the probability of obtaining erroneous or unreliable results is significantly reduced due to the presence of only 3 resonances in working range. The calculated loaded Q-factor for a resonator with one spherical mirror with an operating mode TEM_{005} is not high, but it is quite sufficient to determine the dielectric constant of a dielectric sample with high resonance frequency sensitivity. From the values of the loaded Q-factor it is possible to obtain the values of the intrinsic Q-factor, which is necessary to determine the tangent of the dielectric loss angle of the material.

Drawings were developed, a calculated hemispherical OR was manufactured by our colleagues from China, and an experiment was carried out using various samples of dielectrics. It was found that the resonance frequencies of OR practically coincide according to the data from the CST calculation and the experiment in Wuhu (China). For example, the average difference in resonance frequency is 7 MHz for air and 20 MHz for a single crystal of aluminum. The experimental loaded Q-factors of OR at resonant frequencies for air are much higher than the calculated ones, for a sapphire single crystal sample they are slightly lower than the calculated ones. Thus, the experiment performed showed that the calculation for CST corresponds to the experiment.

- [1] R. Olmi, S. Priori, A. Toccafondi and F. Puggelli "An Open-Resonator Sensor for Measuring the Dielectric Properties of Antarctic Ice", Sensors, 19(9), 13 p. (2019).
- [2] J. Choi and W. Seo "Measurements of Dielectric Properties at Ka-Band Using a Fabry-Perot Hemispherical Open Resonator", International Journal of Infrared and Millimeter Waves 22, pp. 1837-1851 (2001).

Synchrotron diffraction study of the high-pressure behaviour of the multiferroic $\text{BiFe}_{0.5}\text{Sc}_{0.5}\text{O}_3$ perovskite

J.P. Cardoso¹, D.D. Khalyavin², D. Delmonte³, E. Gilioli³, A. Barbier⁴, M.R. Soares¹, J.M. Vieira¹, A.N. Salak¹

¹Department of Materials and Ceramics Engineering and CICECO - Aveiro Institute of Materials, 3810-193 Aveiro, Portugal

²ISIS Facility, Rutherford Appleton Laboratory, Chilton, Didcot, OX11 0QX, UK

³Institute of Materials for Electronics and Magnetism, 43124 Parma, Italy

⁴SPEC, CEA, CNRS, Université Paris-Saclay, CEA-Saclay, 91191 Gif-sur-Yvette Cedex, France
joaopcardoso@ua.pt

The phenomenon of conversion polymorphism, implying an irreversible transformation of one structural phase to another through an annealing, was first reported in the BiFeO_3 - BiFeScO_3 system [1]. Solid solutions of this system are processed via high-pressure synthesis, allowing to stabilize perovskite phases at ambient conditions. BiFeO_3 is a multiferroic perovskite produced via conventional methods. It is a cycloidal antiferromagnet with a polar rhombohedral structure of the $R\bar{3}c$ space group [2]. A substitution of Fe^{3+} by the large Sc^{3+} from BiScO_3 results in a formation of novel structural phases with new combinations of magnetic and ferroelectric orderings.

The equimolar composition of the system, $\text{BiFe}_{0.5}\text{Sc}_{0.5}\text{O}_3$, exhibits a unique path upon annealing. On heating, it irreversibly transforms from the as prepared antipolar $Pnma$ polymorph to the high temperature $R\bar{3}c$ one, isostructural to that of the endmember BiFeO_3 . On cooling, the high-

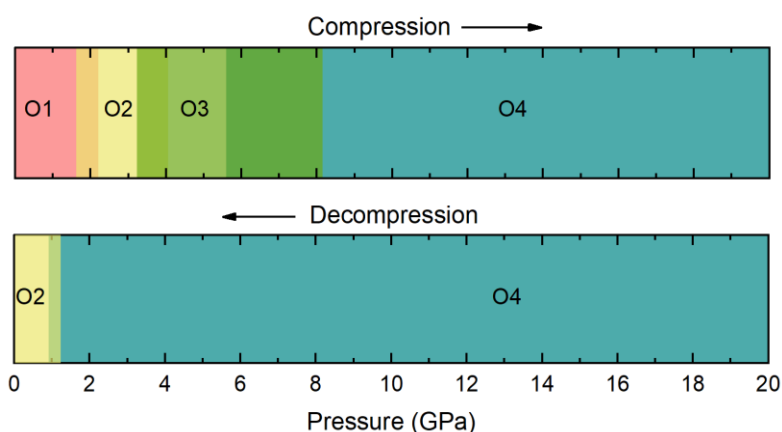


Fig.1. Schematic presentation of the pressure-induced structural transformations in the polar orthorhombic polymorph of $\text{BiFe}_{0.5}\text{Sc}_{0.5}\text{O}_3$ upon compression (top panel) and upon decompression (bottom panel). The phases identified correspond to: O1—orthorhombic polar $Ima2$; O2—orthorhombic antipolar $Pnma$; O3—possibly a novel orthorhombic phase; O4—possibly nonpolar orthorhombic $Pnma$.

will provide useful information to fabricate them in thin film form as well as to further study these phases using first principles calculations and neutron diffraction.

[1] D.D. Khalyavin, A.N. Salak, E.L. Fertman, O.V. Kotlyar, E. Eardley, N.M. Olekhovich, A.V. Pushkarev, Y.V. Radyush, A.V. Fedorchenco, V.A. Desnenko, P. Manuel, L. Ding, E. Čižmár and A. Feher, Chem. Commun. 55, 4683 (2019).

[2] M. Čebela, D. Zagorac, K. Batalović, J. Radaković, B. Stojadinović, V. Spasojević and R. Hercigonja, Ceram. Int. 43, 1256 (2017).

[3] D.D. Khalyavin, A.N. Salak, N.M. Olekhovich, A.V. Pushkarev, Y.V. Radyush, P. Manuel, I.P. Raevski, M.L. Zheludkevich and M.G.S. Ferreira, Phys Rev. B 89, 174414 (2014).

temperature polymorph transforms into the orthorhombic polar $Ima2$ modification [3]. To better understand this transformation path and explore a possibility to stabilize new phases via thermal and pressure cycling, we assessed the behaviour of $\text{BiFe}_{0.5}\text{Sc}_{0.5}\text{O}_3$ under pressure using in situ X-ray synchrotron diffraction. We explored stability ranges of different phases under pressure up to 9 GPa. The collected data revealed four distinct orthorhombic phases, denoted as O₁-O₄ in Fig. 1, with the phase O₄ having the largest stability range. The determined structural parameters and stability ranges of these phases

Nanostructures on the (001) surface of strontium titanate

V.O. Hamalii, N.V. Krainyukova

B.Verkin Institute for Low Temperature Physics and Engineering of NAS of Ukraine,
47 Nauky Ave., Kharkiv, 61103, Ukraine
gamalii@ilt.kharkov.ua

Two types of nanostructures formed on the atomically smooth single crystal (001) surface of SrTiO_3 (STO) were studied by means of the reflection high-energy electron diffraction (RHEED) method in the wide temperature range 5–300 K [1,2]. One appears due to the regular steps on a surface, the other is a system of protruding bumps on a single crystal surface emerging at a certain surface treatment.

By changing the miscut angle between the real surface and crystallographic planes one can create a regular sequence of steps on an atomically smooth single crystal surface. At the cut angle ~ 0.9 deg the diffraction patterns are close to ideal. We have found in this case applying the Selyakov–Scherrer formula (SSF) to reflections for the deepest electron penetration in a crystal (largest angles) that the regions of coherent scattering coincide with a step width ≈ 250 Å if their height is equal to the lattice parameter ~ 3.9 Å (L_{\max} in Fig. 1). But for smaller angles such regions are about twice shorter than was ascribed to the misfit dislocations formed in this case (Fig. 1). For a miscut angle ~ 7 deg the diffraction patterns formed for the azimuthal direction of incident electrons along the step edges exhibit a new type of order with ‘superstructural’ reflections separated by $1/L$, where L coincides with a step width ~ 30 Å in this case (Fig. 2).

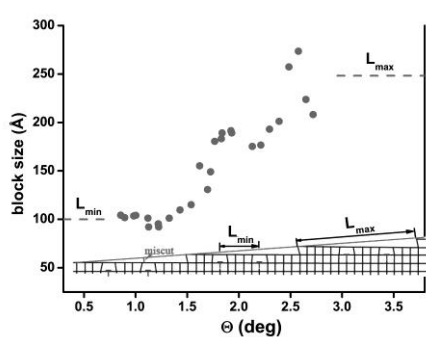


Fig. 1

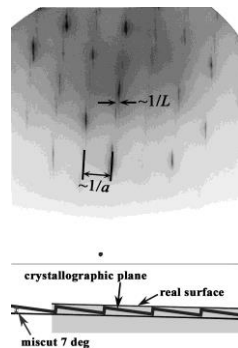


Fig. 2

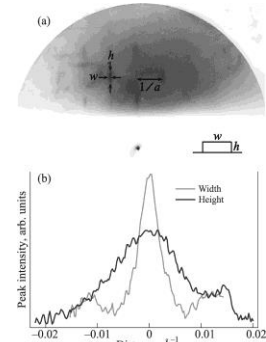


Fig. 3

Using aggressive solvents (such as acetone) in the surface treatment process, we observed the formation of small protruding bumps (Fig. 3). Both the bump width $w \approx 245$ Å and their height $h \approx 75$ Å were calculated applying the SSF. Evidently, these sizes depend on the etching degree. The protrusions are formed on the single crystal surface and therefore they all have the same orientations. They can be a qualitative alternative to systems of ferroelectric nanoparticles, which are differently ordered [3].

The ordered nanostructures on the single crystal surface of STO, as well as the ability to control their properties, open new prospects in engineering many devices such as high-storage-density capacitors, for example, dynamic random access memory (DRAM), as well as sensors and nanotransducers.

- [1] N.V. Krainyukova, V.O. Hamalii, A.V. Peschanskii, A.I. Popov, and E.A. Kotomin, *Low Temp. Phys.* 46, 1170 (2020).
- [2] N.V. Krainyukova, V.O. Hamalii, A.V. Peschanskii, A.I. Popov, and E.A. Kotomin, *Low Temp. Phys.* 46, 740 (2020).
- [3] D. Lee, H. Lu, Y. Gu, S.-Y. Choi, S.-D. Li, S. Ryu, T. R. Paudel, K. Song, E. Mikheev, S. Lee, S. Stemmer, D. A. Tenne, S. H. Oh, E. Y. Tsymbal, X. Wu, L.-Q. Chen, A. Gruverman, and C. B. Eom, *Science* 349, 1314 (2015).

Optical response of novel structures to detect approaching vehicles

L. Illyashenko

*Kharkiv National University of Radio Electronics,
14 Nauky Ave., Kharkiv, 61166, Ukraine
mila.illyashenko@gmail.com*

During the last years lots of investigations in academic world, research and industry were done to develop novel materials, in particular those, which may protect vehicles from extreme radiation and temperature variations. Electronic systems must be protected from extreme heat and cold, while storage containers holding liquid propellants must be shielded from solar radiation. From another side it is difficult to detect approaching vehicle, when coating of vehicle is done from novel material, which is not investigated well enough. The goal of this work is to develop methods and techniques to investigate optical response of novel nanostructures with purpose to use these achievements in the device design for detection of approaching vehicles.

Materials for the vehicle coating may be artificial. Those are a class of materials possibly with tunable properties [1-3]. Artificial materials are possible to be produced by using alloys or mixture of several materials, including those with ordered arrangement of elements, so that new artificial material will have such properties, which do not exist in nature. If the materials and the geometries of particles are optimally selected, the resulting novel material for coatings of vehicles could be more mechanically robust, optically reflective, thermally insulating and electrically conductive. This work mostly focuses on aspects of optical reflectivity of resulting nanomaterials. To study optical reflectivity spectral Boundary Integral Equation method [4] is used in conjunction with conformal mapping method for parametrization of the element cross sections, with analytical regularization based on singularity subtraction for accurate evaluation of resulting singular integrals, and with Fast Fourier Transform for fast numerics in addition to high accuracy.

The results provide insight into fundamental aspects of optical reflectivity for such systems of particles that act collectively. While the overall objective is to understand how different geometries and materials affect the optical characteristics of resulted coating material not only for aircrafts, but also for watercrafts, as well as for spacecrafts, this research could also have beneficial applications on Earth. Since the coatings have specific optical properties, they may also be used as coatings for buildings to decrease their energy consumption for heating and air-conditioning.

Acknowledgements: Author expresses her great appreciation to Professor Monakov V.P. for his valuable and constructive suggestions during the planning and development of this research work. His willingness to give his time so generously has been very much appreciated. Author would like to express her deep gratitude to Academic Yakaovenko V.M. for his patient guidance and assistance, for his advices and enthusiastic encouragement.

- [1] J.D. Joannopoulos, S.G. Johnson, J.N. Winn, R.D. Meade, Photonic Crystals: Molding the Flow of Light, 2nd Edition, Princeton University Press, p.304, (2008).
- [2] W. Cai, V. Shalaev, Optical Metamaterials: Fundamentals and Applications, New York; London: Springer, p. 197, (2009).
- [3] S.A. Maier, Plasmonics: Fundamentals and Applications, New York: Springer, p. 245, (2007)
- [4] G.C. Hsiao, O. Steinbach, and W.L. Wendland, Boundary Element Methods: Foundation and Error Analysis, vol. Encyclopedia of Computational Mechanics, John Wiley & Sons, p. 62, 2018.

Influence of aluminum ion substitution on EPR spectra of lithium ferrites

L. Kaykan¹, J. Mazurenko², N.V. Ostapovych², I.R. Pavliuk²

¹*G.V. Kurdyumov Institute for Metal Physics, N.A.S. of Ukraine, 36 Academician Vernadsky Boulevard, UA-03142*

²*Ivano-Frankivsk National Medical University, Halytska Str. 2, Ivano-Frankivsk, 76018, Ukraine
larysa.kaykan@gmail.com*

Lithium and substituted lithium ferrites play an important role in microwave technology and memory cells due to the high Curie temperature, high saturation magnetization, excellent hysteresis loops and low voltage sensitivity [1-3]. In addition, lithium ferrites do not contain expensive ingredients [4]. Lithium ferrites behave like an n-type semiconductor with an inverse spinel structure and have a high electrical resistance ($10^5 - 10^6 \text{ Ohm}\cdot\text{cm}$) and high Curie temperature ($640 - 680 {}^\circ\text{C}$), and can be used in gas sensors [5].

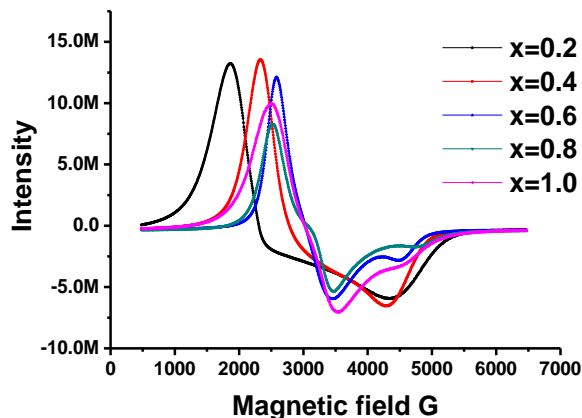


Fig.1. EPR spectra of Aluminum-substituted lithium spinels of general composition
 $\text{Li}_{0.5}\text{Fe}_{2.5-x}\text{Al}_x\text{O}_4$

In a number of works on the basis of X-ray studies it was found that aluminum ions, having an advantage to octahedral positions in the presence of lithium can occupy also tetrahedral positions. However, the exact location of lithium ions by the X-ray method is problematic due to the small number of electrons of the latter, therefore, for the most part, the positions of lithium ions are set indirectly. The use of EPR spectroscopy makes it possible to more accurately determine the distribution of cations in the studied systems, because it is more sensitive than the X-ray method. In addition, in the lithium-containing EPR structures, the Al^{3+} spectra in the 16d positions of the spinel were interpreted from the position of the relaxation mechanism. As can be seen from Figure 1, two additional weak signals corresponding to the localization of Al^{3+} ions near oxygen vacancies and Al^{3+} ions in a lithium-enriched environment were registered. These Al^{3+} defects are sensitive to the Li/Al ratio. It is shown that EPR studies of Al^{3+} make it possible to more accurately determine the cationic distribution in lithium spinels replaced by aluminum ions.

- [1] S. Gul, M. A. Yousuf, A. Anwar, and M. Shahid, Ceramics International 46, 14195 (2020).
- [2] H. Sartaj Aziz, R. Ali Khan, and A. Rahman Khan, Materials Science and Engineering: B 243, 47 (2019).
- [3] L. Kaykan, A. K. Sijo, A. Źywczak, and K. Bandura, Appl Nanosci 10, 4577 (2020).
- [4] K. Malaie, Z. Heydari, and M. R. Ganjali, International Journal of Hydrogen Energy 46, 3510 (2021).
- [5] K. Tian, W. Zhang, S.-N. Sun, and H.-Y. Li, Sensors and Actuators B: Chemical 329, 129076 (2021).

Stability of $\text{Y}_2\text{Ti}_2\text{O}_7$ in ODS steels under swift heavy ions irradiation

E.A. Korneeva¹, A. Ibrayeva², J. O'Connell³, A.S. Sohatsky¹, V.A. Skuratov¹

¹*Joint Institute for Nuclear Research,*

6 Joliot-Curie, Dubna, 141980, Russia

²*Nur-Sultan Branch of Institute of Nuclear Physics,*

2/1 Abylay Khan Ave, Nur-Sultan, 010000, Kazakhstan

³*Centre for HRTEM, Nelson Mandela University,*

University Way, Summerstrand, Port Elizabeth, 6001, South Africa

e-mail: ekorneeva@jinr.ru

Nowadays development of the nuclear industry meets with new challenges to follow modern requirements for safety, sustainability and effectiveness. Therefore, one of the key-note topic in radiation material science is an extensive research of candidate materials for the next-generation fission and future fusion reactors, that can sustain high doses and high temperatures. Oxide dispersion strengthened (ODS) steels are considered as promising constructive materials for fuel claddings of Gen IV nuclear reactors [1]. Nanosized thermostable particles including pyrochlore $\text{Y}_2\text{Ti}_2\text{O}_7$ embedded in the ferritic matrix can act as a sink for radiation defects and assist for effective capture of gas bubbles and helium. As a result ODS steels demonstrate significant values of high temperature creep strength and radiation resistance to void swelling under neutron irradiation in comparison with conventional reactor steels [2]. Nowadays the most of literature data devoted to the examination of ODS radiation stability under neutron and low energy ion irradiation didn't show any significant effect on the materials structure [3,4]. At the same time the critical examination of structure stability of nanoparticles in ODS alloys under fission fragment (FF) irradiation is required because high levels of electronic excitation during FF impact can lead to severe structure transformation of dielectric materials up to complete amorphization [5,6]. Yet another essential question is possible influence of surrounding metallic matrix on the defect formation processes in nanoparticles during irradiation.

In present work ODS steels were irradiated by swift heavy ions (SHI) irradiation simulating FF impact. It was shown that during irradiation the latent tracks can form in the structure of $\text{Y}_2\text{Ti}_2\text{O}_7$ (Fig.1). The track size diameter dependence on the electronic stopping power and threshold stopping power for latent track formation were found. Additional irradiation experiments on individual $\text{Y}_2\text{Ti}_2\text{O}_7$ particles were made for verification of the thermal spike model relevance for describing the process of the track formation.

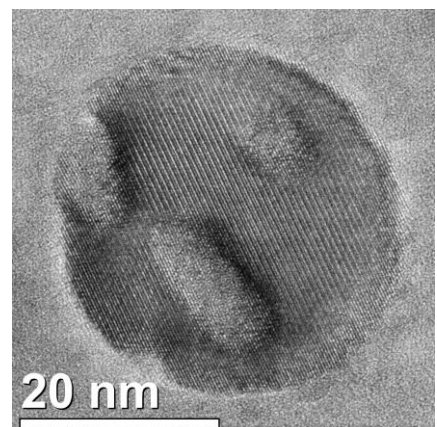


Fig.1 TEM micrograph of latent tracks in $\text{Y}_2\text{Ti}_2\text{O}_7$ in EP450 ODS steel irradiated with $1 \times 10^{12} \text{ cm}^{-2}$ of 167 MeV Xe ions.

- [1] De Carlan, Y., Bechade, J.L., Dubuisson, P., Seran, J.L., Billot, P., Bougault, A., Cozzika, T., Doriot, S., Hamon, D., Henry, J., Ratti, M., J. Nucl. Mater. 386, 430-432 (2009).
- [2] Alamo A, Bertin J.L., Shamardin V.K., Wident P. J. Nucl. Mater. 367, 54-59 (2007).
- [3] He J., Wan F., Sridharan K., Allen T.R., Certain A., Shutthanandan V., Wu Y.Q. J. Nucl. Mater. 455 (1-3), 41-45 (2014).
- [4] Miller M.K., Hoelzer D.T. J. Nucl. Mater. 418(1-3), 307-310 (2011).
- [5] Moll S., Sattonnay G., Thomé L., Jagielski J., Legros C., Monnet I. Nucl. Instr. Meth. B 268 (19), 2933-2936 (2010).
- [6] Monnet I., Grygiel C., Lescoat M.L., Ribis, J. J. Nucl. Mater. 424 (1-3), 12-16 (2012).

CH₄ trapping ability of double vacancy graphene Cu-embedded surface: A DFT study

H. Küçük

Gazi University, Department of Physics, Emniyet Mahallesi, 06500, Teknikokullar, Ankara, Turkey
hilalkucuk@gazi.edu.tr

The detection of methane gas (CH₄) plays a crucial role in developing industry and technology because it causes the greenhouse effect and is getting higher hazardous level the atmosphere day by day that might be the reason for suffocation. The usage of two-dimensional (2D) material is quite wide in order to investigate active single-atom catalysts (SACs). The modification (doping, embedding, decorating) on the surface of 2D materials can provide a significant change in structural, electronic and magnetic behavior of surface and also the detection of dangerous gases. In this study, graphene is modified with double vacancy (DV) embedding with transition metal (Cu) and the adsorption of CH₄ were investigated on surface using Density-functional theory calculations (DFT) in the Van der Waals interactions with DFT-D2 the method of Grimme through Quantum ESPRESSO input generator. The optimum configuration over the Cu-embedded graphene surface is geometrically optimized, and adsorption energy, adsorption distance, bader charge transfer, partial density of states (pDOS) analysis is calculated and reported. The results indicate that CH₄ adsorption on SV modified graphene was the most stable, with an adsorption energy of 0.21 eV and an equilibrium distance of 2.61 Å between CH₄ and graphene surface.

Keywords: The adsorption of CH₄, Graphene Surface with vacancy modification, Binding Energy, Adsorption Energy, Density Functional Theory.

Influence of extreme factors (low temperatures, corpuscular and electromagnetic radiation) on the mechanical properties of polyimide Kapton H films of different thicknesses

V.A. Lototskaya¹, L.F. Yakovenko¹, E.N. Alekseenko¹, N.I. Velichko¹, G.I. Saltevskiy¹, I.P. Zaritskiy¹, Yu.S. Doronin¹, A.A. Tkachenko¹, V.V. Abraimov², W.Z. Shao²

¹*B.Verkin Institute for Low Temperature Physics and Engineering of NAS of Ukraine,
47 Nauky Ave., Kharkiv, 61103, Ukraine*

²*Harbin Institute of Technology, Harbin, the People's Republic of China
lototskaya@ilt.kharkov.ua*

Mechanical characteristics (limit of forced elasticity σ_{forc} , rupture stress σ_r , relative deformation before rupture ε_r and its components) under conditions of uniaxial tension along the direction of drawing of Kapton H polyimide films (made in China) of different thicknesses (25, 75 and 125 μm) were studied:

1) in the initial state in the temperature range (4.2-293 K) and deformation rates (10^{-5} - 10^{-3} s^{-1});

2) after irradiation separately by the fluxes of corpuscular radiation of the Earth's radiation belts (protons and electrons) and the electromagnetic radiation of the transatmospheric Sun, simulated in the laboratory, at room temperature and a strain rate of 10^{-4} s^{-1} .

It was discovered, that the forced-elastic state remains in all deformation conditions in films as in initial state so as after irradiation - $\sigma_{\text{force}} < \sigma_r$. The deformation curves have two or three stages, depending on the thickness. Three stages of deformation are characteristic of the most amorphous film 25 μm thick.

The reserve of elasticity with a decrease in temperature significantly depends on the thickness of the initial film, after irradiation - on the type of exposure and thickness.

A sharp decrease in ε_r occurs in films: 125 μm thick - at 77 K, 75 μm thick - at 4.2 K. Two variants of deformation curves are possible in a 25 μm thick film at 4.2 K: with a short nonlinear stage or with a long one proceeding jumpily. The working surface of the samples that have undergone jump deformation is covered with a deformation relief, partially representing a delayed highly elastic deformation.

The σ_{forc} limit is most sensitive to the strain rate. The nature of the strain rate sensitivity $\sigma_{\text{forc}}(\dot{\varepsilon})$ depends on the temperature and film thickness. The change to the opposite in the character of $\sigma_{\text{forc}}(\dot{\varepsilon})$ and $\sigma_r(\dot{\varepsilon})$ with a decrease in temperature to 4.2 K in 75 and 125 thick films was found for a first time. Change in the character of $\sigma_{\text{forc}}(\dot{\varepsilon})$ is not observed in 25 μm thick film which retains the maximum reserve of elasticity at 4.2 K.

Irradiation with protons leads to the most significant changes of all mechanical characteristics. An increase in the forced elasticity limit σ_{forc} , decrease in the rupture stress σ_r and a decrease in the relative deformation before rupture ε_r are observed. All changes of characteristics increase with decreasing film thickness.

After all types of irradiation, there is a redistribution of the values of the contributions of highly elastic deformation reversible at the test temperature, delayed highly elastic deformation and irreversible deformation into the relative deformation before rupture ε_r . The nature and magnitude of the redistribution depend on the type of exposure.

Irradiation with protons leads to a significant decrease in the contribution of irreversible deformation to ε_r . The amount of reduction increases with decreasing thickness. At the same time, the elasticity of the film is preserved.

On the contrary, irradiation with vacuum ultraviolet and ultrasoft X-rays reduces the contribution of highly elastic deformation reversible at the test temperature. The degree of decrease in the value of the contribution increases with increasing thickness of the film and may be due to a change in its structure (degree of amorphism).

Comparative study of Tl-1223 superconductors prepared by the sol-gel route and solid-state reaction

I.R. Metskhvarishvili^{1,2}, T.E. Lobzhanidze³, G.N. Dgebuadze¹, B.G. Bendeliani¹, M.R. Metskhvarishvili², M.Sh. Rusia³, G.R. Giorganashvili¹, V.M. Gabunia^{1,4}

¹*Ilia Vekua Sukhumi Institute of Physics and Technology, Laboratory of Cryogenic Technique and Technologies, Mindeli St. 7, 0186 Tbilisi, Georgia*

²*Georgian Technical University, Faculty of Informatics and Control Systems, Department of Microprocessor and Measurement Systems, Kostava St. 77, 0175 Tbilisi, Georgia*

³*Ivane Javakhishvili Tbilisi State University, Faculty of Exact and Natural Sciences, Department of Chemistry, Chavchavadze Ave. 3, 0179 Tbilisi, Georgia*

⁴*Petre Melikishvili Institute of Physical and Organic Chemistry of the Iv. Javakhishvili Tbilisi State University, Jikia str 5, 0186, Tbilisi, Georgia
i.metskhvarishvili@sipt.org.ge*

The $TlBa_2Ca_2Cu_3O_y$ high-temperature superconductor shows superconducting transition temperature T_c above 115 K when these are prepared at ambient conditions and when under high pressures, the critical temperature can reach 133.5 K. These characteristics make the Tl-1223 phase a potentially valuable material for producing superconducting wires, tapes, and thin-films. Formation of the Tl-based superconducting materials critically depends on the used precursor and synthesis conditions. Using the wet chemistry offers some advantages in comparison with the classical solid-state ceramics processing, especially, better chemical homogeneity and higher reactivity of the precursor powder.

The present study devoted to synthesizing the precursors by two different methods. It is must note that for both sol-gel and solid-state reaction ways, oxides and carbonate-containing materials were used as starting materials. For the sol-gel route, poly(vinyl alcohol)/poly(vinyl acetate) was used as the complexing agent. In presenting work also investigated precursors properties dependence on heat treatments. A characterization of precursors obtained by the SG and SSR approaches on the superconducting parameters of $TlBa_2Ca_2Cu_3Dy_xO_{8+\delta}$ is investigated, analyzing comparatively the results of their X-ray diffraction, FTIR analysis, ac magnetic susceptibility, and transport critical current densities. The phase method was used to study the real parts $-4\pi\chi'$ of the linear susceptibility. For the measurements of intergranular critical current densities, we used the method of high harmonics.

As a result, we could conclude that the sol-gel process has the potential advantage over the solid-state reaction method, for achieving homogeneous mixing of the component cations on the atomic scale but also higher reactivity of the precursor powder, and in the result leads to the promotion of the high- T_c phase and enhancement of the transport critical current densities J_c .

Acknowledgments

This work was supported by Shota Rustaveli National Science Foundation of Georgia (SRNSFG), under GENIE project, grant number: CARYS-19-1832, Project title: Innovative Cryostat for Studying High-temperature Superconductors.

Use of Cr³⁺ and Mn²⁺ ions in study of the structure and radiation defects in Mg-Al spinel

N. Mironova-Ulmane¹, M. Brik², A.I. Popov¹, G. Krieke¹, A. Antuzevics¹, V. Skvortsova¹, E. Elsts¹, A. Sarakovskis¹

¹*Institute of Solid State Physics, University of Latvia, Kengaraga Street 8, LV-1063 Riga, Latvia*

²*Institute of Physics, University of Tartu, W. Ostwald Str. 1, 50411 Tartu, Estonia*

nina@cfi.lu.lv

Magnesium aluminum spinel is double oxides with high melting temperature at 2135 °C. It has good thermal and mechanical properties, high hardness and low electrical loss. MgAl₂O₄ is highly resistant to neutron irradiation and has attracted strong attention for its promising use in a future fusion reactor. MgAl₂O₄ is part of the spinel family with general formula AB₂O₄ and Fd3m space group. Oxygen ions create close-packed arrangement with 64 tetrahedral and 32 octahedral interstices per a cell. Divalent A and trivalent B cations are respectively located on the tetrahedral 8a and octahedral 16d. The review will consider the optical, luminescent and EPR properties of manganese and chromium ions and their use for the study the structure and radiation defects in single Mg-Al-spinel. Preference energy for Cr³⁺ ions in octahedral site is rather big as compared with tetrahedral one. So, chromium ions occupy octahedral sites exclusively, substituting for Al ions. The Mn²⁺ is observed in both tetrahedral and octahedral coordination providing green or orange emission. In the stoichiometric single crystals MgAl₂O₄:Mn²⁺ irradiated with fast neutron, the transition of the manganese impurity ions from tetrahedral to octahedral coordination is detected using luminescence methods [1]. Absorption bands have been explained in terms of the Mn²⁺ configuration model. In stoichiometric MgAl₂O₄:Mn²⁺ single crystals irradiated with fast neutron, the transition of the manganese impurity ions from tetrahedral to octahedral coordination is detected using luminescence methods [1]. The photoluminescence spectra Cr³⁺ in the natural MgAl₂O₄ spinel consist of zero-phonon R- and N-lines due to the ²E_g → ⁴A_{2g} spin-forbidden transition and their Stokes and anti-Stokes one-phonon vibronic sidebands. The doublet zero-phonon R-lines: R₁= 684.4 and R₂ = 684.7 nm was observed at 10 K and resolution 0.1 nm. We have observed that the intensity of zero-phonon L-lines for two natural spinels depends on the chromium concentration. Study the luminescence spectra Cr³⁺ of the natural spinel the irradiated of the fast neutron on Mg-Al- spinel are investigated. The broadening of R- and N-lines takes place after spinel crystals irradiation by fast neutron. The changes in intensities and broadening of the luminescence lines are should be noted that the fast neutron irradiation causes the increasing of the spinel inversion [2, 3]. The energy levels of Cr³⁺ ions in the natural spinel were calculated [4] and the crystal parameters for Cr³⁺ ions were determined. The predominant contribution to the EPR spectra is made by the axial centre, which is formed by the substitution of Cr³⁺ for Al³⁺ sites in the spinel structure.

- [1] N. Mironova-Ulmane, V. Skvortsova, E. Feldbach, A. Lushchik, Ch. Lushchik, V. Churmanov, D. Ivanov and V. Ivanov, Rad. Meas. 90, 122 (2016),
- [2] V. Skvortsova, N. Mironova-Ulmane and U. Ulmanis., Nucl. Instr. Meth. B 191, 256 (2002).
- [3] N. Mironova-Ulmane, A.I.Popov, G. Krieke, A. Antuzevics, V. Skvortsova, E. Elsts and A. Sarakovskis. Low Temperature Physics 46(12), 1154 (2020)
- [4] M.G. Brik, J. Papan, D.J. Jovanović, and M.D. Dramićanin, J. Lumin. 177, 145 (2016)

The obtaining of $Zn_xMg_{1-x}WO_4$ nanopowders for composite scintillators

V. Tinkova, I. Tupitsyna, A. Yakubovskaya, P. Maksimchuk

*Institute for scintillations materials of NAS of Ukraine, 60 Nauky ave., Kharkiv, 61072
ZverevaVS91@gmail.com*

The development of composite materials that have a number of advantages in comparison with single crystals (an absence of linear dimensions, the simple obtaining technic, controlled functional parameters) is a promising direction in the development of scintillation materials science. The prospect of using powder from crushed $ZnWO_4$ single crystal as a filler of a composite scintillator was shown in [1]. However, to reduce the cost of such material, it is necessary to develop a method of obtaining dispersed scintillation filler without the crystal growth and grinding of single crystals.

The aim of this work is obtaining of scintillation $Zn_xMg_{1-x}WO_4$ nanopowders by various methods for using in composite scintillators.

The "nanorods" ($\varnothing 20 \times 200\text{-}250$ nm) and "nanograins" ($\varnothing 10 \times 25\text{-}50$ nm) were been obtained using the hydrothermal method with microwave heating by varying pH value of solutions and the synthesis temperature. It is shown that the intensity of X-ray luminescence of "nanograins" is almost an order of magnitude lower than that of "nanorods". It is related with the higher concentration of oxygen vacancies in the "grains" and high intensity of associated photoluminescence ($\lambda_{ex} = 355$ nm).

Scintillation nanocrystals $ZnWO_4$ (100 nm) were been obtained using the molten salt method. The optimal synthesis conditions (mass ratio "mineralizer-precursor", temperature and time of synthesis) were established. Investigation of crystal structure shown that nanocrystallines obtained at $T = 270$ °C, $t = 16$ h, $ZnWO_4 : LiNO_3 = 1 : 10$ have a minimal deformation of the elementary lattice and demonstrate maximum X-ray luminescence intensity.

The continuous series of $Zn_xMg_{1-x}WO_4$ solid solutions nanocrystals ($x = 0\text{-}1$) were obtained by molten salt method. An abnormal increase of X-ray luminescence intensity (4.5 times relative to $ZnWO_4$ nanopowder) was observed for the sample $Zn_{0.5}Mg_{0.5}WO_4$. This effect can be associated with the peculiarities of the processes of oxygen vacancies formation in the solid solutions nanocrystals.

It was shown that the composite material based on $ZnWO_4$ nanopowder obtained by the molten salt method is promising for use in computed tomography due to the low level of afterglow in the range of 3-5 ms (an order of magnitude lower than $ZnWO_4$).

[1] V. Litichevskyi, S. Galkin, O. Lalaiants, et.al., Funct. Mater. 3, 18 (2011).

2-D multifunctional nanostructures of layered double hydroxides assembled in magnetic field

D.E.L. Vieira¹, E.L. Fertman², A.V. Fedorchenko², R.Yu. Babkin³, Y.G. Pashkevich³, C.M.A. Brett⁴, J.M. Vieira¹, A.N. Salak¹

¹*Department of Materials and Ceramic Engineering, CICECO – Aveiro Institute of Materials, University of Aveiro, 3810-193 Aveiro, Portugal*

²*B. Verkin Institute for Low Temperature Physics and Engineering of the National Academy of Sciences of Ukraine, Kharkiv 61103, Ukraine*

³*O. Galkin Donetsk Institute for Physics and Engineering, National Academy of Sciences of Ukraine, Kyiv 03680, Ukraine*

⁴*Department of Chemistry, CEMMPRE, Faculty of Sciences and Technology, University of Coimbra, 3004-535 Coimbra, Portugal
danielevieira@ua.pt*

Layered double hydroxides (LDH) represent a numerous family of natural 2-D materials. Due to the unique combinations of functionalities, LDH find application in different areas from optoelectronics, catalysis, energy storage, to conversion or sensing [1]. LDH are composed of alternating positively charged mixed metal M^{2+} - M^{3+} hydroxide layers, in which the oxygen octahedral MO_6 are edge-linked, and interlayers occupied by anions (A^{y-}) and water molecules. LDH can be intercalated with different types of anions or anionic complexes, which are arranged in several different ways depending on the M^{2+} - M^{3+} cation ratio, resulting in variation of the interlayer distance.

In LDH containing at least one of Co^{2+} , Ni^{2+} , Mn^{3+} , Cr^{3+} or Fe^{3+} , magnetic ordering appears at very low temperatures[2, 3] which makes their direct practical use improbable. Nevertheless, since the magnetic properties of such LDH are dependent on the cation content and the interlayer distance, they are of interest as potential materials for magnetic nanohybrids.

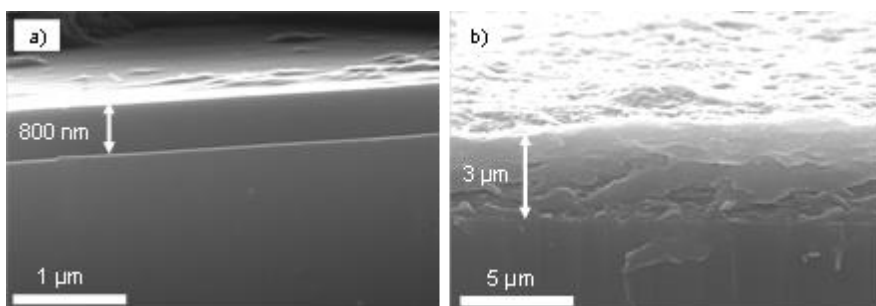


Figure 1 SEM images (cross-section views) of Co_2Al-NO_3 LDH crystallites deposited on glass substrates: (a) with application of an external magnetic field and (b) without magnetic field [4].

to the substrate plane. A mechanism for the field-assisted film formation has been suggested.

In this work, we report the assembly of thin transparent films of crystallites of Co^{2+} - Al^{3+} LDH, with a Co-to-Al ratio of 2, and intercalated with different organic and inorganic anions. Thin films were formed from crystallites of Co_2Al LDH precipitated from dilute suspensions in a magnetic field applied either perpendicularly or parallel

- [1] C. Tan, X. Cao, X.J. Wu, Q. He, J. Yang, X. Zhang, J. Chen, W. Zhao, S. Han, G. H. Nam, M. Sindoro, and H. Zhang, Chem. Rev. 117, 6225-6331 (2017).
- [2] G. Abellán, C. Martí-Gastaldo, A. Rira, E. Coronado, Acc. Chem. Res. 48, 1601-1611 (2015).
- [3] D.E.L. Vieira, A.N. Salak, A.V. Fedorchenko, Yu. G. Pashkevich, E.L. Fertman, V.A. Desnenko, R. Yu Babkin, E. Čižmar, A. Feher, A.B. Lopes, M.G.S. Ferreira, Low Temp. Phys. 43, 977–981 (2017).
- [4] A.N. Salak, D.E.L. Vieira, I.M. Lukienko, Yu.O. Shapovalov, A.V. Fedorchenko, E.L. Fertman, Yu.G. Pashkevich, R.Yu. Babkin, A.D. Shilin, V.V. Rubanik, M.G.S. Ferreira, J.M. Vieira, Chem. Eng. 3, 00062 (2019).

Low thermal conductivity and the evidence of the glassy behavior in $(\text{Pb}_{0.7}\text{Sn}_{0.25}\text{Ge}_{0.05})_2\text{P}_2\text{S}_6$ and $(\text{Pb}_{0.7}\text{Sn}_{0.25}\text{Ge}_{0.05})_2\text{P}_2\text{Se}_6$ mixed crystals

**I. Zamaraite¹, V. Liubachko^{2,3}, R. Yevych², A. Oleaga³, A. Salazar³, A. Dziaugys¹, J. Banys¹,
Yu. Vysochanskii²**

¹*Faculty of Physics, Vilnius University, Sauletekio 9, 10222 Vilnius, Lithuania*

²*Institute for Solid State Physics and Chemistry, Uzhhorod University, Pidgirna Str. 46,
Uzhhorod, 88000, Ukraine*

³*Departamento de Fisica Aplicada I, Escuela de Ingenieria de Bilbao, Universidad del Pais
Vasco UPV/EHU, Plaza Torres Quevedo 1, 48013 Bilbao, Spain
vysochanskii@gmail.com*

The chalcogenide crystals of the $\text{Sn}(\text{Pb})_2\text{P}_2\text{S}(\text{Se})_6$ system are uniaxial ferroelectrics and also demonstrate the quantum paraelectric state appearance at the variation of chemical composition [1]. The dipole ordering temperature of such materials may be tuned by the chemical substitution realizing a ferroelectric quantum phase transition and quantum glassy or relaxor type phenomena in different parts of the phase diagram. The thermal properties of $(\text{Pb}_{0.7}\text{Sn}_{0.25}\text{Ge}_{0.05})_2\text{P}_2\text{S}_6$ and $(\text{Pb}_{0.7}\text{Sn}_{0.25}\text{Ge}_{0.05})_2\text{P}_2\text{Se}_6$ single crystals have been studied by means of measuring their thermal diffusivity D . Thermal conductivity κ has been retrieved by the well-known relation $\kappa = CD$, where C is heat capacity.

As it was found [2] for $(\text{Pb}_{0.98}\text{Ge}_{0.02})_2\text{P}_2\text{S}_6$ crystal, the value of κ at low temperatures (near 50 K) is bigger than that in the case of a pure $\text{Pb}_2\text{P}_2\text{S}_6$ crystal (see fig. 1 (a)). This is obviously related to the Ge induction of polar clusters of the ferroelectric phase. At presenting of Ge the hardening of the optical branch lowers the population of the optical phonons and increases thermal conductivity of the $(\text{Pb}_{0.98}\text{Ge}_{0.02})_2\text{P}_2\text{S}_6$ crystal. In the case of $(\text{Pb}_{0.7}\text{Sn}_{0.25}\text{Ge}_{0.05})_2\text{P}_2(\text{S},\text{Se})_6$ mixed crystals the introduction of Ge slightly increases κ . As it shown in fig. 1 (b), the thermal conductivity behaves on cooling, like in glassy materials, which demonstrates an effective phonon scattering in solid solutions with sublattice of mixed tin and lead cations. Here, germanium impurity induces the dipole glass state, which is manifested in the complex dielectric permittivity frequency dependence below 100 K. Also, the quantum fluctuations are destroyed in the mixed crystals, which follows from the comparison of the low temperature behavior of the thermal diffusivity and the complex dielectric permittivity at different frequencies [2].

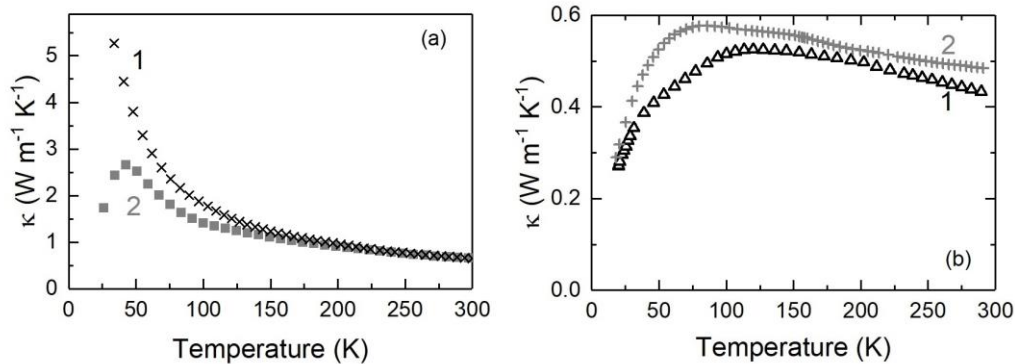


Figure 1. Temperature dependence of thermal conductivity in $(\text{Pb}_{0.98}\text{Ge}_{0.02})_2\text{P}_2\text{S}_6$ (1) and $\text{Pb}_2\text{P}_2\text{S}_6$ (2) (a), $(\text{Pb}_{0.7}\text{Sn}_{0.25}\text{Ge}_{0.05})_2\text{P}_2\text{S}_6$ (1) and $(\text{Pb}_{0.7}\text{Sn}_{0.25}\text{Ge}_{0.05})_2\text{P}_2\text{Se}_6$ (2) (b) mixed crystals.

[1] Yu. M. Vysochanskii, T. Janssen, R. Currat, R. Folk, J. Banys, J. Grigas, and V. Samulionis, Phase Transitions in Ferroelectric Phosphorous Chalcogenide Crystals (Vilnius University Publishing House 2006).

[2] I. Zamaraite, V. Liubachko, R. Yevych, A. Oleaga, A. Salazar, and Yu. Vysochanskii, *J. Appl. Phys.* 128, 234105 (2020).

Cryogenic scintillator based on Li_2MoO_4 single crystal

A.G. Yakubovskaya¹, I.A. Tupitsyna¹, A.M. Dubovik¹, Yu.A. Hizhnyi²

¹*Institute for Scintillation Materials NAS of Ukraine, 60 Nauky Ave., Kharkiv, 61072, Ukraine*

²*Taras Shevchenko National University of Kyiv, Volodymyrskaya st., 64, Kyiv 01033, Ukraine*

nikann2007@gmail.com

A number of experiments are currently being carried out around the world to search for rare nuclear events using low-background nuclear spectrometry. For example, the search of neutrino-free double beta decay using a scintillation bolometric detector is already being carried out in the framework of the international low-background experiment CUPID at Laboratori Nazionali del Gran Sasso. The most promising isotope used to register a $0\nu\beta\beta$ nuclear event is ^{100}Mo . These experiments require certain properties from scintillation crystals: rather high intrinsic radiopurity and light output at low temperature ~ 10 mK, an effective ability to discriminate α and β (γ) events.

The native vacancies, uncontrolled impurities and other defects play the key role in scintillation characteristics of Li_2MoO_4 single crystals.

The studies are aimed to explain peculiarities of the luminescence properties of Li_2MoO_4 using the electronic structure results obtained for a wide range of point defects and their combinations. For investigations, several samples of Li_2MoO_4 with different defectiveness were grown using Czohralski method and characterized by SEM and ICP-OES technique. Luminescence emission spectra of the samples under X-ray and laser excitations, optical and IR absorption spectra, TSL characteristics of the samples were recorded and analyzed.

To study the influence of the charge purity and growing conditions on the optical characteristics, the samples of Li_2MoO_4 crystals of three types were grown:

1. Type I was grown by double crystallization of the material obtained from the cylindrical part of type II crystal boule. Growing environment was dry air.

2. Type II was grown from the charge of 99.99% purity. Growing environment was room atmosphere.

3. Type III was grown using raw materials of 99.5% purity. Growing environment was room atmosphere.



Fig. 1. Images of samples of Li_2MoO_4 crystals of Type I, Type II and Type III (from left to right) of intrinsic and defect-related luminescence, formation of defect-related bands in the optical and IR absorption spectra, dependence of TSL characteristics on sample defectiveness. It was found that the main influence is due to point defects, oxygen vacancies, isovalent and heterovalent impurities

[1] A. Armatol et al. Characterization of cubic $\text{Li}_2^{100}\text{MoO}_4$ crystals for the CUPID experiment. Eur. Phys. J. C 81 (2021) 104.

[2] Yu. Hizhnyi et al. Role of native and impurity defects in optical absorption and luminescence of Li_2MoO_4 scintillation crystals. Journal of Alloys and Compounds 867 (2021) 159148

Catalytic reductive amination of furfural with morpholine at presence of Cu-containing composites

V.M. Asaula

*L.V.Pisarzhevskii Institute of Physical Chemistry of the National Academy of Sciences of Ukraine,
31 Prospect Nauky, Kyiv, 03028, Ukraine
vitaliy.asaula@gmail.com*

Furfural is one of the furan derivatives and is regaining attention as a biobased alternative for the production of everything from antacids and fertilizers to plastics and paints. In particular, furfural is a feedstock for the production of furfuryl alcohol, which is used to produce resins and tetrahydrofuran [1]. However, furfural is toxic when inhaled or swallowed, and is harmful upon contact with skin. The development of new technologies for the treatment of toxic furfural is one of the tasks of modern chemical manufacturing [2]. This task can be fulfilled using reductive amination.

Reductive amination is important reaction widely applied for the preparation of different kinds of amines, which are important building blocks for medicinal chemistry. In such processes, carbonyl compounds react with amines at presence of a reducing agent and form corresponding amines. In particular, interaction of furfural with morpholine or its analogues at presence of gaseous H₂ can lead to one of tetrahydrofuran-2-ylmethylamines as more rigid choline-like derivatives [3], which are important biological compounds exerting neuroprotective activity.

In many cases reactions of reductive amination are carried out with a help of catalysts contained noble metals. Total replacement of noble metals by cheaper readily available and less toxic analogs (3d metals), possessing similar high catalytic activity, is important task of chemical manufacturing. This task can be fulfilled using composites of the non-precious metals and carboneous materials, in particular graphene-like ones.

The aim of this study was to develop new platinum group metals-free catalyst for reductive amination of furfural with morpholine. The composite, containing Cu metal and N-doped carboneous material, was chosen as promising candidate for this study.

The composite was prepared by pyrolysis Cu(II) complex with N-containing ligands such as melamine deposited on active carbon or oxides, in particular, aerosil (highly dispersed SiO₂). The composite contained metallic Cu as crystalline phase. It was found by transmission electronic microscopy that copper nanoparticles had the size of *ca.* 10 -40 nm. Analysis of the Raman spectral data allowed to conclude that the composite contained graphene-like carboneous species.

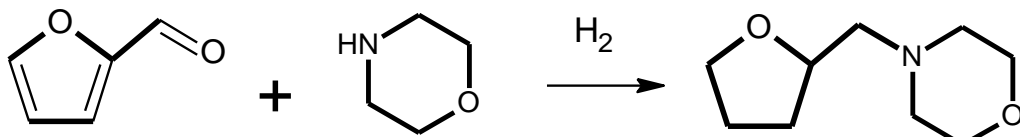


Fig 1. Scheme of the studied reaction

The catalytic activity of the obtained composite was tested in reaction of furfural with morpholine under H₂ pressure (3-5 atm, 50-100 °C) (Fig 1). The reaction products were analyzed by ¹H NMR and gas chromatography. It was found that the 4-(tetrahydrofuran-2-ylmethyl)morpholine formed with *ca.* 90 % yield, while N-(furan-2-ylmethyl)ethanamine was the minor product.

- [1] K. Yan, G. Wu, T. Lafleur, C. Jarvis., Renewable and Sustainable Energy Reviews 38 (2014)
- [2] F. Veisi, M. A. Zazouli, M. A. E. Zadeh, J. Y. Charati, A. S. Dezfuli., Environment Protection Engineering 43, 3 (2017)
- [3] M. Limbeck and D. Gündisch J. Heterocyclic Chem., 40, 895 (2003)

The first principle study of substitutional impurities effect on elastic properties of TlInS₂ layered crystal

T. Babuka¹, O.O. Gomonnai², K.E. Glukhov¹, L.Yu. Kharkhalis¹, A.V. Gomonnai³, M. Makowska-Janusik⁴

¹*Institute for Physics and Chemistry of Solid State, Uzhhorod National University,
54 Voloshin St., 88000 Uzhhorod, Ukraine*

²*Uzhhorod National University, 46 Pidhirna Str., 88000 Uzhhorod, Ukraine*

³*Institute of Electron Physics, Ukr. Nat. Acad. Sci., 21 Universytetska Str.,
88017 Uzhhorod, Ukraine*

⁴*Institute of Physics, Faculty of Mathematics and Natural Science, Jan Dlugosz University in
Czestochowa, Al. Armii Krajowej 13/15, 42-200 Czestochowa, Poland
tanya.babuka@gmail.com*

At this stage of modern materials science development, the search for new promising materials for functional electronics is intensively carried out. Among the important criteria of application of such materials are their elastic properties. Since elastic properties are related to thermodynamic characteristics, such as specific heat, coefficient of thermal expansion, Debye temperature, and melting point, their determination is important for searching materials with promising thermodynamic properties.

One of such materials is TlInS₂ crystal, which belongs to the A^{III}B^{III}C^{VI}₂ group of chalcogenide semiconductors – ferroelectrics [1], and is regarded to be one of the highly anisotropic crystals [2,3]. In the row of TlIn(S_{1-x}Se_x)₂ crystalline solid solutions, the crystal structure changes from C_{2h}^6 to D_{4h}^{18} symmetry at a Se content x near 0.7–0.75 [2,3].

Since the elastic constants are one of the main properties of solid materials, they were obtained for the crystals TlInS₂ and TlIn(S_{0.75}Se_{0.25})₂ using first-principle calculations. The obtained results were compared to identify the effect of impurities substitution on the elastic properties of the TlInS₂ crystal. Thirteen independent elastic constants for TlInS(Se)₂ were calculated using a conditionally deformed state that is in agreement with the Bourne criteria. Among three diagonal components obtained for the TlInS₂ crystal from the first principle calculations, C_{22} ($C_{22} = 48.2 \pm 0.6$) is smaller than C_{11} ($C_{11} = 50.6 \pm 0.5$) and C_{33} ($C_{33} = 60.0 \pm 1.7$). It means, that it is easier to compress the material along the C_{22} direction than along the other two directions. On the other hand, C_{33} shows the highest value. Similar calculations were obtained for the TlInS₂ crystal with selenium substitution.

The bulk modulus elasticity was calculated to find the ability of a material to resist compression under the action of an external force, as well as to describe the chemical bonds in solid. It is known, that the shear modulus measures the resistance of a material to change the shape, if the shear modulus is higher, then harder is material. Pugh established a B/G ratio [4], which describes the ductile or brittle characteristics of materials that are important for technical applications. In our case, B/G is equal to 2.37 for TlInS₂ and 6.66 for TlIn(S_{0.75}Se_{0.25})₂, which indicates that the compounds are characterized by ductility.

Also, using the Christoffel equation, the sound speed for the crystal TlInS₂ and TlIn(S_{0.75}Se_{0.25})₂ in the planes (001), (010), and (100) was calculated.

- [1] V. Grivickas, P. Scajev, V. Bikbajev, O. V. Korolik, A. V. Mazanik, Phys. Chem. Chem. Phys., 21, pp. 2102–2114 (2019).
- [2] A. M. Panich, Journal of Physics: Condensed Matter, 20, pp. 293202 (2008).
- [3] K. R. Allakhverdiev, T. G. Mamedov, B. Akmoğlu, S. S. Ellialtıoğlu, Tr. J. Phys. 18, pp. 1-66. (1994).
- [4] S. Pugh, Philos. Mag., 45, 367, p. 823–843 (1954).

Electron microscope study with in situ video recording of crystal growth in amorphous films

A.G. Bagmut, I.A. Bagmut

*National Technical University “Kharkiv Polytechnic Institute”,
2, Kyrpychova str., 61002, Kharkiv, Ukraine
agbagmut@gmail.com*

In general, crystallization of stoichiometric films occurs according to one of the following schemes [1]: layer polymorphous crystallization (LPC), island polymorphous crystallization (IPC) and dendrite polymorphous crystallization (DPC). The purpose of this work is the electron microscope study with in situ video recording of crystal growth in amorphous films and the systematization of crystallization reactions according to structural and morphological features.

Amorphous films were obtained by thermal evaporation of substance in vacuum, by pulsed laser sputtering targets in oxygen atmosphere and by ion-plasma deposition of metal in argon - oxygen mixture. Phase transformations and structural analysis were performed by the methods of TEM, using microscopes EM-100L and PEM-100-01, operating at the accelerating voltage of 100 kV. The process of crystallization of the films was recorded from the screen of the electron microscope with Canon Power Shot G15 camera in the video recording mode with the frame rate of 30 s^{-1} .

In the case of LPC (V_2O_3 , Fe_2O_3 , Sb_2S_3 , Cr_2O_3 and others) under the action of the electron beam, the crystals with different morphology (disco-shaped, sickle-shaped and needle-shaped crystals) can be formed in the amorphous film, and each film has its own kinetics of evolution. At the fixed density of the electron beam going through the film, the disk-shaped crystals grow at the constant rate and invariable morphology, for which time dependence of crystal fraction $x(t) \sim t^2$. Steps and crystalline layers, moving at different speed into the depth of the amorphous matrix, may accompany the LPC of amorphous films (Fig 1).

In the case of IPC (Al_2O_3 , ZrO_2 , $\text{Yb}_2\text{O}_2\text{S}$, Ni, Re and others) the polycrystalline layer is formed. The average crystal diameter $\langle D \rangle \sim t$, and $x(t)$ is described by the Johnson-Mail-Avrami-Kolmogorov (JMAK) formula $x = 1 - \exp(-nt^k)$, where k is the Avrami coefficient (reaction order) and n is an effective rate constant, describing both nucleation and growth.

In the case of DPC (films of HfO_2 , Fe-C) single crystals in the form of dendrite branches of the first order are the site of formation of branches of the second and third order. The branches are formed from the series of randomly oriented crystals in the process of geometric selection.

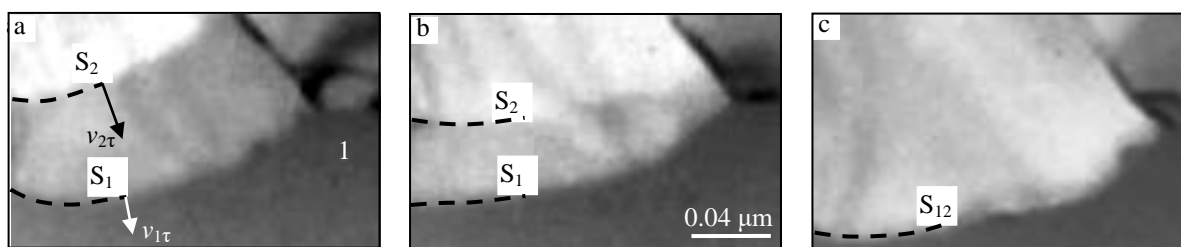


Fig. 1. Film shots of layer crystallization of amorphous film of Cr_2O_3 . Photomicrographs correspond to the periods of time t , that passed after the video recording had started: (a) $t = 0 \text{ s}$; (b) $t = 0.83 \text{ s}$; (c) $t = 1.67 \text{ s}$. 1 - amorphous phase. S_1 is the crystallization front, moving with the velocity $v_{1\tau}$. S_2 is the crystallization front, moving with the velocity $v_{2\tau}$. S_2 - crystallization front after the merger of S_1 and S_2

[1] A.G. Bagmut, Classification of the Amorphous Film Crystallization Types with Respect to Structure and Morphology Features, Tech. Phys. Lett. 38 (2012) 488-491.

Effect of Yb-doping on structural and optical properties of CdTe thin films, their defect structure and type of conductivity

**Yu.P. Gnatenko¹, P.M. Bukivskij¹, R.V. Gamernyk², A.P. Bukivskii¹, M.S. Furyer¹,
M.M. Kolesnyk³, D.I. Kurbatov³, A.S. Opanasyuk³**

¹*Institute of Physics of NAS of Ukraine, 46 Prospect Nauky, Kyiv, 03028, Ukraine*

²*Lviv National University, 8 Kyrylo and Mefodiy Str., Lviv, 29005, Ukraine*

³*Sumy State University, 2 Rymskogo-Korsakova Str., Sumy, 4000, Ukraine*

ap.bukivskii@gmail.com

Cadmium telluride crystals are the basic semiconductor material for many applications in the near infrared spectral region. The efficiency of using such materials largely depends on their crystalline and optical qualities, which in turn determine the electronic properties of materials. It should be noted that cadmium telluride is a *p*-type semiconductor because it contains cadmium vacancies, which are the main acceptor defects in this crystal. The presence of intrinsic and extrinsic defects in CdTe crystals, including residual atoms, can also affect their energy structure and conductivity type. Doping of semiconductor crystals with rare earth elements (REs) is of considerable interest because they can significantly improve the crystal structure and optical quality of such materials.

In this work, we have studied the structural, microstructural and optical properties of Yb doped CdTe thin films obtained by close-spaced sublimation technique at different substrate temperatures, namely (450-500) °C. The investigated films are polycrystalline, homogeneous over the area and have good adhesion to the glass substrate. The films obtained at T_s=450 °C are characterized by a fine structure with an average grain size of 1-2 μm. As the temperature of the substrate increased, the growth mechanism changed and the films had a columnar structure. The large grains in CdTe:Yb films indicate that they are highly crystalline. The average size of the crystallites was about 10 μm. A number of structural and substructural parameters of the investigated films were determined, namely, the lattice parameter, the average size of the coherent scattering region, the level of microdeformation, the level of microstress and the dislocation density.

Analysis of low-temperature photoluminescence spectra allowed us to obtain important information about the nature and energy structure of the defects responsible for the emission of the CdTe:Yb thin films as well as to determine accurate values of their band gap and optical quality. It is shown that the radiative recombination of DAPs occurs with the participation of different acceptor centers. It was found that doping of CdTe thin films with ytterbium allows us to obtain a polycrystalline material of very high crystalline and optical quality. In addition, the conversion of their conductivity from *p*- to *n*-type occurs in this case. It is expected to be a result of a strong decrease in the concentration of shallow acceptor centers associated with residual atoms and cadmium vacancies. This is due to the formation of complex centers with the participation of Yb³⁺ ions and the mentioned acceptors, i.e by gettering of residual atoms in CdTe:Yb thin films. The optical spectra of such films reflect the processes of formation of free excitons and recombination with the participation of bound excitons as well as donor-acceptor pairs. In the latter case, these optical transitions involve shallow and complex acceptor centers. For the first time, emission associated with intracenter optical transitions of Yb³⁺ ions in CdTe was detected and its nature was established. The results obtained open a unique opportunity to control the crystalline and optical qualities as well as type of conductivity of II-VI semiconductor crystals by doping them with rare earth elements.

Study of the polymer - carbon composites electronic structure by positron spectroscopy

Ye.A. Tsapko, Ye.G. Len, I.Ye. Galstian

*G.V.Kurdyumov Institute for Metal Physics of NAS of Ukraine,
36 Academician Vernadsky Boulevard, UA-03142 Kyiv, Ukraine
stenforti@ukr.net*

An important peculiarity of polymer matrix composites – carbon nanotubes is that they consist of two substantially different systems - an insulator matrix with electrons, which are strictly associated with certain σ - and π - atoms, and a network of direct-interaction conducting nanotubes, where π - electrons are collectivized and make an infinite movement. The interaction between these systems is weak, (hydrogen and/or van der Waals). When the charge is redistributed between them (only π -electrons are redistributed), a qualitative change in the state of π -electrons occurs – a transition from a finite to an infinite state or v.v. In such a composite model, the concept of free volume [1] becomes even more relevant not only in understanding segmental molecular motion in a polymer matrix, but also in the exchange and interaction of its systems.

The peculiarities of the electronic structure of composites based on polymers (polypropylene (PP), polytetrafluoroethylene (PTFE), polyvinylchloride (PVC)) with the addition of multi-walled carbon nanotubes (MWCNTs) in the range of concentrations from 0 to 5 wt.% MWCNTs were studied by positron spectroscopy. The angular correlation of annihilation radiation spectra (ACAR) for the studied specimens were obtained using a long-slit spectrometer with an angular resolution of 1.07 mrad and decomposed into components according to the method described in [2].

It was found that the spectrum of the ACAR for polymers consists of three Gaussians: a wide one, due to the annihilation of positrons in defects in polymer chains, a medium one, due to the annihilation of positrons with core electrons, and a narrow one, due to annihilation from the orthopositronium state in the pores of the free volume. The ACAR spectrum for MWCNTs consists of three components – two Gaussians: a medium one, due to annihilation of positrons with core electrons of carbon atoms, a wide one, due to annihilation of positrons in Stone-Welsh defects, and a parabolic contribution due to annihilation of positrons with free electrons. The ACAR spectrum for polymer + MWCNT composites consists of four components – three Gaussians: a wide one, caused by the annihilation of positrons in the Stone-Welsh defects of MWCNTs and polymeric chains, a medium one, caused by annihilation of positrons with core electrons, and a narrow one, caused by annihilation from the orthopositronium state to the pores of the free volume and the parabolic contribution due to the annihilation of positrons with free electrons. The radii of the nanopores decrease with increasing concentration from 0.45 nm to 0.35 nm, and at 5 wt.% CNTs in the composite nanopore by positron spectroscopy are not detected. It was found that the probability of annihilation of positrons with free electrons rapidly increases at low additive concentrations and, with a further increase in this concentration, saturation occurs. Obviously, charge transfer occurs in the composite from the polymer matrix to MWCNTs and weakly bound electrons of the charged layer of the free volume of the polymer, when flowing into MWCNTs, pass into a qualitatively different state - free, which leads to significant changes in the electronic structure of the composites.

The change in the positron annihilation parameters with a change in the concentration of CNTs in the polymer indicates a change in the electronic properties of both the matrix and CNTs.

[1].Y. C. Jean, J. David Van Horn, Wei-Song Hung and Kuier-Rarn Lee. Perspective of Positron Annihilation Spectroscopy in Polymers. *Macromolecules* 2013, 46 (18), 7133–7145.

[2].E. A. Tsapko and I. Ye. Galstian, Positron Spectroscopy Study of Structural Defects and Electronic Properties of Carbon Nanotubes, *Progress in Physics of Metals*, 21, No. 2: 153–179 (2020).

Scattering by molecules of the Kapton H polymer. Amorphous films

D.E. Hurova¹, V.G. Geidarov¹, N.A. Aksanova^{1,2}, N.N. Galtsov¹

¹*B.Verkin Institute for Low Temperature Physics and Engineering of NAS of Ukraine
47 Nauky Ave., Kharkiv, 61103, Ukraine*

²*Ukrainian State University of Railway Transport, Feuerbach Square 7, 61050, Kharkiv
hurova@ilt.kharkov.ua*

A qualitative analysis of X-ray diffraction patterns obtained from amorphous polymer films of the Kapton H type was performed in [1, 2]. These films were stretched both at room temperature and at the temperatures of liquid nitrogen and helium.

The authors found that, as a result of deformation and low temperatures, regions are formed in the samples, which are different in density from the films in the starting state.

This behavior was explained by the fact that in polymer films, by the action of external loads, the ordering of molecules occurs, the same as in molecular crystals [3, 4].

In order to confirm or dispel the conclusions of works [1, 2], it is necessary to calculate the position of atoms in the sample. Due to the lack of long-range ordering, determining the position of atoms in an amorphous Kapton H film is no easy problem.

To solve this objective, in this work we use the construction of the radial distribution function of atoms, whereby we can talk about the mutual arrangement of atoms in the sample.

- [1] I. S. Braude, N. N. Gal'tsov, V. G. Geidarov, G. I. Kirichenko, and V. V. Abraimov, *Low Temp. Phys.* 42, 204 (2016).
- [2] V.G. Geidarov, I.S. Braude, N.N. Gal'tsov, Y.M. Pohribnaya, *Molecular Crystals and Liquid Crystals*, 661 (1), 20-24, (2018)
- [3] N.N. Galtsov, O.A. Klenova, and M.A. Strzhemechny, *Low Temp. Phys.* 29, 365 (2002).
- [4] L. Jin, C. Bower, and O. Zhou, *Appl. Phys. Lett.* 73, 1197 (1998).

Effect of annealing temperature on the elementary composition of CZTSe thin films obtained by 3D printing

S. Kakherskyi, R. Pshenychnyi, O. Dobrozhany, A. Opanasyuk

*Sumy State University, Rimsky-Korsakov str., 2, Sumy, UA-40007, Ukraine
s.kacherski@ekt.sumdu.edu.ua*

$\text{Cu}_2\text{ZnSnSe}_4$ (CZTSe) is the four-component compound of the kesterite phase that nowadays increasingly considered as an alternative to such traditional materials as CdTe, CIS (CuInS_2), CIGS (CuInGaS_2), because it eliminates their main disadvantages, such as indium, gallium deficiency in nature and the toxicity of cadmium, which limit the possibility of mass production of thin film solar cells (SC) using these compounds as absorbers. This compound's main advantage is the content of only low-toxic, widespread in the earth's crust and cheap elements. Also, it is characterized by p-type conductivity, high light absorption coefficient and optimal for use in the solar energy bandgap.

As for other solar energy (SE) absorbers, heat treatment is a mandatory step for CZTSe layers to obtain thin films of high structural quality. However, one of the problems encountered in the annealing process is the loss of Se at high annealing temperatures. ($T > 400 \text{ }^{\circ}\text{C}$). This leads to a change in the stoichiometry of the four-component compound. The emergence of its own defects and additional phases impairs their properties as absorbers of photo converters.

CZTSe thin films were obtained using a 3D printer developed by us, in which traditional inks were replaced by special nanoinks based on suspensions of nanocrystals (NC). Nano inks were obtained by mixing CZTSe NCs synthesized according to the method described in [1] with triethylene glycol and subsequent mixing in an ultrasonic bath. After obtaining CZTSe thin films on glass substrates, they were annealed at temperatures from 300 to $550 \text{ }^{\circ}\text{C}$ with a step of 50 degrees and one hour in the air. Before and after annealing, the chemical composition of the films was studied using an energy dispersion spectrometer AZtecOne with detector X-MaxN20 (manufacturer Oxford Instruments plc), structural characteristics by X-ray diffraction method. The results of determining the atomic concentration of Se in the layers are shown in table 1.

Table 1.

Annealing temperature $^{\circ}\text{C}$	300	350	400	450	500	550
Atomic percentage C_{Se}	37.89	25.1	19.13	10.09	4.93	2.62

Analysis of the results allows us to conclude that the annealing should be done at temperatures not exceeding $350 \text{ }^{\circ}\text{C}$. However, such low temperatures do not allow to completely burn the organic matter used during the synthesis of NC and develop nanoinks from the deposited films. Therefore, it is proposed to increase the annealing time, or in the case of high-temperature annealing of films to use additional gases or mixtures thereof that prevent the release of selenium from the films, such as those containing selenium.

[1] S. Kakherskyi, O. Dobrozhany, R. Pshenychnyi, D. Kurbatov and N. Opanasyuk, "Cu₂ZnSnS₄, Cu₂ZnSnSe₄ Nanocrystals As Absorbers In 3rd Generation Solar Cells," 2020 IEEE 40th International Conference on Electronics and Nanotechnology (ELNANO), Kyiv, Ukraine, 2020, pp. 100-104.

Magnetic composite materials based on chitosan: low temperature synthesis, characterization and application

O. Kalinkevich¹, Y. Zinchenko¹, V. Bilyk¹, A. Kalinkevich¹, A. Sklyar², S. Danilchenko¹

¹*Institute of applied physics of NAS of Ukraine,
58 Petropavlovskaya St., Sumy, 40000, Ukraine*

²*A.S. Makarenko Sumy State Pedagogical University,
87 Romenskaya St., Sumy, 40002, Ukraine
kalinkevich@gmail.com*

Bioadsorbents based on natural compounds, often waste products (cellulose, chitin, etc.), are of great interest today. Inexpensive materials such as walnut shells [1], apricot kernels, acorns, shells of fly larvae [2] are used to clean the environment from various pollutants, and can also be used as enterosorbents, and materials for the immobilization of various compounds. Imparting magnetic properties to such sorbents or matrices for immobilization allows controlling them using an external magnetic field, for example, to separate sorbents from solutions, to carry out targeted delivery of drugs, etc.

In our work, we obtained magnetic composites based on chitosan (a chitin derivative). The materials were obtained in various forms using both simple fast methods of imparting magnetic properties to materials, and more complex procedures. Beads were obtained by coprecipitation in an alkali solution of chitosan and precursors of magnetite, apatite at room temperature [3], sponges by processing frozen solutions of chitosan with magnetite precursors with a mixture of alkali and alcohol at temperatures below zero, and powders by adhesion of pre-synthesized nanomagnetite particles on the powders of chitosan and brushite [4]. The materials were investigated by SEM, X-ray diffraction, and PIXE methods. Their ability to bind some compounds, in particular proteins, amino acids, dyes was also studied.

The synthesis of magnetite using microwave [4] leads to the formation of nanoparticles, which stick together into conglomerates upon removal of the solvent. Chitosan and brushite containing powders in micrographs look homogeneous (particles of irregular shape for chitosan, mainly plate-like for calcium phosphate), do not contain individual magnetic particles. Beads and sponges have a porous structure, nanoparticles of magnetite and calcium phosphates form a single composite with chitosan and do not form separate conglomerates. Diffraction patterns of samples obtained by coprecipitation and by modification of powders with magnetite show peaks of magnetite, as well as calcium phosphates (brushite and hydroxyapatite, in the case of coprecipitation). Magnetite beads are high in iron, while calcium phosphate beads contain significant amounts of calcium and phosphorus. Beads containing both magnetite and calcium phosphates contain all three elements, which indicate the formation of all components during the synthesis process. The study of the sorption capacity of the materials indicates that the beads absorb amino acids and proteins better, magnetic powders have shown a great sorption activity in relation to low-molecular compounds, in particular to dyes.

Acknowledgments. The work was supported by bilateral project of AS of Czech Republic and NAS of Ukraine “Low cost, easy to prepare magnetic chitosan composites for cell and enzyme immobilization, biosorption, biosensing and biomedicine”, 2020-2022.

- [1] A.Safinejad, M. Arab Chamjangali, N.Goudarzi, and G.Bagherian, J. Environ. Chem. Engineer. 5, 1429 (2017).
- [2] O. Gyliene, R. Rekertas, and M. Salkauskas, Water Res. 36, 4128 (2002).
- [3] S.N. Danilchenko, V.N. Kuznetsov, A.S. Stanislavov, O.V. Kalinkevich, A.N. Kalinkevich, M.G. Demidenko, K.V. Tischenko, and L.F. Sukhodub, J. Nano- Electron. Phys. 3, 126 (2011).
- [4] I. Safarik, J. Prochazkova, and K. Pospiskova. J. Magnetism Magnet. Materials (2020).

Topology of chemical bonds and electron band structure of In_6Se_7 monoclinic crystal doped by Sn atoms

L.Yu. Kharkhalis, K.E. Glukhov, T.Ya. Babuka, M.V. Liakh

*Institute for Physics and Chemistry of Solid State, Uzhhorod National University,
54 Voloshin St., Uzhhorod, 88000, Ukraine
lkharkhalis@gmail.com*

A new crystal In_6Se_7 which possesses potential in thermoelectric performance has been found among the phases existing in the In-Se system. Nowadays, it is very little information about this binary compound. As it is known the considered structure is described by a spatial group $P2_1/m$. The unit cell consists of two separate closed packets oriented in equivalent directions at an angle of 61° and contains 26 atoms. Some physical properties (thermoelectric, kinetic, and optical) of both crystals of In_6Se_7 and its polycrystalline thin films are presented in [1–4]. Recent investigations showed that substitution of In^+ site by Sn and Pb impurities can change the conduction type, charge concentration, tend to reduce the lattice thermal conductivity, and as in consequence, lead to the significant enhancement of the thermoelectric performance. Therefore, it is of interest to study the peculiarities of the chemical bonds and the electron band structure of In_6Se_7 crystal and to investigate their evolution due to the doping by substitutional atoms too.

In the present work, we aimed at the calculations of the electron properties of both the undoped and doped by Sn impurities In_6Se_7 . As it is noted in [1], the compound In_6Se_7 can be described as $\text{In}^+[\text{In}2]^{4+}(\text{In}^{3+})_3(\text{Se}^{2-})_7$ presuming that the oxidation state of Se is 2^- , where the $[\text{In}2]^{4+}$ and In^{3+} ions occupy two and three different sites respectively. Such crystal structure suggests that the incorporation of the Sn contents at different In sites is possible. Therefore we considered some models of the Sn atoms substitution for indium and calculated the cohesion energy for the investigation of the stability of $\text{In}_{6-x}\text{Sn}_x\text{Se}_7$ compounds.

Using density functional theory (DFT) within local approximation for exchange-correlation interaction (LDA) we investigated the spatial distribution of electron density, band structures, and total and partial density of states in the In_6Se_7 and $\text{In}_{6-x}\text{Sn}_x\text{Se}_7$ crystals

Our analysis shows that the band structure is very complicated, and the direct minimal energy gap is localized in Γ -Z directions. From the calculation of the total and partial density of states in undoped In_6Se_7 follows that it has resulted from *s*- and *p*-orbitals from In and Se atoms. The *d*-orbitals of indium make the main contribution in the low energy part of the density of states (in the region $E \sim -13 \div -15$ eV). The energy edge of the valence band is formed by the *p*-states of selenium. The doping by Sn atoms influences the topology of band structure and redistribution of the total and partial density of states.

- [1] J. Cui, M. Cheng, W. Wu, Z. Du, Y. Chao, *Appl. Mater. Interfaces*, 8, 23175 (2016).
- [2] Anuroop R, B Pradeep, *Journal of Alloys and Compounds*, 702, 432 (2017).
- [3] A.F. El-Deeb, H.S. Metwally and H A Shehata, *J. Phys. D: Appl. Phys.* 41, 125305 (2008).
- [4] R. Anuroop, B. Pradeep. *J. of Materials Science: Materials in Electronics*, 29, 19499 (2018).

Deviation from the Hall-Petch relationship for Cu-Mo vacuum condensates

E. Lutsenko¹, A. Zybkov², M. Zhadko²

¹*National Science Center “Kharkiv Institute of Physics and Technology”,*

1, Akademichna str., Kharkiv 61108, Ukraine

²*National Technical University “Kharkiv Polytechnic Institute”,*

2, Kyrpychova str., 61002 Kharkiv, Ukraine

lytsenko87@gmail.com

The efficiency of grain boundary strengthening of metallic materials is mainly determined by two factors: the grain size and the value of the coefficient (k) in the Hall-Petch equation. Most of the research associates the problem of increasing the strength properties of metals with the refinement of their grain structure. Less attention is paid to ways for increasing the Hall-Petch coefficient, which is due to several reasons, for example, the need to test grain boundaries at the atomic level, many parameters that affect the Hall-Petch coefficient, etc. In this regard, the purpose of this work was to study the conditions of crystallization and heat treatment for the Hall-Petch relationship for vacuum condensates of the Cu-Mo binary system.

The objects of research were foils of condensates with a thickness of up to 50 μm , obtained at different temperatures of the deposition surface. The molybdenum concentration was varied in the range from 0.1 to 2 at. %. Annealing was carried out in the temperature range from 400°C to 1000°C. The exposure time was varied from 15 minutes to 2 hours. The structure of the foils was studied by electron microscopy and X-ray diffractometry. The elemental composition was controlled by the X-ray spectral method. The strength properties were investigated in the active tension mode and by the microhardness measurement.

It has been established that alloying of copper condensates with molybdenum leads to a decrease in the grain size of the copper matrix from $\sim 1 \mu\text{m}$ to $\sim 0.1 \mu\text{m}$. With an increase in the Mo concentration to 0.5 at. %, a sharp decrease in the value of the grain size is observed, followed by saturation. It is shown that alloying of copper condensates with molybdenum leads to an increase in the Hall-Petch coefficient, and an increase in the substrate temperature leads to a decrease in this value.

Different modes of heat treatment lead to a deviation from the Hall-Petch dependence constructed for samples in the initial condensed state. The experimental points are located above the $\sigma_y = \sigma_0 + kL^{-1/2}$ dependence. A similar pattern was observed by the authors of other studies [1]. An analysis of electron microscopic images shows that annealing changes the state of grain boundaries: for example, finely dispersed molybdenum particles appear, the morphology of which depends on the conditions of heat treatment. The presence of these particles leads to additional hardening. Therefore, with an insignificant increase in the grain size, the experimental points for the annealed condensates are located above the initial dependence. A further increase in the annealing temperature and holding time leads to the destruction of the adsorption layers of molybdenum at the grain boundaries of the copper matrix. The superposition of these simultaneously or sequentially proceeding processes leads to the observed phenomena.

Thus, the experimental results obtained in this study indicate that the change in the slope of the Hall-Petch dependence can be caused by the segregation of atoms or particles of alloying elements at the grain boundaries of the matrix metal. They can be formed both during crystallization from various media and as a result of heat treatment.

- [1] Giga, A., Kimoto, Y., Takigawa, Y., & Higashi, K. Demonstration of an inverse Hall-Petch relationship in electrodeposited nanocrystalline Ni–W alloys through tensile testing. *Scripta Materialia*, (2006) 55(2), 143–146.

The formation of ZrO₂-Y₂O₃-nanoparticles from fluoride solutions

E.S. Gevorkyan¹, O.M. Morozova¹, D.S. Sofronov², V.P. Nerubatskyi¹, N.S. Ponomarenko³

¹Ukrainian State University of Railway Transport, Feierbakh sq., 7, Kharkiv, 61050, Ukraine

²SSI "Institute for Single Crystals" NAS of Ukraine, Nauky ave. 60, Kharkiv, 61001, Ukraine

³Kharkiv National Medical University, Nauky ave. 4, Kharkiv, 61000, Ukraine

oksanabakan2012@gmail.com

High-tech characteristics of zirconium dioxide (ZrO₂) make it possible to use it to obtain highly refractory products, heat-resistant enamels, refractory glasses, various types of ceramics, pigments, solid electrolytes, catalysts. The latter serve as a material for the creation of heat shields for spacecraft, in fields of endoprosthetics and dentistry, in jewelry, fiber optics, as well as for the manufacture of cutting tools and abrasive materials [1,2]. The widespread use of the material in the technological industry involves the studying of the synthesis of ZrO₂-Y₂O₃-particles and their morphology, which was done in this work.

The hydrofluoric acid (HF), concentrated nitric acid (HNO₃), aqueous ammonia (NH₄OH), metallic zirconium and polyvinyl alcohol produced by Reakhim were used to obtain particles of ZrO₂-Y₂O₃. Distilled water was used for the preparation of solutions.

The exploring of the surface morphology of obtained powders was carried out by using a JSM-6390LV scanning microscope (SEM). IR spectra were obtained by a spectrophotometer SPECTRUM ONE (Perkin Elmer) in potassium bromide tablets.

Precursor particles are formed to obtain zirconium dioxide, which is formed mainly by small spherical particles with sizes less than 100 nm, as the result of the precipitating from a fluoride solution. In the process of thermal annealing of the precursor, a slight decrease in the particle size at 300 °C is observed. With a subsequent increase in temperature, the formation of strongly agglomerated shapeless particles occurs. They have sizes up to several micrometers and consist of spherical particles with sizes of about 100 nm.

The use of the supplements of polyvinyl alcohol in the synthetic mixture results in the formation of particles in the form of thin plates. In this case, the higher the concentration of the supplements, the larger plates are formed.

It was found that the synthesis temperature and the concentration of components in solution significantly affect on the formation of ZrO₂-Y₂O₃ - particles. An increase of the deposition temperature of the gel leads to the formation of rod-shaped particles up to several micrometers in length, the thickness of which varies depending on the additive content and varies in the range of 100-500 nm. With a decreasing of the concentration in 5 times (Figs. 1a, b), the effect is practically unnoticeable. According to XRD data, zirconium dioxide with a baddeleyite structure is formed.

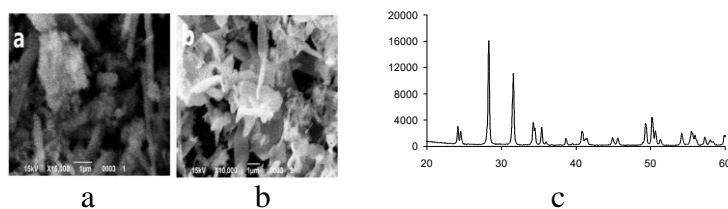


Fig. 1. Micrographs of ZrO₂-Y₂O₃-nanoparticles obtained during deposition from an aqueous solution (a, b) and XRD of a ZrO₂-Y₂O₃ sample obtained after annealing at 800 °C with the addition of polyvinyl alcohol (c).

[1] Novoselov I.Yu., Karengin A.G., Shamanin I.V., Alyukov E.S., Plasma-chemical synthesis of nanodispersed powders of yttrium and zirconium oxides from dispersed aqueous-salt-organic compositions, Polzunovsky Vestnik. № 3, 142-148, (2017).

[2] P. F. Manicone, P. R. Iommetti, L. Raffaelli, An overview of zirconia ceramics: basic properties and clinical applications, Journal of Dentistry. V. 35, 819–826, 2007.

Estimation of iron concentration in silicon solar cell by kinetics of light-induced change in short-circuit current

O. Olikh¹, V. Kostylyov², V. Vlasiuk², R. Korkishko²

¹Taras Shevchenko National University of Kyiv, 64/13, Volodymyrska Str., Kyiv, 03028, Ukraine

²V. Lashkaryov Institute of Semiconductor Physic Institute of NAS of Ukraine,
41 Nauky Ave., Kyiv, 03028, Ukraine
olegolikh@knu.ua

The iron is a major contaminant as well as one of the most detrimental metal impurities in silicon photovoltaic devices. Therefore non-destructive methods of iron concentration (N_{Fe}) estimation in solar cells (SCs) are important from an applied point of view. To date, a not little collection of both direct and indirect methods has been developed to solve this problem. But almost all of them require special sample preparing or/and specialized equipment. At the same time, the current-voltage curve (IVC) measurement is a common method of SC characterization. Short-circuit current (I_{SC}) is among the fundamental SC parameters, which easy determined from IVC as well as depend on N_{Fe} . The proposed method is based on ability of pair FeB to dissociate under carriers injection and to associate in the dark [1] and involves for the measurement of I_{SC} kinetics after intense illumination.

During the kinetic fit it was assumed, that I_{SC} under monochromatic light described by

$$I_{SC} = \frac{W_{ph}(1-R)q\beta\lambda}{hc} \frac{\alpha\sqrt{D\tau}}{1+\alpha\sqrt{D\tau}}, \quad (1)$$

where W_{ph} is the irradiance, D is the diffusion coefficient, τ is minority carrier lifetime in SC base:

$$\tau^{-1} = \tau_i^{-1} + \tau_{Fei}^{-1} + \tau_{FeB}^{-1} + \tau_{rest}^{-1}, \quad (2)$$

where τ_i describes intrinsic recombination, τ_{Fei} and τ_{FeB} concern to Shockley-Read-Hall recombination on interstitial iron Fe_i and FeB pair; τ_{rest} deals with other processes. The time dependence of the Fe_i concentration was used from [2] and it was believed that associate characteristic time can be written as

$$t_{ass} = 1.3 \cdot 10^3 N_A^{-2/3} \exp(E_m/kT), \quad (3)$$

where E_m is the Fe_i migration energy, N_A is the doping level.

The n+-p-p+-Si diffusion-field type SCs were used in experiments. SCs were fabricated by using single-crystal p -silicon wafer with a resistivity of $10 \Omega \cdot cm$. Some examples of I_{SC} kinetic curve are presented on Fig. We use Eqs. (1)-(3) by taking W_{ph} , E_m and N_{Fe} as fitting parameters to fit the experimental data. The obtained values were following: $W_{ph} \approx 0.3 \text{ mW}$; this value is in according with data, obtained by Power Meter Rk-5720 for used light source; $E_m \approx 0.679 \text{ meV}$; this value is in according to known [2] Fe_i migration energy; $N_{Fe} \approx 2 \cdot 10^{13} \text{ cm}^{-3}$; this value is close to one, obtained by long-wavelength spectrum of internal quantum efficiency.

Thus, the proposed method allows to estimate the iron concentration in silicon solar cell. The work was supported by NRFU (project 2020.02/0036)

[1] L. J. Geerligs and D. Macdonald, Appl. Phys. Lett. 85, 5227 (2004).

[2] W. Wijaranakula, J. Electrochem. Soc. 140, 275 (1993).

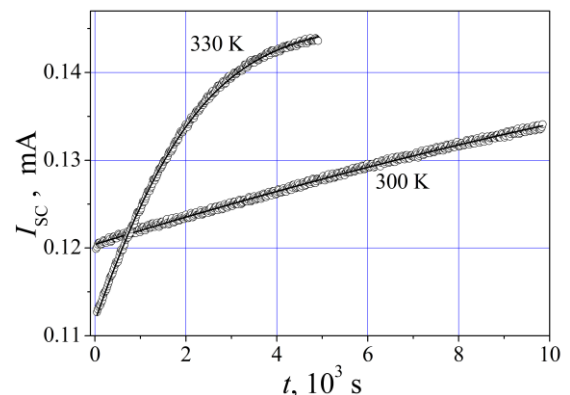


Fig. I_{SC} vs time after halogen lamp illumination (0.25 W/cm^2 , 15 s). The marks are the experimental results, and the solid lines are the fitted curves. I_{SC} corresponds to the LED illumination (940 nm, 0.3 mW).

Influence of the structure formed by condensation on thermal stability of Cu-Mo pseudoalloys

V. Riaboshtan, A. Zubkov, V. Kucherskyi, M. Zhadko

National Technical University «Kharkiv Polytechnic Institute», 61000,
2, Kyrpychova str., 61002 Kharkiv, Ukraine
obibobbivalkinobi@gmail.com

The paper considers the main disadvantage of nanomaterials – their low thermal stability. Recent studies have shown that some alloying elements, such as Mo or Ta, increase the resistance to the grain coarsening of the copper matrix at elevated temperatures. [1] However, the physical mechanism of this process is insufficiently studied.

It is known that the main thermostabilizing factors of the grain structure are the second phase particles (formed at high deposition temperatures) or grain boundary segregation (formed at low deposition temperatures) at the grain boundaries of the matrix metal. To compare the degree of these factors, samples of Cu-Mo system with a thickness of 20 μm in the form of a thin film were used. These films contained 0.3at.% Mo and were obtained by PVD technology at condensation temperatures of 150°C and 450°C. For these samples grain size and microhardness were measured before and after vacuum annealing, which was carried out at 900°C for 30 minutes.

Studies of samples by TEM in the initial condensed state showed that molybdenum has a tendency to concentrate at the grain boundaries of the cooper matrix and its structural state depends on the condensation temperature. In the thin films obtained at a substrate temperature of 150°C, molybdenum form monatomic adsorption layers. Increasing the temperature to 450°C leads to the formation of highly dispersed particles.

The results of annealing showed that the condensates obtained at a lower temperature have a smaller tendency to increase the grain size under the influence of temperature, as well as a smaller decrease in microhardness than the condensates obtained at 450°C (Fig. 1).

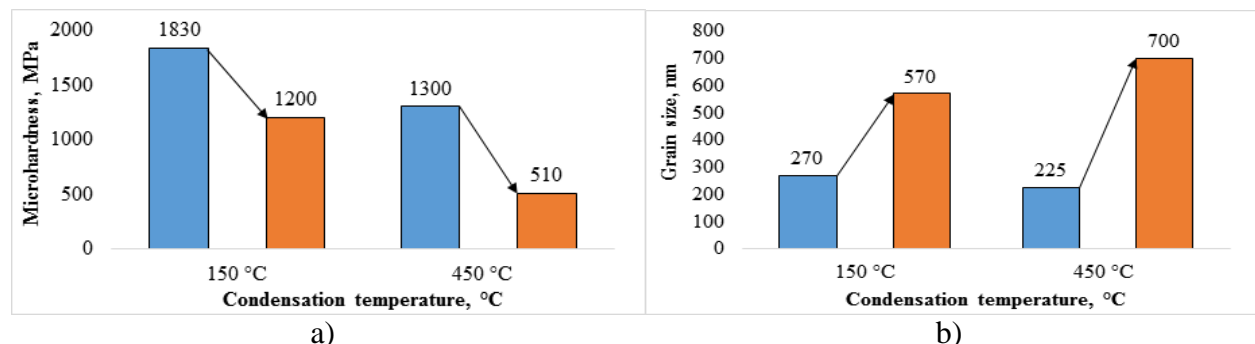


Figure 1 - Dependence of microhardness (a) and grain size (b) on the condensation temperature of the Cu-Mo system after annealing.

This means that grain boundary segregation in the form of monoatomic layers increases thermal stability more efficiently than the second phase particles at the grain boundaries.

[1] A.I. Zubkov, E.N. Zubarev, O.V. Sobol, M.A. Hlushchenko, E.V. Lutsenko, Structure of Vacuum Cu—Ta Condensates, Phys. Metal. Mettallog. 118 No. 2, 158 (2017).

The effect of carbon on the microhardness of $\text{Co}_{0.25-x}\text{Cr}_{0.25}\text{Fe}_{0.25}\text{Ni}_{0.25}\text{C}_x$ alloy

H.V. Rusakova¹, L.S. Fomenko¹, Yi Huang^{2,3}, E.D. Tabachnikova¹, I.V. Kolodiy⁴, A.V. Levenets⁴, M.A. Tikhonovsky⁴, T.G. Langdon³

¹*B.Verkin Institute for Low Temperature Physics and Engineering of NAS of Ukraine,
47 Nauky Ave., Kharkiv, 61103, Ukraine*

²*Department of Design and Engineering, Faculty of Science and Technology,
Bournemouth University, Poole, Dorset BH12 5BB, UK*

³*Department of Mechanical Engineering, University of Southampton,
Southampton, SO17 1BJ, UK*

⁴*National Science Center “Kharkov Institute of Physics and Technology” of NAS of Ukraine,
1 Akademichna Str., Kharkiv, 61108, Ukraine
rusakova@ilt.kharkov.ua*

Samples of $\text{Co}_{0.25-x}\text{Cr}_{0.25}\text{Fe}_{0.25}\text{Ni}_{0.25}\text{C}_x$ ($x = 0; 0.01; 0.03$) high entropy alloy were studied. All samples were subjected to high-pressure torsion of 6 GPa per 1 revolution at room temperature. During torsion, the magnitude of the shear strain γ depends on the distance from the rotation axis r and can be calculated by the equation $\gamma = 2\pi Nr/h$, where N is the number of revolutions and h is the thickness of the disk.

At room temperature we measured the microhardness depending on the coordinate along the diameter of the disk (see figure). Each point in Fig. corresponds to the value of microhardness calculated from one impression. The microhardness is determined by the microstructure formed during the torsion of the sample. It is seen that significant changes in the microhardness with the coordinate took place near the central part of the disk. Closer to the periphery (at a distance of about 2 mm from the edge of the circle bounding the disk), the dependence $H_V(x)$ weakens, thereby indicating a sufficient homogeneity of the microstructure of this region.

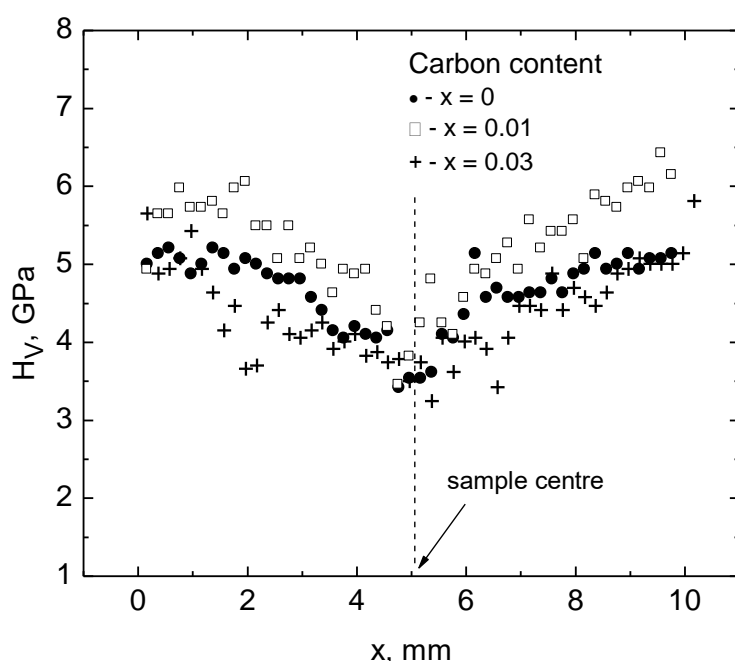


Fig. The dependence of microhardness on the coordinate along the disk diameter of the $\text{Co}_{0.25-x}\text{Cr}_{0.25}\text{Fe}_{0.25}\text{Ni}_{0.25}\text{C}_x$ alloy. Indentation load $P = 1.5$ N, loading duration $t = 10$ s, $T = 300$ K.

From Fig. it is seen that the addition of 1 at.% carbon ($x = 0.01$) into the alloy is accompanied by a remarkable increase in microhardness. At the same time, a further increase in the carbon concentration to $x = 0.03$ leads to an unexpected drop in microhardness to the level of the initial sample and even lower.

Note that for cast specimens of the $\text{Co}_{0.25-x}\text{Cr}_{0.25}\text{Fe}_{0.25}\text{Ni}_{0.25}\text{C}_x$ alloy that were not subjected to torsion a monotonic increase in microhardness is observed with an increase in carbon concentration. So, apparently, it is the torsional deformation that leads to the observed anomalous change in the microhardness. For the interpretation of the results obtained, X-ray structural analysis data were used.

Forced elasticity of amorphous polymers

V.D. Natsik, H.V. Rusakova

*B.Verkin Institute for Low Temperature Physics and Engineering of NASU, Kharkiv, Ukraine
rusakova@ilt.kharkov.ua*

Two features of the mechanical properties of amorphous solid-state polymers are discussed [1]: when cooled below a certain temperature, they pass from a state with high elasticity (elastomers) to a state of glass-like brittle solids; the elasticity of frozen polymers is restored under the action of sufficiently high mechanical stresses (forced elasticity).

The analysis of the mechanisms and kinetics of forced elasticity was carried out within the framework of the well-known model of an amorphous polymer - a macroscopic coil formed by a molecular chain [1]. It consists of a series of rigid monomer units with nanometer-scale lengths, which are connected by single valence bonds and can rotate like rods connected by hinges. In the state of thermodynamic equilibrium, random configurations of units correspond to a minimum in the energy of dispersion interaction between them and a maximum in configurational entropy. Tension deformations of the coil by external stress σ prevent and cause its reversibility by the forces of attraction between the units and thermodynamic forces due to the decrease in entropy due to straightening of the chain. The action of internal entropy stresses σ_i is the main reason for the high elasticity of amorphous polymers. The elementary kinetic unit of the deformation process is several adjacent units, and their excitation (straightening) is considered as an elementary act of highly elastic deformation. The activation of such a process in a small section of the chain under the action of the effective stress $\sigma^* = \sigma - \sigma_i$ is accompanied by overcoming a certain potential barrier $U = U_0 - v\sigma^*$, where U_0 and v are the parameters of the model. At $\sigma^* < U_0/v$ and temperature T , the kinetics of these processes is described by the Arrhenius formula for the activation frequency in the forward and reverse directions:

$$v = v_0 \left[\exp\left(-\frac{U_0 - v\sigma^*}{k_B T}\right) - \exp\left(-\frac{U_0 + v\sigma^*}{k_B T}\right) \right] = 2v_0 \exp\left(-\frac{U_0}{k_B T}\right) \operatorname{sh}\left(\frac{v\sigma^*}{k_B T}\right). \quad (1)$$

Here v_0 is the characteristic libration frequency of molecular units. When deriving the main rheological equation, which connects the consistent changes in the deforming stress $\sigma(t)$ and relative strain $\varepsilon(t)$, we represent the total strain as the sum $\varepsilon = \varepsilon_e + \varepsilon_{he}$ of elastic $\varepsilon_e(t) = M_e^{-1} \sigma(t)$ and highly elastic $\varepsilon_{he}(t)$ components, where the dependence $\varepsilon_{he}(t)$ is determined by the kinetics of the relaxation response of the polymer to the excitation of elementary deformation events by stress $\sigma^* = \sigma - \sigma_i$, and $\sigma_i = M_{he}(t)$. Here M_e and M_{he} are the unrelaxed and relaxed elastic moduli of the polymer with respect to unilateral tensile deformation. The rate of highly elastic deformation $\frac{d}{dt} \varepsilon_{he} = \dot{\varepsilon}_{he} = \epsilon_0 v(t)$ is determined by the total contribution ϵ_0 of elementary kinetic units and the frequency of their excitation $v(t)$. Using the relation $\dot{\varepsilon} = \dot{\varepsilon}_e + \dot{\varepsilon}_{he} = M_e^{-1} \dot{\sigma} + \epsilon_0 v$ and formula (1), we obtain a nonlinear differential equation:

$$\dot{\varepsilon} = M_e^{-1} \dot{\sigma} + 2\epsilon_0 v_0 \exp\left(-\frac{U_0}{k_B T}\right) \operatorname{sh}\left[\frac{v(\sigma - M_{he} \varepsilon)}{k_B T}\right]. \quad (2)$$

This rheological equation describes the regularities of deformation of disordered polymers at both high and low temperatures. When $\sigma \ll k_B T/v$, it turns into the equation of deformation of a standard linear body, which describes the properties of elastic-viscous polymers (elastomers) [1]. In the range of low temperatures and high stresses $\sigma \gtrsim k_B T/v$, its solutions make it possible to describe and interpret various nonlinear deformation effects, which are called "forced elasticity".

[1] G.M. Bartenev and Yu.V. Zelenov, Physics and Mechanics of Polymers (Vysshaya Shkola, Moscow 1983).

Microhardness of ultrafine-grained oxygen-free copper produced by hydrostatic extrusion

H.V. Rusakova, S.V. Lubenets, L.S. Fomenko

*B.Verkin Institute for Low Temperature Physics and Engineering of NAS of Ukraine,
47 Nauky Ave., Kharkiv, 61103, Ukraine
rusakova@ilt.kharkov.ua*

In studies of strength and mechanisms of plastic deformation of solids, fine-grained materials are widely used as topical subjects in view of their particular properties. To obtain such materials, various methods of severe plastic deformation are applied. These include equal-channel angular pressing, direct (DE) and equal-channel angular hydrostatic extrusion (ECAE), high-pressure torsion, a combination of the above processing methods [1-4], which make it possible to synthesize ultrafine-grained (UFG) or nanocrystalline (NC) materials with high mechanical strength. Various methods and modes of processing enable to obtain materials with significantly different properties, for the estimate of which wide microstructural and deformation studies are carried out. The purpose of the work was to use a number of advantages of the indentation method for determining the micromechanical properties of oxygen-free hydroextruded copper in the temperature range 77-300 K.

NC metals are characterized by the instability of their structural state, especially under the action of mechanical loads. Spontaneous grain growth during long-term exposure of NC material at room temperature is due to an excess of internal energy associated with grain boundaries [5].

The microstructure of oxygen-free copper subjected to direct and angular hydroextrusion is described in [6]. The average grain size of samples after DE is $\sim 0.6 \mu\text{m}$, and of samples after ECAE is $\sim 0.5 \mu\text{m}$. These samples showed higher yield strength in tensile experiments [6] compared to NC copper that is due to the texture formed as a result of extrusion.

When studying the degree of heterogeneity of extruded copper billets, it was found that in their central part the Vickers microhardness H_V is approximately 25% higher than at the periphery. The depth of the less hard near-surface layer is $\sim 2-3 \text{ mm}$ when a billet diameter is 15 mm. Copper subjected to ECAE showed a higher hardness: at room temperature the average values of $H_V \approx 1.4 \text{ GPa}$ (ECAE) versus $H_V \approx 1.3 \text{ GPa}$ (DE).

It was found that holding the extruded samples at room temperature for several years did not change their microhardness. This indicates the stability of copper with UFG structure, in contrast to nanocrystalline copper.

Microhardness of copper after ECAE is higher than the H_V of copper after DE over all temperature range of 77-300 K, and its temperature dependence is stronger. So if the difference in microhardness values at room temperature is $\sim 10\%$, at $T = 77 \text{ K}$ it is more than 20%.

- [1] V.M. Segal, V.I. Reznikov, A.E. Drobyshevskij, V.I. Kopylov, Izv. AN Soviet Union 1, 115 (1981).
- [2] V.M. Segal, Mater. Sci Eng. A 386, 268 (2004).
- [3] Y. Iwahashi, Z. Horita, M. Nemoto, T.G. Langdon, Acta Mater. 46, 3317 (1998).
- [4] T. Hebesberger, H.P. Stüwe, A. Vorhauer, F. Wetscher, R. Pippa, Acta Mater. 53, 393 (2005).
- [5] K. Zhang, J. R. Weertman, Appl. Phys. Letters 87, 061921 (2005).
- [6] N.V. Isaev, T.V. Grigorova, O.V. Mendiuk, O.A. Davydenko, S.S. Polishchuk, and V.G. Geidarov, Low Temp. Phys. 42, 825 (2016).

The effect of temperature on micromechanical properties of graphene oxide/polypropylene nanocomposite

H.V. Rusakova¹, L.S. Fomenko¹, S.V. Lubenets¹, A.V. Dolbin¹, N.A. Vinnikov¹, R.M. Basnukaeva¹, M.V. Khlistyuck¹, A.V. Blyznyuk²

¹*B.Verkin Institute for Low Temperature Physics and Engineering of NAS of Ukraine,
47 Nauky Ave., Kharkiv, 61103, Ukraine*

²*National Technical University "Kharkiv Polytechnic Institute",
2 Kyrpychova Str., Kharkiv, 61102, Ukraine
rusakova@ilt.kharkov.ua*

Among the polymers produced by industry, one of the most widely used is semi-crystalline polypropylene (PP) due to its low density, high chemical stability and relatively low cost. However, PP does not have high enough strength characteristics. The properties of neat PP can be significantly improved by adding various nanofillers, in particular graphene and its oxide.

Nanocomposite PP-0.3 wt. % graphene oxide was obtained by high-speed gradient extrusion at $T = 460$ K; samples of neat PP were subjected to similar treatment. Microindentation was performed at temperatures from 295 K to 77 K. In Figure 1, the temperature dependences of the microhardness of the samples studied in the range 175 - 295 K are given. When the temperature decreases, there is a strong increase (5 times) in the microhardness approximately according to the linear law for both the neat PP and the nanocomposite. For all temperatures, the microhardness value of the nanocomposite exceeds the microhardness value of pure PP, the maximum difference is achieved at room temperature, that is probably due to the different values of the glass transition temperature for neat PP and the nanocomposite. At room temperature, which is close to the glass

transition temperature of neat PP, there is a sharp decrease in its microhardness, while the microhardness of the nanocomposite, which has a higher glass transition temperature, retains a linear dependence on temperature.

For the neat PP ($T < 174.5$ K) and the nanocomposite ($T < 226.5$ K), the reversibility of the deformation was detected: when the load was removed and the samples were heated up to room temperature, the indenter impressions completely disappeared. This effect is obviously related to the influence of the adsorption-active medium on the formation of craze (fibrillar-porous nanostructures) with reduced glass transition temperature compared to the block polymer [1].

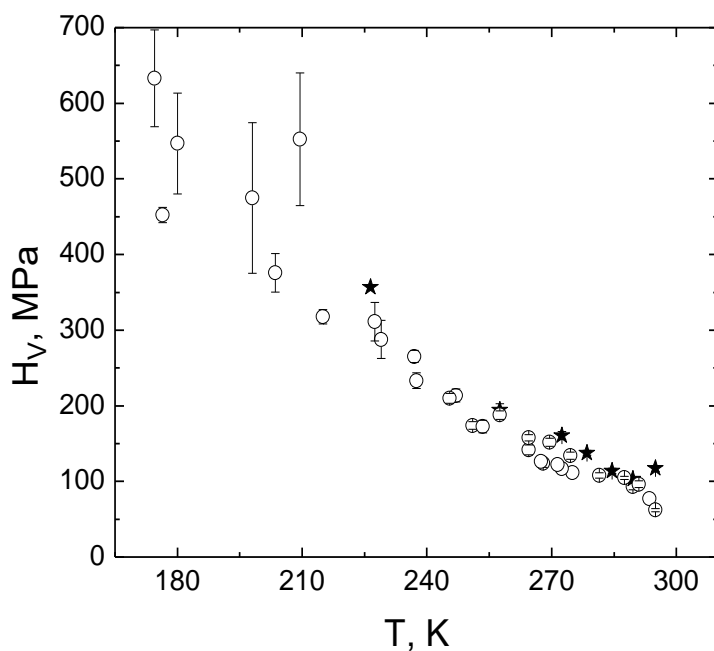


Figure 1. Temperature dependences of the microhardness of the neat PP (empty symbols) and nanocomposite PP-0.3 wt. % GO (complete symbols). $P = 0.25$ N, $t = 10$ s.

[1] A.L. Volynskii and N.F. Bakeev, Solvent Crazing of Polymers, Elsevier, Amsterdam (1995).

The effect of casting conditions on superplastic properties of the eutectic alloy Sn-38wt%Pb

Yu.O. Shapovalov¹, V.F. Korshak²

¹*B.Verkin Institute for Low Temperature Physics and Engineering of NAS of Ukraine,*

47 Nauky Ave., Kharkiv, 61103, Ukraine

²*V. N. Karazin Kharkiv National University,*

4 Svobody Sq., Kharkiv, 61022, Ukraine

shapovalov@ilt.kharkov.ua

Structural superplasticity occurs in alloys with ultrafine grains. Such a structure can be obtained during casting with a rapid crystallization. Alloys are usually treated by severe plastic deformation after casting for achieving a uniform equiaxial structure. The rapid crystallization can also be a reason for a nonequilibrium phase state formation, although as a decisive factor for superplasticity effect occurrence a grain size and grains uniformity are usually considered.

In this work, mechanical properties of the Sn-38wt%Pb were investigated, subject to crystallization conditions. Casting was performed in two ways: 1) onto a massive copper substrate with the initial melt temperature of 425°C (state **I**), and 2) to a massive copper square mold ($25 \times 25 \text{ mm}^2$) ~5 mm thick with the initial melt temperature of 450°C (state **II**). The cooling curves were received by placing a copper-constantan thermocouple junction at a distance of 1 mm from the upper (atmosphere) and bottom (substrate) surfaces in the middle of the ingot. The temperature was measured with accuracy of 0.2 K 10 times per second. The ingots were subjected to compression on a hydraulic press with reduction in thickness up to ~75%. The mechanical tests were conducted at 293 K under conditions of creep in the range of external stress $\sigma = 3 \div 16 \text{ MPa}$.

There cooling curves of the alloy for both cases are shown in fig. 1 (a, b). An average cooling rate of the melt to the eutectic temperature in the state **I** is 600 K/s, and in the state **II** is 200 K/s. During further cooling to the initial crystallization temperature the cooling rate is order of magnitude lower and becomes 60 K/s for the state **I** and 20 K/s for the state **II**. An undercooling level ΔT in the state **I** is 30 K (fig. 1a), in the state **II** $\Delta T=34$ K (fig. 1b). The crystallization runs with decrease in temperature that indicates of nonequilibrium crystallization [1]. An average grain size after compression is almost the same in both cases: 1.5 μm (**I**) and 1.4 μm (**II**).

The change in casting conditions leads to the change in maximal elongations from ~300% in the state **I** to ~200% in the state **II**. The optimal stress for superplasticity moves to lower stress region from 7.5 MPa (**I**) to 4.3 MPa (**II**). At $\sigma = 7.5 \text{ MPa}$ strain rate in the state **II** is order of magnitude higher than in the state **I**: $2 \times 10^{-4} \text{ s}^{-1}$ against $3.5 \times 10^{-5} \text{ s}^{-1}$ (fig. 1c).

It was established in a separate research that phase state of the investigated alloy is nonequilibrium. Change in casting conditions leads to the changes in the initial structural-phase state that has an effect on superplastic properties.

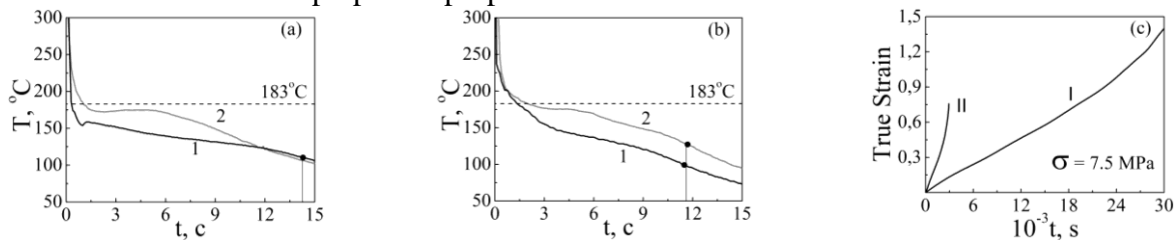


Fig. 1. Cooling curves of the Sn-38wt%Pb alloy during casting onto a massive copper substrate (a) and into a square mold in a copper substrate (b), where 1 corresponds to the bottom part of the ingot and 2 is for upper one; and deformation curves (c) of the samples produced from the ingots in state **I** and **II** respectively.

[1] Yu.M. Lahtin, Metallovedenie i Termicheskaya Obrabotka Metallov (Metallurgiya, Moscow 1983)

Some peculiarities of structural changes of the eutectic alloy Bi-43wt%Sn under conditions of superplasticity

Yu.O. Shapovalov

B.Verkin Institute for Low Temperature Physics and Engineering of NAS of Ukraine,
47 Nauky Ave., Kharkiv, 61103, Ukraine
shapovalov@ilt.kharkov.ua

The present work is devoted to the investigation of microstructure of the Bi-43wt%Sn alloy during deformation under conditions of creep at an applied constant stress σ in the range of 4.5 – 18.5 MPa. It was established that elongation to failure δ (770%) is maximum at $\sigma = 9$ MPa, and δ exceed 300% in the range of 6 – 17 MPa so the alloy demonstrate superplastic deformation (SPD).

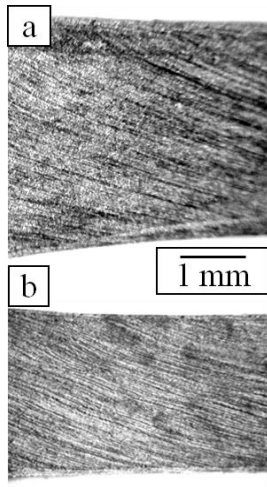


Fig. 1. Structure of samples parts of the Bi-43wt%Sn alloy deformed to failure:
a – $\sigma = 9$ MPa;
b – $\sigma = 17$ MPa

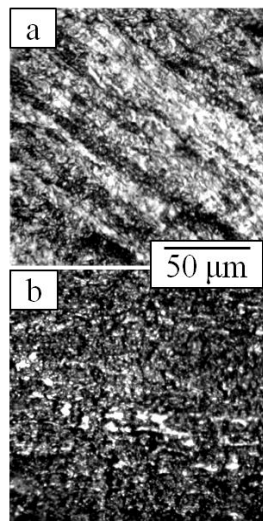


Fig. 2. Structure of the surface of the Bi-43wt%Sn alloy at different local strain ϵ : a – $\epsilon \approx 30\%$; b – $\epsilon \approx 640\%$. $\sigma = 6$ MPa

The emergence and development of a specific relief is observed on the surface of samples during deformation in the studied stress range (Fig. 1). A system of deformation macrobands at the initial stage of creep is oriented along the direction of the maximum shear stress. The orientation of the macrobands gradually approaches the direction of strain axis as the relative elongations increase, and the macrobands become less evident and finally disappear.

Mesoscopic images in fig. 2 show microstructure at different local deformation of a gage portion of the sample of the investigated alloy after tension to failure at $\sigma = 6$ MPa. Comparison of the microstructure changes during increase in local deformation and during increase in the same nominal deformation of a whole sample supposed to be reasonable because at SPD the deformation is quasiuniform and the stresses at different parts of the sample although become higher are still in the range where SPD is possible.

As for the lower local deformation, there are very little changes occur in structure in these parts due to high strain-rate sensitivity and much lower strain rates. It is seen in fig. 2 that at the initial stage of creep narrow regions (10-25 μm width) are subjected to deformation process and separated by wide zones of undeformed material. Localized deformation bands (LDB) are directed at an angle close to 45° to the strain axis. Further development of the deformation process leads to the expansion of the LDB into the region of the undeformed material. At a certain stage of the flow almost all material is involved in the deformation process except separate small regions (fig. 2b).

The present results are in good agreement with the earlier obtained data on the alloy Sn-38wt.%Pb [1] and could be explained by the interdependence of plastic deformation processes and deformation induced structural-phase changes (decomposition of Sn-based supersaturated solid solution of Bi and dynamic recrystallization). Initial nonequilibrium phase state of the investigated alloy was established in the previous investigation [2].

[1] V.F. Korshak, A.P. Krysztal', Yu.A. Shapovalov, A.L. Samsonik, Phys. Met. Metallogr. 110, 385 (2010).

[2] V.F. Korshak, P.V. Mateychenko & Yu.A. Shapovalov Phys. Met. Metallogr. 115, 1249 (2014).

Low-temperature physical and mechanical properties of high-entropy alloy $\text{Fe}_{50}\text{Mn}_{30}\text{Co}_{10}\text{Cr}_{10}$

**T.V. Hryhorova¹, S.E. Shumilin¹, Yu.O. Shapovalov¹, Yu.O. Semerenko¹, S.N. Smirnov¹,
O.D. Tabachnikova¹, M.A. Tikhonovsky³, A.V. Levenets³, M.I. Zehetbauer², E. Schafler²**

¹*B.Verkin Institute for Low Temperature Physics and Engineering of NAS of Ukraine,
47 Nauky Ave., Kharkiv, 61103, Ukraine*

²*University of Vienna, Nanocrystalline Materials Department,
Strudlhofgasse 4, Wien, AT-1090 Austria*

³*National Science Center Kharkov Institute of Physics and Technology,
1 Akademichna St., Kharkov, 61108, Ukraine
shapovalov@ilt.kharkov.ua*

The work investigated the low-temperature mechanical and acoustic properties of the nonequiatomic high-entropy alloy (HEA) $\text{Fe}_{50}\text{Mn}_{30}\text{Co}_{10}\text{Cr}_{10}$. In this HEA during plastic deformation, a transformation of the martensitic type occurs - from the fcc to the hcp phase, which leads to an increase in the plasticity of the alloy. This effect, known in the literature as "transformation induced plasticity" (TRIP), is significantly influenced by the deformation temperature [1]; therefore, it is of particular interest to study the mechanical properties of TRIP alloys at low and ultralow temperatures, where systematic data are currently lacking.

In a wide temperature range (from room temperature to a record low temperature of 0.5 K), the regularities of the plastic deformation \square of the alloy during uniaxial tension of the samples at a constant rate were experimentally studied. Information on the phase composition and microstructure of the alloy at different deformation and temperatures of deformation was obtained by methods of X-ray diffraction analysis and electron microscopy. Also, in the temperature range of 5–415 K, the temperature dependences of acoustic absorption and dynamic modulus of elasticity for an undeformed alloy are obtained.

It was found that as the deformation temperature T decreases from 295 to 4.2 K, strong strengthening is observed in the investigated HEA. Thus, the increase in the yield point $\sigma_{0.2}$ is 160% (from 233 to 612 MPa), and the ultimate strength σ_U at 4.2 K is 2074 MPa. The most interesting and important result is that in the entire investigated temperature range, along with high strength (see Table), high ductility of ~35–40% is observed in the alloy. Note that at the cryogenic temperatures the nature of plastic deformation changes from smooth to serrated flow. In addition, in the temperature range 0.5–4.2 K, an anomalous phenomenon was found - a decrease in the yield stress with decreasing temperature.

It was found that as the temperature rises from 5 to 415 K the dynamic Young's modulus of an undeformed HEA decreases monotonically and almost linearly from 244 to 202 GPa, while the acoustic absorption increases monotonically and has a wide peak at 350 K, which corresponds to a blurred step on the temperature dependence of the dynamic elastic modulus. It is shown that the acoustic properties of an undeformed HEA in the investigated temperature range do not have features characteristic of structural-phase rearrangements.

The paper discusses the physical mechanisms responsible for the observed low-temperature features of the investigated HEA.

Table

T, K	295	77	30	4,2	0,5
$\sigma_{0.2}$, MPa	233	457	586	612	545
σ_U , MPa	1066	1909	1983	2074	1832
ε	0.39	0.36	0.35	0.35	0.40

[1] Z. Li, D. Raabe, JOM, 69, 11, (2017).

Thermoactivated amplitude-dependent dislocation internal friction in deformed samples of pure magnesium

P.P. Pal-Val¹, O.M. Vatazhuk¹, A.A. Ostapovets², L. Král², J. Pinc³

¹*B.Verkin Institute for Low Temperature Physics and Engineering of NAS of Ukraine,
47 Nauky Ave., Kharkiv, 61103 Ukraine*

²*Institute of Physics of Materials, Czech Academy of Sciences, Žižkova 22,
Brno, 61662 Czech Republic*

³*Institute of Physics, Czech Academy of Sciences, Na Slovance 2, Prague 8, 18221 Czech Republic
vatazhuk@ilt.kharkov.ua*

Dislocation motion in crystals containing impurities in most cases is controlled by thermally activated unpinning of dislocations from weak pinning centers. Experimental study of the thermoactivated dislocation motion is therefore one of the most important tasks of physics of strength and plasticity. Of particular interest, these studies are due to the possibility of changing the mechanisms that control the dislocation movement, especially in the range of low temperatures. Studying the dislocation motion using mechanical tests does not provide sufficient accuracy to identify the fine details of the dislocation interaction with the pinning centers due to possible irreversible changes in the dislocation structure of samples. Acoustic spectroscopy methods, on the contrary, make it possible to study the same processes in a wide range of temperatures and stresses more precisely and in a non-destructive manner.

Two sets of 99.95% pure Mg samples were studied. The samples of the first type were rolled at room temperature up to 20% of total plastic deformation value. The samples of the second type were obtained by the warm extrusion at 300°C with extrusion ratio 10:1 and deformation rate 5 mm/s. The samples were characterized by EBSD technique using electron microscope equipped with EBSD detector. Average grain sizes in rolled and extruded samples were 49 μm and 15 μm, respectively. The samples have strong crystallographic texture that can be characterized by the basal planes aligned with the rolling or extrusion directions.

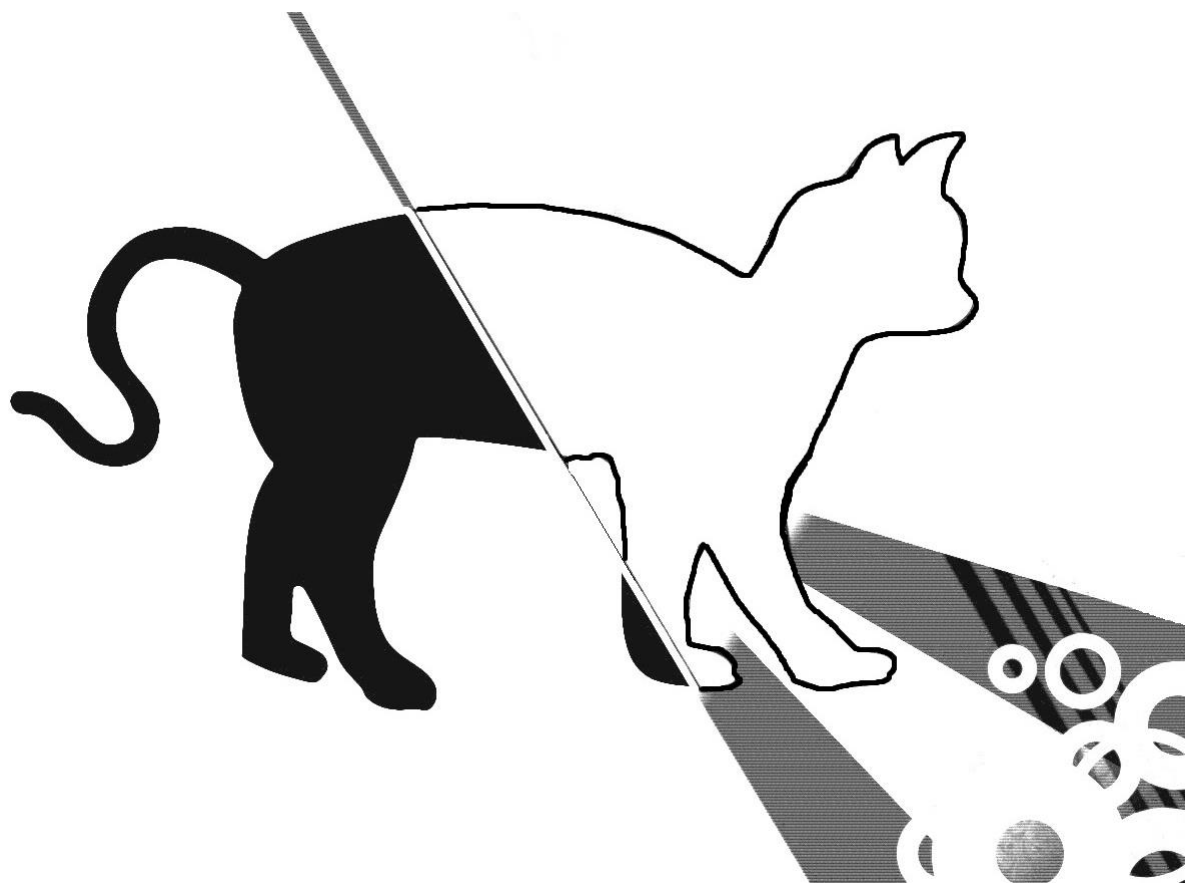
Investigations of the acoustic properties of Mg in the frequency range 50 - 350 kHz were performed by the two-component composite vibrator technique. Longitudinal standing waves were excited in the samples by piezoelectric quartz transducers [1]. Measurements of the logarithmic decrement δ , and the dynamic Young's modulus E were carried out at the resonant frequencies of the composite vibrators in the temperature range 50.5 - 310 K.

Over a certain critical deformation amplitude ε_{0c} , distinctive increase of the values of δ and E was observed when measuring the amplitude dependences $\delta(\varepsilon_0)$ and $(\Delta E/E)(\varepsilon_0)$. When increasing temperature from 50.5 K to 250 K, the critical amplitude ε_{0c} decreases monotonically. After that, ε_{0c} stops or even shifts to the higher amplitudes, i.e., a non-monotonic changes in $\varepsilon_{0c}(T)$ are observed. Qualitatively, the same behavior of $\varepsilon_{0c}(T)$ was observed for the rolled samples, but the anomalous behaviour was observed near 180 K as opposed to 250 K for extruded samples.

The most probable reason for the observed amplitude dependence is the nonlinear effects associated with the motion of dislocations through local potential barriers created by point defects in crystals. Analysis of the results obtained shows that at low enough temperatures the experimental data may be described within the Indenbom-Chernov theory of the thermally activated dislocation hysteresis [2]. The agreement of the theory with experiment makes it possible to determine the main quantitative characteristics of the process of overcoming the pinning centers by dislocations. The data obtained at temperatures above 250 K for the extruded samples and 180 K for the rolled samples may confirm the change of the microscopic mechanism that governs the dislocation motion in the deformed magnesium in the vicinity of these temperatures.

[1] V.D. Natsik, P.P. Pal-Val, S.N. Smirnov, *Acoust. Phys.*, 44, 553 (1998).

[2] V.L. Indenbom, V.M. Chernov, *Phys. Stat. Sol. (a)*, 14, 347 (1972).



THEORY OF CONDENSED MATTER PHYSICS

Schrödinger-cat states generation via mechanical vibrations entangled with a charge qubit

O.M. Bahrova¹, L.Y. Gorelik², S.I. Kulinich¹

¹*B.Verkin Institute for Low Temperature Physics and Engineering of NAS of Ukraine,
47 Nauky Ave., Kharkiv, 61103, Ukraine*

²*Department of Physics, Chalmers University of Technology, SE-412 96 Göteborg, Sweden
bahrova@ilt.kharkov.ua*

Nanoelectromechanical (NEM) devices are in the spotlight of state-of-the-art technology as well as fundamental condensed matter physics. Recent advantages in nanotechnologies acquire a promising platform for studying the phenomena generated by the interplay between mechanical and electronic subsystems. Systems which dynamics are determined by the mutual influence of superconducting quantum bit and nanomechanical resonator, belong to a hot topic of research in quantum computing science.[1,2]

We have considered a NEM system that consists of the superconducting nanowire which is suspended between two bulk superconductors and capacitively coupled to the two gate electrodes.[3] The suspended superconducting nanowire modelled as a movable Cooper-pair box (CPB) coupled to the leads via tunneling processes. A CPB is a charge qubit whose basic state are two charge state – states which represent the presence or absence of the excess Cooper pair on the superconducting dot. The bending oscillations of the nanowire are described by the harmonic oscillator. The bias voltage applied between the superconducting leads induces the time evolution of superconducting phase difference according to the Josephson relation. It leads to the fact that mechanical vibrations come to be highly affected by qubit dynamics. The perturbation theory over the electromechanical coupling induced by the electrostatic force is used.

We demonstrate that due to the bias voltage applied between superconducting electrodes, the initial pure state of the system evolves in time into the charge qubit states entangled with coherent states of harmonic oscillator. Moreover, we suggest simple bias voltage manipulation protocol that results in the formation of the entanglement between the qubit states and so-called Schrödinger-cat states (i.e. the superposition of coherent states) of nanomechanical resonator. To characterize the organization and evolution of such states, we calculate the entropy of entanglement and the corresponding Wigner function. In addition, the time-averaged Josephson current is considered. The examined phenomena may be employed in quantum communications for the encoding quantum information from charge qubit into a superposition of the coherent mechanical states.

- [1] S.M. Girvin, Phys.Rev.Lett. 123, 250501 (2019).
- [2] S.M. Girvin, arXiv: 1710.03179v1 [quant-ph] (2017).
- [3] O.M. Bahrova, L.Y. Gorelik, S.I. Kulinich, Fiz.Nizk.Temp. 47, №4, 315 (2021).

Depending on the angle of the functionalization of twisted graphene

A.A. Belosludtseva, Y.A. Chymakov, N.G. Bobenko

*Institute of Strength Physics and Materials Science of Siberian Branch of Russian Academy of Sciences (ISPMS SB RAS),
2/4, pr. Akademicheskii, Tomsk, 634055, Russia
anna.bel@ispms.tsc.ru*

Twisted graphene, wherein structure is determined by the rotation angle of the graphene layers relative to each other, has only attracted attention recently, compared to the well-studied single-layer graphene. Rotation, as a new degree of freedom, leads to the dependence of the properties on the rotation angle of the twisted bigraphene. The surface of such a material is divided into areas with AA, AB stacking and turbostratic structures, which the ratio is determined by the rotation angle.

Experimental studies [1] and theoretical calculations [2] have shown that the fluorination and hydrogenation of the surface of twisted graphene is uneven. There are adsorption centers determined by the rotation angle. It was shown [2] that adsorption centers will be AA and AB structures for rotation angles 0-16 and 44-60 degrees, and it will be fullerene-like structures C48 and C72 at twisted angles of 16-44 degrees. Determination of correlation between the relation of different types areas (AA and AB) and rotation angle is important to create a material with a given concentration of adsorbed atoms.

We have created software using dynamic modeling to construct the crystal lattice of twisted graphene, with the ability to set the lattice size, rotation angle, and determine the sizes of areas with AA and AB stacking with different accuracy. The results of calculating the dependence of the relative areas of AA and AB areas on the angle are shown in Figure 1. It is shown that the number of AA and AB areas is minimal at rotation angle 20-40 degrees. They change abruptly in the ranges from 0 to 1 and 59 to 60 degrees. Thus, the best functionalization by fluorine and hydrogen of twisted graphene will be at rotation angles of 0-16 and 44-60 degrees.

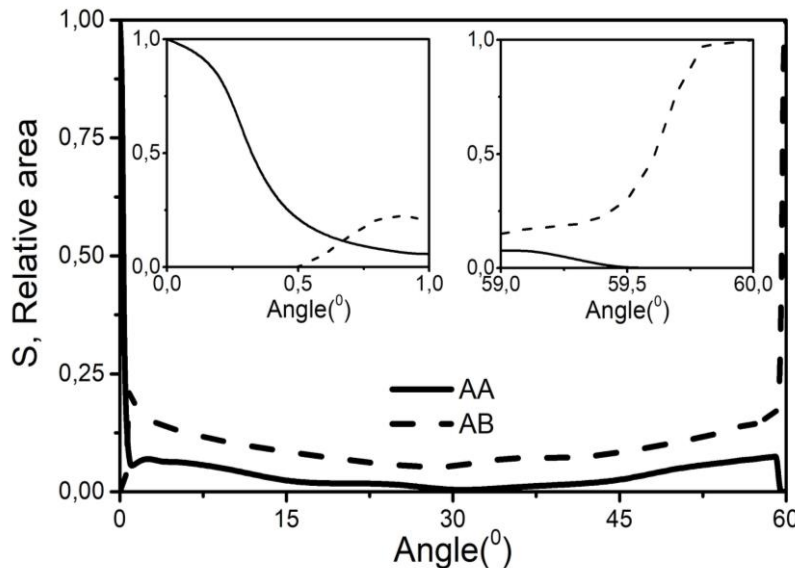


Figure 1 - Dependence of the ratio areas of different types on the rotation angle in twisted graphene.

The study was supported by a grant Russian Science Foundation (project № 20-72-00138)

- [1] J.E. Weis, S.D. Costa, O. Frank, Z. Bastl and M. Kalbac, Chem. Eur. J. 21, 1081-1087 (2015)
[2] A.R. Muniz and D. Maroudas, J. Phys. Chem. 117, 7315-7325 (2013).

Resonant modes in cavity layered microwave resonator with axial symmetry

Z.E. Eremenko, I.N. Volovichev, A.A. Breslavets

*O. Ya. Usikov Institute for Radiophysics and Electronics of NAS of Ukraine,
12 Ac. Proskura St., Kharkiv, 61085, Ukraine
zoya.eremenko@gmail.com*

The study of bulk microwave resonators with random inhomogeneities of shape or/and volume is an urgent problem because there is currently no strict theory that can describe electrodynamic processes in microwave resonators with random inhomogeneities. Spherical shape dielectrics have been studied in numerous papers. Some of them study electromagnetic problem in a dielectric sphere with an eccentric spherical dielectric [1].

We present both a computational method and the theory it is based on, which allow calculating the frequency spectrum of axially symmetric resonators. In this report, we consider as an example a layered spherical cavity resonator with a constant permittivity of each layer. The permeability of the layers is equals unity. The considered resonator structure is surrounded by a perfect metal. Dielectric losses are neglected.

To reduce the number of variables in the problem, the electromagnetic field in each layer is described using the Hertz functions [2] in the form of a superposition of spherical waves — eigenmodes of the uniform spherical resonator. Moreover, each eigenmode of the system is presented as a sum of transverse electric (TE) and transverse magnetic (TM) components.

The equality of the tangential components of the electric and magnetic fields on the inner sphere must be met. In this paper, we propose to use a common coordinate system with reference at the center of the inner sphere. This choice allows us to obtain simple analytical boundary conditions (BCs) for matching fields on the inner sphere.

The main feature of the proposed method is the way the BCs on the outer sphere are formulated. The BCs are stated at a given number of points on the boundary. At each of the points the physical requirements of vanishing of the tangential components of the electric field at the interface between a dielectric and perfect metal are fulfilled. The necessary number of BCs to write down the characteristic equation is formulated as a weighted sum of BCs at these points. This approach eliminates the need for numerical integration over the surface of the outer sphere and avoids the difficulties due to round-off errors. We present a detailed discussion of these issues, as well as the optimal number and selection criteria for the points on the surface and the weight coefficients. The described procedure provides the characteristic equation, the roots of which are found numerically. The developed theory and software were verified by comparing the results for a model problem calculated by our approach with the frequency spectra computed by CST Microwave Studio. It is the powerful simulation platform for all kinds of electromagnetic field problems and related applications. The sensitivity of the resonator eigenfrequencies to the size and the offset of the inner sphere is investigated. It is confirmed that violation of the central symmetry of the problem (displacement of the inner sphere) leads to hybridization of axially non-uniform eigenmodes of the resonant system. There exist only axially uniform TE and TM eigenmodes in this case.

The advantage of the developed method is the reduction in the required computing resources. In addition, the proposed approach allows one to separate *a priori* the degenerated resonances in the spectrum. This avoids difficulties related to rounding errors for close eigenfrequencies when computing the statistical properties of the spectrum and studying the wave chaos in the system.

[1] F. Vervelidou and D. Chrissoulidis, J. Opt. Soc. Am. A, Vol. 29, No. 4, 605 (2007).

[2] J. Stratton, Electromagnetic Theory (Wiley, 2007).

Nonlinear thermoelectric properties of a magnetic single-electron shuttle

O.A. Ilinskaya¹, I.V. Krive¹, R.I. Shekhter²

¹*B.Verkin Institute for Low Temperature Physics and Engineering of NAS of Ukraine,
47 Nauky Ave., Kharkiv, 61103, Ukraine*

²*Department of Physics, University of Gothenburg, SE-412 96, Göteborg, Sweden
ilinskaya@ilt.kharkov.ua*

In recent years, nanostructured thermoelectrics are actively studied both theoretically [1] and experimentally [2]. In this talk, we theoretically investigate nonlinear thermoelectric properties of a magnetic single-electron shuttle device [3]. In an electron shuttle [4], a quantum dot transfers electrons from the source electrode to the drain one by its periodical motion.

The model considered is the following: a movable single-level quantum dot is tunnel coupled to the leads kept at different temperatures and chemical potentials. The leads are fully spin-polarized in opposite directions, and a spin blockade of an electric current is lifted by an external magnetic field applied perpendicular to the plane of the electrodes' magnetization. An interplay of Coulomb and exchange forces, acting on the dot, leads to an interesting behavior of the shuttle amplitude as a function of the bias voltage, which implies peculiarities in current-voltage characteristics such as negative differential conductance [5]. These peculiarities influence the voltage dependence of the differential Seebeck coefficient which is defined as [6]

$$S_d = - \left(\frac{\partial V}{\partial \delta T} \right)_I = - \left(\frac{\partial I}{\partial \delta T} \right)_V \left/ \left(\frac{\partial I}{\partial V} \right)_{\delta T} \right. ,$$

where V and δT are the bias voltage and the temperature difference and I is the electric current. Large values of Seebeck coefficient which we found are important for high-efficient thermoelectrics.

- [1] G. Benenti, G. Casati, K. Saito, R.S. Whitney, Phys. Rep. 694, 1 (2017).
- [2] S. Yazdani and M.T. Pettes, Nanotechnology 29, 432001 (2018).
- [3] S.I. Kulinich, L.Y. Gorelik, A.N. Kalinenko, I.V. Krive, R.I. Shekhter, Y.W. Park, M. Jonson, Phys. Rev. Lett. 112, 117206 (2014).
- [4] L.Y. Gorelik, A. Isacsson, M.V. Voinova, B. Kasemo, R.I. Shekhter, M. Jonson, Phys. Rev. Lett. 80, 4526 (1998).
- [5] O.A. Ilinskaya, D. Radic, H.C. Park, I.V. Krive, R.I. Shekhter, M. Jonson, Physica E: Low-dimensional Systems and Nanostructures 122, 114151 (2020).
- [6] U. Eckern and K.I. Wysokinski, New J. Phys. 22, 013045 (2020).

Strong drag force fluctuations in disordered ensembles of scatterers and effects of nonlinear dynamical screening

O.V. Kliushnichenko, S.P. Lukyanets

*Institute of Physics, Nat. Acad. of Sci. of Ukraine,
46 Nauky Ave., Kyiv, 03028, Ukraine
kliushnichenko@iop.kiev.ua*

We consider the nonequilibrium correlations and interactions between constituent particles of a bunch or pulsed beam, arising in course of its motion through a medium, or under the scattering of particle stream on a cluster or finite cloud of impurities. Formally, these correlations are determined by the effect of dynamical screening [1,2]. The induced correlations and dynamical friction forces on impurity bunch are manifested most pronouncedly in the case of collective dynamical screening effect and are enhanced in the case of a nonlinear medium when strong local fluctuations of scattered field begin to act as additional scattering elements along with impurities. Due to the spatial finiteness of impurity clusters, the main contribution to the average quantities can be from the heavy tails of probability density distribution function [3]. Besides, collective scattering effects essentially depend on the degree of spatial impurity disorder within a cluster [4]. We focus on effects provoked by the collective scattering on randomly inhomogeneous structures and by the presence of local fluctuations. The presence of strong fluctuations of the scattered field is shown to give rise to strong local fluctuations of nonequilibrium forces acting on certain particles within the impurity cluster that can be a precursor of the dynamical instability of the cluster. It is manifested in the peculiar behavior of the tails of the probability distribution function of the local drag force [5]. The description of the impurity cluster in terms of effective parameters breaks down due to the presence of such fluctuations.

- [1] O.V. Kliushnichenko, S.P. Lukyanets, J. Exp. Theor. Phys. 118, 976 (2014).
- [2] O.V. Kliushnichenko, S.P. Lukyanets, Phys. Rev. E 95, 012150 (2017).
- [3] I.M. Lifshitz, S.A. Gredeskul, and L.A. Pastur, Introduction to the Theory of Disordered Systems (Nauka, Moscow 1982; Wiley, New York 1988).
- [4] O.V. Kliushnichenko, S.P. Lukyanets, Phys. Rev. E 98, 020101(R) (2018).
- [5] O.V. Kliushnichenko, S.P. Lukyanets, arXiv: 2012.09266 (2020).

Studying the magnetic peculiarities of the frustrated spin chain using the effective model without frustration

O.O. Kryvchikov

*B.Verkin Institute for Low Temperature Physics and Engineering of NAS of Ukraine,
47 Nauky Ave., Kharkiv, 61103, Ukraine
Kryvchikov@ilt.kharkov.ua*

The magnetism of numerous Co-based and Cu-based compounds, such as $\text{Na}_2\text{Co}_2(\text{C}_2\text{O}_4)_3(\text{H}_2\text{O})_2$, $\text{ACo}_2\text{V}_2\text{O}_8$ ($\text{A}=\text{Ba, Sr}$), Li_2CuO_2 , LiCuSbO_4 , LiCuVO_4 , $\text{Li}_2\text{ZrCuO}_2$, $\text{Rb}_2\text{Cu}_2\text{Mo}_3\text{O}_{12}$ etc. could be described by the Heisenberg model on the zigzag ladder[1]. These compounds have been a major focus for researchers in recent times due to their promising applications in next-generation memory devices, sensors, microwave devices, battery materials, and so on. The magnetic properties of the ladder in the case of the antiferromagnetic exchange interaction between spins were studied. We consider the spin-1/2 Heisenberg XXX model on the chain of finite length that consists of triangles. Each triangle of the chain is connected by the two vertices with their neighbor triangles. The spins are located on the sites of the triangles. The triangular geometry and antiferromagnetic interaction lead to the geometrical frustration of the system. The global minimum of the energy cannot be obtained by minimization of the local minimum of energies for each site and the system has a highly degenerate ground state. In general, that makes the analytical approach very hard for this class of systems[2,3]. Recently, approximate numerical methods such as density matrix renorm group (DMRG) became the practical tool to study such ladders. The state of the system could be represented by a vector in a Hilbert space. The dimension of the space increases exponentially with the number of spins. DMRG is based on the reducing dimension of the Hamiltonian space while maintaining its lowest energy states. The algorithm allows calculating the ground state and the correlation functions between particles of frustrated quantum systems up to several hundreds of particles.

Based on the calculations of the DMRG the ground state and the lowest energy states of different spin sub-spaces of the Hamiltonian were found. Using the dependence of the energy states on the external field for each spin quantum number the magnetization of the system was obtained. To analyze the magnetic peculiarities of the system an effective model with similar properties was built. This model has no frustrations and can be studied by analytical methods. The magnetic peculiarities of the model were studied and compared with the result that was get using the DMRG method. The dependence of the magnetization on the external field has 2 areas of growth and plateau. The parameters of the curve could be described by the parameters of the effective model. It is interesting that in this particular case the properties of frustrated system can be qualitatively described by the system without frustration.

- [1] M. Kurmoo, Chem. Soc. Rev. V.38, 1353 (2009).
- [2] V.O.Cheranovskii, V.V.Slatin, E.V.Ezerskaya, A.L.Tchougréeff, R.Dronskowski, Crystals V.9, 251 (2019).
- [3] V.O.Cheranovskii, V.V.Slatin, A.L.Tchougréeff, R.Dronskowski, J. Phys.: Condens. Matter 31, 305601 (2019).

Thermal coulomb drag between quantum wires hosting 1D wigner crystals

M.V. Mazanov¹, S.S. Apostolov^{1,2}

¹*V. N. Karazin Kharkov National University, 61077 Kharkov, Ukraine*

²*A. Ya. Usikov Institute for Radiophysics and Electronics NASU, 61085 Kharkov, Ukraine
mazanovmax@gmail.com*

The one dimensional (1D) electron systems which form in nanowires, nanotubes, nanostrings etc. are of special interest due to their unusual properties. The main paradigm usually applied to such systems is the Luttinger liquid model [1]. However, the elementary excitations in the Luttinger liquid, which are the waves of electron density, do not interact, leading to the lack of the equilibration. For the special conditions, the electron system can be considered in terms of the so-called Wigner crystal [2], which is a limiting case of the nonlinear Luttinger liquid when the liquid crystallizes, and the phonons within it (which are plasmons) have finite relaxation rate. Such crystals represent unique nearly-integrable quantum systems with unusual regimes of conductance and electronic thermalization [3,4].

In work [4] the main focus was on finding the thermal conductance and the dynamics of electron thermal quench relaxation in a single gated quantum wire hosting 1D Wigner crystal. It was found that the leading process, which renders relaxation time finite, is the “two-into-two” plasmon scattering when the plasmon spectrum nonlinearity is considered. A size effect was found for the thermal conductance of the crystal, governed by the interaction-induced inelastic plasmon relaxation length, which was found to obey T^5 -temperature dependence.

In the present work, we study the effect of thermal Coulomb drag between two close parallel quantum wires coupled by the inter-wire electron interaction. When one of the wires is thermally biased, hot plasmons in this biased wire scatter via inter-wire electron interactions into plasmons in the unbiased wire driving it to oppositely biased state. Treating the intra-wire interaction similar to the previous work [1] and accounting for the leading inter-wire “one-into-one” plasmon scattering process, we derive analytic expressions for the thermal Coulomb drag factor in the first order of the temperature bias and analyze it for the different regimes. In particular, we find two distinct temperature regimes for the inter-wire plasmon scattering, with transitional temperature T_2 governed by the parameter (Δ/a) , where Δ is the inter-wire distance and a is the lattice constant. For the thermal Coulomb drag factor χ , we obtain scaling behavior as depicted in Fig.1: at low temperatures $T \ll T_1$ (where T_1 is determined by the ratio of effective intra- and inter-wire plasmon scattering lengths), χ scales as T^2 and is determined by intra-wire scattering amplitude, while at high temperatures $T \gg T_1$, χ decreases by power law, changing the exponent at transitional temperature T_2 (where T_2 is inversely proportional to the inter-wire distance). The maximum thermal Coulomb drag factor χ_{max} saturates for long wires and is of the order of 1.

We gratefully acknowledge support from the National Research Foundation of Ukraine, Project No. 2020.02/0149 “Quantum phenomena in the interaction of electromagnetic waves with solid-state nanostructures”.

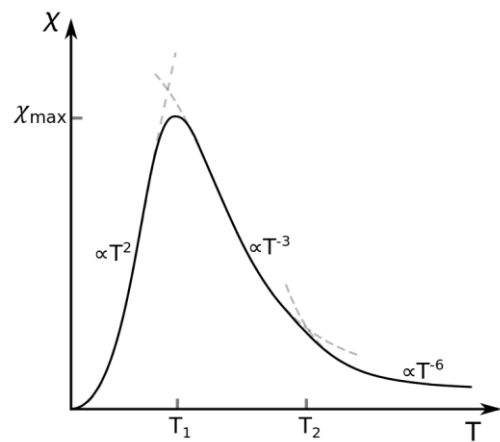


Fig. 1. The scaling dependence of thermal Coulomb drag factor χ on the temperature.

- [1] F. D. M. Haldane, J. Phys. C 14, 2585 (1981).
- [2] J. S. Meyer and K. A. Matveev, J. Phys.: Condens. Matter 21, 023203 (2009).
- [3] J. Lin, K. A. Matveev, M. Pustilnik, Phys. Rev. Lett. 110, 016401 (2013).
- [4] S. Apostolov, D. E. Liu, Z. Maizelis, A. Levchenko, Physical Review B 88, 045435 (2013).

Propagation and intensity-dependent focusing of THz laser radiation in layered superconductors

H.V. Ovcharenko¹, Z.A. Maizelis^{1,2}, S.S. Apostolov^{1,2}

¹*V.N. Karazin Kharkov National University, 4 Svobody Sq., Kharkiv, 61022, Ukraine*

²*O.Ya. Usikov Institute for Radiophysics and Electronics NASU,*

12 Ac. Proskura st., Kharkiv, 61085, Ukraine

greg.ovcharenko@gmail.com

Family of high-temperature cuprate layered superconductors are of high interest for both experimental and theoretical investigations. Mainly the interest is related to the nonlinear Cooper pairs tunneling effect between layers of superconductor, namely, Josephson effect. The so-called Josephson plasma waves can propagate inside the layered superconductors and can be described using coupled sine-Gordon equations for gauge-invariant phase difference of order parameter [1]. These waves can give origin to a number of nonlinear effects, such as self-focusing of electromagnetic waves, stimulated transparency, stopping of light, etc. The theoretical investigations show that strong nonlinear effects take place even for the relatively low intensity when frequency of radiation is close to Josephson plasma frequency. In particular, the theoretical studies show the existence of the nonlinear localized Josephson plasma waves [2] and the amplitude-dependent reflectance and transmittance of layered superconductor slabs [3]. It should be noted that the most of the theoretical investigations deal with a plane wave incident on the infinite slab of layered superconductor. However, from experimental perspectives it is more relevant to use THz laser radiation. Therefore, the model of the plane wave cannot correctly describe the laser propagation inside of the superconductor slab, because of finite sizes of laser beam cross-section.

In the present investigation we use the sine-Gordon equations to describe the nonlinear propagation of Gaussian laser beam inside the layered superconductor. Despite of the nonlinearity, we show that electromagnetic field inside of the slab can be presented as a superposition of two nonlinearly interacting, forward and backward propagating waves. We show that in main approximation these waves are also Gaussian, but their parameters, such as amplitude, width, phase and curvature are changing nonlinearly. Using assumption of weak nonlinearity, we obtained set of equations, describing evolution of these quantities. As a result, we get the dependence of transmittance on amplitude, which qualitatively agrees with the one obtained for plane waves in [3]. Main result, obtained in this investigation, is the intensity-dependent focusing of laser beam transmitted through the layered superconductor. We analyze the focal distance and the focal-spot radius as the functions of both amplitude and frequency of radiation and observed strong focusing effect for high enough amplitudes and for the frequencies, close to the Josephson plasma frequency.

To investigate focusing effect more accurately, we support our theoretical results by the numerical simulations. In the simulations we verify and confirm the dependence of focal-spot radius and focal length on the amplitude of the beam from our analytical solution. This allows us to expect these focusing effects in real experimental setups.

We gratefully acknowledge support from the National Research Foundation of Ukraine, Project No. 2020.02/0149 “Quantum phenomena in the interaction of electromagnetic waves with solid-state nanostructures”.

[1] S. Savel’ev, V. A. Yampol’skii, A. L. Rakhmanov, F. Nori, Rep. Prog. Phys. 73, 026501 (2010).

[2] S.S. Apostolov, D.V. Kadygrob, Z.A. Maizelis, A.A. Nikolaenko, V.A. Yampol’skii, Low Temperature Physics 44, 238 (2018).

[3] T. N. Rokhmanova, S. S. Apostolov, Z. A. Maizelis, V. A. Yampol’skii, F. Nori, Phys. Rev. B 88, 014506 (2013).

Ideal Bose gas in steep traps

A. Rovenchak, Yu. Krynytskyi

*Department for Theoretical Physics, Ivan Franko National University of Lviv,
12 Drahomanov St., Lviv, 79005, Ukraine
andrij.rovenchak@gmail.com*

We report the results of studies of the ideal Bose gas thermodynamics in one-dimensional traps having a steep shape, $U(x) = U_0 \exp[(x/a)^b]$. We consider this trap on the half-line $x > 0$ with a hard wall at the origin. While a rapid growth of the potential curve suggests significant similarities with a rigid box, the properties of the respective trapped systems appear more interesting as shown below.

Using the approach from [1], for a particle of mass m we can obtain the following asymptotic expression for energy levels in such potentials:

$$E_n = \frac{\hbar^2}{2m} \left(\frac{\pi(n + \frac{3}{4})}{a} \right)^2 \left[\frac{2}{b} W \left(\frac{b}{2} \left(\frac{2}{e} \frac{\hbar}{\sqrt{2mU_0}} \frac{\pi(n + \frac{3}{4})}{a} \right)^b \right) \right]^{-2/b},$$

where $W(z)$ is the Lambert W function solving the equation $We^W = z$.

We calculate thermodynamic functions of the ideal Bose gas using both the semiclassical expressions with the space region within classical turning points [2] and direct summations over energy levels. While in power-law traps $\sim x^\eta$ an effective space dimensionality is constant, $D_{\text{eff}} = 1 + 2/\eta$, cf. [2,3], for more complex potentials a dependence of D_{eff} on temperature can be expected. Such a situation, in turn, creates a richer thermodynamics picture as shown in Figure below with the specific heat as an example.

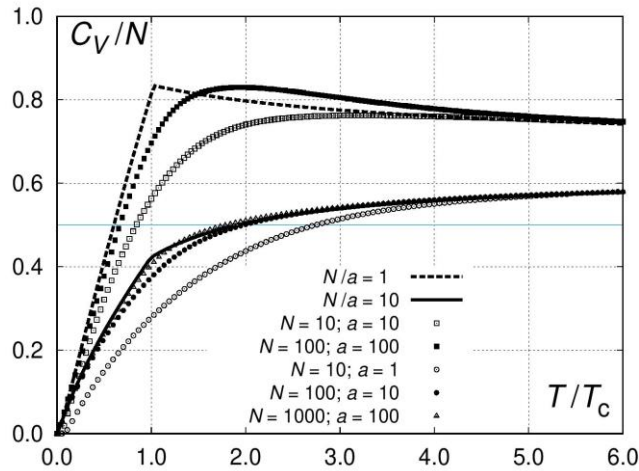


Figure: Specific heat of the ideal Bose gas in a simple exponential potential ($b = 1$) for several values of the parameter a and the number of particles N . The units are chosen so that $k_B = 1$, $\hbar^2/2m = 1$, and $U_0 = 1$. Lines correspond to the thermodynamic limit while points stand for different values of a and N obtained using direct summations. Note that – as expected – they approach the respective limiting curves as N grows.

In the thermodynamic limit, cusps are observed on the temperature dependences of the specific heat at some critical temperature T_c corresponding to the fugacity $z = 1$ as for an ordinary 3D Bose gas. We thus expect the Bose–Einstein condensation to occur in 1D systems trapped by steep potentials. Detailed studies of this phenomenon are under way.

- [1] Yu. Krynytskyi and A. Rovenchak, Asymptotic estimation for eigenvalues in the exponential potential and for zeros of $K_{iv}(z)$ with respect to order, arXiv:2103.01732 (2021).
- [2] V. Bagnato and D. Kleppner, Phys. Rev. A 44, 7439 (1991).
- [3] A. Rovenchak, Physics of Bose Systems (Lviv University Press, 2015).

Landau-Zener-Stückelberg-Majorana quantum logic gates

A.I. Ryzhov¹, O.V. Ivakhnenko¹, S.N. Shevchenko^{1,2}, F. Nori^{3,4}

¹*B. Verkin Institute for Low Temperature Physics and Engineering of the National Academy of Sciences of Ukraine, Kharkiv 61103, Ukraine*

²*V. N. Karazin Kharkiv National University, Kharkiv 61022, Ukraine*

³*Theoretical Quantum Physics Laboratory, RIKEN Cluster for Pioneering Research, Wakoshi, Saitama 351-0198, Japan*

⁴*Physics Department, University of Michigan, Ann Arbor, MI 48109-1040, USA
artem.ryzhov.14@gmail.com*

All quantum algorithms can be implemented using only a universal set of single-qubit logic gates and one two-qubit logic gate. A quantum gate is a controlled non-adiabatic excitation of the system realized by changing certain external fields, applied to the system, resulting in a specific transformation of its state. The most common realization of quantum gates and quantum control is based on Rabi oscillations, which cause a periodic *resonant* excitation of the system. This approach has been quite successful. However, under resonant driving, certain limitations may arise, including achievable gate speeds and additional complications, like counter-rotating terms [1-3]. Other approaches are being developed, which could have advantages over the Rabi oscillations method.

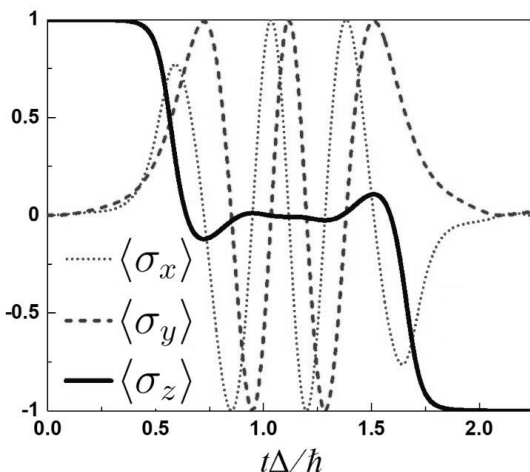


Fig 1. Time dependence of the expectation values of Pauli operators. Demonstration of an X-gate. Two LZSM transitions with constructive interference transfer a qubit from state 0 to state 1.

relaxation, and coupling with the environment. We consider analytical approximations and also numerically solve the master equation (see the figure).

Here we study a qubit control technique based on Landau-Zener-Stückelberg-Majorana (LZSM) interferometry [4], which allows a complementary approach to quantum control based on *non-resonant driving* with the alternation of adiabatic evolution and non-adiabatic transitions. This enables ultrafast qubit gates controlled solely using baseband pulses, reducing the need for pulsed-microwave control signals [3,5]. Its main differences, compared to the Rabi oscillations method, are a non-resonant excitation frequency, large excitation amplitude, and a small number of periods in the external excitation. Compared to Rabi oscillations, it could potentially increase the duration and fidelity of quantum gates. Both of these characteristics have major importance for experimental realizations of quantum computers, as these define the number of quantum operations that could be performed during the coherence time of the system. We study different aspects of LZSM excitations: qubit dynamics,

Acknowledgments: This research is sponsored by the Army Research Office under Grant Number W911NF-20-1-0261.

- [1] N. V. Vitanov, L. P. Yatsenko, and K. Bergmann, Phys. Rev. A **68**, 043401 (2003).
- [2] S. Longhi, G. L. Giorgi, and R. Zambrini, Adv. Quant. Tech. **2**, 1800090 (2019).
- [3] D. L. Campbell, Y.-P. Shim, B. Kannan, R. Winik, A. Melville, B. M. Niedzielski, J. L. Yoder, C. Tahan, S. Gustavsson, and W. D. Oliver, Phys. Rev. X **10**, 041051 (2020).
- [4] S. N. Shevchenko, S. Ashhab, and F. Nori, Phys. Rep. **492**, 1 (2010).
- [5] G. Cao, H.-O. Li, T. Tu, L. Wang, C. Zhou, M. Xiao, G.-C. Guo, H.-W. Jiang, and G.-P. Guo, Nat. Commun. **4**, 1401 (2013).

Thermoelectric and vibronic effects in tunneling of spin-polarized electrons in a molecular transistor

A.D. Shkop

*B.Verkin Institute for Low Temperature Physics and Engineering of NAS of Ukraine,
47 Nauky Ave., Kharkiv, 61103, Ukraine
shkop@ilt.kharkiv.ua*

Scientific community is interested in thermoelectric phenomena due to the possibility of creating thermoelectric devices that convert heat, dissipated in physical processes, into useful electrical energy. Transistors based on a quantum dot placed between electrodes are seemed to have high thermoelectric efficiency and good ability of integration into microcircuits.

The following system is considered. The molecule, represented as a single-level vibrating quantum dot, is placed between two magnetic electrodes that are fully spin-polarized in opposite directions. The electrodes are hold at different temperatures. An external magnetic field applied perpendicular to the plane of the magnetization vectors of the electrodes causes spin flips in the dot.

Such a system is interesting due to the influence of electron-vibron interaction on its transport properties at low temperatures [1]. Heat current and thermoelectric phenomena are considered. The problem is solved using density matrix method in perturbation theory over weak tunnel couplings. It is shown that for strong electron-vibron interaction the system is characterized by negative thermoconductance. The suppression of the thermoconductance is caused by the dissipation of energy when new vibronic channels are opened when temperature raises.

Thermopower is obtained in linear response to voltage and temperature difference, using the expression for charge current found in our previous work [2]. Optimal thermopower values are needed for high efficiency of the thermoelectric device. Depending on the position of the energy level at the quantum dot relative to the resonance points and the point of electron-hole symmetry of the system the thermopower changes its sign and magnitude, according to the feature of nanodevices based on a quantum dot [3]. Moreover, the number of such points for our model is greater than for conventional molecular transistor due to the Zeeman splitting of the energy level in an external magnetic field. It was also revealed that in a spintronic molecular transistor the dependence of the thermopower on dot energy has a sawtooth behavior with a step of the order of magnitude of the quantum of molecular oscillations.

- [1] J. Koch, F. von Oppen. Phys. Rev. Lett., 94, 206804 (2005)
- [2] A.D. Shkop, O.M. Bahrova, S.I. Kulinich, I.V. Krive, Superlattices and Microstructures, 137, 106356 (2020)
- [3] J. Koch, F. von Oppen, Y. Oreg, and E. Sela, Phys. Rev. B 70, 195107 (2004)

Approximately isospectral isomers for antiferromagnetic Heisenberg model

V.V. Tokarev

*V. N. Karazin Kharkiv National University, School of Chemistry,
4 Svobody Sq., Kharkiv, 61077, Ukraine
victor.tokarev@karazin.ua*

Heisenberg model is a paradigmatic model of magnetism in transition metal-based insulators with quenched orbital momentum. Compounds with small isolated magnetic subsystems, also known as magnetic molecules, have perspective applications for information storage, quantum computing and magnetic cooling. Increase of the number of magnetic ions leads to exponential increase of the number of different structures and the complexity of exact diagonalization. But to efficiently build pseudo-phase diagrams for finite antiferromagnetic clusters and to find new isomers with new or extreme properties it's highly desirable to partition that structure space in terms of observable zero- or finite-temperature values. While this partitioning using exact diagonalization quickly becomes infeasible for moderately-sized systems, it can be done with help of approximate methods. This study is motivated by early works, where families of strictly isospectral 3-and 4-spin systems [1] and multiple sets of exchange parameters that reproduce low-energy excitation energies of magnetic wheel Fe_{18} in spin wave approximation [2] were found.

Here we focus on finite clusters that have different exchange couplings but almost equal ground state and lower excitation energies. Earlier we showed that spin- S regular bipartite antiferromagnets with isospectral exchange matrices J are approximately isospectral, and that in lowest order of perturbation theory spin wave interactions in bipartite double covers of strongly regular graphs with same parameters do not change ground state energy. Using spin wave approximation and perturbation theory we extend this result and find which unitary transformations of exchange matrix approximately conserve lowest part of energy spectrum of non-regular and non-bipartite Heisenberg clusters, and confirm these findings using exact diagonalization and SSE Monte-Carlo calculations. We estimate the number of such approximately isospectral clusters with isospectral exchange matrices and investigate how inclusion of 4th order effective Hamiltonian for half-filled Hubbard model change these results.

- [1] H.-J. Schmidt and M. Luban, J. Phys. A: Math. Gen. 34, 2839 (2001).
- [2] J. Ummethum, J. Nehrkorn, S. Mukherjee, N. B. Ivanov, S. Stuiber, Th. Strässle, P. L. W. Tregenna-Piggott, H. Mutka, G. Christou, O. Waldmann, and J. Schnack, Phys. Rev. B 86, 104403 (2012).

Low-temperature phases of SU(4)-symmetric fermionic mixtures in optical lattices

V.I. Unukovych¹, A.G. Sotnikov^{1,2}

¹*Karazin Kharkiv National University, 4 Svobody Square, Kharkiv, 61000, Ukraine*

²*Akhiezer Institute for Theoretical Physics, NSC KIPT, Kharkiv, 61108, Ukraine*

unukovich.vladislav@gmail.com

The quantum gases of alkaline-earth-like atoms are playing a significant role in understanding of physically rich phenomena of multiflavored fermionic mixtures, due to their properties at low temperatures. Since experimentally accessible values for the entropy per particle are currently too high for direct exploration of magnetic phases in the ultracold fermionic gases, the theoretical studies allow to handle such case [1,2].

We apply dynamical mean-field approach to the Hubbard model for the case of four-component SU(4)-symmetric fermionic gas to study both paramagnetic hysteresis between metallic and Mott-insulating phases, as well as transitions between the paramagnetic metal/insulator and antiferromagnetic (AFM) insulator phases. In contrast to previous studies of the half-filled SU(4)-symmetric Hubbard model [3], at quarter filling (one particle per site) we identify both the two-sublattice AFM and plaquette-ordered/four-sublattice AFM phases with the corresponding entropy-driven hierarchy for critical temperatures. Experimentally-relevant observables, such as the double occupancy, compressibility, and entropy per particle are studied in detail.

- [1] A. Sotnikov, N. Darkwah Oppong, Y. Zambrano, and A. Cichy, Phys. Rev. Research 2, 023188 (2020).
- [2] P. Corboz, A. M. Läuchli, K. Penc, M. Troyer, and F. Mila, Phys. Rev. Lett. 107, 215301 (2011).
- [3] A. Golubeva, A. Sotnikov, A. Cichy, J. Kuneš, and W. Hofstetter, Phys. Rev. B 95, 125108 (2017).

Bose-Einstein condensation of ideal gas in the external harmonic potential**E.O. Bilokon¹, A.S. Peletinskii^{1,2}**¹*Karazin Kharkiv National University, 4 Svobody Square, Kharkiv, 61000, Ukraine*²*Akhiezer Institute for Theoretical Physics, NSC KIPT, Kharkiv, 61108, Ukraine**elyabilokon@gmail.com*

We study Bose-Einstein condensation of ideal gas trapped in the harmonic potential within a semiclassical theoretical approach valid at temperatures much higher than characteristic oscillator energies. For experimentally relevant parameters, we obtain the density profile as a function of temperature and compare it with that observed in the experiment with the trapped lithium-7 gas in a magneto-optical trap [1]. We estimate the correctness of the semiclassical description and provide a purely quantum-mechanical approach to study thermodynamic properties of a trapped Bose gas in the low-temperature limit.

[1] A. G. Truscott et al., Science 291, 2570 (2001).

Thermodynamics of quantum Fermi gases in magneto-optical traps

V.O. Bilokon¹, A.G. Sotnikov^{1,2}

¹*Karazin Kharkiv National University, 4 Svobody Square, Kharkiv, 61000, Ukraine*

²*Akhiezer Institute for Theoretical Physics, NSC KIPT, Kharkiv, 61108, Ukraine*

lera.bilokon@gmail.com

We theoretically examine thermodynamic properties of the trapped Fermi gases in the quantum degeneracy regime. The trapping potential profiles and number of atoms are relevant to the experiments with ultracold lithium-6 atoms [1]. We calculate corrections to the chemical potentials in the experimentally-accessible range of temperatures and compare the obtained density distributions to the experimental ones. Other relevant thermodynamic quantities as functions of temperature for the trapped gas are analyzed.

[1] A. G. Truscott et al., Science 291, 2570 (2001).

Magnetic phases and phase diagram of spin-1 condensate with quadrupole degrees of freedom

M. Bulakhov^{1,2}, **A.S. Peletminskii**^{1,2}, **S.V. Peletminskii**¹, **Yu.V. Slyusarenko**^{1,2}

¹*Akhiezer Institute for Theoretical Physics, NSC KIPT, 61108 Kharkiv, Ukraine*

²*V.N. Karazin Kharkiv National University, 61022 Kharkiv, Ukraine*

bulakh@kipt.kharkov.ua

We obtain and justify a many-body Hamiltonian of pairwise interacting spin-1 atoms, which includes eight generators of the SU(3) group associated with spin and quadrupole degrees of freedom. It is shown that this Hamiltonian is valid for non-local interaction potential, whereas for local interaction specified by s-wave scattering length, the Hamiltonian should be bilinear in spin operators only (of the Heisenberg type). We apply the obtained Hamiltonian to study the ground-state properties and single-particle excitations in a weakly interacting gas of spin-1 atoms with Bose-Einstein condensate taking into account the quadrupole degrees of freedom. It is shown that the system under consideration can be in ferromagnetic, quadrupolar, and paramagnetic phases. The corresponding phase diagram is constructed and discussed. The main characteristics such as the density of the grand thermodynamic potential, condensate density, and single-particle excitation spectra modified by quadrupole degrees of freedom are determined in different phases [1].

[1] Bulakhov et al 2021 J. Phys. A: Math. Theor. <https://doi.org/10.1088/1751-8121/abed16>

Breather Birth and Wave Radiation in the sine-Gordon Systems with Oscillating Kinks

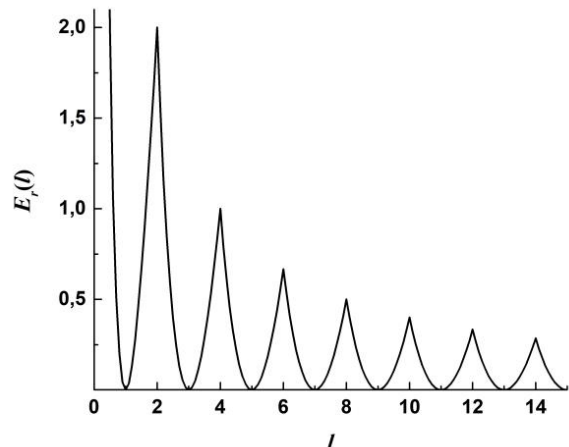
O.V. Charkina¹, M.M. Bogdan^{1,2}

¹*B.Verkin Institute for Low Temperature Physics and Engineering of NAS of Ukraine,
47 Nauky Ave., Kharkiv, 61103, Ukraine*

²*V.N. Karazin Kharkiv National University, 4 Svobody Sq., Kharkiv, 610022, Ukraine
charkina@ukr.net*

The structure and dynamics of topological defects and inhomogeneities in solid state physics are described by nonlinear equations. Well-known examples of such topological objects are domain walls in anisotropic magnets, fluxons in long Josephson junctions, and dislocations in crystals. Typically, the stationary dynamics of these topological objects is described by the sine-Gordon equation. In the present contribution the nonstationary dynamics of topological defects and inhomogeneities is studied. In particular, the evolution of initially nonequilibrium profiles of these topological objects is investigated, and their oscillation regimes of the approach to static configurations are considered in terms of nonlinear excitations of the sine-Gordon equation, namely kinks and breathers. In order to describe explicitly oscillatory behavior of these objects, the Cauchy problem for the equation linearized near the exact static kink is solved for the small addition to the kink shape. The obtained solution describes explicitly the regime of long-living oscillations of the kink, named in Ref. 1 the kink quasimode. It is shown that the kink deformations leading to its initial compression and tension evolve as weakly damped oscillations with the frequency lying just above the lowest edge of the continuous spectrum. The specially combined deformation leads to a great rate of damping the kink oscillation and to the formation of the well-separated running wave packet carrying away all the exceed energy of the initial kink profile. The corresponding patterns of the kink evolution and the time dependencies of its effective length have been found.

The nonlinear stage of evolution of the kink with the deformed shape is investigated in the framework of the inverse scattering method. In fact, the direct scattering problem solution appears to be enough to find exactly the conditions of arising the breathers from the nonequilibrium kink and to determine their amplitudes, frequencies and finally their energies. In general, we reduce the direct scattering problem, considered in Ref.2, first to our knowledge, to solving the spectral problem of the one-dimensional Schrödinger operator. In the case of the nonequilibrium kink, the obtained equation corresponds to the well-known one in quantum mechanics [3] with the famous spectrum of discrete levels. After exact finding parameters of all breathers for the multi-frequency oscillating kink, we have constructed the complex solution consisting of the kink, arising breathers and wave packets generated by the kink. We have calculated the dependence of the radiation energy on the effective length of the initial kink profile (see fig.), which has maxima in points of a new breather birth. At last, we note the advantage of using the obtained Schrödinger equation that makes it possible to determine whether or not a small deformation of the exact sine-Gordon kink leads to the small-amplitude breather birth.



The dependence of the radiation energy on the effective length of the initial kink profile.

- [1] R. Boesch and C.R.Willis, *Phys. Rev. B* **42**, 2290 (1990).
- [2] R. Buckingham and P.D. Miller, *Physica D* **237**, 2296 (2008).
- [3] L.D. Landau and E.M. Lifshitz, *Quantum Mechanics* (Pergamon, New York, 1977).

Raman Scattering and Theoretical Investigations of CuInP₂S₆ Layered Ferrielectric Crystal

K. Glukhov, R. Yevych, A. Kohutych, K. Medulych, V. Hryts, Yu. Shiposh, M. Kundria, Yu. Vysochanskii

*Institute for Solid State Physics and Chemistry, Uzhhorod University,
Pidgirna Str. 46, 88000 Uzhhorod, Ukraine
kglukhov@gmail.com*

For van der Waals family CuInP₂S₆ crystals with ferrielectric ordering below T_c ≈ 315 K earlier the possibility of spontaneous polarization switching in samples with a thickness of several structural layers was discovered [1]. This discovering has opened a new direction of basic and applied investigations in the field of nanoelectronics based on van der Waals multiferroics.

The ferrielectric polarization of considered crystals is determined by opposite shifts of Cu⁺ and In³⁺ cations out of structural layers that are built by (P₂S₆)⁴⁻ anionic structural groups. Such ferrielectric ordering below T_c can be presented as freezing of Cu⁺ cations in the four-well (or quadruple) local potential. The origin of such a complicated potential landscape for the copper atoms moving inside crystal lattice elementary cells can be related to the second-order Jahn-Teller effect destabilizing the Cu⁺ cations in positions in the middle of structural layers.

Data of previous Raman scattering investigations [2] illustrate the temperature-dependent transformation of the low-frequency spectral lines intensity, which is related to Cu⁺ cations redistribution between wells of the local potential. For further analysis of CuInP₂S₆ crystal anharmonic lattice dynamics, we performed DFT calculations of its phonon spectra in the GGA approach with considering of s, p, and d valence orbitals of atoms constituting the crystal lattice. For the ferrielectric phase in groundstate the phonon branches across the monoclinic Brillouin zone, the eigenvectors of long-wave phonons, and partial phonon states were calculated. Also, the Raman spectral intensity at different temperatures was calculated and compared with observed Raman spectra temperature dependence. Such comparison illustrates anharmonic effects – redistribution of spectral lines intensities that can be related to changes of Cu⁺ cations population in different wells of quadruple local potential at heating in the ferrielectric phase.

The Raman spectra temperature dependence also is compared with calculated pseudospin fluctuations spectra in the four-well quantum anharmonic oscillators model. At this, the shape of local potential was determined following data [3] about the scattering of electrons by Cu⁺ cations in CuInP₂S₆ crystal at different temperatures. Comparative analysis of DFT calculated phonon spectra, experimental Raman scattering data, and simulations in four-well quantum anharmonic oscillators model characterize anharmonic dynamics of copper and indium sublattices in CuInP₂S₆ crystal. In this background investigations of uniaxial pressure influence on phonon spectra and ferrielectric phase transition in CuInP₂S₆ crystal are analyzed.

- [1] A. Belianinov, Q. He, A. Dziaugys, P. Maksymovych, E. Eliseev, A. Borisevich, A. Morozovska, J. Banys, Yu. Vysochanskii, and S.V. Kalinin, Nano Lett. 15, 3808 (2015).
- [2] Yu.M. Vysochanskii, V.A. Stephanovich, A.A. Molnar, V.B. Cajipe, and X. Bourdon, Phys. Rev. B 58, 9119 (1998).
- [3] V. Maisonneuve, V.B. Cajipe, A. Simon, R. Von Der Muhll, and J. Ravez, Phys. Rev. B 56, 10860 (1997).

Driven quantum systems: Majorana's approach

P.O. Kofman¹, O.V. Ivakhnenko², S.N. Shevchenko^{1,2}

¹*V.N. Karazin Kharkiv National University, Kharkov 61022, Ukraine*

²*B.Verkin Institute for Low Temperature Physics and Engineering, Kharkov 61103, Ukraine
poly.kofman@icloud.com*

One of the base problems in studying dynamics of quantum two-level systems (qubits) is the transition between the two quantum states under the influence of a time-dependent excitation, Fig. 1(a). It is important for further developing our understanding of quantum mechanics.

This transition relates to the well-known Landau-Zener-Stückelberg-Majorana (LZSM) transitions [1]. The difference in approaches of these four authors lays in a way of solving the Schrödinger equation. E. Majorana used Laplace transform method and the saddle-point method that gives the asymptotic result [2,3]. Paradoxically enough, Majorana's approach is often underestimated in the context of non-adiabatic transitions, even though it has several advantages over other approaches by LZS [2,4].

We consider and develop the Majorana approach in several aspects. Firstly, we reproduce the non-adiabatic probability in detail, which is not always clear from the original work [2]; these relates to direct and inverse Laplace transforms including the integrations along the circuits in Fig. 1(b). We derive more general formulas, including the ones describing the time dependence. These results are important for different applications in quantum engineering, where both the time dependence and interference are important.

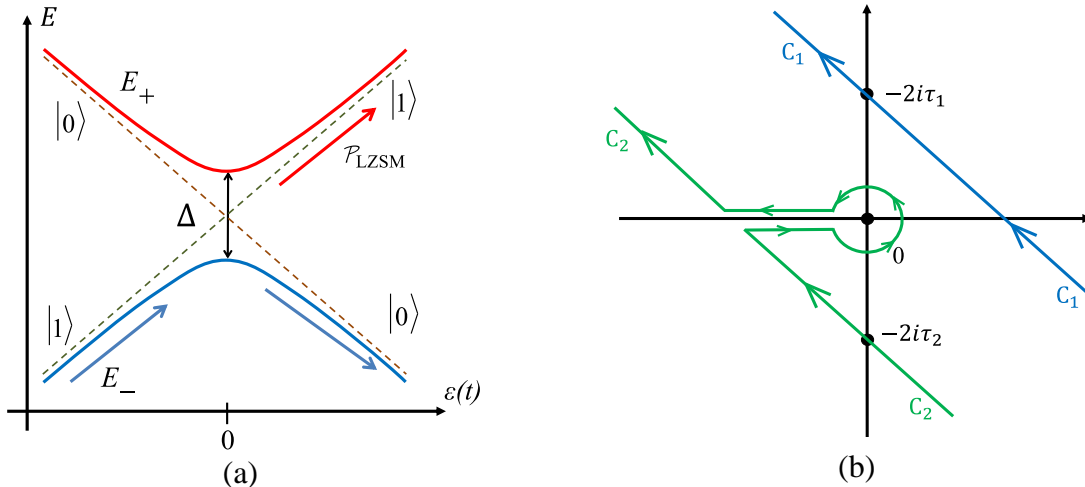


Fig. 1. (a) Two-level system in dependence on the energy. (b) Contours of integration in the saddle-point method.

Acknowledgments: This research is sponsored by the Army Research Office under Grant Number W911NF-20-1-0261.

- [1] F. D. Giacomo and E. E. Nikitin, “The Majorana formula and the Landau–Zener–Stückelberg treatment of the avoided crossing problem,” Phys. Usp. 48, 515 (2005)
- [2] E. Majorana, “Atomi orientati in campo magnetico variabile,” Il Nuovo Cimento 9, 43 (1932).
- [3] F. Wilczek, “Majorana and condensed matter physics,” ArXiv ,1404.0637 (2014)
- [4] S. N. Shevchenko, S. Ashhab and F. Nori «Landau-Zener-Stückelberg interferometry», Phys. Rep., 2010, 492, 1.

Simultaneous Effect of Short-Range Atomic and Magnetic Orderings on Magnetic Phase Diagrams of Substitution Binary Alloys

E.G. Len^{1,2}, T.D. Shatnii¹, V.V. Lizunov¹, M.V. Ushakov¹, T.S. Len³

¹*G. V. Kurdyumov Institute for Metal Physics NASU, Kyiv, Ukraine*

²*Kyiv Academic University, NAS and MES of Ukraine, Kyiv, Ukraine*

³*National Aviation University, Kyiv, Ukraine*

len@imp.kiev.ua

The Pauli principle and Coulomb repulsion of itinerant electrons determine the unique physical properties of strongly correlated systems. The theories of such systems try to solve two major problems, namely, the nonlocality of correlations in time and in space. The first problem is mainly solved within the method of dynamical mean-field theory and the second—by cluster methods. We consider the absolute zero of temperature and corresponding static approximation; also we use the one of the cluster expansion methods for one-particle Green function to describe the spatial nonlocality of correlations. This approach was early extended to magnetic alloys with strong electron-electron correlations and with arbitrary degrees of short and long atomic and magnetic orders [1]. At the present work we investigate the simultaneous effect of short-range atomic and magnetic orderings ($\varepsilon_{a,m}$) on electronic structure and magnetic phase diagrams (MPDs) of substitution binary alloys with strong electron correlations.

To solve this complex problem, at the beginning, we use a semi-elliptical model for initial electron density of states. The numerical calculations show (Fig. 1) a qualitative agreement between magnetic phase diagrams of atomically disordered alloys within the scope of semi-elliptical model and real electron dispersion law for b.c.c. crystals obtained in Refs. [1, 2]. As determined, in a semi-elliptical model of magnetic alloys the correlations in orientation of localized magnetic moments at nearest sites lead to a violation of electron–hole symmetry, which results in both the threshold character of antiferromagnetic ordering at half filling and the asymmetry of MPDs relative to corresponding value of average electron density per one site ($n=1$). However, in comparison with Refs. [1, 2], we observe the other quantitative values of all characteristics described the alloys. Different magnetic moments on ions of different types (A, B) and corresponding equilibrium parameter of correlation in their orientations (ε_m) lead to different splitting of impurity bands into Hubbard subzones due to the Coulomb potential (U) of electrons repulsion at one site, and to appearance on MPDs the region with paramagnetic (PM), full antiferro- (AFM) and ferromagnetic (FM) orders, as well as the regions of transitions between them characterised by partial orders (PO). The dispositions of these regions substantially depend on value of atomic short-range parameter ε_a (Fig. 1), which negative values determine a tendency to ordering and positive values—to phase separation in atomic system. Some specific details of given MPDs, such as PM region inside of FM-phase (Fig. 1, *b*) or concrete structure of PO regions, need further investigations.

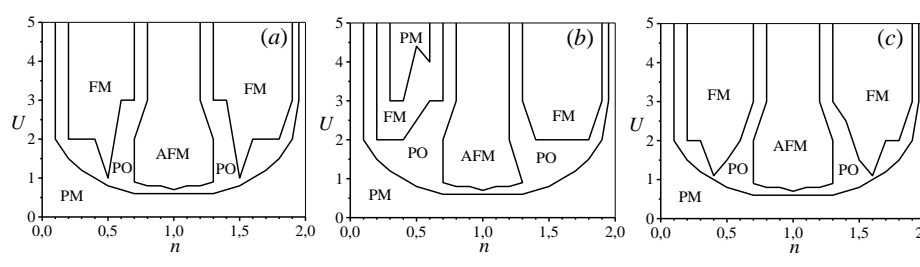


Fig. 1. MPDs of atomically disordered ($\varepsilon_a=0$) (a), partially phase-separated ($\varepsilon_a=+0.1$) (b), and partially ordered ($\varepsilon_a=-0.1$) (c) alloys in the semi-elliptical model; concentration of binary alloy components $P_A=P_B=0.5$, impurity scattering potential $W=V_B-V_A=-0.2$.

- [1] E.G.Len, V.V.Lizunov, T.S.Len, M.V.Ushakov, V.A.Tatarenko, Metallofiz. Noveishie Tekhnol. 37, 1405 (2015).
- [2] E.G.Len, V.V.Lizunov, T.D.Shatnii, M.V.Ushakov, T.S.Len, E.A.Tsapko, A.O.Bilots'ka, Metallofiz. Noveishie Tekhnol., 42, 289 (2020).

Theoretical Cross-Sections of the Ionization of the K atom by Electron Impact

V. Roman

*Institute of Electron Physics of NAS of Ukraine, 21 Universytetska Str., Uzhhorod 88017, Ukraine
viktoriyaroman11@gmail.com*

Electron impact ionization cross-sections are widely used in applications such as modeling of plasma syntheses in tokamaks, modeling of radiation effects for both materials and medical research and aeronomy, as well as in basic research in astrophysics, atomic, molecular and plasma physics. Therefore, the study of ionization of atoms is very relevant today. This is confirmed by a large number of experimental and theoretical studies of the ionization process of atoms, in particular alkali metal atoms [1–4]. Previously, we studied the ionization cross sections for the rubidium atom [5]. Here we consider the capabilities of the most widely used theoretical approaches, relativistic Coulomb-Born (CB) distorted-wave (DW) and binary-encounter-dipole (BED), for the single electron impact ionization of the K atom in the impact energy range from the $4s$ threshold up to 700 eV using the standard software package Flexible Atomic Code (FAC) [6].

Figure 1 shows a comparison of the single ionization cross-sections of the $4s$, $3p^6$, and $3s^2$ shells of the K atom calculated in the DW, BED, CB approximations with the data [4] obtained using the plane wave Born (PWB) approximation. Note that the experimental data are available only for the $4s$ shell and only below the excitation threshold of the $3p^6$ shell [1]. In fig. 1 these data [1] are normalized to the absolute values from [2] at 500 eV.

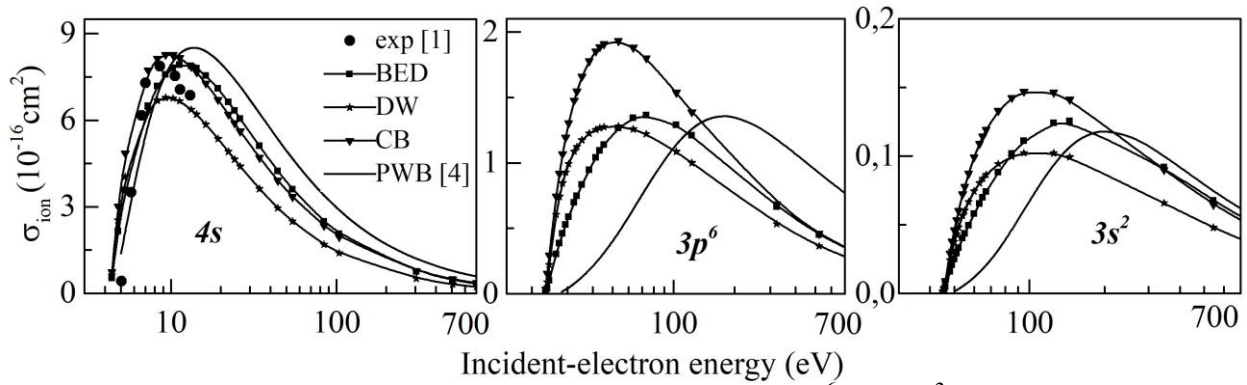


Fig. 1. The single ionization cross-sections of the $4s$, $3p^6$, and $3s^2$ shells of the K atom

The comparison of the ionization cross-sections of the $4s$ shell shows that the absolute values of the BED data are the best match with the experiment, however the maximum of the cross-section is strongly shifted. As for the maxima position, the CB and DW data are in the best agreement with the experiment. The $4s$ -shell ionization cross-section obtained using PWB approximation [4] shows the largest discrepancy with experiment regarding the absolute values as well as maxima position. As for the K atom $3p^6$ and $3s^2$ shells, their ionization cross-sections strongly differ between themselves. Unfortunately, one is unable to obtain the experimental cross-section of a specific electron shell. However, we are currently calculating the excitation cross-sections of the K atom which allow us to compare the calculated total cross-section with the experimental cross-section of the K atom direct ionization.

- [1] J. Tate, P. Smith, Phys. Rev. 46, 773 (1934).
- [2] R. Mcfarland, et al, Phys. Rev. 137, 1058 (1965).
- [3] B. Roy, D. Rai, Phys. Rev. A. 8, 849 (1973).
- [4] P. Bartlett, A. Stelbovics, Atomic Data and Nuclear Data Tables 86, 235 (2004).
- [5] V. Roman, A. Kupliauskiené and A. Borovik, J. Phys. B. 48, 205204 (2015).
- [6] M. Gu, Can. J. Phys. 86, 675 (2008).

Exploration of the Phase Diagram of $(\text{Pb}_y\text{Sn}_{1-y})_2\text{P}_2(\text{Se}_x\text{S}_{1-x})_6$ Ferroelectrics within the Framework of a Combined BEG – ANNNI Model

V. Liubachko¹, A. Oleaga², A. Salazar², R. Yevych¹, A. Kohutych¹, Yu. Vysochanskii¹

¹*Institute for Solid State Physics and Chemistry, Uzhhorod University, Pidgirna Str. 46, Uzhhorod 88000, Ukraine*

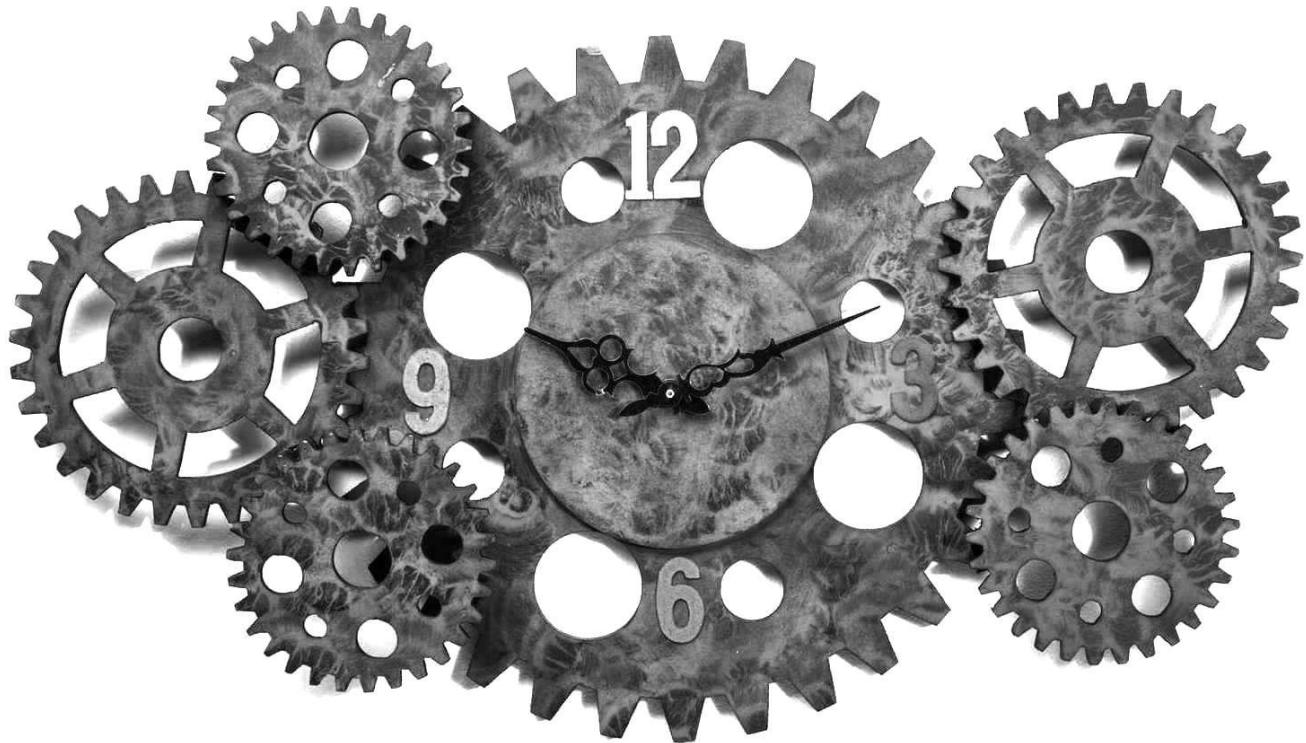
²*Departamento de Fisica Aplicada I, Escuela de Ingenieria de Bilbao, Universidad del Pais Vasco UPV/EHU, Plaza Torres Quevedo 1, 48013 Bilbao, Spain
vysochanskii@gmail.com*

Static and dynamic critical behavior of $\text{Sn}_2\text{P}_2\text{S}_6$ type ferroelectrics and $(\text{Pb}_y\text{Sn}_{1-y})_2\text{P}_2(\text{Se}_x\text{S}_{1-x})_6$ mixed crystals with line of tricritical points and line of Lifshitz points on the $T - x - y$ phase diagram, which meet at the tricritical Lifshitz point, can be described in the combined Blume - Emery - Griffiths – axial next nearest neighbor Ising model (BEG – ANNNI). Such model considers first and second neighbor interactions for pseudospins in a local three-well potential. Below the temperature of tricritical Lifshitz point, the “chaotic” state accompanied by the coexistence of ferroelectric, metastable paraelectric and modulated phases is expected [1].

In order to investigate the topology of the experimental phase diagram of $(\text{Pb}_y\text{Sn}_{1-y})_2\text{P}_2(\text{Se}_x\text{S}_{1-x})_6$ ferroelectrics we have built the theoretical $t - \Delta - \lambda$ phase diagram within the framework of the Blume - Capel spin-1 Ising model (which is a simpler version of BEG model) with competing interactions [2], and afterward, we have compared the latter with the experimental phase diagram. From this, it follows that the Lifshitz points line terminates at tricritical Lifshitz point, and this multicritical point can be considered as a “Lifshitz end point”. The Lifshitz points line in tricritical Lifshitz point splits into the tricritical points line and the end points line. At big Δ parameter, the paraelectric - modulated critical line terminates at the end point.

For high lead concentrations ($y > 0.2$), at low temperatures a “chaotic” state can be observed [1]. This state presents a mixture of paraelectric, ferroelectric and modulated phases. Such peculiarity can be seen on the excess heat capacity ΔC_p and anomalous temperature dependencies of dielectric susceptibility ε' in $(\text{Pb}_y\text{Sn}_{1-y})_2\text{P}_2\text{Se}_6$ crystals, according to previous investigation [3,4]. For small lead concentrations, there are clear anomalies of $\Delta C_p(T)$ and $\varepsilon'(T)$ at paraelectric – incommensurate and incommensurate – ferroelectric phase transitions. However, for high lead concentrations the $\Delta C_p(T)$ and $\varepsilon'(T)$ anomalies in the vicinity of the lock-in transition are strongly smeared. Such chaotization can be related to a synergy of frustration effects and nonlinearity of the system with the three - well local potential for spontaneous polarization fluctuations.

- [1] V. Liubachko, A. Oleaga, A. Salazar, R. Yevych, A. Kohutych, Yu. Vysochanskii, Phys. Rev. B 101, 224110 (2020).
- [2] T. Tomé, S. R. Salinas, Phys. Rev. A 39, 2206 (1989).
- [3] K. Moriya, T. Yamada, K. Sakai, S. Yano, S. Baluja, T. Matsuo, I. Pritz, Y. M. Vysochanskii, J. Ther. Anal. and Cal. 70, 321 (2002).
- [4] Maior M. M., Molnar S. B., Vysochanski, Y. M., Gurzan, M. I., van Loosdrecht P. H. M., van der Linden P. J. E. M., van Kempen H., Appl. Phys. Let. 62, 2646 (1993).



TECHNOLOGIES AND INSTRUMENTATION FOR PHYSICAL EXPERIMENTS

Development of universal experimental cell for Yanson point-contact spectroscopy and sensor research

P.O. Dmitriyev¹, A.V. Savytskyi¹, A.P. Pospelov², E. Faulques³, G.V. Kamarchuk¹

¹*Department of Spectroscopy of Molecular Systems and Nanostructured Materials, B. Verkin Institute for Low Temperature Physics & Engineering, 47 Nauky Ave., Kharkiv, 61103, Ukraine*

²*Department of Physical Chemistry, National Technical University “Kharkiv Polytechnic Institute”, 21 Kyrpychov Str., Kharkiv, 61002, Ukraine*

³*MIOPS, Jean Rouxel Institute of Materials, 2 Chemin de la Houssinière, 44300 Nantes, France
dmitriyev@ilt.kharkov.ua*

Sensor technology has become one of the most dynamic and perspective research and development areas in modern life. It has already resulted in creating a large variety of sensor devices, including nanosized ones, and their everyday applications. The use of modern nanosensors to detect different gases is now a common practice. Gas media control is of great importance for both reliable operations of numerous technological cycles and protection of the environment.

Bearing this in mind, we proposed a novel approach [1] that applies the Yanson point-contact spectroscopy [2] to sensor techniques. The original basic properties of Yanson point contacts make it possible to discover new sensory effects and develop innovative sensor technologies. One of these is a new method for quantum detection of liquid and gaseous media we proposed. The clue is discovering the cyclic electrochemical switchover effect alongside the introduction of the concept of a point-contact nanostructured gapless electrode system for modeling processes occurring at the atomic scale [1, 3]. The proposed method is based on the characterization of the energy of interaction of point-contact structures with gas and liquid media through quantum conductivity parameters of dendritic Yanson point contacts synthesized electrochemically in the medium under study [4]. *In situ* synthesis of nanoscale dendritic point-contacts is part of the cyclic switching effect [3] that takes place in the electrolyte in contact with the analyzed medium and consists of alternating cycles of formation and destruction of point contacts.

During the *in-situ* experiment, a large number of parameters are being controlled and investigated. For this purpose, a universal complex for Yanson point-contact spectroscopy is applied. However, to carry out full-fledged observations, especially during sensor research, it was also necessary to create a universal experimental cell, to which this work is devoted.

Three iterations of experimental cells have been designed and manufactured to conduct simultaneous electrical, electrochemical, and optical experiments in a multichannel regime. During the development, the problems of precise electrode positioning and sample optical accessibility were resolved. We also overcame the challenge of the automation of electrode movement and optimized the dimensions and the weight. All the blueprints were tested for manufacturability and are now ready to be replicated. The cell has been tested in all operating modes and calibrated following the specified requirements. At the moment, the experimental cell is being successfully integrated into the universal complex for Yanson point-contact spectroscopy and sensor research.

- [1] G.V. Kamarchuk, A.P. Pospelov, L.V. Kamarchuk, and I.G. Kushch, “Point-Contact Sensors and Their Medical Applications for Breath Analysis: A Review”, in Nanobiophysics: Fundamentals and Applications, V.A. Karachevtsev, ed. (Pan Stanford Publishing, Singapore, 2015).
- [2] Yu.G. Naidyuk and I.K. Yanson, Point-contact spectroscopy (Springer, 2005).
- [3] A.P. Pospelov, A.I. Pilipenko, G.V. Kamarchuk, V.V. Fisun, I.K. Yanson, and E. Faulques, J. Phys. Chem. C 119, 632-639 (2015).
- [4] G.V. Kamarchuk, A.P. Pospelov, A.V. Savytskyi, A.O. Herus, Yu.S. Doronin, V.L. Vakula, E. Faulques, Conductance quantization as a new selective sensing mechanism in dendritic point contacts. Springer Nature Applied Sciences, 2019. 1(3): 244 (7).

Investigation of the Voltage Sensitivity of Selectively Doped Microwave Diodes on "Hot" Electrons in a Wide Temperature Range

V. Derkach¹, R. Golovashchenko¹, Y. Ostryzhnyi¹, J. Gradauskas^{2,3}, A. Sužiedėlis², M. Anbinderis^{2,3}

¹O. Ya. Usikov Institute for Radiophysics and Electronics of NAS of Ukraine,
12 Acad. Proskura St, Kharkiv, 61085, Ukraine
derkach@ire.kharkov.ua

²Center for Physical Sciences and Technology, Savanorių av. 231, Vilnius, LT-02300, Lithuania

³Vilnius Gediminas Technical University, Saulėtekio al. 11, Vilnius, LT-10223, Lithuania
jonas.gradauskas@ftmc.lt

The paper presents the results of joint research of promising microwave sensors by Ukrainian and Lithuanian research groups within the framework of a joint project. Microwave diodes of novel design based on the selectively doped GaAs / AlGaAs semiconductor structure of asymmetrical shape with gates over a narrow and wide part of the active layer, developed by Lithuanian co-authors [1] (Fig. 1), were investigated. The operation of diodes is based on the principle of non-uniform electron heating due to the influence of a microwave electric field. This is realized by using an asymmetric isthmus of a thin semiconductor film, where the bigradient electromotive forces are induced [2]. Such diode structures have a number of advantages over traditionally used: small size, stability of parameters, insensitivity to external magnetic and electrostatic fields, operation without a reference voltage, etc. They can be effectively used in the gigahertz and terahertz frequency ranges [2].

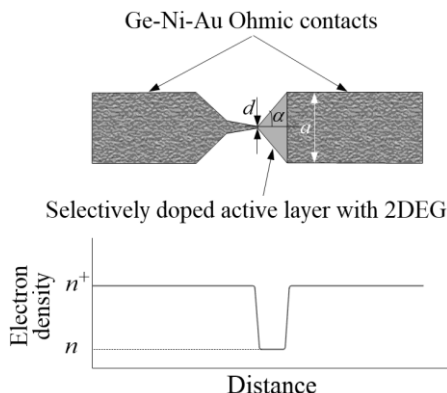


Fig. 1. Schematic view of the ungated diode and electron density distribution in the diode.

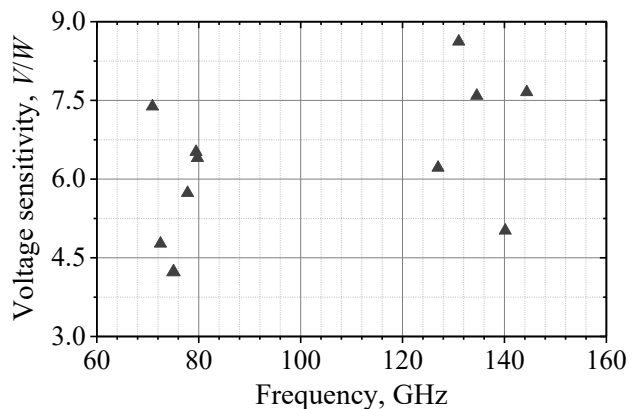


Fig. 2. Frequency dependence of the voltage sensitivity of a diode on a polyimide film at room temperature.

As a result, the voltage-power characteristics of semiconductor diode structures on a crystal substrate and on a polyimide film were measured in the frequency range of 70 – 146 GHz and in the temperature range from room to nitrogen temperature (an example of the characteristic is shown in Fig. 2). In order to measure the temperature dependence of properties of diodes a special electrodynamic unit was manufactured and tested. In the near future, it is planned to measure the characteristics of microwave diodes using this unit and the Tornado cryodielelectrometer [3] in the in the temperature range from nitrogen to helium temperature.

- [1] A. Sužiedėlis, S. Ašmontas, J. Gradauskas, A. Šilėnas, A. Čerškus, A. Lučun, Č. Paškevič, M. Anbinderis, and O. Žalys, Lithuanian Journ. Physics 57, 225 (2018).
- [2] S. Ašmontas and A. Sužiedelis, Int. Journ. Infr. Millimeter Waves 15, 525 (1994).
- [3] R. V. Golovashchenko, V. N. Derkach, M. K. Zaetz, V. G. Korzh, A. S. Plevako, and S. I. Tarapov, Telecommunications and Radio Engineering 73, 993 (2014).

Phase-Resolved Visualization of Radio Frequency Standing Waves in Superconducting Spiral Resonator for Metamaterial Applications

A.P. Zhuravel¹, A. Karpov², A.V. Lukashenko³, A.A. Leha¹, A.V. Ustinov^{2,3}

¹*B.Verkin Institute for Low Temperature Physics and Engineering of NAS of Ukraine,
47 Nauky Ave., Kharkiv, 61103, Ukraine*

²*National University of Science and Technology(MISiS),
4 Leninskiy prosp., 119049 Moscow, Russia*

³*Karlsruhe Institute of Technology (KIT), 76131 Karlsruhe, Germany
zhuravel@ilt.kharkov.ua*

A recent trend in the field of electromagnetic metamaterials is the development of planar resonant structures comprising artificially engineered unit elements. Among them, superconducting spiral resonators are especially attractive for the metamaterials research because of their magneto-active permittivity (with a μ -negative response) and ultra-compact design. The deep sub-wavelength spiral resonator has been realized with a size smaller than $\lambda_0/800$ [1], where λ_0 is free space wavelengths. Moreover, superconductors have small values of the surface resistance at radio frequencies (RF) and can cause large inductance values without the associated losses found in their normal metal-based counterparts.

However, the RF performance of a superconducting resonator with a planar spiral geometry is often influenced by nonlinear effects at high RF power. The dominant sources of these nonlinearities can be strongly localized in the dissipative area of the overcritical RF current densities generated underneath the crests of standing wave patterns at the edges of adjacent turns. Therefore, an imaging contrast of the RF field distribution was examined in detail with a laser scanning microscope (LSM) at different electromagnetic modes of spiral [2].

To probe the spatial distribution of the laser-beam-induced RF photoresponse in usual LSM modes of the RF imaging contrast, a modulated laser beam is focused onto and scanned over the surface of a superconducting resonator. The imaging contrast of these changes is recognized in terms of the local RF current densities squared. Clearly, this measurement alone does not allow visualization of RF current flow vector field over probed geometry due to inadequate data on the phase of the electric field distribution. To avoid the problem of incorrect phase presentation in the RF LSM response we apply a newly developed RF LSM regime.

The general idea is to synchronize signals of the RF drive and a laser beam modulation, adjusting them in such a way as to tailor the phase-sensitive photoresponse. In order to present imaging LSM contrast of the vector RF current density in terms of both phase and amplitude of oscillating components, the nonlinear mixed signals are heterodyne detected in the function of the laser probe position (x-y). This approach removes frequency limitations of the existing RF LSM regime and brings the phase-sensitive LSM regime to the level required for exploring the physics of superconductive metamaterials.

We demonstrate the feasibility of LSM imaging the magnitude and phase components of an RF current density vector field. As an example, radial magnitude and phase profiles of the concentric circular patterns of RF standing waves in the superconducting spiral resonators are imaged for the first three resonant modes. We performed the time-domain and frequency-domain simulations of the RF signal propagation and found an excellent agreement with experimental data obtained. The developed experimental technique allows to image the internal electrodynamics of superconducting metamaterials and provides new opportunities for their characterization.

This work was partially supported by the Volkswagen Foundation (Grant Az97768).

[1] A. P. Zhuravel, C. Kurter, A. V. Ustinov, and S. M. Anlage, Phys. Rev. B 85, 134535 (2012).

[2] A. Karpov, A. P. Zhuravel, A. S. Averkin, V. I. Chichkov, and A. V. Ustinov, Appl. Phys. Lett. 114, 232601 (2019).

Spatial Distribution of Resonances in rf-SQUIDs Array

A.P. Zhuravel¹, A.V. Lukashenko², A.V. Ustinov^{2,3}, Y.D. Oboznyi^{1,4}, S.M. Anlage⁵

¹*B.Verkin Institute for Low Temperature Physics and Engineering of NAS of Ukraine,
47 Nauky Ave., Kharkiv, 61103, Ukraine*

²*Karlsruhe Institute of Technology (KIT), 76131 Karlsruhe, Germany*

³*National University of Science and Technology(MISiS),
4 Leninskiy prosp., 119049 Moscow, Russia*

⁴*V.N. Karazin Kharkov National University, Kharkov 61000, Ukraine*

⁵*Center for Nanophysics and Advanced Materials, Department of Physics, University of Maryland,
College Park, Maryland 20742, USA
zhuravel@ilt.kharkov.ua*

Two-dimensional metamaterials (MMs) have attracted increasing attention as an effective left-handed medium that can be used for controllable routing and manipulating electromagnetic wave propagation in the radio frequency (rf) or microwave (mw) ranges. The main idea of developing such MMs is to arrange a periodic array of subwavelength planar resonators on a flat dielectric substrate to create spatially varying phase jumps and artificially controlled amplitudes in the incident wave structure. It has been shown that the Superconducting Quantum Interference Devices (rf-SQUIDs) based MMs offer many interesting opportunities for novel MM structures due to their extreme tunability and nonlinearity. One of the challenges [1] of such rf-SQUID based nonlinear MMs is understanding and controlling their collective electrodynamics, which is not a simple linear superposition of the responses of constituted metaatoms: rf-SQUIDs.

Addressing this issue, we investigate the collective behavior of the rf SQUID array. Whole structure under test consists of 6x6 individual SQUIDs, which are equidistantly spaced to form a planar network of magnetically coupled resonant oscillators. The rf SQUIDs interact in array with each other via a nonlocal magnetic dipole-dipole forth, which makes their coherent synchronization possible even in the case of randomly distributed natural resonances. However, spontaneous desynchronization of resonances in constituting SQUIDs can arise as a result of spatial rearrangement of discrete resonances to the tuning of the resonance frequency of the meta-atom depending on temperature, as well as external dc and rf magnetic flux bias. The problem of finding out the internal causes of desynchronization becomes extremely confusing for the usual global methods of its recognition, since there is no spatially resolved data.

Using low-temperature laser scanning microscopy (LSM), we visualize microwave resonances in a two-dimensional network of presumably identical coupled 6x6 rf-SQUIDs and identify spatial coherence, clustering and disordering of oscillating meta-atoms. The LSM method [2] allows us to investigate the contributions of individual meta-atoms to macroscopic response and thus provides a useful tool for characterization and optimization. We found that the rf current distribution over the SQUID array at zero dc flux and small rf flux exhibits a low degree of coherence. In contrast, spatial coherence improves dramatically with increasing rf flux amplitude, which is consistent with our simulation results.

We have shown the versatility of the LSM method with an array of rf SQUIDs visualizing its microwave response on a scale from the entire array to individual meta-atoms. This method can be extended to various planar superconducting metamaterials and microelectronic circuits to detect and ultimately overcome the technological and experimental difficulties inherent in this technology.

This work was partially supported by the Volkswagen Foundation (Grant Az97768).

- [1] M. Trepanier, D. Zhang, O. Mukhanov, V. P. Koshelets, P. Jung, S. Butz, E. Ott, T. M. Antonsen, A. V. Ustinov, and S. M. Anlage, Phys. Rev. E **95**, 050201(R) (2017)
- [2] A. P. Zhuravel, S. Bae, A.V. Lukashenko, A.S. Averkin, A.V. Ustinov, S.M. Anlage, Appl. Phys. Lett. 114, 082601 (2019).

Application of deep learning for improvement of particle flow algorithm for dijet events

A. Charkin-Gorbulin, E. Gross, S. Ganguly

*Weizmann Institute of Science, Herzl St 234, Rehovot, 76100, Israel
anton.charkingorbulin@gmail.com*

The particle flow (PFlow) [1] algorithm application made it possible to significantly improve event reconstruction accuracy in the Large Hadron Collider experiments. The association of charged particle tracks with energy deposition in calorimeter cells made it possible to fully use the composition of data obtained from the internal tracking detector and the electromagnetic and hadronic calorimeter system. In this thesis, deep learning algorithms were proposed to replace the PFlow in separating the deposition of charged and neutral particles in a calorimeter system.

A simplified model of a cylindrical detector close to the ATLAS detector was built to obtain data to analyze various event reconstruction methods. With its help, a calorimeter response was obtained for dijet events. As in ATLAS, the obtained data have a noise component, which is suppressed when we use the implemented topological cell clustering algorithm. The topo-clusters formed due to the algorithm operation are the main objects participating in the reconstruction of the jets.

The PFlow algorithm is the baseline challenging the deep learning (DL) algorithms [2,3]. The PFlow algorithm used in ATLAS was taken as the basis, but since the geometry of SCD differs in some details from the atlas detector, some numerical values of the parameters were changed, while the procedure itself was unchanged.

The primary purpose of the work was to analyze possible DL algorithms capable of replacing PFlow. Four architectures, widely used in the field of computer vision, CNN, U-Net, EdgeConv, and DS, were considered. All four algorithms have demonstrated better jet reconstruction ability compared to the implemented PFlow and topological cell clustering algorithms. The best one turned out to be the U-Net working with data in the form of images. This representation of data limits the applicability of such an architecture to a grid topology. At the same time, Deep Set and EdgeConv working with data in the representation of a point cloud are devoid of such a drawback and can work with cells of any shape, significantly increasing its scope. Thus, it is possible to choose an optimal architecture depending on the calorimetric cells geometry.

- [1] Morad Aaboud et al. *Eur. Phys. J. C* 77.7, 466 (2017).
- [2] Francesco Armando Di Bello et al. arXiv: 2003.08863 (2020).
- [3] Jonathan Shlomi, Peter Battaglia, and Jean-Roch Vlimant. *Machine Learning: Science and Technology* 2.2, 021001 (2021).

Creation of a remote presence robot based on the TI-RLSK development board

V. Chekubasheva, O. Glukhov, O. Kravchuk, V. Rohovets

*Kharkiv National University of Radio Electronics, 14 Nauka Ave, Kharkov, 61166, Ukraine
valeriia.chekubasheva@nure.ua*

The automation of complicated, harmful, tedious and monotonous work in various fields is specially attended nowadays. The method of simultaneous localization and mapping (SLAM) allows to significantly expand the functionality of modern autonomous robots of an unknown space.

A Kalman filter (extended Kalman filter EKF) is used to minimize the error that accumulates over time. There is a comparison of each new result with the previous data and the covariance matrix when using it. If the result was not found in the previous records, the new data is added to the covariance matrix. Thus, the matrix is constantly growing, and it is necessary to compare at each step with a larger number of data, which takes a certain processing power of the processor. Therefore, the system design is based on the low-power MSP432P401R microcontroller. Sensitivity and intelligent perception in the robotic equipment is realized by means of the 2Y0A21 based IR rangefinder.

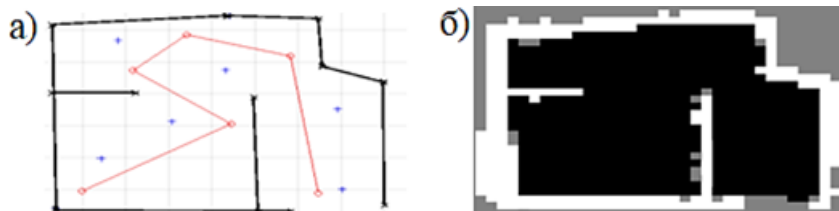


Fig. 1. The area under study (a) and the resulting map (b)

There is the evaluation of the EKF SLAM method operation principle. The simulation and the mapping (Fig. 1) was performed using the Matlab software. Over time accumulated errors analysis graphs (Fig. 2) according to the performed area research are shown below. It is studied how the errors affect the general uncertainty of the results of the mapping and the simultaneous localization of the object. The error minimization task accomplishment is visible from the received data.

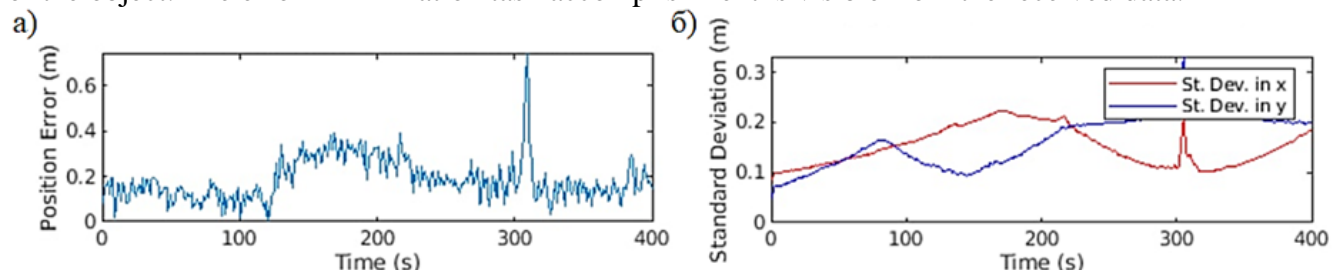


Fig. 2. Dependence of position error on time (a) and dependence standard deviation on time (b)

Fig. 2, a shows that a large error occurs in places of sharp turns. The filtering result is shown in Fig. 2, b. The total uncertainty error does not exceed 0.3 m (Fig. 2, b), despite an error of 0.1–0.65 m appearing every second (Fig. 2, a). As a result, the task of minimizing the error is performed. Thus, a robotic system TI-RLSK can build an unknown area map with a minimum error based on the data received from the sensors. This hardware platform is simplifying and accelerating the learning of work process on automated mapping systems.

- [1] M. Emharraf, M. Bourhaleb, M. Saber, M. Rahmoun, J. of Computer Science, No 2, 106 (2016).
- [2] G. Welch, G. Bishop. An Introduction to the Kalman Filter, 35 (Department of Computer Science University of North Carolina, 2006).
- [3] TI-RSLK Texas Instruments Robotics System Learning Kit The Maze Edition – Basic, 242 (Texas Instruments Incorporated, 2018).

Optimized Model of Hybrid Solar PV/Thermal Systems

K.O. Minakova, R.V. Zaitsev, M.V. Kirichenko

*National Technical University “Kharkiv Polytechnic Institute”,
2, Kyrpychova str., Kharkiv, 61002, Ukraine
zaitsev.poman@gmail.com*

The efficiency of using solar energy as a source of electricity is currently limited by the efficiency of solar cells, which for devices available to the mass consumer (operating without solar concentration) is at the level of 20-22%. A promising way to increase the efficiency of solar energy is the use of hybrid photovoltaic/concentrated solar-thermal systems that combine solar cells and solar thermal collectors, which may provide a combined conversion of solar radiation into electricity and heat energy with an overall system efficiency in excess of 80%.

The main goal of the work is to develop and numerically evaluate the computational optimization model of a hybrid solar PV/thermal system, which takes into account the variable properties of the system components, with the goal to maximize the whole solar spectrum harvesting and to achieve highly efficient combined conversion of solar energy in a hybrid system. To solve such problems, robust and accurate models and algorithms are needed to model and optimize the thermodynamic properties of hybrid systems using calculations based on general principles of thermodynamics.

Existing prototypes of solar PV/thermal systems are typically equipped with conventional solar cells based on crystalline silicon using primitive thermal layers, which reduces the efficiency of thermal energy generation, as well as significantly increases the systems cost. A general model of physical processes in such systems is needed to allow to solve optimization problems at a stage of development and designing.

During the our work implementation, a generalized theoretical and computational model of a hybrid system for solar energy into electricity and heat conversion will be created on the basis of both high-level thermodynamic analysis and realistic measured electrical and thermal transport properties of common solar cells, solar-thermal absorbers, spectral splitters, optical concentrators, thermoelectric generators, and structural materials. Modeling and optimization of hybrid system components will be performed in the COMSOL software environment. The development of a detailed model with realistic material parameters will allow to streamline the process of hybrid systems development and to optimize the power generated by both the electrical and the thermal conversion unit with a full variation of any components properties of the system that may include solar concentrators, spectrally-splitting optical filters, spectrally-selective and protective PV cell coatings, solar PV cells, heat-conducting adhesive, heat-receiving plates, or heat transfer fluids.

The developed model will be used in the proposed project to optimize hybrid systems that combine readily commercially available solar elements and construction materials. Based on the optimized system parameters, we plan to make a laboratory prototype of a hybrid system for solar energy conversion into electricity and heat, and to test the prototype to validate the model experimentally.

- [1] K.A. Minakova, R.V. Zaitsev, J. Nano- Electron. Phys. 12 No 4, 04028 (2020).
- [2] R.V. Zaitsev, Electrical engineering & electromechanics No 4, 57 (2017).
- [3] R.V. Zaitsev, M.V. Kirichenko, G.S. Khrypunov et. al., J. Nano- Electron. Phys. 10 No 6, 06017 (2018).

Medical masks filter resistance change measurement for their humidification monitoring

V. Rohovets, Y. Levchenko, O. Kravchuk, V. Chekubasheva

*Kharkiv National University of Radio Electronics, 14 Nauky Ave, Kharkiv, 61166, Ukraine
volodymyr.rohovets@nure.ua*

Over the last year, the question of respiratory protection effectiveness has become aggravated. The masks with replaceable filters which service many times longer and offer much better protection compared to disposable masks are much more convenient and environmentally friendly.

Resistance change measurement was used as the simplest and the most effective method to estimate humidification of the filters during their usage. Overwetting the filter reduces its efficiency, increases humidity of the inhaled air and carbon dioxide concentration in it – threatening the health of the user. Therefore, even long-life filters are recommended to be replaced at least every two hours. Moreover, the term of overwetting can be much shorter than that. Although filters restore after drying

Three-layer disposable masks, three-layer changed filters, five-layer changed filters for masks with and without valve were studied. Masks satisfy TS EN 14683 for the type I masks, three-layer filters satisfy type II masks requirements. Five-layer filters satisfy TS EN 143/149: KN95 (FFP2).

The electrodes of the device developed on the microcontroller basis were fixed on the filters. Filters are made of polypropylene which resistivity is about 10^{17} , that cannot be measured by the microcontroller. However, the microdroplets soaking the mask during respiration gradually reduce the filter resistance to tens of kOhms. Fig. 1 shows the dependence of resistance on time for each filter.

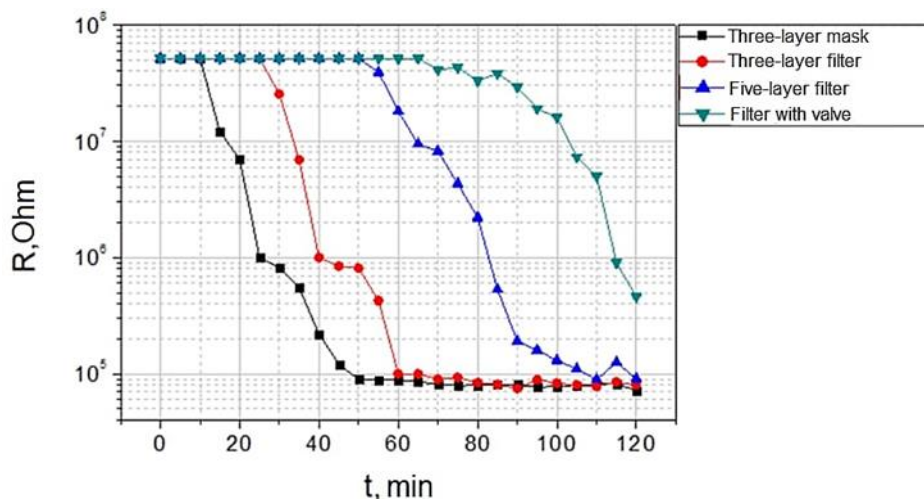


Fig. 1 – Graph of filters resistance dependence on usage duration

The graph illustrates the difference in time required to overwet different filters. It was found that even the most moisture-resistant filter lasts for approximately two hours. It is hardly possible to set a precise time interval for filter replacement even for specific model and usage conditions. The developed system makes it possible to monitor this parameter in real time, avoiding health threatening.

- [1] D. Bunyan, L. Ritchie, D. Jenkins, J. Coia, J. of Hospital Infection, 85 (3), 165-169 (2013).
- [2] Shu-An Lee, Dong-Chir Hwang, He-Yi Li, Chieh-Fu Tsai, Chun-Wan Chen, Jen-Kun Chen. Particle Size-Selective Assessment of Protection of European Standard FFP Respirators and Surgical Masks against Particles-Tested with Human Subjects, 12 (2016).
- [3] A. Tcharkhtchia, N. Abbasnezhadab, N. Zirak, Bioactive Materials, 6 (1), 106-122 (2021)

Energy Storage Development for High Voltage Electromagnetic Pulse Generator

D.S. Shkoda, M.V. Kirichenko, K.O. Minakova

*National Technical University "Kharkiv Polytechnic Institute",
2, Kyrpychova str., Kharkiv, 61002, Ukraine
shckoda.dm@gmail.com*

Recently, more and more attention is paid to electromagnetic stability, electronic equipment(EE), which means the ability to maintain operating parameters during and after the action of electromagnetic pulses (EMP) of various origins [1, 2]. Under the influence of EMP, overvoltage pulses appear in the circuits of the circuit, and with decreasing in the size of semiconductor device structures, the energy level sufficient to damage them decreases and for integrated circuits it is from 10^{-3} J to 10^{-7} J. As fuses, elements of protection of electronic equipment from impulse overvoltages are usually used, which are connected in parallel to the protected device and, when the threshold voltage is activated, in a short time can reduce its resistance to a value significantly lower than the input resistance of the electronic equipment.

To conduct research on the protection elements of electronic equipment in previous works [3,4], a generator based on a charge line made of coaxial cable with an electronic power supply and control unit was developed, which allowed to generate rectangular pulses with a rise front of 2.5 ns and an amplitude of up to 200 V. However, for a charging line, the pulse amplitude is half the charging voltage of the cable, which when charging such a line to 400 V, limited the pulse amplitude to 200 V, and the pulse duration specified by the length of the charging line was limited to 100 ns for technological reasons, which did not allow to reproduce the energy parameters of real EMP, destructively effecting EE.

In this regard, the purpose of this work was to modernize the previously developed nanosecond pulse generator to ensure the generation of high-energy pulses.

For the practical implementation of this approach industrial high-speed capacitors can be used.

Obviously, to increase the energy of the generated EMP is possible either by increasing the amplitude of the pulse, or by increasing its duration. Model calculations have shown that in the first case it is necessary to increase the pulse amplitude to 1 kV and more, which is unacceptable for safety reasons and requires the creation of an expensive high-voltage power supply.

To solve this problem, model calculations of the discharge rate of the capacitor were performed, which demonstrated that using common capacitors with a capacity of 20-25 μ F, one can get pulses with a duration of 50-100 μ s. Using a battery of capacitors connected in parallel, one can gradually adjust the pulse duration, and charging the capacitors to voltage, less than the maximum, one can also vary the amplitude of the generated pulses.

The combined use of energy storage devices based on the charge line and capacitors in the generator of electromagnetic pulses will allow, if necessary, to implement a rectangular pulse to study the time characteristics of switching or to investigate the limit characteristics of protection elements under high energy pulses.

- [1] C.N. Ghosh, Strategic Analysis 24, 1333 (2008).
- [2] V.P. Dyakonov, Generation and Signal Generators (DMK Press., Moscow 2009)..
- [3] A.M. Drozdov, R.V. Zaitsev, M.V. Kirichenko, G.S. Khrypunov, Nanosecond Pulse Generator Control System (NTU "KhPI", Kharkiv 2019).
- [4] D.S. Shkoda, M.V. Kirichenko, Development of Energy Storage for High Voltage EMP Generator, in Proceedings of XIV International Conference for Master and Postgraduate Students "Theoretical and Practical Research of Young Scientists", 01 – 04 December 2020, NTU "KhPI", Kharkiv, p. 438-439.

On Determination of Neutral Oxygen Atoms Density During Testing of Spacecraft Polymer Materials in a Rarefied Plasma Flow

V. Shuvalov, Yu. Kuchugurnyi, D. Lazuchenkov, G. Kochubei

*Institute of Technical Mechanics of NAS of Ukraine and SSA of Ukraine,
15 Leshko-Popelya St., Dnipro, 49600, Ukraine
vashuvalov@ukr.net*

Polymer materials are widely used in space technology: thermostatic coatings, solar panel coverings, components of screen-vacuum thermal insulation, etc. In the ionospheric plasma, polymer materials are damaged by the atomic oxygen (AO). The main destruction mechanism is chemical etching. The selection of polymer structural materials and the prediction of the rate of their degradation in the ionosphere is carried out by the results of the exposure of material samples on spacecraft, for example, on the International Space Station, and during accelerated resource tests in rarefied atomic-molecular oxygen plasma flows in specialized test sets. The mass loss of polymers is proportional to the fluence, density of neutral atoms and atomic ions of oxygen. The primary problem in this case is to determine the fluence and density of neutral oxygen atoms. In the ionospheric plasma and on the test set, the polymer materials are affected by flows of neutral atoms and atomic ions of oxygen. At altitudes of 200-400 km in a weakly ionized plasma, the effect of AO ions on polymer degradation is negligible. The density of neutral oxygen atoms is determined by the mass loss of the reference polymer Kapton-H, which is defined by US and ESA standards as the "polyimide equivalent" for polymers – structural spacecraft materials. Plasma is strongly ionized in the ionosphere at altitudes of 400-700 km and on the test benches. Then both neutrals and ions of AO affect polymers, and the contribution of AO ions becomes significant. In this case, the mass loss of exposed polymers is proportional to the total AO fluence. Determination of the neutral oxygen atoms density by the Kapton-H mass loss leads to significant error.

To improve the accuracy of the procedure for determining the neutral oxygen atoms in the atomic-molecular oxygen plasma flow, we propose to use cylindrical electric probe oriented transversely in the rarefied plasma flow in addition to the Kapton-H polymer. The current-voltage characteristic (CVC) of such a probe is used to determine the degree of dissociation of the ionic component and the density of AO ions. The mass loss of the Kapton-H is proportional to the total content of neutrals and ions in the rarefied AO plasma flow. With the known (determined by the CVC of the electric probe) density of AO ions and the total AO density (obtained by the Kapton-H mass loss), the density of neutral oxygen atoms in the rarefied plasma flow is calculated carrying out accelerated resource tests of polymers for resistance to AO and interpretation of the results of the polymer materials exposure in the ionospheric plasma on spacecraft.

The procedure was implemented in accelerated resource tests of polymers on the plasma electrodynamic test set of the ITM.

AUTHOR INDEX

A

- Abaloszew O. ... 52
 Abaloszewska I. ... 52
 Abraimov V.V. ... 172
 Ada Bibang P. ... 107
 Adda C. ... 164
 Agnihotri A.N. ... 107
 Aksanova N.A. ... 109, 184

B

- Babich A. ... 135
 Babich D. ... 164
 Babkin R.Yu. ... 176
 Babuka T. ... 180, 187
 Baczewski L.T. ... 31
 Bagatskii M.I. ... 127
 Bagmut A.G. ... 181
 Bagmut I.A. ... 181
 Bahrova O.M. ... 201
 Balciunas S. ... 29
 Baltrunas D. ... 74
 Ban H. ... 140
 Banys J. ... 29, 177
 Barabashko M.S. ... 127
 Barannik A.A. ... 55, 68
 Barbier A. ... 166
 Basnukaeva R.M. .128, 130, 195
 Batyuk L.V. ... 149

C

- Cardoso J.P. ... 166
 Cario L. ... 164
 Chabanenko V.V. ... 31, 52
 Chagovets V.K. ... 117
 Chareev D.A. ... 78
 Charkina O.V. ... 217

D

- Danilchenko S. ... 186
 Danylchenko P. ... 72
 Danylchenko O.G. ... 133
 Delmonte D. ... 39, 166
 Derenko S. ... 91
 Derkach V. ... 225
 Dgebuadze G.N. ... 56, 173
 Diachenko D.G. ... 119

E

- Eliseev E.A. ... 44
 Elsts E. ... 174

F

- Faulques E. ... 224
 Fedorchenko A.V. ... 176

- Al S. ... 162, 163
 Alekseeva L.A. ... 109
 Aleksenko E.N. ... 172
 Anbinderis M. ... 225
 Andrievskii V. ... 137
 Andriyevsky B. ... 94
 Anlage S.M. ... 227

- Antuzevics A. ... 174
 Apostolov S.S. ... 207, 208
 Asaula V.M. ... 179
 Averkov Yu. ... 126
 Ayachit N.H. ... 125

- Belan V.I. ... 124, 145
 Beliayev E. ... 60, 137
 Belosludtseva A.A. ... 202
 Bendeliani B.G. ... 56, 173
 Bereznyak E. ... 150
 Bernath B. ... 35
 Bertoncini P. ... 164
 Besland M.-P. ... 164
 Bespalova I.I. ... 143
 Bezrodna T.V. ... 92
 Bilokon E.O. ... 214
 Bilokon V.O. ... 215
 Bilych I.V. ... 78
 Bilyk V. ... 186
 Bludov O. ... 74
 Bludov A.N. ... 78
 Bludov M.A. ... 106, 112
 Blyzniuk Iu. ... 150

- Blyznyuk A.V. ... 195
 Bobenko N.G. ... 202
 Bodiu O.S. ... 46
 Boduch P. ... 107
 Bogdan M.M. ... 217
 Boichenko A.P. ... 129
 Bondarenko S.I. ... 61
 Bondarenko P. ... 77
 Borovkova M. ... 85
 Boryak O.A. ... 155, 156
 Breslavets A. ... 165, 203
 Brett C.M.A. ... 176
 Brik M. ... 174
 Bukivskii A.P. ... 182
 Bukivskij P.M. ... 182
 Bulakhov M. ... 216
 Büscher F. ... 36
 Bykov A. ... 85

- Charkin-Gorbulin A. ... 228
 Cheipesh T. ... 151
 Chekubasheva V. ... 229, 231
 Cherednychenko S.V. 128, 130
 Cherpak N.T. ... 55
 Chiang Yu.N. ... 57

- Choi S.S. ... 30
 Chumak O.M. ... 31, 52
 Chymakov Y.A. ... 202
 Čižmár E. ... 72, 75
 Corraze B. ... 164
 Curmei M.D. ... 92

- Dmitriyev P.O. ... 224
 Dobrovolskiy O.V. ... 32
 Dobrozhan O. ... 185
 Dolbin A.V. ... 128, 130, 195
 Domaracka A. ... 107
 Doronin Yu.S. ... 93, 106, 172
 Dovbeshko G.I. ... 66
 Dryhailo M. ... 120

- Dubovik A.M. ... 178
 Dukhnovskiy S.K. ... 68
 Dukhopelnykov E. ... 150
 Duma V.-F. ... 33
 Dzhenzherov O. ... 73
 Dzhimieva T. ... 151
 Dziaugys A. ... 177
 Dzyuba M.O. ... 57

- Eremenko Z.E. 147, 165, 203
 Esel'son V.B. ... 128, 130

- Ezerskaya E. ... 73, 76

- Fedosov S. ... 142
 Feher A. ... 75

- Felser C. ... 36
 Feodosyev S.B. ... 113

Fertman E.L. ... 39, 176
 Fil V.D. ... 78

G

Gabáni S. ... 34
 Gabunia V.M. ... 173
 Gagor A. ... 29
 Gal D. ... 140
 Galstian I.Ye. ... 183
 Galtsov N.N. ... 109, 184
 Gamayunova N.V. ... 58
 Gamernyk R.V. ... 182
 Gang Z. ... 165
 Ganguly S. ... 228
 Garbaras A. ... 29
 Gavrilko V.G. ... 128, 130
 Gawryluk D.J. ... 61
 Gažo E. ... 34
 Geidarov V.G. ... 184

H

Hamalii V.O. ... 167
 Harbuz D. ... 124, 145
 Haysak A. ... 140
 He Y.-S. ... 55
 Herashchenko N.O. ... 103
 Heraskevych V. ... 137
 Hizhnyi Yu.A. ... 178

I

Ibrayeva A. ... 170
 Ilchuk H. ... 94, 99
 Ilinskaya O.A. ... 204

J

Janod E. ... 164

K

Kabatova A. ... 76
 Kačmarčík J. ... 58
 Kačmarčík J. ... 34
 Kakherskyi S. ... 185
 Kalinkevich A. ... 186
 Kalinkevich O. ... 186
 Kamarchuk G.V. 93, 106, 124, 145, 224
 Kamarchuk L. ... 124, 145
 Kamenskii D. ... 35, 80
 Kanuchova Z. ... 107
 Kapustianyk V. ... 98
 Kapuza S.S. ... 117
 Karachevtsev M.V. ... 154
 Karachevtsev V.A. ... 155, 159
 Karachevtseva A.V. ... 110, 111
 Karpov A. ... 226
 Kashuba A. ... 94
 Kashuba N. ... 99

Fil D.V. ... 78
 Flachbart K. ... 34

Gevorkyan E.S. ... 189
 Gilioli E. ... 39, 166
 Giorganashvili G.R. ... 56, 173
 Gladkovskaya N. ... 150
 Glibitskiy D. ... 151
 Glibitskiy G. ... 151
 Glukhov K. 74, 180, 187, 218
 Glukhov O. ... 229
 Gnatenko Yu.P. ... 182
 Gnezdilov V. ... 36
 Gnida D. ... 137
 Golovashchenko R. ... 225
 Golub V. ... 77
 Gomonnai O.O. ... 180
 Gomonnai A.V. ... 180

Fomenko L.S. ... 192, 194, 195
 Furyer M.S. ... 182

Gonchar L. ... 70
 Gorbenko G. ... 160
 Gorelik L.Y. ... 201
 Gorobchenko O. ... 151
 Gradauskas J. ... 225
 Grankina I.I. ... 43
 Grechnev G.E. ... 63
 Grib A. ... 59
 Grigalaitis R. ... 29
 Gritsyna V. ... 95
 Gross E. ... 228
 Gudimenko V.A. ... 145
 Guminilovich R. ... 94

Holub M. ... 75
 Horbatenko Yu.V. ... 108
 Horielyi V.A. ... 60
 Hreb V.M. ... 63
 Hryhorova T.V. ... 198
 Hryshko V. ... 95
 Hryts V. ... 218

Huang Y. ... 192
 Hubenko K.O. ... 132
 Humbert B. ... 164
 Hurova D.E. ... 109, 184
 Husak O.S. ... 146
 Hushcha T.O. ... 152, 153

Illyashenko L. ... 84, 168
 Isaev N.V. ... 130
 Ivakhnenko O.V. ... 210, 219

Iwanowski P. ... 79

Jeżowski A. ... 127

Kavok N.S. ... 132
 Kaykan L. ... 169
 Kazarinov Yu. ... 95
 Khalyavin D.D ... 39, 106
 Kharchenko Yu.M. ... 81
 Kharchenko M.F. ... 81
 Kharkhalis L.Yu. ... 180, 187
 Kharlan J. ... 77
 Khlistyuck M.V. ... 195
 Khmelevskyi S. ... 35
 Khyzhniy I.V. ... 106, 112
 Kinka M. ... 29
 Kirichenko M.V. ... 230, 232
 Kizilova N.N. ... 149
 Klishevich G.V. ... 92
 Kliushnichenko O.V. ... 205
 Klochkov V.K. ... 132
 Kobyakov V. ... 95
 Kochubei G. ... 233

Koechlin J. ... 45
 Kofman P.O. ... 219
 Kohutych A. ... 218, 222
 Kolesnyk M.M. ... 182
 Kolkundi S.S. ... 125
 Kolodiazhna M.P. ... 78
 Kolodiy I.V. ... 192
 Kondratenko S. ... 91
 Konopelnyk Y.T. ... 79
 Konotop O.P. ... 133
 Konstantinov A.M. ... 104
 Konstantinov V.A. ... 110, 111
 Kordan V. ... 94
 Kordyuk A.A. ... 53
 Korkishko R. ... 190
 Korneeva E.A. ... 170
 Korolyuk O.A. ... 108
 Korotchenkov O. ... 134
 Korotun A. ... 135, 141

Korshak V. ... 136, 196
 Korshikov E. ... 96
 Kosevich M.V. ... 155, 156
 Kostylyov V. ... 190
 Kotvytska L. ... 82
 Kovalevsky A.V. ... 63
 Koverya V.P. ... 61
 Kozachenko V. ... 134
 Krainyukova N.V. ... 119, 167
 Král L. ... 199
 Kravchuk O. ... 229, 231

L

Langdon T.G. ... 192
 Lazuchenkov D. ... 233
 Lederová L. ... 82
 Leha A.A. ... 226
 Lemmens P. ... 36
 Len T. ... 137
 Len Ye.G. ... 183, 220
 Len T.S. ... 220
 Leonov V.O. ... 138
 Levchenko Y. ... 231

M

Maczka M. ... 29
 Maizelis Z.A. ... 208
 Makowska-Janusik M. ... 180
 Maksimchuk P. ... 132, 175
 Malyi T. ... 94
 Manna K. ... 36
 Manzhelii E.V. ... 113
 Marcin M. ... 34
 Marinchenko A. ... 77
 Marsagishvili T.A ... 123
 Martunov A.V. ... 147
 Masajada J. ... 45
 Matchavariani M.N. ... 123
 Matzui L. ... 137

N

Nabiałek A. ... 31, 52
 Nadtochiy A. ... 134
 Naidyuk Yu.G. ... 58
 Natsik V.D. ... 193
 Nemchenko K.E. ... 103, 121

O

O'Connell J. ... 170
 Oboznyi Y.D. ... 227
 Ogurtsov N.A. ... 65
 Ohta H. ... 80
 Oleaga A. ... 177, 222
 Olikh O. ... 190

P

Pal-Val P.P. ... 199

Krieke G. ... 174
 Krivchikov A.I. ... 108, 111
 Krive I.V. ... 204
 Kruhllov S.O. ... 62
 Krynytskyi Yu. ... 209
 Kryvchikov O.O. ... 206
 Kucherskyi V. ... 191
 Kuchugurnyi Yu. ... 233
 Kuchuk O.I. ... 52
 Küçük H. ... 171
 Kulinich S.I. ... 201

Levenets A.V. ... 192, 198
 Liakh M.V. ... 187
 Liubachko V. ... 177, 222
 Liul M.P. ... 139
 Lizunov V.V. ... 220
 Lobzhanidze T.E. ... 56, 173
 Lopez-Mago D. ... 45
 Lopushenko I.V. ... 85
 Lototskaya V.A. ... 172
 Lubenets S.V. ... 194, 195

Mazanov M.V. ... 207
 Mazurenko J. ... 169
 Medintseva T.V. ... 121
 Medulych K. ... 218
 Meglinski I. ... 85
 Meleshko V.V. ... 61
 Melnyk S.S. ... 87
 Melnyk V.I. ... 92
 Menesenko D.P. ... 53
 Metskhvarishvili I.R. ... 56, 173
 Metskhvarishvili M.R. ... 56, 173
 Mévellec J.-Y. ... 164
 Mikhin N.P. ... 105
 Miloslavskaya O.V. ... 81

Nerubatskyi V.P. ... 189
 Nesprava V.V. ... 92
 Nikolaienko T.Yu. ... 146
 Nikolenko A.S. ... 65
 Nikolov O. ... 151

Omelchenko L.V. ... 64
 Opanasyuk A. ... 182, 185
 Orendáč M. ... 34, 72
 Orendáčová A. ... 72, 82
 Orlov V.V. ... 155, 156
 Ostapovets A.A. ... 199

Panfilov A.S. ... 63

Kundria M. ... 218
 Kurbatov D.I. ... 182
 Kurbatsky V. ... 141
 Kurkcu C. ... 162, 163
 Kurutos A. ... 160
 Kutko K. ... 35, 80
 Kuznetsov V.L. ... 127
 Kuznetsova K.S. ... 147
 Kvitsnitskaya O.E. ... 58
 Kychka E. ... 81

Lukashenko A.V. ... 226, 227
 Lukyanets S.P. ... 205
 Lutsenko E. ... 188
 Lyagushyn S. ... 86
 Lyakhno V.Yu. ... 129
 Lykah V.A. ... 157
 Lyogenkaya A.A. ... 63
 Lyubchanskii I.L. ... 50

Minakova K.O. ... 230, 232
 Mironova-Ulmane N. ... 174
 Miroshnychenko K.V. ... 158
 Mirzoev I. ... 60, 137
 Molnar A. ... 140
 Mori T. ... 34
 Morozova O.M. ... 189
 Morozovska A.N. ... 44
 Moseenkov S.I. ... 127
 Müllner S. ... 36
 Mykhailyk V. ... 98
 Mykula M.S. ... 152
 Mysiura A. ... 148
 Mysko-Krutik N.S. ... 114, 115

Nori F. ... 37, 210
 Noskov Yu.V. ... 65
 Nurmukan A. ... 96

Ostapovych N.V. ... 169
 Ostryzhnyi Y. ... 225
 Ovcharenko H.V. ... 208
 Ovsienko I. ... 137

Pashchenko V. ... 63, 74

Pashitskii E.A. ... 54
 Pashkevich Y.G. ... 36, 176
 Pashynska V.A. ... 147
 Pavlishche N. ... 141
 Pavliuk I.R. ... 169
 Pawłowski M. ... 99
 Pękała M. ... 79
 Peletminskii A.S. ... 214, 216
 Peletminskii S.V. ... 216
 Pentegov V.I. ... 54
 Pereira M.F. ... 38
 Petrenko E.V. ... 64
 Petrov E.G. ... 138
 Petrus R. ... 94

R

Radelytskyi I. ... 79
 Ramya S. ... 125
 Riaboshtan V. ... 191
 Rogacki K. ... 64
 Rohovets V. ... 229, 231
 Roman V. ... 221
 Romantsova O.O. ... 108
 Rong L. ... 165

S

Sagan V.V. ... 110, 111
 Sakhnyuk V. ... 142
 Sakurai T. ... 80
 Salak A.N. ... 39, 166, 176
 Salazar A. ... 177, 222
 Saltevskiy G.I. ... 172
 Samuely P. ... 34, 58
 Samulionis V. ... 29
 Sarakovskis A. ... 174
 Savasta S. ... 40
 Savchenko E.V. ... 106, 112
 Savytskyi A.V. ... 224
 Schafler E. ... 198
 Seki T. ... 31
 Semenov A.V. ... 54, 67
 Semenov M. ... 151
 Semerenko Yu.O. ... 198
 Semkiv I. ... 94, 99
 Shahnazaryan V. ... 41
 Shao W.Z. ... 172
 Shapovalov Yu.O. 196, 197, 198
 Shatnii T.D. ... 220
 Shchuka M. ... 160
 Shekhar Ch. ... 36
 Shekhter R.I. ... 204
 Shekovsky V.S. ... 155
 Shestopalova A.V. ... 158

T

Tabachnikova E.D. ... 192, 198
 Takanashi K. ... 31

Petrychuk M.V. ... 65
 Piętosa J. ... 61
 Pinc J. ... 199
 Pisklova P. ... 88
 Plohotnichenko A.M. ... 128
 Plokhotnichenko A.M. 155, 159
 Podolian A. ... 134
 Pokhila A.S. ... 62
 Pomorski K. ... 122
 Ponomarenko N.S. ... 189
 Ponomarev A.N. ... 127
 Poperezhai S. ... 35
 Popov A.I. ... 174
 Poroshin V.M. ... 65, 66

Ropakova I. ... 43, 88, 97
 Roshal A. ... 151
 Roshchin O.M. ... 92
 Rostami H. ... 41
 Rothard H. ... 107
 Rovenchak A. ... 209
 Rudenko R.M. ... 65, 66
 Rudko M. ... 98

Shevchenko S.I. ... 104
 Shevchenko Ye.V. ... 138
 Shevchenko S.N. 139, 210, 219
 Shiposh Yu. ... 218
 Shitov N.V. ... 64
 Shitsevalova N. ... 34
 Shkoda D.S. ... 232
 Shkop A.D. ... 211
 Shmid V. ... 134
 Shnyrkov V.I. ... 129
 Shubniy O.I. ... 147
 Shubnyi A.I. ... 68
 Shumilin S.E. ... 198
 Shutovskyi A. ... 142
 Shuvalov V. ... 233
 Shvartsman V.V. ... 42
 Siddanna S. ... 125
 Sieradzki A. ... 29
 Simenas M. ... 29
 Sivakov A.G. ... 62
 Sklyar A. ... 186
 Skrypnyk T.V. ... 143
 Skuratov V.A. ... 170
 Skvortsova V. ... 174
 Sluchanko N. ... 34
 Slyusarenko Yu.V. ... 216
 Smirnov S.N. ... 198

Tarabara U. ... 160
 Taranets Yu. ... 120

Pospelov A. ... 124, 145, 224
 Pourovskii L.V. ... 35
 Pribulová Z. ... 34
 Pristáš G. ... 34
 Prodán L. ... 80
 Prokhorov A.A. ... 61
 Prokhvatilov A.I. ... 61
 Prokopenko Yu. ... 126
 Pshenychnyi R. ... 185
 Pud A.A. ... 65
 Pustovit Yu.V. ... 53
 Puzniak R. ... 52
 Pužniak R. ... 61

Rudnev G. ... 165
 Rusakov V.F. ... 52
 Rusakova H.V. 192, 193, 194, 195
 Rusia M.Sh. ... 173
 Rutkevich S.B. ... 71
 Ryzhov A.I. ... 139, 210

Soares M.R. ... 166
 Sofronov D.S. ... 189
 Sohatsky A.S. ... 170
 Sokolov D. ... 96
 Sokolov S. ... 105, 116
 Sokolova E. ... 116
 Solodovnik A.O. ... 114, 115
 Solovjov A.L. ... 64
 Soroka A.A. ... 129
 Sorokin A.V. ... 43, 88, 143
 Sotnikov A.G. ... 213, 215
 Stadnyk O. ... 89
 Starodub T.N. ... 75
 Starodub V.A. ... 75
 Stolyarov E.V. ... 100
 Strikha M.V. ... 44
 Sumarokov V.V. ... 127
 Sun L. ... 55
 Sužiedėlis A. ... 225
 Svirskas S. ... 29
 Sydorov D.O. ... 65
 Syrkin E.S. ... 109, 157
 Syvokon V. ... 116
 Szabó P. ... 58
 Szatkowski M. ... 45
 Szewczyk D. ... 127
 Szymczak H. ... 31

Tarasenko R. ... 72, 82
 Tarasov Yu. ... 89

Tatishvili G.D. ... 123

Tikhonovsky M.A. ... 192, 198

Timofeev V.P. ... 61

Tinkova V. ... 175

Titov I. ... 141

Tkáč V. ... 72

U

Udachan S.L. ... 125

Udachan L.A ... 125

Uhrinová A. ... 72

V

Vakula V. ... 93, 106, 124, 145

Vasylechko L.O. ... 63

Vatazhuk O.M. ... 199

Velichko N.I. ... 172

Velyhotskyi D. ... 148

Vieira J.M. ... 166, 176

Vieira D.E.L. ... 176

Vikhtinskaya T.G. ... 103, 121

W

Wiśniewski A. ... 61

Y

Yakovenko V. ... 126

Yakovenko L.F. ... 172

Yakub L.N. ... 46

Z

Zabrodin P.A. ... 130

Zaitsev R.V. ... 230

Zaitseva I. ... 151

Zakuťanská K. ... 82

Zamaraitė I. ... 177

Zamurujeva O. ... 142

Zaritskiy I.P. ... 172

Zaytseva V. ... 76

Tkachenko A.A. 93, 106, 172

Tkachuk V.M. ... 101

Tokarev V.V. ... 212

Tomašovičová N. ... 82

Tranchant J. ... 164

Trotskii E.N. ... 157

Unukovych V.I. ... 213

Usatenko O.V. ... 87

Ushakov M.V. ... 220

Vinnik O. ... 82

Vinnikov N.A. ... 128, 130, 195

Vitusevich S.A. ... 68

Vlasiuk V. ... 190

Voitovich O. ... 165

Voitsihovska O.O. ... 65, 66

Volkova Y. ... 124, 145

Volovichev I.N. ... 203

Wu Y. ... 55

Yakubovskaya A. ... 175, 178

Yampol'skii V.A. ... 87

Yefimova S. ... 43, 88, 132, 143

Zehetbauer M.I. ... 198

Zhadko M. ... 188, 191

Zhaxybekov D. ... 96

Zhekov K.R. ... 78

Zherlitsyn S. ... 47

Zhuravel A.P. ... 226, 227

Zhytniakivska O. ... 160

Zibarov A. ... 151

Trusova V. ... 160

Tsapko Ye.A. ... 183

Tupitsyna I. ... 175, 178

Turutanov O.G. ... 129

Tyutrina L.V. ... 58

Ustinov A.V. ... 226, 227

Uyutnov S.A. ... 106, 112

Vovk A.I. ... 152, 153

Vovnyuk M.V. ... 68

Vrakina V.A. ... 117

Vus K. ... 160

Vysochanskii Yu. 74, 177, 218, 222

Wulferding D. ... 36

Yermakov O. ... 90

Yevych R. ... 177, 218, 222

Zinchenko Y. ... 186

Zloshchastiev K.G. ... 48

Zobnina V.G. ... 155

Zubkov A. ... 191

Zvyagin S. ... 49

Zvyagin A.A. ... 97

Zvyagina G.A. ... 78

Zybkov A. ... 188

Наукове видання

**2-а Міжнародна конференція передових досліджень
Фізики твердого тіла та низьких температур 2021
CM<P 2021**

**Конференційна програма
Книга тез**

Формат 60x84/16. Ум.друк. арк. 13,95. Тир. 250 прим. Зам. 806-20

Видавець та виготовлювач ФОП Бровін О.В.
61022, м. Харків, вул. Трінклера, 2, корп. 1, к. 19. Т. (066) 822-71-30
Свідоцтво про внесення суб'єкта до Державного реєстру
видавців та виготовників видавничої продукції серія ДК 3587 від 23.09.09 р.





SPIE. STUDENT CHAPTER

INSTITUTE OF
RADIOPHYSICS
AND ELECTRONICS